TISSUE TRANSGLUTAMINASE AS A NOVEL THERAPEUTIC BIOMARKER IN THE DEVELOPMENT OF ENDOMETRIOSIS

by

İnci Kurt Celep

Submitted to Graduate School of Natural and Applied Sciences

in Partial Fulfillment of the Requirements

for the Degree of Doctor of Philosophy in

Biotechnology

Yeditepe University

2019

TISSUE TRANSGLUTAMINASE AS A NOVEL THERAPEUTIC BIOMARKER IN THE DEVELOPMENT OF ENDOMETRIOSIS

APPROVED BY:

Prof. Dr. Dilek Telci Temeltaş .....
(Thesis Supervisor)
(Yeditepe University)

Prof. Dr. Elif Damla Arısan .....
(İstanbul Kültür University)

Prof. Dr. Ertuğrul Kılıç .....
(Medipol University)

Prof. Dr. Fikrettin Şahin .....
(Yeditepe University)

Prof. Dr. Rukset Attar .....
(Yeditepe University)

DATE OF APPROVAL: ..../..../2019

Dedicated to my little prince, my brother

EVREN...

ACKNOWLEDGMENTS

To begin with, I would like to convey my deep gratitude to my supervisor Prof. Dr. Dilek Telci Temeltaş for her invaluable guidance and for never ending support throughout the course of the preparation of this dissertation. She never hesitated to share her knowledge with me and guided me with patience. I will always feel gratitude for her and be indebted to her. It is a genuine honor for me that TUBİTAK has granted financial support (Tübitak Project Code: 118S153) for my dissertation.

I would like to give my sincere thanks to Dr. Melike Batukan and Prof.Dr. Rukset Attar for providing patient population and biopsy samples as well as their guidance through the study. I would like to express my sincerest gratefulness to Dr. Hüseyin Çimen for making me feel as a part of his research team. He supported me in any way I needed in every moment of my dissertation.

I am also special gratitude to Dr. Ayşe Hande Nayman, MSc. Hazal Erkan and MSc. Cansu Atılgan, with whom I walked the same road together, for their support and understanding as well. I would like to thank my working mates Zeynep Bolat, Ece Nezir, Halime İlhan Sığınç, Meltem Önal, Kaan Öztürk, Deniz Yeşil, Serra Şener, Selen Tiryaki, Bihter Öztürk, M. Ali Karaca, Polen Koçak, Melike Sarıçam, Deniz Uzunoğlu, Mine Altunbek, Zehra Çobandede, and special thanks to Burçin Asutay and Murat Özpolat for technical support in flow cytometry. I am also thankful to my friends Dr. Hilal Bardakcı and Selin Akyüz for giving me the support I needed when I felt tired.

I would like to express my last and deepest gratitude to my family. I would not succeed if it weren't for you. My dearest parents, İnsaf &Vala Kurt, and my little prince Evren Kurt, I love you very much. My dearest husband, my soulmate Dr. M. Engin Celep, this would never finish without your support, help and patience.

ABSTRACT

TISSUE TRANSGLUTAMINASE AS A NOVEL THERAPEUTIC BIOMARKER IN THE DEVELOPMENT OF ENDOMETRIOSIS

Endometriosis is the growth endometrium, the tissue that normally lines the inner surface of the uterus of a reproductive woman and is lost upon thickening during menstruation, at abnormal sites in the body other than the uterus. Viable cells present in the endometriosis tissue behave as the endometrial cells and are discarded during menstruation. Given that endometriosis depends on the migration of endometrial cells out of uterus, a recently identified and ubiquitously expressed cell adhesion molecule called tissue transglutaminase (TG2) may play an important role in the development of endomteriosis. In order to elucidate the role of TG2 in migratory and invasive phenotype for endometrial stem cells (eMSCs), cells isolated from healthy and endometriosis patients were used in experimenatal setups. In support of our hypothesis, patient eMSCs (peMSCs) showed higher TG2 protein expression than healthy eMSC (heMSCs). In addition, the analysis of TG2 activity suggested that TG2 enzyme was more active in heMSC when compared to peMSCs. Co-IP experiments showing that TG2 was in complex with Integrin β-1 and syndecan-4 only on the cell surface of peMSCs, suggested that TG2 may be important for the survival and invasion abilities of these cells. Silencing of TG2 in peMSCs using shRNA technology revealed that increased cell proliferation, migration and invasion properties displayed by peMSCs was lost, resulting in a phenotype like heMSCs. The high MMP-2 and -9 activity in the peMSCs was also reduced back to basal heMSCs levels following shRNA targeting of TG2. In conclusion, results from this thesis, for the first time in literature, showed that TG2 was an important orchestrator for the stemness, survival, proliferation and invasion of eMSCs therefore can be considered as a novel molecular target to prevent the development of endometriosis. This study was supported by TUBITAK (118S153).

ÖZET

ENDOMETRİYOZ GELİŞİMİNDE YENİ BİR TERAPÖTİK BİYOMARKER OLARAK DOKU TRANSGLUTAMİNAZ

Endometriozis; üreme çağındaki kadınların rahmin iç tabakasını döşeyen ve her ay adet döneminde kalınlaşıp dökülen endometrium dokusunun rahim dışına çıkarak vücudun diğer bölgelerine implante olmasıdır. Adet döneminde kalınlaşıp dökülen endometrium dokusunun içerisinde hala yaşamaya devam eden endometrium hücreleri bulunmaktadır. Endometrioz gelişiminin endometriyal hücrelerin rahim dışına göçüne bağlı olduğu göz önüne alındığında, hücre adezyon/göçünü güdümleyen bir protein olan doku transglutaminaz (dTG) molekününün endometioz sürecinde önemli bir rol oynayabileceği düşünülmüştür. dTG'nin endometrial kök hücrelerin (eMKH) göç ve invaziv fenotipteki rolünü açıklamak amacıyla sağlıklı (keMKH) ve endometriozis hastalarından (heMKH) izole edilen hücreler kullanılmıştır. Hipotezimizi destekleyen sonuçlarımız, heMKH'lerin keMKH'lere kıyasla daha yüksek TG2 protein sentezlediğini göstermiştir. Ayrıca enzim aktivite deneyinde dTG aktivitesinin, keMKH'lerde daha aktif olduğunu gösterilmiştir. dTG'nin sadece heMKH 'lerin hücre yüzeyinde Integrin β-1 ve Sindekan-4 ile kompleks olduğunu gösteren immuno çökeltme deneyleri, dTG'nin bu hücrelerin hayatta kalma ve istila yetenekleri için önemli olabileceğini düşündürmektedir. dTG ifadesinin heMKH'lere shRNA teknolojisi ile susturulması sonucunda bu hücrelerde hücre çoğalması, göçü ve invasif potansiyeli kayıp olmuştur. Ayrıca heMKH'lerde yüksek MMP-2 ve -9 sentezi ve aktivitesi, shRNA uygulamasını takiben keMKH'lerde bulunan bazal seviyelere düşmüştür. Sonuç olarak literatürde ilk kez, dTG'nin, eMKH'lerin köklülüğü, hayatta kalması, çoğalması ve yayılması için önemli olduğu bu tez sonuçlarıyla gösterilerek, dTG endometriozis gelişimini önlemek için yeni bir hedef olarak gösterilebileceği ortaya konmuştur. Bu çalışma TÜBİTAK (118S153) tarafından desteklenmiştir.

TABLE OF CONTENTS

LIST OF FIGURES

LIST OF TABLES

LIST OF SYMBOLS / ABBREVATIONS

AML	Acute myeloid leukaemia
ANG	Angiopoietin
ASRM	American society for reproductive medicine
BSA	Bovine serum albumine
BTC	Biotin cadaverine, trifluoroacetate salt (N-(5-aminopentyl) biotinamide, trifluoroacetic acid salt)
CALC	Calcitonin hormone
CAM	Cell adhesion molecule
CD	Clusters of differentiation
CFU	Colony forming units
Cq	Quantitation cycle
Cys277	Cysteine 277
DMSO	Dimethyl sulfoxide
E-cad	E-cadherin
ECM	Extracellular matrix
ECs	Epithelial cells
eECs	Endometrial epithelial cells
EGF	Epithelial growth factor
EGFR	Epidermal growth factor receptor
eMSCs	Endometrial mesenchymal stem cells
eNOS	Endothelial nitric oxide synthase
EPO	Erythropoietin
FAS	Focal adhesion kinase
FAS-L	FAS-ligand
FAS-R	FAS-receptor
FBS	Fetal bovine serum

FCS	Fetal calf serum
FGFR	Fibroblast growth factor receptor
FN	Fibronectin
heMSCs	Healthy endometrial mesenchymal stem cells
HGF	Hepatocyte growth factor
ICAM	Intracellular adhesion molecule
ICAM-1	Intercellular adhesion molecule-1
IGF-1	Insulin-like growth factor-1
IGF1R	Insulin-like growth factor 1 receptor
IgSF	Immunoglobulin superfamily
IL	Interleukin
IL-6	Interleukin-6
iNOS	Inducible nitric oxide synthase
ITGβ-1	Integrin beta-1
KGF	Keratinocyte growth factor
LAP	Latency associated peptide
LTBP	Latent transforming growth factor-beta 1 binding protein
LTGF-β	Latent transforming growth factor-beta
MAPK	Mitogen activated protein kinase
M-CSF	Macrophage colony stimulating factor
MFR	Monthly fecundity rate
MIP	Macrophage inflammatory protein
MMP-2	Matrix metalloproteinase-2
MMP-9	Matrix metalloproteinase-9
MMPs	Matrix metalloproteinases
MSCs	Mesenchymal Stem Cells
MTGase	Microbial transglutaminase
MT-MMPs	Membrane-type matrix metalloproteinases
Na3VO4	Sodium orthovanadate

NEAA	Nonessential amino acid
NF-κB	Nuclear factor-kappa B
NK	Natural killer
NPM1	Nucleophosmin 1
OPD	O-phenylenediamine dihydrochloride
pAKT	phosphorylated AKT
PBS	Phosphate buffered saline
PDGFR	Platelet-derived growth factor receptor
peMSCs	Patient endometrial mesenchymal stem cells
PI	Protein inhibitor
PI3K	Phosphatidylinositol-3-kinase
PMC	Peritoneal mesothelial cell
PMSF	Phenylmethyl sulfonyl fluoride
PPAR-γ	Peroxisome proliferator-activated receptor- γ
pRb	Retinoblastoma protein
PTEN	Phosphatase and tensin homolog
Q-PCR	Quantitative polymerase chain reaction
RARE	Retinoic acid response element
ROS	Reactive oxygen species
RT-PCR	Reverse transcriptase polymerase chain reaction
SCF	Stem cell factor
SDC-4	Syndecan-4
SDF	Stromal induced factor
SDS	Sodium dodecyl sulphate
shRNA	Small hairpin ribonucleic acid
SLE	Systemic lupus erythematosus
SS	Sjogren syndrome
TCP	Tissue culture plastic
TEM	Transmission electron microscopy

TG2	Tissue transglutaminase-2 protein
TGF-β	Transforming growth factor-beta
TIMP	Transcription of tissue inhibitor of metalloproteinases
TMB	3,3’,5,5’-tetramethyl benzidine
VCAM	Vascular cell adhesion protein
VEGF	Vascular endothelial growth factor
VHL	Von-hippel-lin
WST-1	Water soluble tetrazolium
M	Molar
mg	Milligram
Ml	Milliliter
nm	Nanometer
µg	Microgram
µl	Microliter
µM	Micromolar

1. INTRODUCTION

Uterus has three layers namely, endometrium, myometrium and perimetrium from the innermost to outermost. Endometrial tissue is shed every month during the menstrual cycle. Myometrium is the thickest layer of the uterine wall and consists of three distinct layers of smooth muscle. The middle muscle layer contains many large blood vessels (venous plexuses) and lymphatics [1]. The perimetrium, which is known as the visceral peritoneum layer or the outer serous layer covering the uterus, consists of mesothelium and a loose connective tissue layer [1]. Endometriosis is seen in women of reproductive age and can be defined as the implantation of endometrium in other parts of body [2, 3,4]. Surgery is the most common method used in the diagnosis of endometriosis yet causing many risks. The exact prevalence of endometriosis in the community is not known since surgery is performed only in patients with suspected endometriosis or demonstrating the symptoms. Endometriosis disease is seen in 10-15 percent of reproductive-age women and 9-50% in the infertile population. This rate increases up to 50 percent in adolescents with chronic pelvic pain and dysmenorrhea [5]. Clinical symptoms such as headache [6], arthralgia and myalgia [7], allergies, eczema, hypothyroidism, fibromyalgia, chronic fatigue syndrome [8] and predisposition to vaginal yeast infection [9] are common in the endometriosis disorder. These symptoms related to the disease significantly affect women's daily life activities and quality of life. A multidisciplinary team approach should be carried out in the treatment of endometriosis to improve the quality of life of the patients and to reduce the negative effects of the disease [10].

Endometriosis is defined as the migration of endometrial tissue to a place outside the uterine cavity, settling in this region resulting in endometrial spreading [11]. As a result, migrating endometrial tissue causes complex immune development, inflammation and fibrotic tissue formation in new regions where they are implanted [12]. Recent findings showing the presence of viable cells in the tissue discarded during menstruation supported the basis of the retrograde theory put forward by Sampson stating that the backflow of menstrual blood

towards ovaries might have been the cause of endometriosis [2]. One recently notified protein responsible for increased cell migration and adhesion in cells is tissue transglutaminase [13,14]. As a ubiquitously expressed protein TG2 might have a potential role in the transition of endometrial cells from the stationary to the locomotion profile causing the disease. In this respect, this thesis aimed to determine the role of TG2 in migratory phenotype of mesenchymal stem cells (MSCs) isolated from endometrium tissue samples of healthy women and those diagnosed with endometriosis. Our hypothesis relies on the findings that endometriosis is caused by the menstrual blood MSCs reflux to the peritoneal cavity [15].

1.1 FEMALE REPRODUCTIVE SYSTEM

Female reproductive organs (*Organa genitalia feminina*) have a more complex structure than male reproductive organs. Female reproductive organs, such as their male counterparts, are divided into two parts such as external reproductive and internal reproductive organs [16]. Latin name for the external female reproductive organ is "*Organa genitalia feminina externa*" [17]. Nevertheless, vulva is more commonly used instead. Labia major, labia minor, clitoris, bartholin gland, and vestibulum vagina compose the external female reproductive organs [18].

The second part of the female reproductive system is the *organa genitalia feminina interna* or the internal female reproductive organs [16,17]. The internal organs are sorted from the inside to the outside, such as: the ovaries, tuba uterine, uterus, and vagina [19]. The internal female reproductive organs and layers are shown in Figure 1.1 of the anterior section from left to right [20]. The development of endometriosis disease originates from the female reproductive organs of uterus [21].

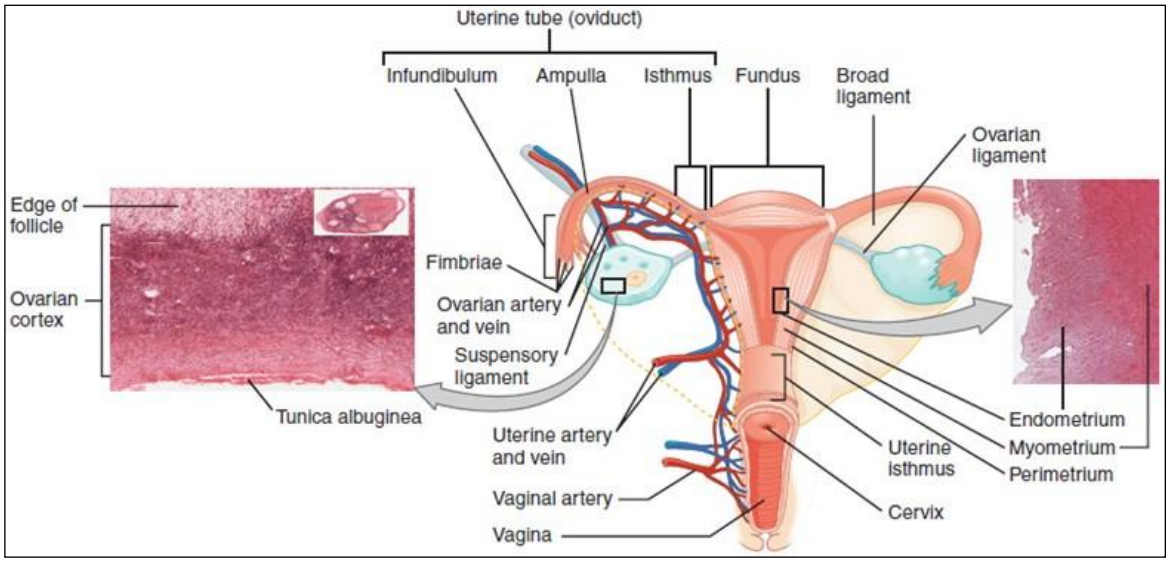

Figure 1.1. The anterior view shows the female reproductive organs and layers from left to right [20].

1.1.1. Uterus Structure and Histology

The uterus is a thick-walled hollow organ found along the midline and located between the bladder and the rectum in the pelvic cavity [16]. It resembles a truncated cone, flattened from front-to-rear. The uterus is normally in the forwardly tilted position and is a moving organ. In the fullness of neighbouring organs and during pregnancy, the uterus is elevated forward and upward. Its height can increase up to 3-6 times in pregnancy [16, 17]. It is restored following the delivery. There are ligaments responsible for the maintaining of the position of the uterus. These ligaments are ligamentum latum, ligamentum cardinale, ligamentum rotundum, ligamentum sacro uterine. The uterus has a length of 7 cm as well as a width of 4 cm, a thickness of 2.5 cm. Anatomically, it is composed of four parts, which are fundus, corpus, isthmus and cervix [22]. The histological structure of uterus fits to those of the tubular organs, and no submucosa is found. The wall of the uterus is made of three main layers from the inside to outside, such as tunica mucosa (endometrium), tunica muskularis (myometrium) and tunica serosa (perimetrium) [23]. Figure 1.2 shows the layers of the uterine wall, the blood vessels feeding the uterus, and the location of the uterine glands [24].

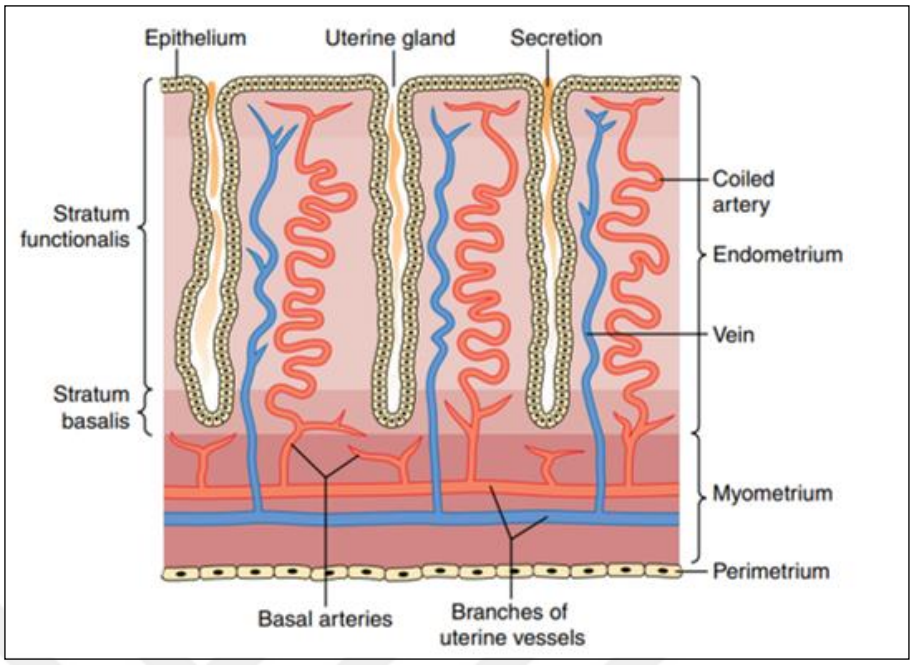

Figure 1.2. The structure of the uterine wall [24].

1.1.1.1. Endometrium

It is the innermost layer of the uterus. Creating a bed suitable for the implantation of the blastocyst, participating in implantation and performing a maternal placenta, and protecting and feeding it by hosting live until birth are among its main tasks.

The endometrium undergoes cyclic structural changes parallel to the development of the ovary in each month from puberty to menopause. It thickens, its glandular secretions increase, and stromal cells store glycogen. Unless pregnancy occurs at the end of this preparation phase, endometrial layer cannot return its beginning state and is poured out with a small amount of blood [16] This condition is known as menstruation. Following this step, the changes initiate again. The regulation of menstrual cycle is carried out by ovarian hormones [25].

Endometrium consists of two sub-layers the lamina epithelialis and lamina propria [25]. The first layer lamina epithelialis is composed of single-layer prismatic epithelium and possesses two different types of cells. The first epithelium has a ciliated structure known as kinocilium.

The stroke direction of these cilia is towards the uterus. The movement of the zygote occurs by means of this stroke direction. The second epithelium has a glandular epithelial structure.

The inner endometrial layer lamina propria, is composed of a specific type of connective tissue, where blood and lymphatic vessels are abundant. In this layer, there are shuttle and star-shaped stromal cells and reticular connective tissue fibers [16, 25]. The uterus glands are found inside the cellular connective tissue of lamina propria. The walls of these simple tubular structures were composed of prismatic cells without cilia. In some cases, the diameters of the glands extending up to the myometrium are forked. The number and activity of the glands might show alterations due to the menstrual cycle [26]. The 1/3 basal part of the lamina propria is composed of fibrous connective tissue called stratum basale, which does not participate in cyclic changes. The 2/3 upper part showing cyclic changes is called stratum fungus. At the end of each cycle, this part is restored by the stratum basalis. The stratum compactum is the most superficial layer of stratum functionalis which contains narrow neck portions of the glands, and the wide part adjacent to the stratum basal is called stratum [26].

1.1.1.2. Myometrium

Myometrium forms the thickest layer of the uterus wall (approximately 12 mm). The longest smooth muscle fibers in the organism are found here. In particular, during pregnancy, the length of these smooth muscle fibers reaches a maximum (approximately 10-fold increase). The smooth muscle fibers form four separate layers, which are inseparable by any distinct borders [27]. Those layers are stratum submucosum, which is adjacent to the endometrium, with the longitudinal course, stratum vasculature, which is circular or spiral course, veins are abundantly found among the muscle fibers, stratum supravasculare, which is a layer of thin muscle fibers with circular or longitudinal course, stratum subserosum, which is the longitudinal muscles, adjacent to the serosa [28, 1].

During pregnancy, the muscle fibers increase by hypertrophy or by the presence of mitotic division of existing muscle fibers. Following the delivery, some of the increased muscle fibers shrink; some are phagocytosed by macrophages and degenerate. The collagen fibers that provide endomysium increase also undergo an enzymatic degradation as the uterus gains its former size. Uterine contractions in non-pregnant people are too small to be felt. Contractions may cause increased cramp-like pain during sexual stimulation or menstruation [1].

In pregnancy, myometrium contractions are suppressed by progesterone and in particular by relaxin hormone. Removal of this pressure at the end of pregnancy initiates the delivery. Uterine contractions at birth are increased with oxytocin secreted by neurohypophysis [29]. This hormone is sometimes used by the gynecologists to initiate birth or to strengthen weak contractions. Estrogen is required to maintain the normal volume and cytology of the myometrium, and the uterus becomes atrophic in the absence of estrogen [29].

1.1.1.3. Perimetrium

Perimetrium is the outermost layer of the uterus, located between the peritoneum and myometrium. It provides lubrication of the outer surface of the uterus and facilitates its mobility. It is rich in veins, nerves and lymph nodes [23].

1.2. MENSTRUATION AND ITS PHASES

The menstrual cycle is regulated by estrogen and progesterone, secreted from both pars distalis of pituitary gland and the ovary. The menstrual cycle begins at the age of 12-15; and continues until the age of 45-50. In this process, morphological and functional changes occur in the endometrium. The menstrual cycle initiates on the day of the onset of bleeding and consists of 3 stages including proliferation stage, secretion stage and menstrual phase that

repeat every 28 days [30, 31, 32]. Figure 1.3 presents the changes in the hormones and endometrium during the menstrual cycle [24].

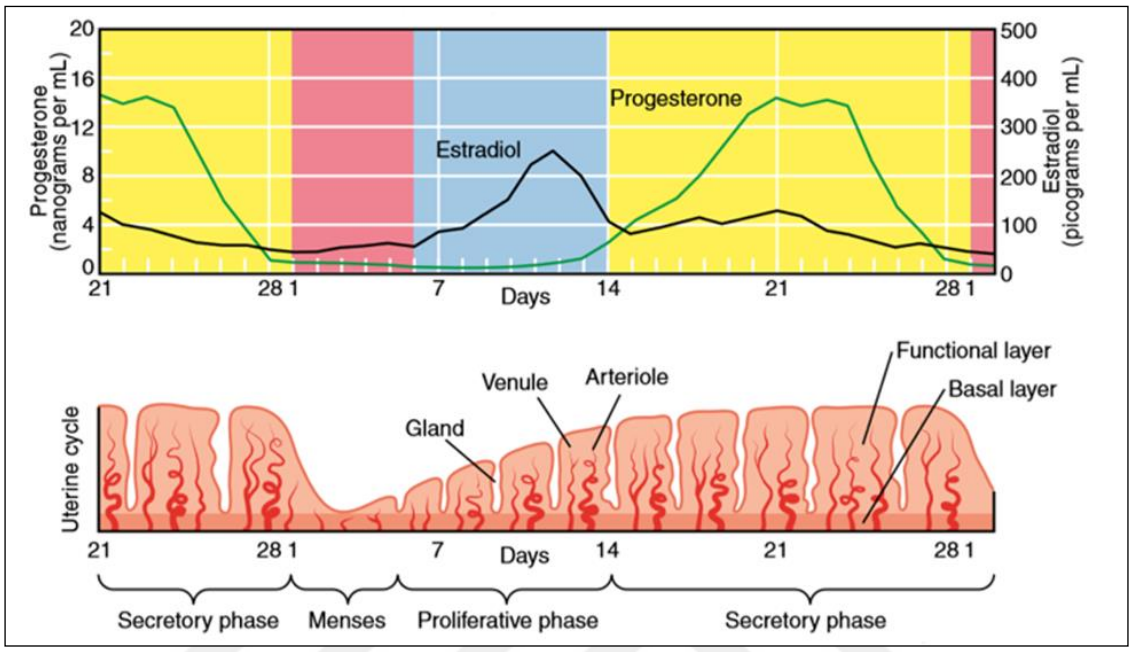

Figure 1.3. Levels of estrogen and progesterone in the blood and changes in the uterine during the menstrual cycle [24].

Proliferation stage also known as follicular stage or estrogenic stage is the phase between follicular maturation and the 5th to 14th day after uterine bleeding, which is regulated by the estrogen hormone released by the developing follicles in ovaries. At this stage, the endometrium is approximately 1 mm thick, including the basal parts of the uterine glands (stratum basal) and connective tissue [24]. Following the endometrial shedding, proliferation begins with the estrogenic influence leading to the rapid proliferation of stroma cells and endothelial cells. Stromal cells in the basal parts of the glands not only reproduce and migrate to the upper layers of endometrium but also differentiate to reshape the uterine epithelium [1] through synthesis of collagen and other extracellular matrix proteins. As the proliferation stage progresses glandular epithelial cells gradually increase the size of their granular endoplasmic reticulum and Golgi body as a preparation for the next stage secretory phase. At the end of the proliferation phase, the thickness of the endometrium reaches approximately 3 mm [1].

Secretion stage (Luteal stage) is the phase between the 14th to 28th days, beginning right after the ovulation. The secretion phase coincides with the formation of corpus luteum and is regulated by the progesterone hormone released by corpus luteum. Endometrium thickness reaches upto 5-6 mm in this phase. The thickening at this stage is due to the edematous function of endometrium, increased vascularity, and hypertrophy of epithelial cells [24]. At this stage, the glands are lengthened, folded, and the lumens are expanded by the glycoprotein secretion [30, 31]. If fertilization takes place, the stromal cells are transformed into decidual cells with the influence of estrogen and progesterone as a result of the blastocyst implantation. Decidual cells form a cellular structure that has a high glycogen content and provides the necessary environment for embryo development [1].

The final phase of menstruation (the bleeding phase) lasts about 5 days. If there is no fertilization, the corpus luteum decreases after actively producing hormone for about 10 days. With this reduction, the secretion of progesterone and estrogen drops abruptly, and necrosis begins in the endometrium. In the spiral arteries, regular contractions begin, and the functional layer becomes ischemic. Locally secreted prostaglandins, cytokines and nitric oxide lead to rupture of the blood vessel walls together with basal membrane disintegration. In addition, collagen in the endometrium lamina propria is degraded. In the endometrial stroma, edema decreases, and the endometrium shrinks [32]. With the rupture of the spiral arteries, the lumens of the glands are filled with blood, the surface epithelium is destroyed, and the hormone secretion is terminated. As tissue fragments break off from the functional layer of the endometrium, the open ends of the veins, arteries, and glands appear. This spill continues to the basal layer, and the functional layer is completely lost. During the menstrual bleeding period, approximately 35-50 ml of blood is lost, and blood clotting is inhibited at this stage [30, 31, 32, 1].

1.3. CELL TYPES OF ENDOMETRIUM

Human endometrium is a chimeric structure with many different cell types including endometrial glands, stromal cells, fibroblasts, endothelial cells, lymphoid cells, and smooth

muscle cells surrounding the endometrial wall [33]. This complex structure of the endometrium is undoubtedly dependent on an organized extracellular matrix (ECM) structure consisting of fibronectin, laminin and collagen, which contribute to the cell distribution, cell traffic and intercellular communication.

1.3.1. Epithelial Cells

The prismatic secretory cells in endometrium are a kind of epithelial cells (ECs) with typical features of high mitotic activity and tendency to break off from endometrial surface [34]. They assist the formation of endometrial glands in the endometrium. According to the most emphasized theory, endometrial tissues should be implanted to the peritoneal surface, invade the basal membrane and the ECM, and survive to take place in the development of endometriosis [35, 36, 37, 38]. Witz *et al.* support the theory of Sampson with *in vitro* studies showing that both the epithelia and the stroma of endometrium can easily adhere to the mesothelium [39]. In the experimental setup, attachment of the Ecs, which were isolated from the ectopic endometrial samples taken from the peritonea, was observed using transmission electron microscopy (TEM) and confocal laser scanning microscopy. The data indicated that attachment of the Ecs to the mesothelia occurs within an hour, and invasion proceeds through the 18-24 hours that follow [40]. High migration, adhesion, and invasion potentials were determined for the prismatic secretory Ecs via these experiments.

1.3.2. Mesenchymal Stem Cells

As clarified in the literature, both the functional layer and the basal layer of the endometrium possess many mesenchymal stem cells and hence stromal cells originating from these mesenchymal stem cells [41]. Stem cells are the cells that have the property of being able to renew themselves and at the same time they can be transformed into other tissue cells by differentiating according to the needs of the body. Mesenchymal stem cells (MSCs) are adult

stem cell types generally found in the connective tissue that have the ability to differentiate into cells such as fat, bone, cartilage, muscle, tendon and ligament, as mentioned earlier.

MSCs were first described by Fridenstein who showed that the cell isolates from fetal bone marrow formed cell colonies that were morphologically similar to fibroblasts with the capacity to differentiate into bone and fat cells [42]. Years later, it was demonstrated that these cells were multipotent stem cells with no hematopoietic properties and differentiation ability [43]. MScs provide homeostasis of tissues by providing replacement for cells die through routine cellular turnover and repair tissues after an acute injury [44].

MSCs, which could previously be isolated only from bone marrow, can now be obtained from muscle [45], bone [42,46], cartilage [47], fat tissue [48], dental pulp [49], periodontal tissue, liver, lung, thymus, ovary, testis, amniotic fluid, placenta and umbilical cord (Figure 1.4.) [50]. When intravenously administered MSCs first directed is bone marrow [51]. However, when there is a tissue damage in the organism, mediators like integrin, selectin, chemokine interact with the surface receptors on the MSCs and lead these cells to the damaged tissue [52].

Bone marrow-derived MSCs secrete growth factors such as the macrophage colony stimulating factor (M-CSF), Flt-ligand, stem cell factor (SCF) required for hematopoietic cells. In addition, MSCs synthesize cytokines such as interleukin (IL) -1, -6, -7, -8, -11, -12, -14, stromal induced factor (SDF) -1, and chemokines such as monocyte chemoattractant proteins [53].

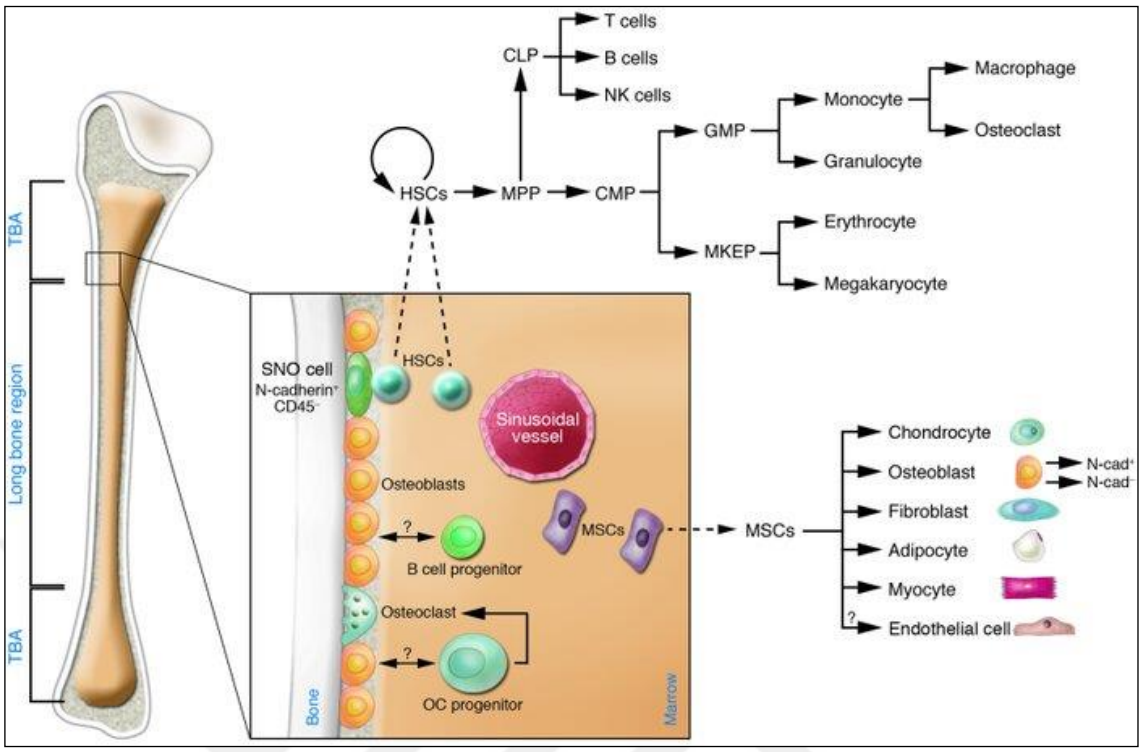

Figure 1.4. Hematopoietic and stromal stem cell differentiation [50].

MSCs have many important roles in cell homeostasis. MSCs move to the inflammatory site through the cytokines and chemical chemokines and play a proliferative [54], anti-inflammatory [55, 56, 57] and anti-apoptotic [58] in that region. It is important that mesenchymal stem cells exhibit paracrine activity and growth factor and cytokine secretion play an antifibrotic role and vascularity. When the angiogenic response is impaired, mesenchymal stem cells release stromal cell-derived factor-1 (SDF-1), vascular endothelial growth factor (VEGF), insulin-like growth factor-1 (IGF-1), epidermal growth factor (EGF), keratinocyte growth factor (KGF), angiopoietin (ANG) -1, macrophage inflammatory protein (MIP) -1α and β, erythropoietin (EPO), matrix metalloproteinases (MMPs) and many cytokines, and ensure angiogenesis and tissue regeneration [59, 60]. VEGF secreted by mesenchymal stem cells is a critical factor responsible for the angiogenic potential of these cells [60]. In addition to VEGF, other molecules expressed by mesenchymal stem cells, including transforming growth factor-Beta1 (TGF-β1) and MMPs also contribute to the interaction of mesenchymal stem cells with endothelial cells [61, 62].

Paracrine secretion of mesenchymal stem cells was shown by a research team 15 years ago, with broad spectrum growth factors such as VEGF, FGF, MCP-1, hepatocyte growth factor (HGF), IGF-I, SDF-1, and thrombopoietin, which affect cells in the immediate vicinity of mesenchymal stem cells, and cytokine synthesis and release [63]. These factors promote arteriogenesis; supporting stem cell crypt in the gut, protecting against ischemic kidney and extremity tissue damage. It has been shown to support and maintain hematopoiesis and support the formation of megakaryocytes and proplatelet. Most of these factors have been shown to demonstrate beneficial effects, including neovascularization and increased angiogenesis [64].

Mesenchymal stem cells also show anti-inflammatory properties through dendritic cells and macrophages. TGF-β, HGF, indolamine 2,3 dioxygenase and prostaglandin E are known to play a role in this feature [65]. Mesenchymal stem cells have been shown to inhibit B-cell proliferation, differentiation and antibody secretion both in-vitro and in-vivo [66].

In support Sampson's theory, it has been hypothesized that endometrial stem cells are refluxed together with their niche (nest) cells into the peritoneal cavity through retrograde menstruation in women with endometriosis [67, 68, 69, 70]. The mesenchymal stem cells isolated from menstrual blood taken from baboons with menstrual cycle were shown to induce experimental environment endometriosis [71]. In other studies, stem cells were isolated from human menstrual blood [72, 73].

Endometrial regeneration is seen in postmenopausal women after each menstrual cycle and after estrogen replacement therapy [74]. This level of tissue regeneration is similar to regeneration in the intestinal epithelium and epidermis. In this way, the adult stem cells in the constantly renewed tissues continue the cellular production [74]. Initially, it was assumed that adult root or progenitor cells were present in the basal layer, responsible for the cyclic regeneration of the endometrial functional layer. However, studies have shown that endometrial stem / progenitor cells are identified by specific markers, both in functional and basal layers [74,75]. A rare population of mesenchymal stem cells (eMSC) of endometrial origin has been identified in the human and mouse endometrium. These eMSCs have similar

properties and phenotype with the mesenchymal stem cells derived from bone marrow or adipose tissue [75]. The gene expression profile of mesenchymal stem cells of endometrium is more similar to fibroblasts than endothelial cells. In addition, these features, together with their genetic potential and angiogenic capacities to respond to perivascular sites, hypoxic, inflammatory and proteolytic stimuli, indicate that endometrial stem cells play a major role in endometrial regeneration [15]. This observation reinforces the role of endometrial-derived mesenchymal stem cells in endometrial regeneration [74]. Initially, it was assumed that adult stem cells or progenitor cells were present in the basal layer, responsible for the cyclic regeneration of the functional endometrial layer [39]. Epithelial precursor cells in human endometrium are localized at the base of the st. bazal layer, yet endometrial mesenchymal stem cells are located near both basalis and functional layer [76, 77]. Information on the presence of human adult stem cells in the endometrium has been shown in publications in which colony forming capabilities of single-cell suspensions of endometrial stem cells have been studied [76, 78]. It is thought that these cells in the endometrium of perimenopausal women may be responsible for the regeneration of the gland in the cyclic and atrophic endometrium, during the normal menstrual cycle [41, 76, 79]. MSCs are the ancestors of stromal cells and have been proven to be precursor stromal cells. These studies demonstrated that 0.22% of the human endometrial cells have colony-forming units (CFU). Two types of CFU are available. 0.9% of these types are large, and 0.14% are small colonies [76, 80].

Adult stem cells in the mouse endometrium are located at the base of the uterus and especially in the luminal epithelium; also perivascularly located at the endometrial-myometral junction region corresponding to the human basal layer (Figure 1.5) [75].

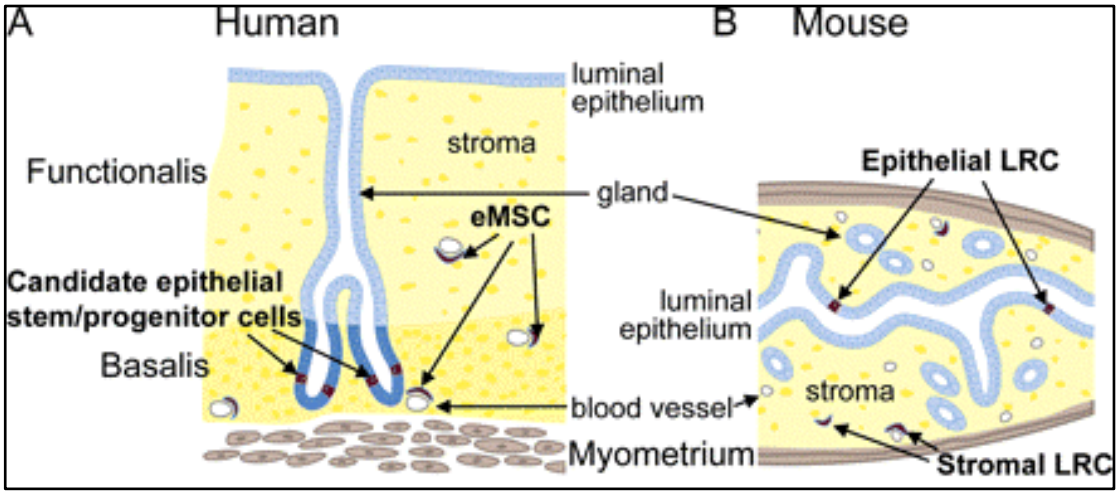

Figure 1.5. The location of stem / progenitor cells in human (A) and mouse (B) endometrium (eMSC: endometrial mesenchymal stem cells; LRC: labeled in the mouse endometrium stem cells) [75].

Endometrial stem cells have been shown to be located in endometrial luminal epithelium rather than glandular epithelium in the postpartum period (days 3-5) in mice. 3% of endometrial luminal epithelial cells are epithelial stem / progenitor cells. Luminal epithelial stem / progenitor cells are thought to be responsible for the growth and development of glands during the cycle [75, 80]. Since the functional layer of the endometrium includes the mesenchymal stem cells in addition to the basal layer, endometrium-derived stem cells can be taken from patients without anesthesia by means of biopsy; thus, endometrial stem cells can be cultured and differentiated. Even in the case of endometrial injury encountered in such cases as fine dysfunctional endometrium or Asherman syndrome, this allows the use of autologous cells for the patient [80, 81].

1.4. ENDOMETRIOSIS

Endometriosis is named after endometrium, the inner membrane of the mammalian uterus that thickens and gets discarded from the body during menstruation. During endometriosis, the tissue that normally lies on the inner surface of the uterus migrates and becomes implanted to other sites in the body [82]. These migrated ectopic tissues exert activity during

each menstrual cycle and lead to the formation of cysts, and formation of fibrotic tissues, at the sites they are implanted [83, 84]. The condition often results in severe pelvic pain and infertility. Etiologic of endometriosis points to age, chronic inflammation, multiple miscarriages in a row, and endocrine problems; particularly, chronic inflammation and fibrotic tissue formation play a critical role in the emergence and progression of the disease [84, 85]. The prevalence of endometriosis is between 3-37 percent in fertile women [86].

Although endometriosis was described in 1860 [87], its etiologic and pathogenesis are still not clear. There are different theories on the pathogenesis of endometriosis [88, 89]. The so-called theories are retrograde menstruation/transplantation [2, 90], coelomic metaplasia [91], changes in immune response [92], metastasis [93], genetic factors [94, 95], environmental influences [96], and epigenetics [97]. Main focus is on the retrograde menstruation theory, which was first presented in 1920s, stating that the disease results from the invasion of the endometrium tissue into the peritoneal cavity [2, 98].

The presence of endometrial tissue as sub-peritoneal implants indicates a pathological condition. The reflux of endometrium tissue fragments from the fallopian tubes towards the peritoneal cavity results in their adhesion onto the peritoneal surface, followed by the initiation of the invasion and progression of the disease. The first line of defence is the peritoneal immune system that stays alert in the abdominal cavity. Here, a local peritoneal immune response is initiated, immune system is upregulated, and the tissue is degraded into fragments to be phagocytosed by hyper-activated macrophages [99]. The fragments that evade this defence mechanism adhere to the peritoneal surface, invade, and form the endometriotic lesions [89].

Even though endometriosis disease is a gynecological problem for females; it also leads to other pathological conditions with different cell homeostasis. Clinical symptoms such as headache [6] arthralgia and myalgia, allergies, eczema, hypothyroidism, fibromyalgia [7], chronic fatigue syndrome [8] and predisposition to vaginal yeast infection [9] are common in endometriosis disorder. In a retrospective study in 2002, endometriosis patients were observed to be statistically more prone to disorders such as hypothyroidism, rheumatoid

arthritis, systemic lupus erythematosus (SLE), Sjogren syndrome (SS), multiple sclerosis, allergies and asthma than healthy controls, however no significant difference was found in terms of hyperthyroidism and diabetes [8]. In a cohort study involving a small number of patient groups, no significant relationship was found between SLE and endometriosis, between SS and endometriosis [100].

1.4.1. Theories About Endometriosis Development

In 1927, Sampson proposed the first theory of the etiopathogenesis of endometriosis [2]. According to this theory, endometriosis is expressed as a result of menstrual spread of endometrial tissue to the peritoneal cavity. Although there is not a single mechanism to explain all cases of endometriosis, a growing body of evidence supports that Sampson's theory of retrograde menstruation and implantation of living endometrial tissue may be the primary mechanism, particularly in the pathogenesis of peritoneal endometriosis. In the light of recent studies, seven major theories of etiopathogenesis have been proposed.

1.4.1.1. Sampson's Retrograde Menstruation Theory

As mentioned previously, there are many theories about the formation of endometriosis. The Sampson Retrograde is the most widely accepted and popular theory. When the early literature is examined, it has been understood that in the time Sampson started writing results of his works on this disease, the term endometriosis was not in use yet.

A chocolate-shaped cyst was first reported by Lackyer in 1913, followed by Cullen in 1914, and then described by Sampson as a severe and invasive disease, occurring usually in the ovaries. It has been shown in the studies that the chocolate-shaped cyst completely destroys *cul de sac* by adherence to rectum and vagina. In the publication of Sampson in 1918, he published x-ray graphs that he had taken after injecting gelatinase bismuth or barium gelatinase into the surgically excised uterus [101]. Sampson mentioned the direct retrograde

model in this publication. According to him, the menstrual blood, which is supposed to be discarded in a menstrual cycle every month, still contains living cells, and that these cells migrate to different places, stick to the migrated area and other neighbouring organs and possess the growth potential there. Sampson's findings indicated that if the endometrium integrity is intact, the injected material does not flow through the uterine arteries and veins. In the same publication, it was pointed out that the material injected through the collecting veins under the endometrial tissue could flow through the veins located on both sides of the uterus, if the hysterectomy was performed during menstrual bleeding or if the endometrial integrity was impaired by curettage. It was also shown that the material used in this study could flow through the fallopian tubes [90, 101, 102]. These findings have been a popular theory in the field of endometriosis, since it responds to the causes and consequences of the retrograde flow. In the light of this and earlier findings, in 1925, Sampson clarified that women undergoing menstruation may have endometrial tissue with uterine veins as a disease seen outside adenomyosis and pelvis [90, 101, 102, 103]

In another frequently cited study by Sampson in 1921, it was reported that only 9 out of 23 patients with chocolate cysts had ovarian cysts of endometrial type. Other cysts were found to have a corpus luteum-like appearance or were covered with flat, cubic cells. In their highly detailed observations, the majority of patients were diagnosed with “deeply invasive” cysts on pelvic surfaces [103]. Another result obtained from the same study revealed that the blood or chocolate liquid leaking from the reproductive cysts causes the endometrial cells to spread to the pelvic surface leading to the development of the implantation adenomas, similar to the spread of malign cells in ovarian cancer [90, 102, 103].

In another article published by Sampson's group in 1922, it has been demonstrated that the reflux of endometrial cells from the fallopian tubes has a critical role in the development of superficially located lesions in the ovarian tissue or deep-settled chocolate cysts [90, 102]. In the same publication, the reason for the spread of endometriosis to the pelvic tissue was stated as the migration of cells in the exploding chocolate cysts. In another article, published in the same year [90, 102], the first incision, proliferation or invasion of endometrial cells

on the peritoneal wall was illustrated. This paper was regarded as the continuation of the other study in 1922 and supported the reality of the theory. In this article, the reflux of menstrual blood was also indicated as the cause of endometriosis. It was proposed that endometrial-type ovarian cysts and implantation adenomas were resulted from the misplaced euctopic endometrium. According to Sampson, when the benign endometrium tissue fell into a suitable soil, it could cling to the site, proliferate and spread deeper, and cause menstruation bleeding in the regions where they were found.

Sampson's theory was supported by Dr. J.W. Williams by the statement "I believe in everything Sampson has said and tried to prove" [2]. Sampson published another article in 1925, for the purpose of explaining the relationship between endometriosis formation and endometrial cancer. Here, he reported that peritoneal metastases of both benign implantations and endometrial cancer occur as a result of the reflux of endometrial tissue from the fallopian tubes [103].

After all these scientific data, this theory has still been the subject of debate among the scientists who have revealed findings that Sampson did not consider in his interpretation of the results. The most important of these overlooked evaluations is Iwanoff's serosal metaplasia theory. Although this theory is limited to peritoneum, it has been suggested that totipotent features may also be present in cells in the anterior lower abdominal wall, where surgical wound is also present. In these tissues, it is stated that there may be cells that are transformed into endometriosis tissue due to the effects of the growth factors taking part in wound healing. Over time, due to Sampson's missing interpretations and the linguistic gaps that cannot be elucidated; Sampson abandoned the term 'implantation adenoma' in his 1925 paper and used the term "endometriosis" for the first time [2, 103]. In this article, he tried to define the colors of the lesions and he stated that the stage of the disease would be determined by the colors [2].

Sampson explained all these theorems and experimental results without any biochemical evidence [2, 90, 102, 103]. He claimed that the blood that is refluxed by menstruation possesses more irritating properties for the pelvis than the normal blood, which resulted in

significant adhesion in some patients [2, 90, 102, 103]. He did not consider that endometrial glands could be biologically active and could release some paracrine substances leading to inflammation, bleeding, and adhesion [2, 90, 102, 103].

Sampson, in his 1926 article, cited menstruation blood as “magical and mysterious” and described it as “a never-ending super tissue” [104]. What Sampson actually tried to explain was that there are living cells dwelling in the menstrual blood, and these cells can still migrate to areas outside the uterus, with the ability of implantation resulting in adhesion in these regions. Owing to their listed properties, these cells formed endometrial foci and led to endometrial cyst development [104].

1.4.1.2. Coelomic Metaplasia Theory of Endometriosis

In the 1960s, Ferguson suggested that coelomic metaplasia could contribute to the development of endometrosis in the metaplasia [105]. This suggestion was derived from the assumption that there were undifferentiated cells in the peritoneum that could differ in the direction of endometrial cells [105, 106]. This theory is not supported by strong clinical or experimental data [107].

1.4.1.3. Induction Theory

The theory of induction is, in principle, an extension of the systemic metaplasia theory. It is thought that an endogenous biochemical factor can induce the development of differentiated tissue in the direction of the peritoneal cells. Although it was observed in rabbits there have been no findings supporting this theory in women and primates [107].

1.4.1.4. Genetic Factors

Epidemiological studies have shown that endometriosis is inherited as polygenic / multifactorial [108, 109, 110, 111, 112, 113]. The disease shows hereditary predisposition in first degree relatives between 5% and 7%. The incidence of an individual's sister being diagnosed with endometriosis increases the risk by a factor of 5.2 in that individual [113].

A number of potential loci have been identified in genomic level studies to accommodate mutations in endometriosis patients [114]. Association studies were carried out in order to illuminate the biological susceptibility. The largest of these studies examined pairs of siblings affected by endometriosis in two or more families of a total 1100 families, and the 10q26 region was found to be significant in terms of sensitivity [115].

Both eutopic endometrial and ectopic endometriotic foci of women with endometriosis have a group of changes that are not observed in the endometrium of healthy women. The anti-apoptotic gene BCL-2 up-regulation was shown in the ectopic and eutopic endometrium of affected women [116, 117]. This finding explained why in addition to a decrease in apoptosis, an increase in selective survival was observed in endometrial proliferation and ectopic endometrial tissues in women with susceptibility to endometriosis [116, 118]. The loss of heterozygosity in the PTEN (Phosphatase and Tensin Homolog) tumor suppressor gene have been also shown to be related to solitary endometrial cysts in the ovary [119]. In addition, new evidence indicates that the response of endometrium to steroid hormones is controlled by epigenetic regulation and these mechanisms are impaired in women with endometriosis [120, 121]. Progesterone resistance has been shown in animal models as a result of abnormal methylation of the promoter genes that constitute the normal progesterone response of the endometrium [122].

1.4.1.5. Immunologic Factors

As the endometrial tissue, which is normally refluxed, is removed from the peritoneum by the immune system, the deterioration of this cleansing mechanism predisposes the tissue to the implantation and growth of endometrial cells in non-uterine location. Unlike the individual cells, large tissue fragments have a higher implantation capacity, probably because the cell cluster inside the fragment is protected from the immune system [123]. In patients with endometriosis, the eutopic endometrium is more resistant to the lysis by natural killer (NK) cells than normal women [124], suggesting that a disruption in NK cell function may predispose endometrial cells to escape from the immune system and develop endometriosis.

In vitro studies have shown that endometrial fragments can adhere to the peritoneum only in case of the emergence of basal membrane and extracellular matrix due to mesothelial layer damage [125]. Menstrual fluid exerts harmful effects on mesothelium and may induce a local damage facilitating the implantation of endometrial cells [126]. However, the main mediators that cause mesothelial damage have not been elucidated, yet. Matrix metalloproteinase-3 (MMP-3) upregulation during luteal phase in patients with endometriosis, and the upregulation of transforming growth factor beta (TGF-β), intercellular adhesion molecule-1 (ICAM-1) and interleukin-6 (IL-6) during menstruation occur [127]. Variable expression of these cytokines and growth factors may facilitate the formation of a microenvironment that eases the endometrial cell implantation or causes difficulty in the removal of these cells by the immune system. In women with endometriosis, the role of TGF-α among different cytokines in peritoneal fluids is different and it has been observed to induce endometrial cell invasion in *in vitro* model of the peritoneum [128].

1.4.1.6. Environmental Factors

Although the current epidemiological data for endometriosis is limited, some dietary and lifestyle factors are likely to cause predisposition. High fruit and vegetable consumption and

low meat consumption have been found to protect against the development of endometriosis [129, 130]. Women who do not have children and have a low body mass index have a higher risk of developing endometriosis [130]. Synthetic compounds such as dioxin and other polychlorinated biphenyls can induce endometriosis by affecting the endocrine system. Dioxin appears as a by-product of the chlorine bleaching process used as bleaching agent in the paper industry and is also used in the manufacture of buffers. Information on association of dioxin and endometriosis is based on animal studies, and the effect of dioxin on endometriosis in human data is controversial [131].

1.5. MOLECULAR MECHANISMS FOR THE DEVELOPMENT OF ENDOMETRIOSIS

Apart from being the most common gynaecological problems of our age, endometriosis is a complex disease to treat and to diagnose. In recent years, the treatment of endometriosis has been facilitated by examining and illuminating the molecular pathways involved in the development of the disease [132]. In the literature, it has been shown that changes in cellular responses and molecular mechanisms might occur inside or outside the endometrium [133]. These changes affecting the physiological activity of the endometrium have been demonstrated to cause endometriosis [134]. Most of the molecular studies regarding the endometrial tissues or menstrual blood of women with endometriosis provided such results that support the Sampson's Retrograde and Implantation Theory [135]. The first phenomenon described in women with endometriosis and providing significant biological contributions to this theory is programmed cell death (apoptosis) [136]. In studies with electron microscopy, healthy endometrial cells have been proven to possess apoptotic bodies in the late secretion phase [136, 137, 138]. The mechanism of apoptotic bodies and apoptosis is important for the elimination of aged cells in the endometrium and for the maintenance of cellular homeostasis [32]. Each month, dysfunctional cells in the endometrium of healthy and reproductive women undergo apoptosis and removed from the body by menstrual blood [138]. When the cells of menstrual blood of women with endometriosis were compared with

healthy women, the cells in the endometriosis samples were determined to have less apoptosis [136]. In studies, some major differences were observed when the healthy endometrium was compared to the patient's endometrium [139]. These differences lead to endometriosis by causing the survival of endometrial cells with reflux to the peritoneal cavity. Another study revealed that the percentage of apoptosis in endometrial cells that have refluxed peritoneal cavity in women with endometriosis was very low [140]. In the same study, the apoptosis index in women with endometriosis was lower than that in the control group, and the cyclic change in apoptosis was reported to be lost in patients with endometriosis. In a study by Dmowski et al., apoptotic index analysis was performed according to the stage of the disease in women with endometriosis and increased endometriosis stage and decreased tendency of apoptosis were observed [141].

Another study conducted on the anti-apoptotic Bcl-2 protein elucidated its role in the formation of endometriosis. Bcl-2 protein and gene expression were analysed by immunohistochemical staining. When the Bcl-2 gene was examined in endometriosis tissues, this gene was observed to be expressed at a high rate, and cell survival was increased by escaping the apoptotic pathway through increased Bcl-2 expression of cells [116, 142] suggesting that Bcl-2 acts as the suppressor of the apoptotic pathway in endometriosis. Another Bcl-2 protein family member Bax was proposed to play a role in the development of endometriosis [143, 144]. The expression of Bax, an inducer of apoptosis protein, was found to be decreased in women with endometriosis when compared to the endometrium of healthy women [143, 144]. The increased expression of Bcl-2 in women with endometriosis and the inability to express Bax may cause the decreased sensitivity to apoptosis and survival of endometrial cells in an ectopic environment [145, 146]. In another study using the immunohistochemical staining method, the anti-apoptotic Bcl-2 was shown to be highly expressed in the basal layer of the endometriotic tissue, while the expression of death receptor Fas and caspase-3 was lower in the basal layer of the endometrium but higher in the functional layer [147].

Bcl-x is another member of the Bcl-2 family whose role in endometriosis has been identified. Bcl-x gene encodes both inducing and suppressive protein of apoptosis by alternative splicing mechanisms [148]. Bcl-xl (long form of Bcl-x) acts as anti-apoptotic protein while Bcl-xs (short form) acts as a pro-apoptotic protein [149]. In that, Bcl-xl provides resistance to apoptotic cell death in the absence of growth factors, while bcl-xs breaks the resistance of bcl-2 against apoptotic cell death [150, 151]. A comparative study was conducted in 2007 with ten different women with endometriosis and ten healthy women. In this study, mRNA levels of Bcl-xs and Bcl-xl were analysed in epithelial tissues of women with/without endometriosis. In the menstrual phase, women with endometriosis had a high Bcl-xl gene expression while no expression of the Bcl-xs gene was found, while high Bcl-xs gene expression was determined in the menstrual phase of healthy women [152]. These results suggested that the development of apoptotic resistance in eutopic and ectopic epithelial cells of women with endometriosis resulted in an increased cell survival leading to the development of disease pathogenesis [152].

FAS receptor (FAS-R) from the TNF family, which plays an active role in programmed cell death, participates in inducing apoptosis after it binds to its ligand, FAS-L [153]. Therefore, it is another target molecule that is investigated as a molecular marker in endometriosis disease. FAS-R/FAS-L is expressed throughout the menstrual cycle in endometrial cells of a healthy woman and induces apoptotic cell death [154]. FAS-R/FAS-L analysis was performed on 33 women with severe endometriosis and 18 women without endometriosis. According to the immunohistochemical staining and quantitative gene expression analysis results of this study, FAS-R and FAS-L were stained more intensively during the secretion phase of the menstrual cycle in healthy epithelial cells, while endometriotic epithelial cells showed low staining for Fas-L although Fas receptor staining was found to be high [154]. Despite the increased expression of FAS-R in epithelial cells of women with endometriosis, these cells have been shown to be resistant to apoptosis due to intense inflammation and impaired immune response in the peritoneal environment. Balanced expression of FAS-R/FAS-L in healthy endometrium indicates that the immune system is active, and apoptosis occurs in these tissues [154, 155].

The impaired apoptotic signalling pathway in endometriosis has led to the need to illuminate the relationship between cancer and endometriosis by many researchers. It is known that phosphatidylinositol-3-kinase (PI3K)/AKT pathway inhibits apoptosis in endometrial-derived cancers and PI3K/AKT pathway has an effective role in cell differentiation/growth [156]. Stimulation of this pathway is mediated by the activation of numerous receptors, including the epidermal growth factor receptor (EGFR), insulin-like growth factor 1 receptor (IGFIR), and fibroblast growth factor receptor 2 (FGFR2) [157]. In endometriosis formation, PI3K/AKT activation, as in endometrial cancers, is the result of the loss of PTEN tumor suppressor gene activity or the mutation of PIK3CA encoding the α-catalytic subunit of PI3K [158, 159]. Besides, mutations in AKT and overexpression of these pathway tyrosine kinase receptors play an important role in PI3K/AKT dysregulation [160]. Most of the molecular anomalies associated with endometriosis and endometrial cancers are directly or indirectly related to the PI3K/AKT pathway. The most critical changes by PIK3CA, PTEN and AKT mutations in this pathway and expression of phosphorylated mTOR and phosphorylated AKT (pAKT) are important [161]. When stromal cells from endometriosis patients were compared to that of healthy individuals a high rate of PI3K/AKT was found in the cells of patients. In addition, pAKT was found to be over-expressed in these cells, leading to the development of endometriosis by the silencing the programmed cell death [158, 162, 163, 164, 165, 166]. One of the new approaches on the treatment of endometriosis or endometrial carcinoma is the use of specific inhibitors targeting the PI3K/AKT pathway [158, 162,163, 166].

Another factor affecting the development of endometriosis is the oxidative stress [167, 168]. Oxidative stress causes infertility by negatively affecting ovulation, fertilization, and embryo implantation. Generally, oxidative stress occurs due to low antioxidant levels and the overproduction of reactive oxygen species (ROS), both of which is present during the development of endometriosis [168, 169, 170]. It has been observed that high rates of ROS are synthesized by mononuclear cells and macrophages localized in peritoneal fluids of women with endometriosis. ROS production is regulated by NF-κB transcription factor [171, 172] which is also responsible for the synthesis of proinflammatory cytokines, growth

factors, angiogenic factors, adhesion molecule expression and expression of the inducible nitric oxide synthase (iNOS) and COX-2 [173]. All these products take part in the development of endometriosis by stimulating the adhesion, proliferation and neovascularization of endometrial fragments [174]. Lousse *et al.* found that women with endometriosis had significantly higher NF-$_K$B activity in peritoneal macrophages than the control group [175]. Increased iNOS activity due to NF-$_K$B activity raised the question "the role of nitric oxide in the formation of endometriosis". The abnormally high concentration of nitric oxide produced by active macrophages leads to the occurrence of infertility and endometriosis [176]. High levels of nitrite and nitrate content of peritoneal fluid were seen in patients with endometriosis. Interferon-α and γ activate macrophages in endometriotic peritoneal fluid and increase the nitric oxide production through iNOS. Increased nitric oxide has a cytotoxic effect, which may affect endometrial receptivity and prevent embryo implantation. It also stimulates endometrial angiogenesis by increasing endothelial NOS (eNOS) gene expression, thus accelerating endometriosis development [176]. As a result, oxidative stress caused by increased free radical production and an increased amount of nitric oxide plays an essential role in the pathogenesis of endometriosis.

1.6. THE RELATOINSHIP BETWEEN ENDOMETRIOSIS AND INFERTILITY

Although the pathogenesis of endometriosis has not been fully explained for many years, the relationship between endometriosis and infertility has been demonstrated by different reports [100, 177, 178]. Among the basic data for explaining the association between endometriosis and infertility, anatomic distortion or tubal occlusion formed by adhesions are found. In addition, local infection and altered immune response are explained as the cause of subfertility [179].

Although not all women with endometriosis suffer from infertility, 50% of infertile women have been shown to have endometriosis disease [180]. Endometriosis may trigger various anatomic abnormalities [181]. Accordingly, disruption of the pelvic anatomy, distortion of the fallopian tubes, and destruction of the ovarian tissue by endometriosis might simply lead

to mechanical infertility [180]. Monthly fecundity rate in women with endometriosis (MFR) in other words, the average monthly egg productivity, was shown to be decreased [182, 183, 184, 185, 186]. Animal experiments on baboons with minimal endometriosis reported a 18% lower MFR than the normal baboons. Furthermore, MFR was found to be even lower unless the disease is treated [187]. In a study conducted in Spain, MFR of minimally endometriosis women was found to be a minimum 6% [182] of the healthy women. Studies conducted in Canada, on the other hand indicated a 2.5% in the rate of MFR in women with endometriosis [183, 184] showing the relationship of the disease with infertility. In support of these findings suggesting that women with endometriosis have higher risk of infertility, the Nurses Healthy Study II, published in 2016 revealed that women who were previously diagnosed with endometriosis had twice the risk of infertility compared to women without endometriosis [188].

1.7. TRANSGLUTAMINASES

Transglutaminases (TG1, TG2, TG3, TG4, TG5, TG6 and TG7) are a family of structural and functional enzymes that catalyse Ca^{2+}-dependent posttranslational modification of proteins by forming covalent bonds between the γ-carboxyl amides of proteins and the free amine groups of the peptide-bonded glutamines [189, 190, 191, 192]. Transglutaminases regulate cell-matrix interactions by covalent modifying ECM proteins such as fibronectin and collagen [13, 193, 194], as well as binding to cell surface adhesion molecules including integrins and syndecans cell [195, 196]. Although most members of the transglutaminase family show tissue-specific expression, some exhibit co-expression in various tissues [197, 198].

Numerous types of TGases are found in various organisms ranging from single-celled to plants and mammals [189, 199]. In recent studies, it has been discovered that TGases are also synthesized by microbial cells. For instance, *Streptoverticillium moreens* and *Streptoverticillium laudanum* have been found to synthesize extracellular microbial transglutaminase (MTGase) and intracellular MTGases are synthesized by *Bacillus subtilis*

and *Physarum polycephalum* [200]. One of the main uses in the micro gastronomy area is that they are used as a natural glue to prepare the meat obtained from different types of animals [201]. Apart from this usage, the cross-linking properties of transglutaminase enzymes are utilized in the production of milk and milk products and in the storage of dry foods [202].

In humans, nine different genes that encode TGases have been identified: however, only eight of these gene domains code for catalytically active enzymes [203]. The characteristics, locations and diseases of transglutaminase family members are shown in Table 1.1 [adapted from 189].

Table 1.1. Important characteristics of nine different TGases adapted from Mehta et. al. [189].

Names	Main Tasks	Locations	Diseases	Other Names
TG 1	Cell envelope formation during keratinocyte differentiation	Keratinocytes	Lamellar ichthyosis	TG1, TG_K, Keratinocyte TG, Particulate TG
TG 2	Apoptosis, Cell Adhesion, Matrix stabilization, Cell Survival and Signalling	Ubiquitously expressed in various human tissue	Celiac, Epitheal orgin cancers, Cardiovascular, Neurodegenerative disorders	Tissue TG, TG_C, Liver TG, Endothelial TG, Erythrocyte TG, Ghα
TG 3	Cell envelope formation during keratinocyte differentiation	Hair follicle, Epidermis, brain	Head and neck squamous cell carcinoma and laryngeal carcinoma	TG_E, Callus TG, Hair follicle TG, Bovine Snout TG
TG 4	Reproduction in rodents aiding semen coagulation	Prostate	Prostate cancer	Prostate TG, TG_P, Androgen regulated major secretory protein, vesiculate, dorsal protein prostate 1 (DP1)

TG 5	Cornified cell envelope formation during keratinocyte differentiation	Foreskin keratinocytes, epithelial barrier lining and skeleton muscular striatum	Secondary effect of to the hyperkeratotic phenotype in ichthyosis an in psoriasis	TG_X
TG6	Development of central nervous system, Membrane formation in the epidermis and hair follicles	Testis, lung and brain	Schizophrenia, Damage of central nervous system	TG_Y
TG 7	Unknown	Testis, Lung	Unknown	TG_Z
FXIII a	Wound Healing, Bone Development, Bloot Clotting	Chondrocytes, Platelets Heart, Eyes, Bone	Anemia, Alzheimer (Yamada T., 1998), Obesity (Myneni V.D., 2016)	Fibrin Stabilizing Factor, Plasma TG, Laki- Lorand Factor
Band 4.2	Main Element of Erythrocyte, Skeletal Structure (Pretorius E., 2016)	Membranes of Erythrocyte, Bone Marrow, Spleen	Spherocytic elliptocytosis	B.4.2, ATP binding erythrocyte membrane proteins band 4.2.

As explained in Table 1.1, each member of the transglutaminase has different structural roles and functions within the cell. For example, TGases have the ability of tissue remodeling, maintain membrane integrity, and regulate cell adhesion and signal transduction [204, 205, 206, 194]. In addition to the structural roles of transglutaminases, recent studies have revealed that they play an essential role in the cells by regulating the biological activity of the transforming growth factor-β (TGF-β), IL-2 and midkine signalling molecules in the tissue fibrosis pathway though cross-linking [204]. In addition, TGs catalyses post-translational modification of proteins by primary amine addition and deamidation. As a consequence of the incorporation of TG-catalysed amines into proteins or deamidation of protein substrates, the function, stability, and immunogenicity of substrate proteins may change and result in the development of autoimmune diseases [207]. For instance, amidation of gluten proteins or TG2-dependent deamidation of gliadin A, components of wheat and other grains or contributes to the pathogenesis of celiac disease [208].

All the members of TG family have highly similar gene sequences and organization with well-preserved intron distribution and intron splice sequences (insertion, mutation, deletion), which are encoded by closely related genes [198, 194]. TG2, TG3, TG4 and band 4.2 protein contains 13 exons [209, 210], while Factor XIIIa and TG1 are consists of 15 exons [211, 212 194]. In addition to their similar gene sequences, the primary and three-dimensional protein structure and similarities in the catalytic mechanism of TGs are indicative of their origin from a common ancestor gene [198, 194]. All TGases lack the N-terminal hydrophobic sequence, including Factors XIII and TG1 [213, 189, 214].

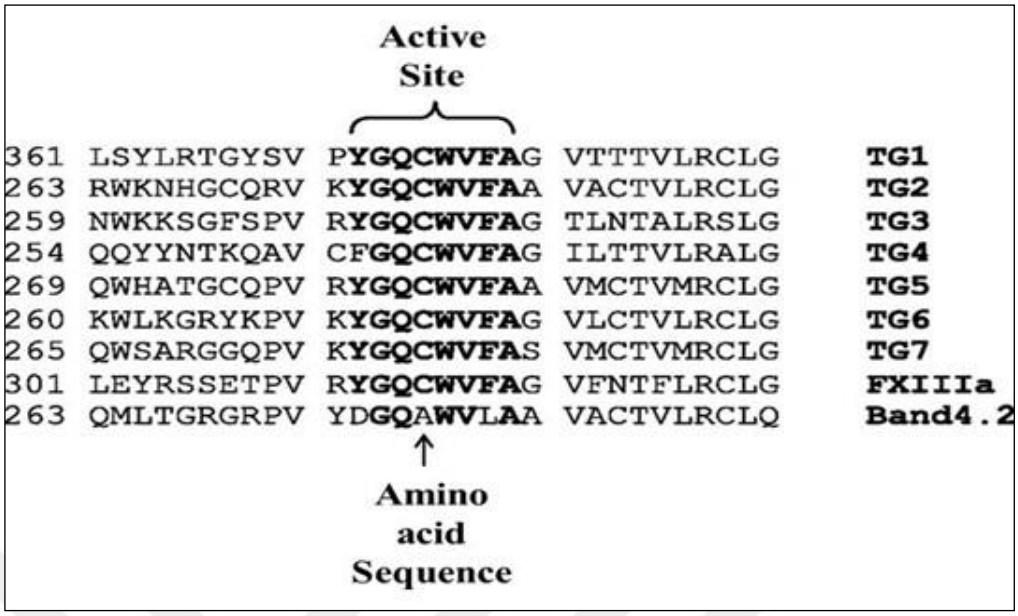

Figure 1.6. Active sites of transglutaminases family members. The cysteine residues in the catalytic region of TGase members are indicated by the arrow (↑) [189].

All members of TGases require calcium for catalytic activity except erythrocyte membrane protein band 4.2 [203] that is catalytically inert and serve as a membrane structural protein. Although the overall structure of the transglutaminase family members varies, they all possess the same amino acid sequence YGQCWVFA in their active site (Figure 1.6), apart from the Band 4.2. [189]. The preserved cysteine residue within YGQCWVFA motif is required for the transamidation activity of TGase members and is replaced with alanine in the catalytically inactive region of Band 4.2. Consequently, the Band 4.2 is the sole transglutaminase member that lacks catalytic activity [189].

1.8. TISSUE TRANSGLUTAMINASE (TG2, TGM2 OR EC 2.3.2.13)

Transglutaminase 2 (TG2, TGM2 or EC 2.3.2.13) is the only member of the nine-membered transglutaminase enzyme family that is expressed in all tissues in human. TG2 is localized on chromosome 20q11-12 with an approximate 37 kb [192]. Human TG2 has a molecular weight of about 78-80 kDa and a sequence of 687 amino acids [215, 216]. In addition to the full length, shorter TG2 isoforms with different properties are produced by the alternative

splicing of *TGM2* gene [217]. A total of four TG2 isoforms have been reported, including TG2-S, TG2-H2, TG2V1, and TG2V2; however, their roles *in vivo* have not been fully identified yet [218]. The main difference between TG2 and its isoforms is that all isoforms contain a specific amino acid sequence at the ends of the C-terminal regions and exhibit high GTPase activity as well as low transamidation activity [218, 219, 189].

The TG2 gene promoter has been shown to contain a retinoic acid response element (RARE), which is localized 1.7 kb upstream of the transcription initiation site, IL-6 specific cis-regulatory element (downstream of the promoter 4 kb), TGF-β1 response element (transcription initiation region 868 bp), and two AP-1 and AP-2 response elements (transcription initiation region 634 bp and above 183 bp), as described in Figure 1.7 [189, 194].

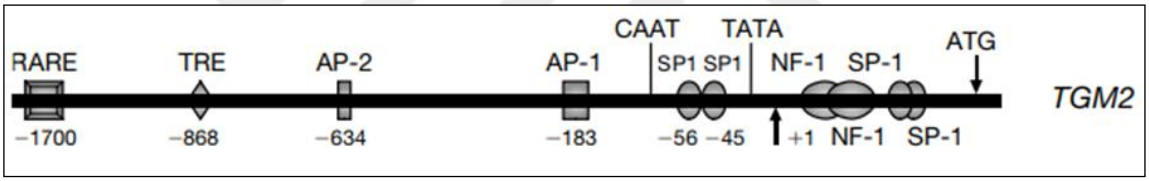

Figure.1.7. The regulatory sequences of the TG2 gene. RARE stands for retinoic acid regulatory element, while TRE stands for TGF β-1 response element (TRE; GAGTTGGTGC), and AP-1 and -2 stand for activator protein-1 and -2. Transcription and translation initiation [189].

The sequence of TG2 was found to have four different SP-1 regions [220, 221]. SP-1 regions contain core DNA binding domains to initiate transcription. TG2 has multifunctional properties due to these specific SP-1 regions, which mediate different molecular pathways for the regulation of TG2 under different cell conditions [221, 206]. Another molecule localized in the transcription initiation site is TGF β-1 (Figure 1.7) [189], which is responsible for regulating TG2 transcription, when cells are exposed to various stress conditions, injury or inflammation [222, 223].

TG2 structurally consists of four different domains. These domains are an NH_2-terminal β-sandwich domain, which contains integrin and fibronectin binding sites, a catalytic triad (Cys277, His335 ve Asp358) for the acyl transfer reaction, and two β-barrels in COOH-terminal, respectively [224, 225, 226]. All these areas were depicted in Figure 1.8 [225].

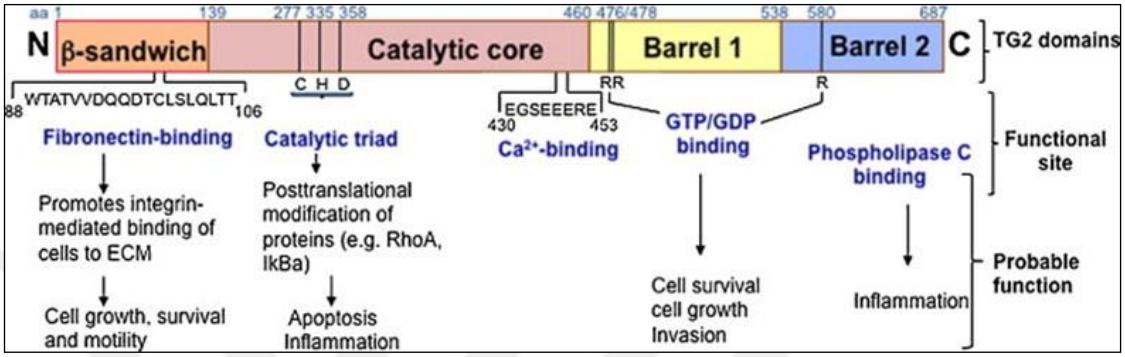

Figure 1.8. The role of the structural and functional domains of TG2 protein in the cell [225].

The N-terminal β-sandwich domain of TG2 possesses a high affinity-binding site for fibronectin and plays a critical role in promoting direct or indirect binding of cells to the ECM [192]. The catalytic domain of TG2 is also responsible for the crosslinking of various cellular proteins by the constitution of highly stable isopeptide bonds [225]. The β1-barrel domain has a GTP/ATP binding region that participates in TG2-mediated signalling pathways [227]. Under certain circumstances (e.g., in GTP-dependent form), the β2-barrel region at the C-terminus can enhance and activate phospholipase C and contribute to the proinflammatory functions of the TG2 protein [228]. In contrast to other transglutaminases, TG2 has a single guanidine nucleotide binding site in the region between the catalytic nucleus and the β-barrel domain, which is encoded by the exon 10 of the TG2 gene. In other transglutaminases, this guanidine nucleotide binding site is homologous and shows poor binding capacity [229, 192]. The conformational change of the four domains in the TG2 structure is related to the interaction with cofactors as presented in Figure 1.8 [225]. The best-known cofactors of TG2 are Ca^{2+} and guanine nucleotides [230, 231, 208]. TG2 activity is regulated by a change in tertiary structure in the presence or absence of Ca^{2+} [232, 233] and as well as its reduction by thioredoxin (Figure 1.9) [194].

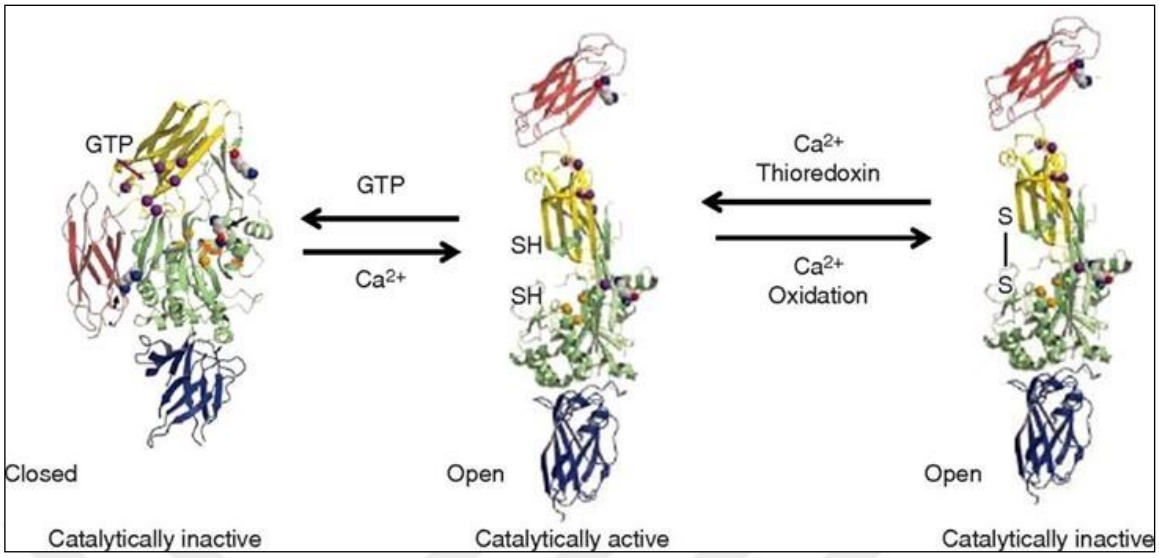

Figure 1.9. The conformational and structural modifications of TG2 due to oxidation or in the presence or absence of Ca 2+. The NH2-terminal area in the figure is indicated in red by the COOH-terminal domain in blue [194].

In the case of calcium binding to the enzyme, the active site of TG2 in the open structure interacts with the substrates. TG2 switches to closed conformation by the binding of guanosine nucleotides (GTP/GDP) to the active site of the enzyme [234, 189, 194] and in this newly formed confirmation, TG2 acts as a GTPase. The GTP/GDP-dependent catalytic domain involved in the transition of TG2 to a closed or compact conformation is controlled by cooperation between the 3rd and 4th domains in the structure of TG2 [235]. This change reduces the availability and activity of the Ca^{+2}-dependent cross-linking region [229]. In contrast, as shown in Figure 1.9, the binding of calcium inactivates the third and fourth domains localized in the β-barrels at the COOH terminal and then shifts the activity to the catalytic core of TG2, the second site. Thus, the catalytic region becomes active and, in that case, TG2 is switched to open conformation [236, 229, 237, 232, 238]. This open configuration is associated with the acyl transfer reaction [232, 238]. However, for TG2 to act as a transamidation enzyme it should not only assume an open confirmation in the presence of Ca^{+2} but also should be reduced at Cys370 and Cys371 by thioredoxin [239]. In that, the oxidation of the open/active conformation causes loss of activity rendering TG2 catalytically inactive although it is in open conformation [240, 241].

The activities and functions regulated by conformational changes of TG2 also affect its location in the cell [242] (Figure 1.10) [243]. TG2 is predominantly a cytosolic protein, yet it is also present in the ECM [244], mitochondria [245], nucleus [246], and on the cell surface. TG2 can serve as a multifunctional cross-linking enzyme with more than 130 intercellular and intracellular substrates [206, 247] as it is the only family member that is secreted and stored in the intercellular matrix [248,249].

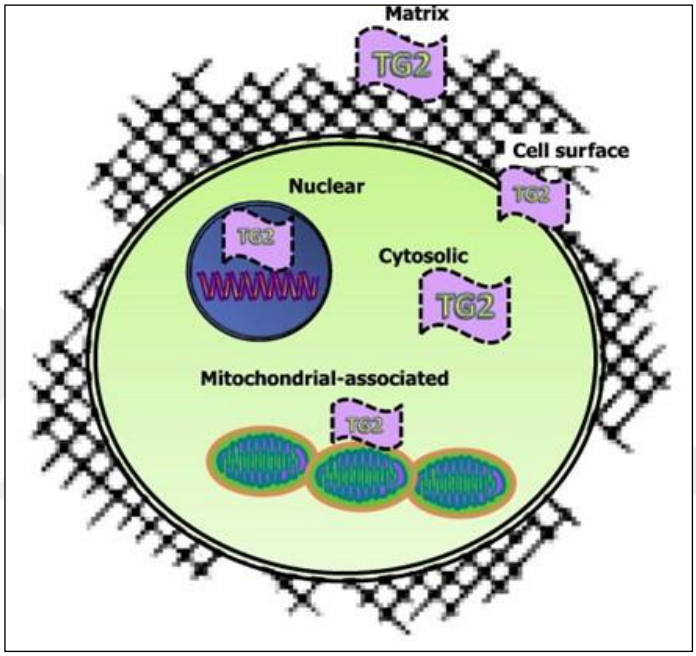

Figure 1.10. Localization of TG2 in cell [243].

The secretion mechanism of TG2 is unusual, since it lacks a signal peptide therefore not secreted through a classical Endoplasmic Reticulum/Golgi-dependent mechanism [195, 196 250]. TG2 secretion is known to require the open conformation of the enzyme [195, 196, 251] and an intact N-terminal FN-binding site [195, 196] however, due to the atypical secretion mechanism, TG2 is not released effectively. Nevertheless, in cellular damage and stress conditions TG2 was shown to be released into the intracellular matrix [252]. Transaminase activity of TG2 plays an important role in extracellular matrix stabilization [253, 254] which is essential in wound healing [255, 256, 257, 254], angiogenesis [258, 259, 254, 260], and bone repair [261, 254]. Transamidation activity takes place in the second step of the cross-linking activity [262, 226, 263]. Cross-linking activity occurs in two parts

(Figure 1.11) [modified from 263]. In the first part, the sulfur atom of the active site cysteine 277 (Cys277) carries out a nucleophilic attack on the γ-carbon of the peptide bound glutamine side chain (acyl donor) and creates a thioester bond between the C277 [262]. Ammonia molecule is formed as a by-product in this step [264, 265, 232, 263]. In the second step, the thioester bond is attacked by the primary amine or water (acyl acceptor). As a result, an intermolecular isopeptide ε- (γ-glutamyl) lysine bond is formed, and TG2 induces internal crosslinking of monomeric protein units [262]. If the reaction group is a primary amine, that is lysine is replaced with low molecular weight amines such as polyamines, this reaction is then called transamidation [262]. Thus, in the presence of high concentration polyamines, such as spermine, TG2 might constitute covalent crosslink in the form of an aduct, such as a dimer between two polypeptide chains or Gln-Gln / Gln-Gly [192]. As a result, an intermolecular isopeptide ε- (γ-glutamyl) lysine bond is formed, and TG2 induces internal crosslinking of monomeric protein units (Figure 1.11) [263].

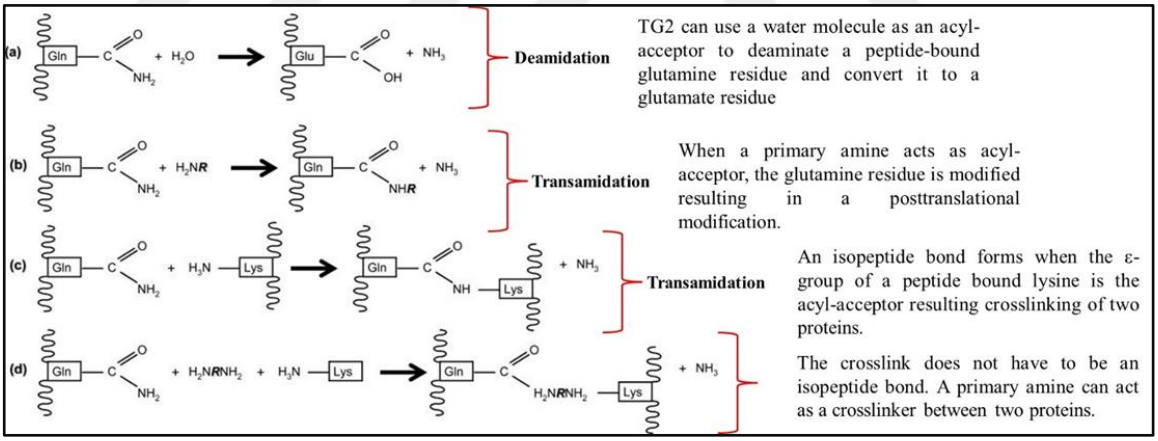

Figure 1.11. Reactions performed by Transglutaminase-2 [modified from 263].

If the attacking group is a water molecule, the reaction is then called deamination [262]. TG2-mediated deamidation reaction is a kind of transamidation reaction in which water acts as nucleophile in the absence of amine co-substrates [266, 238]. The deamidation reaction ends with the conversion of the acyl-transmitting glutamine residue to a glutamate residue as the net result of the reaction [263]. TG2 has the ability to catalyse the deamidation of gliadin-derived peptides, which is formed by digestion of wheat protein gluten contributing

the pathogenesis of celiac disease. In this context, TG2 was reported to be the dominant epitope to activate T cells related to the pathogenesis of celiac disease [267].

In addition to the Ca^{2+}-dependent post-translational modification, TG2 protein can bind and hydrolyse GTP and act like a G protein [268, 207, 235]. For this reason, TG2 can be termed as the bi-functional enzyme. TG2 also acts as a protein disulphide isomerase (PDI) [269,270], a protein kinase [271, 272] and DNA-hydrolyse [273, 207].

1.8.1. Role of TG2 in Cell Process

TG2 plays a role in many cellular processes due to its localization in many places [263], the presence of numerous defined protein substrates [206, 247] and different biological functions [189, 194]. Apoptosis [274, 275], cell survival [276, 277], cell migration-adhesion [13, 278, 279] invasion [280, 281] and drug resistance in cancer cells [276, 277, 282] are some of the biological events in which TG2 was showed to take part in [263].

Initial findings suggested that isopeptide bonds formed by transamination activity of TG2 were functionally important in apoptosis [283, 284, 285]. Following studies showed that TG2 might also be involved in the apoptosis pathway in two different ways, either by acting as a pro-apoptotic or anti-apoptotic protein [286, 284, 192]. In the case where TG2 takes a pro-apoptotic role, aged or damaged cells enter the apoptosis due to its transamidation activity [287, 288]. In damaged cells under stress conditions, the amount of intracellular Ca^{2+} is increased by the endoplasmic reticulum, which leads to the induction of transamination activity of TG2 [289]. The induced transamination activity of TG2 above 1mM Ca^{2+} [192] catalyses the formation of apoptotic bodies around dead cells [287] which results in the phagocytosis of cells [290]. Thereby, TG2 prevents the inflammation by concealing the intracellular content of dying cells in apoptotic bodies [284, 285, 225, 291, 292]. In addition, TG2 transamidation activity triggers programmed cell death (apoptosis) by post-translational modifications of proapoptotic proteins members of the Bcl-2 family such as Bax and Bak. BH3 domain of Bax and Bak has a 70 percent sequence similarity with

TG2 BH3 domain [290]. Through BH3 domain TG2 enzyme can interact with Bax and Bak, which might be advantageous in their mitochondrial localization and proapoptotic activity [290, 292]. Activation of the TG2's cross-linking activity, upon apoptosis induction, leads to TG2-dependent polymerization of these proapoptotic factors on the mitochondrial outer membrane, which increases the rate of mitochondrial membrane potential loss [290]. Also, TG2 mediated post-translational modification of Bax leads to mitochondrial depolarization, mitochondrial outer membrane permeabilization, and the release of cytochrome c [290]. In nucleus, TG2 cross-links and inactivates transcription factor SP-1, which results in caspase-independent cell death. As a result of this reaction, the expression of growth factors such as c-Met and EGF, which are required for the survival of the cells, is reduced [293].

In contrast to the pro-apoptotic pathway, the anti-apoptotic effect of TG2 does not require calcium-dependent transamidation or cross-link activity [294, 225]. The anti-apoptotic activity of TG2 resulting in the survival and proliferation of cells [289] is mainly mediated by the adhesive capability of TG2 in partnership with integrins to fibronectin [279, 295]. Behaving as a cell adhesion protein, TG2 impairs anoikis (detachment-induced apoptosis) that is induced due to the loss of integrin-matrix contact [279]. In addition, TG2 can assume an anti-apoptotic role by binding of cathepsin D and inhibiting its apoptotic activity [296, 289]. On the other hand, in cancer cells, nuclear TG2 interacts with Retinoblastoma protein (pRb) by polymerizing the alpha-inhibiting subunit of nuclear factor-kappa B (NF-κB). As NF-κB is responsible from the transcriptional regulation of some genes involved in the apoptotic pathway, the loss of NF-κB and pRb function due to polymerization helps cells escape from cell death [294, 192].

Previous studies have shown that TG2 plays an essential role in cell survival, drug resistance and invasion mechanisms in cancer cells [297, 298, 299, 300, 276, 277]. For example, overexpression of TG2 in melanoma, breast, kidney, lung and pancreatic cancers was shown to be important in the drug resistance and metastatic profile of these cancer cells [288, 289, 300, 301, 302, 303, 304, 305, 306]. TG2 performs these tasks in the cell by acting as a cell survival protein, stimulating and inducing the focal adhesion kinase (FAK) and its

downstream signal transduction pathways such as PI3-K/Akt and Ras/Erk [13, 304]. It has also been disclosed that the activation of FAK, which plays a crucial role in the cell survival signal pathway, requires TG2 expression [277, 304]. This effect was later on explained by the downregulation of an infamous tumor suppressor protein PTEN, phosphatase and tensin homolog by TG2 [307]. TG2-induced suppression of PTEN via its ubiquitination, results in the activation of FAK and downstream PI3K/AKT survival pathway, which in turn leads to its recognition and phosphorylation by the Src kinase [308]. Once hyperphosphorylated by Src, FAK can activate the PI3K/AKT survival pathway in the downstream and helping cells to escape apoptosis [304, 307]. Finally, another alternative explanation to the cell survival role of TG2 could be the direct interaction between TG2 and PI3K as cells that overexpress TG2 could escape apoptosis induced by the PI3K inhibitor LY294002 [308, 309].

Accumulating evidence suggests that TG2 is directly involved and plays an active role in the regulation of the cell cycle [238]. The first study on the subject is the research conducted by Mian et al. in malignant hamster fibrosarcoma cells in 1995 [310] showing that over-expression of wild type or transamidating activity mutant TG2 disturbs the S to G_2/M phase transition through a process dependent on GTPase activity of TG2. In another study siRNA downregulation of TG2 in endothelial cells caused the cell cycle to be arrested in G_1 due to increased expression of cyclin E and decreased levels of cyclin B [311]. Studies showing the regulatory role of TG2 in cell cycle paved the way for the studies on the role of TG2 in cell proliferation [300]. The overexpression of TG2 in breast cancer and pancreatic cancer cells caused a sharp rise in proliferation of these cells [280, 225, 312] through activation of NF-κB and AKT pathway [304]. As mentioned afore, TG2 has also been shown to reduce the function of phosphatase PTEN, which led to increased activation of the FAK /PI3K-AKT pathway [301, 304, 307, 313]. Von-Hippel-Lin (VHL) is another tumour suppressor whose levels and activity are hindered by TG2 [314]. VHL is part of a ubiquitin ligase complex known for its key regulatory in hypoxia response as well as its hypoxia-independent role to suppress insulin-growth factor-1 (IGF-1R) expression via repressing not only transcription but also mRNA stability [315]. VHL targets hypoxia-inducible factor (HIF) to proteasomal degradation, thereby prevents the expression of genes such as TGFB, VEGF, PDGFR-B and

IGF-1R that are involved in cyst formation and angiogenesis [316]. In both breast and ovarian cancer cell lines, TG2 was found to cross-link and polymerise VHL, which led to the proteasomal degradation of the ubiquitin ligase. This decrease in VHL levels was accompanied by increased levels of angiogenesis-inducing proteins such as IGRF-1R-13, and HIF-1 α as well as increased NF-κB activity resulting in increased cell proliferation [314]. Following studies showed TG2 mediated NF-κB activation in cancer cells caused drug resistance [276, 317, 318]. For example, TG2 mediated activation of NF-κB in ovarian and breast cancer was found to be associated with cisplatin [317] and paclitaxel drug resistance [318], respectively. TG2 was found to trigger NF-κB activation in breast cancer tissue and facilitate its interaction with peroxisome proliferator-activated receptor- γ (PPAR-γ) [319]. As the activity of NF-κB as well as other inflammatory transcriptional factors is inhibited by PPAR-γ [320, 321], the inhibition of PPAR-γ activity resulted in increased NF-κB activation in cancer cells with high TG2 expression [322, 293]. As a result, in these conditions NF-κB activation triggered an increase in cell proliferation and drug resistance [314]. In other words, high levels of TG2 in cancer cells were found to suppress PPAR-γ, thereby increasing NF-κB activation, which conferred cells TG2-mediated-drug resistance [301, 276, 314]. Another protein whom TG2 is associated with in regulation of cell survival anddrug-resistant is nucleophosmin 1 (NPM1). In some types of cancer, especially acute myeloid leukaemia (AML), both TG2 and NPM1 have been overexpressed [292]. In AML, NPM1 over-expression resulted in an increased p53 levels in the nucleus, while decreasing p53 level in the mitochondria [323, 292]. Due to the reduced p53 at the mitochondrial level, the entry of cells into apoptosis has been suppressed, and cell survival have been preserved [323]. There are some studies showing that this effect of NPM1 on p53 is mediated by its polymerization by TG2 [319]. Acting as a TG2 substrate, NPM1 was polymerized and translocated from the cytosol to the mitochondria. Increased levels of NPM1 in mitochondria resulted in suppression of p53 pro-poptotic acivity, conferring cells both drug resistance and increased survivability [319, 323].

1.8.2. TG2 as a Novel Cell Adhesion and Migration Molecule

The first study demonstrating that TG2 may play a role in cell-ECM adhesion and migration was carried out because TG2 overexpressing cells showed resistance to detachment by trypsin [255]. Subsequent studies have supported the role of intracellular TG2 in cell adhesion and migration [254, 324, 257]. In many biological conditions, TG2 acts as a protein responsible for cell adhesion and migration and cell surface [325]. TG2 has assumed these tasks in the cell both though its non-enzymatic adapter/scaffolding property and its cross-linking enzyme activity property [326]. The ability of TG2 to support cell adhesion is mainly due to its co-operation with the two transmembrane proteins, integrins and syndecans, as well as to the modulation of ECM proteins through non-covalent protein-protein interactions [195, 13, 193, 279, 254]. Integrins, sydecans receptors and TG2 are known to interact with FN [254, 324, 327]. In recent studies, it has been shown that TG2 loses its cross-linking enzyme activity upon binding to the extracellular FN and becomes a novel surface adhesion molecule that acts as a co-receptor for integrin and syndecan-4 [327, 328, 329]. Moreover, FN-bound TG2 inhibits anoikis caused by inhibiton of integrin-mediated cell adhesion [279]. Integrins are heterodimers consisting of α and β subunits, which are transmembrane glycoproteins encoded by 18 α and 8 β genes. So far, 24 different αß integrins have been identified [327]. In addition to regulating cell-matrix adhesion by binding to ECM proteins such as FN, collagen, and laminin, integrins support cell-cell adhesion by binding to the surface receptors such as intracellular adhesion molecule (ICAM) and vascular cell adhesion protein (VCAM). While integrin receptors provide a physical linkage between cell surface and matrix proteins via their extracellular domains, they activate the intracellular signalling pathways via their cytosolic domains, through their interactions with the cytoskeleton and kinases [330]. Integrins can be activated either by extracellular ligand binding (outside-in) or upon signals from the cytoskeleton (inside-out). Upon integrin activaiton, FAK and mitogen activated protein kinase (MAPK) pathways can be activated, leading to cell viability and proliferation [331, 332].

Integrins β-1, β-3, and β-5 can non-covalent interact with TG2 on the cell surface [13, 193, 238]. For example, in many different cell types including macrophages 40% of cell surface integrins are in complex with TG2 [13, 333]. In addition to these interactions, cell surface TG2 interacts with FN to form a stable triple complex formation and plays a role in the integrin-mediated cell adhesion (Figure 1.12) [254].

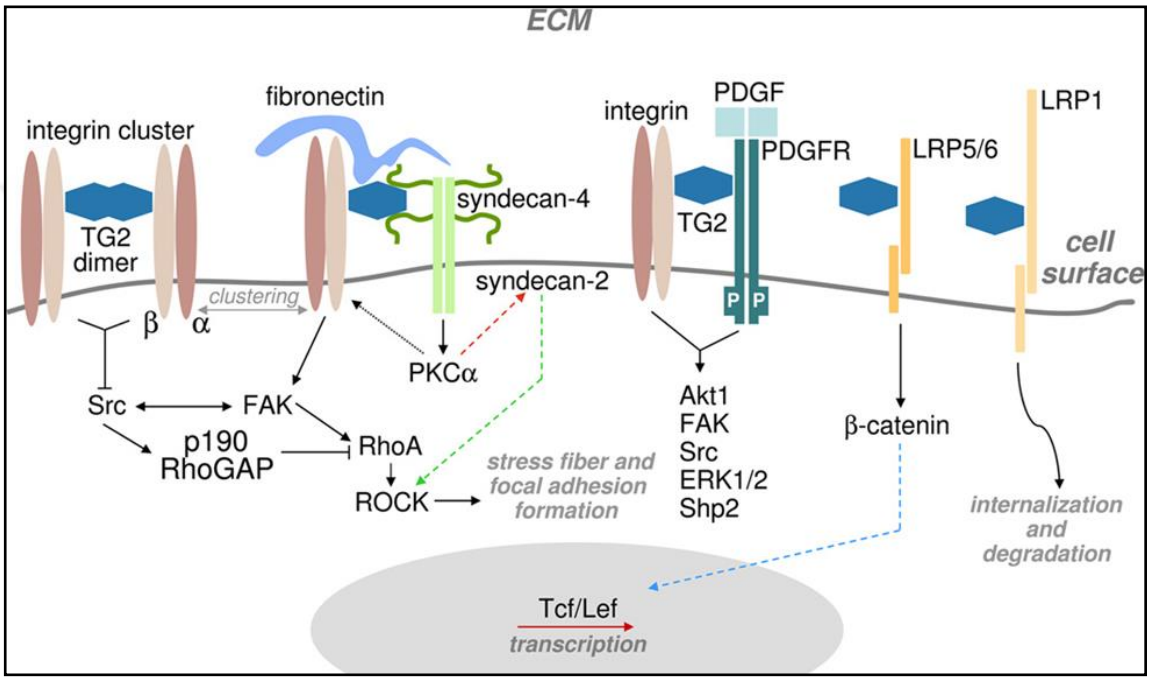

Figure 1.12. Transgulutaminase2-mediated adhesive/signal complexes on the cell surface [254].

Cell surface TG2 increases cell adhesion by acting as a bridge between integrins and FN [13]. On the other hand, it was found that TG2 controls integrin levels in cancer cells leading to increased cell adhesion and migration [281, 334] suggesting that the co-operation between integrins and TG2 can also occur independently of FN [333]. On the cell surface TG2 can induce integrin aggregation even in the absence of integrin-ligand binding [333], though an ill-defined mechanism that may be dependent on the interaction of TG2 with integrin-binding protein caveolin-1 in lipid rafts. Therefore, the observed co-distribution of TG2 and ITGβ-1 in lipid rafts and caveolae [326] is likely not only to enhance the linkage of cell–ECM adhesions in these cholesterol-enriched membrane microdomain but also to affect

membrane protein trafficking and compartmentalization of cell signalling [238]. The association of TG2 with integrins on the cell surface and TG2-mediated integrin aggregation enhances the external signalling triggered by these transmembrane adhesion receptors [254, 326]. Formation of stable complexes between ITGβ-1 and TG2 modulates FAK, src and p190RhoGAP activities, and upregulates the activation levels of RhoA GTPase and its downstream signalling target, ROCK [279, 333]. For this reason, these complexes contribute to increased focal adhesions, stress fibers, and high actomyosin contraction in cells [333]. The FAK, Src and p190RhoGTPase signalling axis is the determinant signalling factors in the induction and regulation of cell migration [335, 336]. There are many studies indicating that the upregulation of TG2 in epithelial cancers including melanomas, breast, lung and pancreas cancers, increases cell migration hence the metastatic potential of the cancer cells [288, 300, 301, 304, 302]. Increased TG2 levels in parallel with integrin ß1 activation resulted in TG2-controlled activation of metastatic behaviour [281, 302, 337].

SDC-4, ubiquitously expressed member of syndecan family, is another transmembrane protein that forms a complex with TG2 to regulate cell adhesion and migration [327, 338] (Figure 1.12). SDCs are the type 1 transmembrane proteins of cell surface heparan sulfate proteoglycan (HSPGs) family with a molecular weight of about 20 to 45 kDa [339, 321]. They are characterized by heparan sulfate and chondroitin sulfate linking sequences at the extracellular N-terminus of single polypeptide chains [340]. SDC-1, SDC-2, SDC-3 and SDC-4 are the four discovered members of SDC family [340] that are expressed in different cell types and have highly conserved single transmembrane domains and short cytoplasmic domains [340]. SDC-1 is localized in epithelial cells and acts as a cell-matrix receptor that binds to various matrix proteins (type I collagen, FN, tenascin) and to members of the fibroblast growth factor (FGF) family [340, 341]. SDC-2 is the main type of syndecan found in mesenchymal cells and in neuronal tissues albeit in co-expression with SDC-3 [340, 342]. SDC-4 is ever-expressed in all tissues and responsible from facilitating the cell adhesion in mature focal adhesions [342]. SDCs are shown to be involved in cell-matrix interaction, cell proliferation, signal transduction, cell adhesion, and migration, and may also provide binding sites for cytoskeleton proteins by recruiting ERM proteins [340, 343].

Although there are nine different types of TGs in mammals, only TG2 is the only family member that contains the conserved heparan sulfate binding site $_{261}$LRRWK$_{265}$ [344, 345, 346, 329]. Owing to this heparan binding site, the formation of a triple complex between the TG2-FN-SDC4 takes place on the cell surface and faciliates cell adhesion [329]. TG2-FN cell adhesion complex induce a SDC4-dependent protein kinase Cα (PKCα) and FAK activation, resulting in the formation of focal adhesions and cell survival signaling in response to matrix fragmentation-mediated integrin blockade [279, 327]. SDC-4 interaction with TG2-FN overcomes the inhibition of ITGB-1 through PKCα signaling, with a subsequent integrin-mediated activation of the FAK leading to an RGD-independent cell adhesion [327]. Besides, a recent study demonstrated that SDC-2 is important to maintain the RGD-independent adhesion of fibroblasts [328] and osteoblasts [324] on TG2-FN by augmenting the downstream signalling and modulating the cytoskeletal organization through the ROCK pathway, without forming a complex with the TG2-FN. These results further demonstrated that FN–TG2–SDC-4 complexes have a significant role in cell adhesion and signalling [345, 346, 347, 348]. SDC-4 interaction with integrin-bound TG2 at the cell surface and/or fibronectin-bound TG2 in the ECM might be necessary for response of tissue to ECM modeling [349, 350]. In this way, increment in TG2 expression during wound healing and tissue remodelling is likely to improve cell adhesion and signalling by increasing integrin activation and assembly of the fibronectin matrix [257, 327, 279, 324]. This may in return promote clustering of TG2 binding partners on the cell surface to improve adhesion, prevent adhesion-mediated apoptosis (anoikis), and facilitate cell survival [279].

1.8.3. The Relationship Between TG2 and Endometriosis

As previously explained in detail, according to Sampson's retrograde menstruation theory, endometriosis may develop as a result of the implantation of living cells (mostly eMSCs) in menstrual blood into the peritoneal cavity [2]. There is no adequate and illuminating study on the investigating the role of TG2 as a cell adhesion protein or enzyme on the migratory potential of these eMSCs which would migrate to a region outside of the uterus.

The first study in literature that associates TG2 with endometrium showed that TG2 enzyme was synthesized 10 times more in the secretive phase of menstrual cycle in women. Here, TG2 removes the aging or deformed endometrial stromal cells from the body by inducing the pro-apoptotic pathway through its cross-linking activity [351]. In an immunohistochemical study on endometrial tissue from horse mares with endometrosis, TG2 levels was found to increase in parallel with MMP-2 [352]. In another animal study in 2009, baboons with/without endometriosis were used [353] to investigate calcitonin hormone (CALC), E-cadherin (E-cad) and TG2 levels on paraffin-embedded formalin fixed tissues obtained at the first, sixth and fifteenth week following the disease formation [353]. Results of the study showed decreased expression of TG2 was in correlation with reduced CALC in ectopic endometrial regions.

Considering the major roles of TG2 in celiac disease, a case study was conducted with Italian patients with endometriosis, and although a potential relevance of the two diseases was found to be possible, the data was not statistically significant [354, 355].

1.9. MATRIX METALLOPROTEINASE

1.9.1. Structure and Function of MMPs

The extracellular matrix is a structure with different types of collagen, protein and proteoglycans, which possess the task of supporting cells and organisms [356]. ECM has a complex structure, which takes part in many biological activities such as cell proliferation, differentiation, adhesion and migration. ECM also acts as a primary barrier to prevent tumor tissue growth and tumor cell proliferation [357, 358]. The relationship between the cell and ECM is regulated by a number of proteolytic enzyme systems responsible for the hydrolysis of ECM components [359]. These enzymes regulate the integrity of the ECM structure and play a critical role in the control of signals generated by the matrix molecules, in the migration, proliferation, differentiation, and apoptosis of cells [359].

ECM degradation seen in various physiological and pathological conditions is performed by four main enzymes groups classified as “cysteine proteases”, “aspartic proteases”, “serine proteases” and “matrix metalloproteases (MMPs)” [360]. MMPs are extracellular proteases, which comprise approximately 28 enzymes playing an important role in the regulation of the cell-matrix composition [361]. MMPs were first described by Jerome Gross and Charles Lapiere in 1962 [362]. In addition, the first compilation article on MMPs was written by Henning Birkedal-Hansen in 1988 [363, 364]. The historical development and illuminated structures of MMPs are given in Table 1.2 [364].

Table 1.2. The structure and illuminated features of the top ten MMPs in history. In addition, the role of MMPs in diseases and the organism in which they were first studied are presented. [364].

Historical Development and Illuminated Structures	**Researchers**
Enzyme degradation of collagen described	Woessner JF
First MMP described	Gross J, and Lapiere CM
MMP-1 purified	Nagai Y
MMP-2 and -3 identified, isolated, and sequenced	Chin JR, Collier IE, Galloway WA, Okada Y, and Woessner JF
MMP-3 as activator of pro-MMP-1	Murphy G
MMP term coined	Okada Y
TIMP-1 and RECK identified as natural MMP inhibitors	Bauer et al. Oh et al, and Sellers et al.
MMP zymogen and mechanism of activation	Chen et al., Milla et al., Rosenblum et al. and Springman et al., among numerous research groups
Crystal structure of collagenase catalytic domain solved	Lovejoy et al.
MMP-7 is the first MMP null mouse generated	Wilson et al.
MMP diversity and expression in human heart failure	Dixon and Spinale and Spinale
MMP diversity and expression in atheromatous plaque	Libby et al.
Plaque rupture and inflammation	Galis et al.
MMP roles in inflammatory and fibrotic responses to myocardial infarction	Lindsey and Zamilpa

All MMPs have a catalytic domain that binds to Zn^{2+} and hence also known as endopeptitases dependent on metal ions [365]. MMPs are secreted in a latent form and activated by separation of the zinc-cysteine bond in their molecular structure [366]. Structural examination of MMPs indicated that they have 5 different domains (Figure 1.13) [367]. These domains: the signal peptide, the propeptide, the Zn-binding region-containing catalyst moiety, the hemopexin-like moiety (which determines the substrate specificity) and the catalyst moiety to the hemopexin-like moiety are proline-rich regions [368]. The first region is a signal peptide sequence, which is defined as predomain, targeting the molecule for secretion, but it is then removed and not found in the latent enzyme [358, 369]. The propeptide region has amino acid structures of 80-90 amino acids and keeps the enzyme in its inactive form by interacting with the catalytic zinc-binding region [369]. Catalytic region consists of 180 amino acids with histidine residues that contain 3 different binding sites for the zinc (Zn^{+2}) ion. The cysteine residue in the propeptide region in inactive MMPs is the fourth binding site for the zinc ion. The catalytic zone consists of 3 alpha helixes and a twisted 5-strand beta layer. The hemopexin-like region ensures the substrate specificity and endogenous inhibitor binding [370].

MMPs are produced by a variety of cell types such as macrophages, neutrophils, endothelial cells, fibroblasts, vascular smooth muscle cells, T-lymphocytes, platelets, chondrocytes, keratinocytes, epithelial cells, mesenchymal cells and osteoblasts [371, 372, 373]. Specific tissue inhibitors (tissue inhibitor of matrix metalloproteinase, TIMP) play a significant role in the regulation of MMP activity [374]. TIMPs are specific MMP inhibitors in the tissue, whereas alpha-2 macroglobulin is the MMP inhibitor in serum [375, 376].

There is a stable balance between MMP activity and their specific endogenous tissue inhibitors in maintaining the tissue homeostasis [377]. The shift in the direction of MMP activity leads to the destruction of the matrix and ultimately to pathophysiological events such as failed wound healing, ulcers and tendon degeneration [378, 379, 380]. MMPs take considerable part in the pathophysiology of various diseases (Table 1.3.) including

rheumatoid arthritis, osteoporosis, multiple sclerosis, emphysema, nephritis and liver fibrosis, particularly cancer, atherosclerosis as well as endometriosis [38, 381, 382].

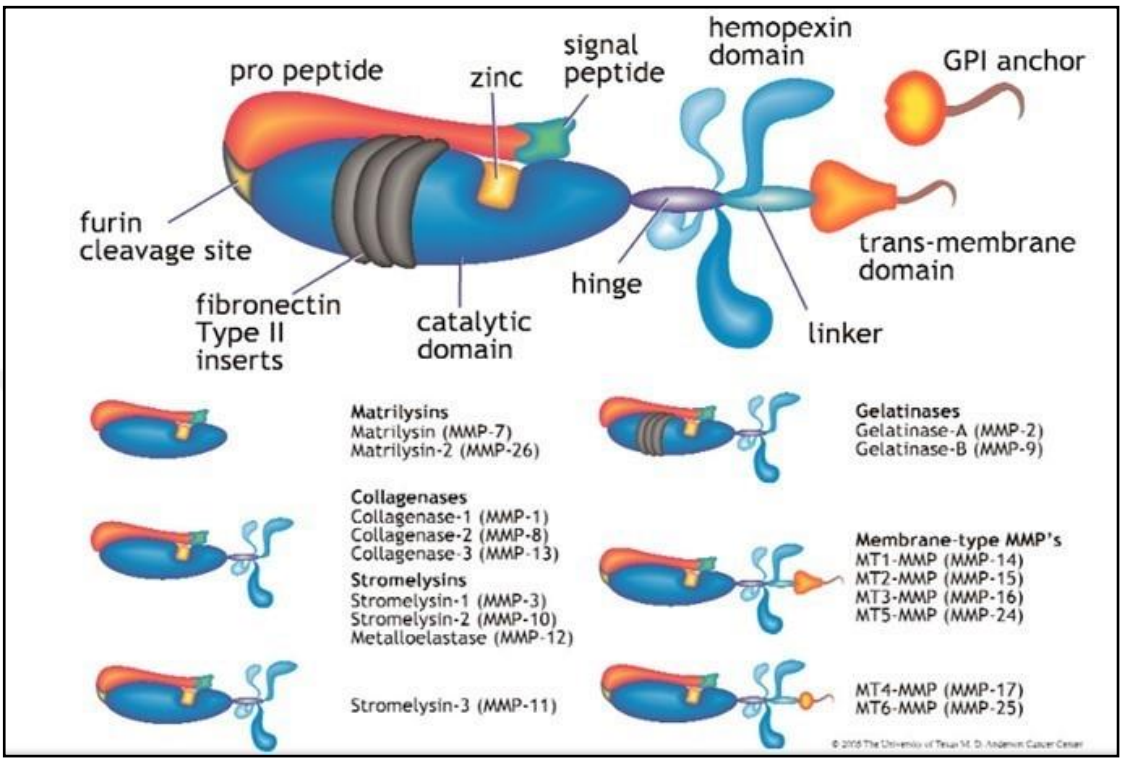

Figure 1.13. The main structural domains of MMPs are schematized [367].

Table 1.3. Expression of different types of MMPs in different cancer types and other diseases

Different types of MMPs	**Types of Cancer**	**Other Diseases**
Collagenase (MMP-1, -8, -13)	• Breast cancer	• Atherosclerosis • Rheumatoid arthritis
Gelatinases (MMP-2, -9)	• Breast Cancer, • Colorectal Cancer, • Lung cancer, • Ovarian cancer, • Malignant glioma	• Bronchiectasis, • Chronic asthma, • Chronic obstructive pulmonary disease, • Cystic fibrosis, • HIV-related dementia, • The hypertension
Stromelysins (MMP-7)	• Pancreatic ductal adeno Carsinoma • Colorectal cancer	• Chronic obstructive pulmonary disease
Membrane type MMP (MMP-14)	• Breast cancer	• Preeclampsia

According to difference in their structure and substrate specificities MMPs were initially classified into 6 groups such as collagenases, stromelysins, gelatinases, matrilysins, membrane type MMPs (MT-MMP), and finally unclassified MMPs [383, 384]. However, different types of MMPs have been rapidly discovered in the last few years and the number of newly discovered metalloproteinases has gradually increased to 26 members. Figure 1.14 demonstrates the classification and substrates of twenty-six different MMP enzyme constructs [384].

MMP	Name of class	Enzyme	EC No.	Substrate	Chromosome location (human)
MMP-1	Collagenases	Collagenase-1	EC 3.4.24.7	Collagens (I-III, VII, VIII, and X), gelatin, aggrecan, L-selectin, IL-1β, proteoglycans, entactin, ovostatin, MMP-2, and MMP-9	11q22-q23
MMP-8	Collagenases	Collagenase-2/ neutrophil collagenase	EC 3.4.24.34	Collagens (I-III, V, VII, VIII, and X), gelatin, aggrecan, and fibronectin	11q21-q22
MMP-13	Collagenases	Collagenase-3	13 EC 3.4.24.B4 (preliminary BRENDA-supplied EC number)	Collagens (I-IV, IX, X, and XIV), gelatin, plasminogen, aggrecan, perlecan, fibronectin, osteonectin, and MMP-9	11q22.3
MMP-18	Collagenases	Collagenase-4		Type I collagen	
MMP-2	Gelatinases	Gelatinase-A	EC 3.4.24. 24	Gelatin, collagen IV-VI and X, elastin, and fibronectin	16q13
MMP-9	Gelatinases	Gelatinase-A	EC 3.4.24.35	Collagens (IV, V, VII, X, and XIV), gelatin, entactin, aggrecan, elastin, fibronectin, osteonectin, plasminogen, MBP, and IL-1β	
MMP-3	Stromelysins	Stromelysin-1	EC 3.4.24.17	Collagens (III-V and IX), gelatin, aggrecan, perlecan, decorin, laminin, elastin, casein, osteonectin, ovostatin, entactin, plasminogen, MBP, IL-1β, MMP-2/TIMP-2, MMP-7, MMP-8, MMP-9, and MMP-13	11q23
MMP-10	Stromelysins	Stromelysin-2	EC 3.4.24.22	Collagens (III-V), gelatin, casein, aggrecan, elastin, MMP-1, and MMP-8	11q22.3-q23
MMP-11	Stromelysins	Stromelysin-3		Unknown (casein)	22q11.2
MMP-17	Stromelysins	Homology tostromelysin-2 (51.6%)			
MMP-7	Matrilysins	Matrilysin (PUMP)	EC 3.4.24.23	Collagens (IV, X), gelatin, aggrecan, decorin, fibronectin, laminin, elastin, casein, transferrin, plasminogen, MBP, β4-integrin, MMP-1, MMP-2, MMP-9, and MMP-9/TIMP-1	11q21-q22
MMP-26	Matrilysins	Matrilysin-2		Collagen IV, fibronectin, fibrinogen, gelatin, α (1)-proteinase inhibitor	11p15
MMP-14	MT-MMP	MT1-MMP (membrane type)	EC 3.4.24.80	Collagens (I-III), gelatin, casein, fibronectin, laminin, vitronectin, laminin, vitronectin, entactin, proteoglycans, MMP-2, and MMP-13	14q11-q12
MMP-15	MT-MMP	MT2-MMP		Fibronectin, entactin, laminin, aggrecan, perlecan, and MMP-2	16q13-q21
MMP-16	MT-MMP	MT3-MMP		Collagen III, gelatin, casein, fibronectin, and MMP-2	8q21
MMP-17	MT-MMP	MT4-MMP			12q24.3
MMP-24	MT-MMP	MT5-MMP		Fibronectin, but not collagen type I or laminin	20q11.2
MMP-25	MT-MMP	MT6-MMP		Progelatinase A	16p13.3
MMP-12	Other enzymes	Macrophage metalloelastase	EC 3.4.24.65	Collagen IV, gelatin, elastin, casein, fibronectin, vitronectin, laminin, entactin, MBP, fibrinogen, fibrin, and plasminogen	11q22.2-q22.3
MMP-19	Other enzymes	RASI-1		Type I collagen	12q14
MMP-20	Other enzymes	Enamelysin		Amelogenin, aggrecan, COMP	11q22.3
MMP-21	Other enzymes	MMP identified on chromosome 1			
MMP-22	Other enzymes	MMP identified on chromosome 1			11q24
MMP-23	Other enzymes	From human ovary cDNA			1p36.3
MMP-28	Other enzymes	Epilysin			17q11.2
MMP-29		Unnamed			

MT-MMP=Membrane type-matrix metalloproteinase, MBP=Myelin basic protein, IL=Interleukin, COMP=Cartilage oligomeric matrix protein

Figure 1.14. In this table, MMP enzymes substrates, enzyme conventions are named according to International Biochemistry Association and their locations in chromosomes are explained [384].

The discovery of metalloproteinases by different research groups has led to a very complex naming system, so each member of the MMP family has been named with more than one name. The International Association of Biochemistry and Molecular Biology has proposed to give specific enzyme numbers (E.C.3.24. X) and number nomenclature for MMP [384]. Interstitial collagenase (MMP 1, Fibroblast collagenase) is prototypic member of the MMP family. The latent form is around 55 kDa and the active form is around 43 kDa [386]. MMP

1 digests Type I, Type II and Type III interstitial collagen found in basement membrane [387]. Collagen types V that is essential for the assembly of collagen fibrils and collagen X that is important for bone and cartilage development are also substrates for MMP-1 [388]. Neutrophil collagenase (MMP 8) has 75 kDa of molecular weight as a proenzyme and 58 kDa as an active enzyme and produced by neutrophils. Gelatine, aggrecan and fibronectin is digested by MMP-8 [389]. Neutrophil collagenase has a crucial task in the connective tissue turnover that accompanies inflammatory processes [390]. In addition, MMP-8 was found to be extremely active in ultraviolet-irradiated dermal fibroblasts [391]. Collagenase 3 or MMP-13 enzyme breaks down Type I collagen. Gelatinase A or MMP-2 has 72 kDa of latent form and the active form is about 66 kDa [392]. The MMP 2 enzyme cleaves type IV collagen, gelatin, as well as type VII, X, collagen, elastin and FN [390]. Gelatinase B or MMP-9 has 92kDa of molecular weight. This enzyme is substrate-specificity for gelatin and type IV basement membrane collagen. The active form of MMP-9 is 84 kDa [392]. Other substrates for MMP-9 are type I, III, V collagen, elastin and FN. Fbronectin type II repeats found in the catalytic domain of these gelatinases enable the binding of these enzymes to be denatured collagens. Stromelysin 1 or MMP-3 has 57 kDa of latent form and active form is 46 kDa. Stromelysin substrates are respectively; proteoglycans, laminin, FN, type III, IV, V, IX, collagen and gelatins [393]. Matrilysin (MMP-7, Putative matrix metalloproteinase 1, PUMP 1) has a latent form of 28 kDa, and an active form of 19 kDa [394]. It is known as a subgroup of stromelysins in the metalloproteinase family. MMP-7 has substrate specificity for gelatin, elastin, FN, and laminin [395]. MMP-7 is the simplest MMP consisting of three regions including catalytic, zinc-binding region, and the propeptide. In addition to these three regions, collagenases and stromelysins contain a hemopexin-like area bound to the catalytic site through a bridge region [396]. Hemopexin-like region allows MMPs to bind to other proteins such as integrins, cell surface receptors, and tissue inhibitors [397]. Membrane-type MMPs (MT-MMP) contain a catalytic, hinge, and hemopexin-like domain adjacent either to a transmembrane domain or a glycosylphosphatidylinositol-linker domain in their structures. Therefore, MT-MMPs bind to the cell surface either with this transmembrane region or with glycosylphosphatidylinositol hooks [367, 398]. Besides, furin recognition sequences located

between propeptides and catalysis domain of MT-MMPs is responsible for intracellular activation of proenzymes [399].

Since MMPs interact with integrins and other cell receptors and also over-expressed in cancer cells similar to TG2, it is desirable to explain the relationship between TG2-(MT)-MMP. MT-MMPs are involved in ECM degradation hence regulates cell adhesion, migration, and invasion [400]. Cell surface TG2 was shown to be proteolytically cleaved by MT1-MMP overexpressed in fibrosarcoma and glioma cells while purified guinea pig liver TG2 was identified as a substrate for MT1-MMP, MT2-MMP, and MT3-MMPs [401]. The resulting suppression of TG2-mediated cell adhesion and migration due to the proteolytic degradation of TG2 by MT1-MMP can be reversed by purified FN or cell-surface FN in association by TG2. Therefore, the interaction between the cell surface protein fibronectin and TG2 has been shown to confer resistance to proteolytic degradation by MT1-MMP and promote cell adhesion and migration [401]. MT1-MMP is also known to be proteolytic activator of MMP-2 and act together to target cell surface TG2. However, by associating with intermediate form of MMP-2, TG2 can limit the maturation of this enzyme hence protect itself from proteolytic degradation by MMP-2 [402]. In other words, this association determines the maturation rate of MMP-2 and protects TG2 against proteolysis [403, 401]. In a follow-up study, overexpression TG2 in epithelial ovarian cancer was found to upregulate the expression and activation of MMP-2 in transcriptional level by increasing the CREB recruitment to MMP-2 promoter region leading to enhanced tissue invasiveness [404].

1.9.2. Role of MMPs in Development of Endometriosis

Endometriosis is defined as the presence of endometrial tissue, in other words, the presence of glandular epithelium and stroma in ectopic sites. Histologically, endometriosis is the growth of the endometrium outside the uterine cavity [405]. Endometrial tissue should undergo some cyclic changes for the growth, displacement, and diffusion of the peritoneal cavity, except for the uterine cavity. Therefore, the pathogenesis of endometriosis requires

the adhesion of endometrial fragments to the peritoneal surfaces and subsequent remodelling, which requires the activation of MMPs [406]. The endometrium is the only tissue exposed to constant cyclic transformations in the female body. The function of hormones, especially estrogen and progesterone, is significant for the proper course of such cyclic transformations. Hormonal changes and release affect the activity of both MMPs, and their tissue inhibitors known as tissue inhibitors of metalloproteinases (TIMPs). The course of endometrial transformation, proliferation, secretion of secretions, exfoliation, and finally re-growth and the coordination of such processes depend directly on MMPs and their inhibitors. There is a dozen of different MMPs, and their expression is affected by sex hormones.

Abnormal expression of MMPs is associated with invasive and destructive diseases [407]. The bioactivity, proliferation, and differentiation of endometrial cells as well as transformation of decidual cells are regulated by MMPs [408]. As MMPs play an active role in the reshaping and structuring of the endometrium under estrogen stimulation, the expression of various MMPs in the female endometrium is different throughout the menstrual cycle. While most MMPs remain undetectable in the proliferative or latent phase of menstrual cycle, their expressions are increased to maximum level during the bleeding phase. The expression of some other MMPs remains constant throughout the entire menstrual cycle [410]. The endometrial tissue dynamics, which is destroyed and reformed by menstrual cycle every month, are maintained through MMP activation [409, 410].

Most MMPs are under the influence of estrogen and activated by it, while they are suppressed by progesterone. Estrogen takes part in the development and proliferation of endometriosis through activation of various biochemical pathways in the formation of endometrial tissue. MMPs responsible from the breakdown of ECM in healthy endometrial tissue help regulate normal endometrial destruction and estrogen-stimulated regrowth [410]. Similar to the process of cancerization, MMPs are highly expressed during the development of endometriosis conferring an invasive potential to the spilled endometrial tissue, thus favouring the progression of the disease [410]. Owing to the ongoing MMP activity in the

spilled endometrial cells, these cells can easily be refluxed on the peritoneal surface and their invasion and proliferation can be facilitated. [411]. Furthermore, in women with endometriosis, secretory endometrial MMP expression is unexpectedly resistant to progesterone suppression [411].

1.10. AIM OF THE STUDY

The theory that explains the pathogenesis of endometriosis by the notion of the reflux of endometrial cells from the tubes during menstruation and their attachment to peritoneum and organs in the abdomen [2, 412] can be linked to the increase in integrin and TG2 expressions in these cells. Walter et al have detected an increase in TG2 enzyme parallel to an increase in MMP-2 in an immunohistochemical study conducted with horses; yet, a role for TG2 in development of endometriosis or a correlation of the increase in MMP-2 level to the presence of TG2 were not shown in the mentioned study [352].

Our hypothesis is that TG2 protein loses its cross-linking activity and acts as an adhesion molecule, being expressed in high levels together with integrin and syndecan-4 in endometriotic tissues. Focusing on this idea, we aim to investigate the role of TG2 in development of endometriosis with a molecular approach using eMSCs isolated from healthy and diseased women. In this respect, the effects of TG2 on adhesion and migration of eMSCs were studied using shRNA technology. An idea is that, using the same techniques, regulation of MMPs - the major protease that degrades the ECM were controlled via TG2 enzyme activity, and development of endometriosis could be prevented by these means. In case our hypothesis is experimentally supported, a probability was revealed such as the inhibitors that are currently in phase studies for cancers can also be used to prevent endometriosis. A potential of such treatment is important for the prevention of the damages arising from complications in a medical surgery.

2. MATERIALS

2.1. INSTRUMENTS

CO2 incubator (In-Vitro Cell ES NU-5800, NuAire, USA), Laminar flow cabinet (ESCO Labculture Class II Biohazard Safety Cabinet, Singapore), Centrifuge (MICRO 22R, Hettich, Germany), Centrifuge (Sigma 2-5, England), Carl Zeiss PrimoVert Microscopy with Axio Cam 105 colour (GmbH 37081, Göttingen, Germany), Flourescence Microscope (Nikon 80i Eclipse Fluorescence Microscope), 80 °C freezer (Thermo Forma -86 C ULT Freezer, USA), pH meter (Hanna instruments PH211, Germany), Vortex (Stuart SA8, UK), Magnetic Stirrer (Heidolph MR 3004, Germany), Heater (Bioer, MB102, China), ELISA Plate reader (Bio-Tek, USA), Mini-PROTEAN Tetra Cell Electrophoresis System (Bio-Rad, USA), Mini Trans-Blot Cell Blotting System (Bio-Rad, USA), ChemiDOC XRS+Gel Imaging System (Bio-Rad, USA), CFX96 Touch Real-Time PCR (Bio-Rad 1855195, USA), FACS Calibur (BD Biosciences, USA), Cytell Cell Imaging System (GE Healthcare, USA).

2.2. EQUIPMENTS

Falcon tubes (15 mL, 50 mL Isolab, Germany), Polypropylene eppendorf tubes (2mL, 1.5 mL, Germany), Electronic pipette (CAPP aid, Denmark), Micropipettes (10µL, 20µL, 100µL, 200µL, 1000µL, Thermo Scientific, USA), Serological pipettes (2 mL, 5 mL, 10mL, 25mL, SPL Life Sciences, USA), Cell culture flasks (T-25, T-75, T-150), cell culture plates and cryovials (TPP Switzerland, Germany), Filter 0.22 µm (TPP, Switzerland), 0.45 µm (Biotech, Germany), Ultra-Low Attachment 24-Well Plate Polystrene, Flat Botrom (Corning-Costar,CLS 3473, USA), Ultra-Low Attachment 96-Well Plate Polystrene, Flat Botrom (Corning-Costar,CLS 3474, USA), Cover Slip (Sigma Aldrich, USA), Bright-Line Hemacytometer (Sigma Aldrich, USA), Graduated Cylinder (50 mL, 250 mL, 500 mL, 1000 mL Isolab, Germany), Whatman Paper (Isolab, Germany), Amersham Hybond- ECL Nitrocellulose Membrane (GE Healthcare, USA), Amersham Rainbow Protein Marker (GE

Healthcare, USA), PVDF membrane 0.45 µm (ThermoFisher Scientific, USA), Corning® BioCoat™ Matrigel® Invasion Chamber, 8.0 µm PET Membrane 24-well Permeable (Corning® BioCoat, 354480, USA).

2.3. CHEMICALS

2.3.1. Cell Line

Endometrial stem cells isolated from healthy and endometriosis patient endometrium by İnci Kurt Celep was used in this study until the passage number 5.

2.3.2. Cell Culture Media

Dulbecco's Modified Eagle Medium low glucose (1x DMEM, 1000 mg/L Glucose, L-glutamine, sodium (Gibco 31885-023, Thermo Fisher).

2.3.3. Growth Supplements

MEM Non-essential amino acid 100x (INVITROGEN / 11140-035), Heat Inactivated Fetal Bovine Serum (FBS) (Gibco 10500-056, Thermo Fisher), Penicilin Steptomycin (Gibco 15140-122, Thermo Fisher Scientific, USA), L-Glutamine (Sigma Aldrich G-7513).

2.3.4. Other Reagents

2-Propanol (AppliChem A3928, Germany), Absolute Ethanol (AppliChem A3928, Germany), Acrylamide/ Bis-acrylamide (29:1) (Sigma A3574, USA), Ammonium Persulfate (APS) (BioRad, 1610700, USA), Bovine Serum Albumin (Santa Cruz, sc-2323, USA), Collagen Type-I from Human Placenta (Sigma C7774, USA), Dimethyl sulfoxide (Santa Cruz sc-202581, USA), Dulbecco's Phosphate Buffered Saline (DPBS) (PAN Biotech P04-

53500, Germany), Ethylenediaminetetraacetic acid (EDTA) (Merck, K40173218 946, Germany), Methanol 99 percent (Sigma, 34885, USA), DPBS (10X) (Lonza, BE17-517Q, Belgium), Phenylmethanesulfonylfluoride (PMSF) (Sigma 78830, USA), Protease Inhibitor (PI) (Sigma, P8340, USA), Protein Assay Reagent A (BioRad, 5000113), Protein Assay Reagent B (BioRad, 5000114), Puromycin dihidrochloride (Santa Cruz, sc-108071), Polybrene (Santa Cruz, sc-134220), Sodium orthovanadate (Na3VO4) (Sigma, S6508, USA), Sodium orthovanadate (Na3VO4), N,N,N′,N′-Tetramethylethylenediamine (TEMED) (Sigma, T7024, USA), Tris-base (Merck 108387), Tris-HCl (Merck 108219), Triton-100X (Biomatik Corporation, A4025), Trizol (Invitrogen, 15596-018), Tween-20 (Merck, 822184), Trypan Blue (0. 4 percent) (Sigma-Aldrich, T8154), 0.05 percent Trypsin (Lonza, BE02-007E, Belgium), WST-1 Cell Proliferation (13489900, Roche, Germany)

2.4. KITS AND SOLUTIONS

Bovine Serum Albumin, Protein (Sigma P0834, USA), ClarityTM Western ECL Substrate, (BioRad, 1705061, USA), EMSA LightShift Optimization Kit (QF219950, Thermo Scientific, USA), RIPA Lysis Buffer (Santa Cruz sc-24948, USA), QuantiTect SYBR Green PCR Kit (Qiagen, 204145, USA), Sensiscript RT Kit (Qiagen, 205213, USA), Peq-Gold Ultra Competent Kit (Agilent technologies), Hs_MMP9_1_SG QuantiTect Primer Assay (208679794, USA), Hs_MMP2_1_SG QuantiTect Primer Assay (208679792, USA), Hs_TGM2_1_SG QuantiTect Primer Assay (202689401, USA), Reagent G Cytell Cell Cycle Kit (GE Healthcare Life Sciences 29-0574-98).

2.5. ANTIBODIES

2.5.1. Primary Antibodies

Mouse-anti-TG2 Antibody (ThermoFisher Scientific, Labvision Cub 7402, MS-224-P, USA), Monoclonal mouse anti-β-Actin antibody (Sigma, USA), Monoclonal mouse anti-

Integrin β1 Antibody (Santa Cruz, sc-8978, USA), Anti-Syndecan 4 antibody (Abcam, ab24511, USA), CDK-2 (CST 2546S, USA), CDK-4 (CST 12790S, USA), Cyclin D3 (CST 2936S, USA), Cyclin E1 (CST 4129S, USA), CyclinD1 (CST 2978S, USA), p27Kip1 (CST3686S, USA), Mouse Anti-mouse CD11b Flow Antibody (B192967, Biolegend, USA), Anti-mouse Sca-1 Flow Antibody (B163257, Biolegend, USA), Anti-mouse CD44 Flow Antibody (B193068, Biolegend, USA), Anti-mouse CD45 Flow Antibody (B187805, Biolegend, USA), Anti-mouse CD73 Flow Antibody (B182619, Biolegend, USA), Anti-mouse CD29 Flow Antibody (B181560, Biolegend, USA), Anti-mouse CD105 Flow Antibody (B178443, Biolegend, USA), Normal mouse IgG FITC sc-2855 (Santa Cruz Biotechnology).

2.5.2. Secondary Antibodies

Anti-rabbit IgG Peroxidase (Sigma A0545) and anti- mouse IgG Peroxidase (Sigma A4416) Conjugates, Normal, Mouse IgG (Santa Cruz Biotechnology sc-2025, USA), Normal Rabbit IgG (Santa Cruz Biotechnology sc-2027, USA).

3. METHODS

3.1. ETHICS COMMITTEE DECISION FOR THE ISOLATION OF ENDOMETRIAL MESENCHYMAL STEM CELLS FROM EUTOPIC AND ECTOPIC ENDOMETRIUM

All isolated cells used in our experiments were isolated from the tissue samples of patients diagnosed with endometriosis and healthy volunteers. Patients and healthy volunteers were enrolled to the study in accordance with the Declaration of Helsinki. The study was approved by the Ethics Committee of Yeditepe University Human Ethical Committee. The ethics committee certificate (Decision No: 63/509) obtained from The Ethics Committee of Yeditepe University Human Ethics Committee has been published as an original copy on the last page of the thesis.

3.2. ESTABLISHMENT OF EXPERIMENT GROUPS

Five groups were constituted for this study in order to maintain statistical significance of all experiments. Each group was comprised of mesenchymal stem cells (MSCs) isolated from two different samples of endometrium tissues, one taken from healthy individuals (heMSCs), and the other from patients (peMSCs) diagnosed with endometriosis, for comparative purposes.

Certain criteria were set for the collection of endometrial tissues both in healthy and patient groups. For both healthy and patient samples, women showing menorrhagia, menometrorrhagia symptoms or were pregnant or breastfeeding in the previous six months were excluded from the study. None of the women included in the study received hormonal treatment in the previous three months. Fertile women under 49 years of age without endometrial polyps in the uterus, or endometrial hyperplasia or endometrial cancer and submucosal myoma and who were not diagnosed with endometriosis were included in the control (healthy) study group. Endometrial tissues were taken from the endometrial wall of

these women who had undergone laparoscopy for tubal sterilization. Surgical excision biopsies of endometrium tissue were collected by Dr. Melike Batukan and Prof. Dr. Rukset Attar. The absence of endometriotic lesions was confirmed in healthy volunteers by comprehensive laparoscopic evaluation and pathologic examination [413].

Patient samples were voluntarily collected from women under the age of 49 with confirmed diagnosis of moderate or severe endometriosis according to American Society for Reproductive Medicine (ASRM) classification system. The patients were selected from clinical cases with ultrasonography findings and later, confirmed by laparoscopic surgery. During the laparoscopic surgery, patients were undergone abdominal cavity examination and total endometriotic tissue excision that was sent to histopathological examination for the confirmation of endometriosis diagnosis. Women with other pathological diseases other than endometriosis, which may affect the results were not included in the study [413].

3.3. CELL CULTURE

Two different methods were applied for the isolation of adult mesenchymal cells from the human endometrial wall and endometriosis tissue. The first one was a nonenzymatic method, and the other was the enzymatic method performed with trypsin.

3.3.1. Non-Enzymatic Isolation of Mesenchymal Stem Cells

As stated above, the tissue biopsy samples in physiological saline solution were transferred to our laboratory and then rinsed trice with PBS pH 7.4 including 3 percent (v/v) penicillin/streptomycin. Following another set of washed with serum-free DMEM tissue biopsy samples were minced into 1-2 mm^2 pieces with the help of scalpel. The minced tissue samples were then centrifuged at 500xg for 5 minutes in 10 mL of serum-free DMEM containing 100 IU/mL penicillin, 100μg/mL streptomycin and the supernatant was discarded. The pellet was transferred to a 60 mm petri dish, and a coverslip was placed onto the pellet. The cells were grown in low glucose (1g/L) DMEM containing 20 percent (v/v)

Fetal Bovine Serum (FBS), 100 IU/mL penicillin, 100 μg/mL streptomycin at 37ºC and 5 percent CO_2-humidified air for 5 days [414, 415, 416]. At the end of the fifth day, minced tissue together with cover slip was removed, cell monolayer dispersed from tissue pieces was cultured in fresh low glucose DMEM containing 20 percent FBS, 100 IU/mL penicillin, 100 μg/mL streptomycin and 1 percent nonessential amino acid (NEAA).

3.3.2. Cell Growth and Maintenance Conditions

The mesenchymal cells isolated from endometrial tissues of healthy and patient women were grown with optimized cell culture media, as previously described [415]. This medium was composed of 20 percent (v/v) inactive FBS, 100 IU / mL penicillin, 100 μg/mL streptomycin and 1 percent NEAA, added in freshly prepared low glucose DMEM (500 mL), and stored at +4ºC until further use. The growing step of all isolated cells were carried out with incubation at 37°C in a 5 percent CO_2-humidified air incubator.

3.3.3. Cell Passaging

When cells reached to the confluency of 80 percent, which was approximately in two days, the medium in the flask was discarded and cells adhered to the surface of the flask were washed with 2 mL of PBS pH 7.4. After washing, PBS pH 7.4 was discarded, and 2 mL of 0.025 percent trypsin-EDTA was added, and the flask was incubated for 5 minutes in the incubator. Cells were then monitored for detachment from the flask surface under a phase-contrast light microscopy (Carl Zeiss Primo Vert). Later, the detached cells were transferred into the 15 mL sterile centrifuge tube with a 1:2 ratio of the complete medium (with 10 percent FBS) to trypsin terminate the trypsin activity. The tube was centrifuged at 300xg for 5 minutes. The supernatant was removed, and the cell pellet was resuspended and placed into a new flask.

3.3.4. Determination of Cell Number

Cells were centrifuged for 5 minutes at 300xg after trypsinization (*Section 3.3.3.*) and resuspended in the complete media. 10 µL-aliquot was taken from the cell suspension and loaded into each mirror-grid of the hemocytometry slide. Two different squares were selected from the areas on the hemocytometry slides and cells falling into these areas were counted under the phase-contrast light microscopy. Attention was paid for the difference between the numbers of cells counted in both areas to be less than 20 and the total number of cells to be no less than 20 and no more than 80. The total cell number was calculated by the Equation 3.1. given below:

$$\text{Total Cell Number/mL} = \frac{\textit{The average number of cells counted in two squares X Dilution Factor}}{10^{-4}} \quad (3.1)$$

3.3.5. Cell Freezing

Subsequent to passage phase described in *Section 3.3.3.*, 1x 10^6 cells were transferred to 1 mL of the freezing mix containing 10 percent dimethyl sulfoxide (DMSO) and 90 percent inactivated FBS inside special cryotubes and then stored at -80ºC for stepwise freezing. If cells were not to be used for more than six months, they were transferred to liquid nitrogen at -196°C and maintained there.

3.3.6. Cell Thawing

Frozen cells taken from the liquid nitrogen tank were quickly thawed at a temperature of approximately 37°C and placed into 15 mL sterile centrifuge tube onto which, 5 mL of low glucose (1g/L) DMEM containing 20 percent (v/v) FBS, 100 IU/mL penicillin, 100 µg/mL streptomycin and 1 percent NEAA medium was added dropwise to avoid the built of osmotic

pressure. The tube was then centrifuged at 300xg for 5 minutes, the supernatant was discarded, and the pellet suspended. Later, 5 mL of low glucose (1g/L) DMEM containing 20 percent (v/v) FBS, 100 IU/mL penicillin, 100 μg/mL streptomycin and %1 NEAA medium was added to the 25 cm^2 flask and $1x10^6$ cells from the suspension were transferred to the flask. The transferred cells were manually treated with cautious circular motion so that they were distributed homogeneously to the inner surface of the flask. After seeding, the flask was incubated at 37°C in a 5% CO_2-humidified air incubator.

3.4. CHARACTERIZATION OF HUMAN ENDOMETRIAL MESENCHYMAL STEM CELLS WITH FLOW CYTOMETRY

Isolated cells were characterized by flow cytometry analysis. The basis of the flow cytometry method is the measurement of the physical or chemical characteristics of cells or biological particles. For this purpose, the targeted constructs or the cells were first labelled with a fluorescent agent or acid-specific propidium iodide. For this technique, $0.3x10^6$ cells/well were plated into six-well plates and allowed to attach overnight. Next day, cells were centrifuged after trypsinization as described in *Section 3.3.3* and harvested cells were fixed in 4 percent (v/v) paraformaldehyde (PFA) for one hour. Next, the fixated cells were rinsed with PBS pH 7.4 for three times and incubated with antibodies (1:1000 diluted in PBS pH 7.4) conjugated with fluorescent dye (Table 3.1) raised against clusters of differentiation marker (CD) CD146, PDGF-R, W5C5, CD44, CD90, CD73, CD105, CD29 and CD Integrin for 16 hours at 4ºC. In addition, isolated heMSCs and peMSCs were incubated with antibodies against hematopoietic stem cell surface markers CD14, CD31, CD34 and CD45 (acting as negative control).

Table 3.1**.** Mesenchymal stem cells markers and their conjugated dye.

CD Marker Name	**Labelling Dye**	**Company**
CD 146	FITC (+)	Abcam
PDGFR	PE (+)	Abcam
W5C5	PE (+)	Abcam
CD 44	PE (+)	Abcam
CD 73	PE (+)	Abcam
CD 29	PE (+)	Abcam
IntegrinB1	PE (+)	Abcam
CD 90	PE (+)	Abcam
CD 105	PE (+)	Abcam
CD 14	FITC (-)	Abcam
CD 31	FITC (-)	Abcam
CD 34	FITC (-)	Biolegend
CD 45	PE (-)	Abcam
Negatif Control (NC)	FITC	Abcam

After overnight incubation, 1 mL of PBS pH 7.4 was added onto the tube containing the cells, and the cells were centrifuged at 300xg for 5 minutes and this process was repeated three times. Following the centrifugation step, the supernatant on the cells was removed and the cell pellets were dissolved in 100 µL of PBS pH 7.4 and ready for flow cytometry reading. In flow cytometry analysis, at least 30,000 events per sample were recorded for each thirteen different CD markers by using negative control IgG as gating control. The purpose of using negative control is to determine background staining resulting from the nonspecific binding or increased autofluorescence from dead cells.

3.5. DETERMINATION OF mRNA EXPRESSION LEVELS OF TG2, INTEGRIN-β1, SDC-4, MMP-2 and MMP-9 IN ALL ISOLATED ENDOMETRIAL MESENCHYMAL STEM CELLS

Quantitative PCR (Q-PCR) was performed to determine changes in the expression of TG2, ITGB-1, SDC-4, and gelatinase group of MMPs (MMP-2 and MMP-9) genes in healthy and patient cells. The mRNAs were isolated with Trizol PeqGOLD RNA Pure (Peqlab) reagent and mRNA levels were determined by reverse transcriptase PCR followed by quantitative real time-PCR technique [417].

3.5.1. mRNA Isolation

Cells isolated from healthy and patient tissues were cultured as described in Sections 3.3.2.and 3.3.3 and seeded in 6-well plates for 24 hours with $0.3x10^6$ cells per well. At the end of the incubation time, cells were rinsed with PBS pH 7.4 following the removal of media and mRNA was isolated according to the protocol of manufacturer (Peqlab).

First, 500 µL of Peqlab reagent was added to each 6-well plates to lyse cells by pipetting and then cell homogenates were transferred to DNase and Rnase free 1.5 mL Eppendorf tube. Following this step, 250 µL of cold chloroform was placed into each tube and then tubes were gently vortexed and kept at room temperature for 2-3 minutes. Next, tubes were centrifuged at 4°C for 15 minutes at 12000 x g and RNA in the supernatant was collected after centrifugation to be transferred in a new tube containing 500 µL of isopropanol. Tubes containing RNA and isopropanol was gently mixed by manually shaking the tubes up and down and kept at room temperature for 10 minutes, prior to centrifugation at 12000 x g for 10 min at 4°C. After removal of the supernatant, 1 mL of 70 percent (v/v) ethanol in deionized water was used to resuspend the pellet by gently vortexing. Next, tubes were centrifuged at 4°C for 10 min at slow speed (7500 x g) to prevent deformation and breaking of RNA. After centrifugation, 70 percent ethanol was disposed of, and the RNA pellet was dried by leaving tube lids open for 10 mins at room temperature. RNA pellet was finally

resuspended in 20-25 μL of Dnase-RNAase-free water and stored at -20°C until analysis and at -80°C for following studies.

3.5.2. cDNA Synthesis

For cDNA synthesis, Sensiscript Reverse Transcriptase enzyme kit and oligo (DT) primer produced by Qiagen were used. The concentration of 1000 ng RNA (measured by Nanodrop) was used as a template.

For cDNA reaction, 2 μL from 10x reaction buffer, 2 μL from dNTP mixture, 2 μL from 10 μm Oligo-DT and 1 μL from reverse transcriptase enzyme and 7 mL of total reaction mixture was prepared. 1000 ng RNA and Rnase-free water were added to the reaction mixture to a final volume of 20 mL (Table 3.2) and incubated at 37°C for 60 minutes. After incubation, samples were kept on ice for 5 minutes. The components of the reverse transcriptase reaction were given in the Table 3.2.

Table 3.2. Components of cDNA reaction mixture

Volumes	**The components of the cDNA reaction**
2 μL	10x Reaction Buffer
2 μL	dNTP mix
2 μL	10 μM Oligo-DT
1 μL	Reverse Transcriptase Enzyme
Changeable	RNase-Free Water
Changeable	1000 ng of template RNA
The total reaction volume should be 20 μL.	

3.5.3. Quantitative Polymerase Chain Reaction (Q-PCR)

Changes in TG2, ITGB-1, SDC-4, MMP-2, and MMP-9 expression levels were detected by real time Q-PCR, following mRNA isolation from mesenchymal stem cells using PeqGold reagent and reverse transcriptase reaction [417].

TG2, ITGB-1, SDC-4, MMP-2, and MMP-9 mRNA levels were amplifed using the pre-designed primers from Qiagen (QuantiTect Primer Assays). The real-time PCR was alos performed using syber-green Quanti-Tech Q-PCR kit (Qiagen) using parameters as shown in Table 3.3. To monitor the specificity of the reaction, melt curve analysis was performed at temperatures starting from 50^{o}C and increased by 0.5^{o}C intervals (Table 3.3). 18sRNA gene was used as the reference housekeeping gene as described [417, 302].

Table 3.3. Conditions of Quantitative-PCR for TG2, ITGB-1, SDC-4, MMP-2, and MMP-9

Cycle	**Temperature**	**Time**	**Phase**
1	94^{o}C	15 minutes	-
2	95^{o}C	5 minutes	Initial denaturation
3 (39 repeat)	95^{o}C	60 second	Denaturation
	55^{o}C	60 seconds	Annealing
	72^{o}C	60 seconds	Extension
4	72^{o}C	10 minutes	Final extension
5 (80 repeat)	50-80^{o}C 0.5^{o}C increase / 12 seconds	-	Melt Curve
6	4^{o}C	∞	Cooling

3.6. DETERMINATION OF PROTEIN EXPRESSION LEVELS OF TG2, INTEGRIN-β1, AND SDC-4 IN ALL ISOLATED ENDOMETRIAL MESENCHYMAL STEM CELLS

3.6.1. Preparation of Cells Lysates

The heMSCs and peMSCs were seeded as $0.3x10^6$ cells/well in 6-well culture plate as described in *Section 3.3.2* and cell monolayer was washed three times with PBS pH 7.4 prior to addition of 15 μL RIPA protein lysis buffer solution per well. The lysis buffer was composed of 50mM NaCl, 1 percent (v/v) Igepal CA-630 detergent, 0.5% (w/v) sodium deoxycholate, 0.1 percent (w/v) sodium dodecyl sulphate (SDS) dissolved in 50 mM Tris buffer at pH 8.0. Prior to protein isolation, fresh 1 mM sodium orthovanadate (Na3VO4), 2 mM phenylmethyl sulfonyl fluoride (PMSF) and 1 percent (v/v) protein inhibitor (PI) were added into the RIPA buffer.

Cells were scraped inside RIPA buffer by the scraper and transferred to 1.5 mL Eppendorf tubes. Later, cell lysates embedded in ice were sonicated with 60 percent strength for 4 seconds using Bandelin Sonopuls Ultrasonic (HD 2070.2) sonicator. The sonicator was stopped 3 times every four seconds and this step was repeated 5 times. At the end of these processes, lysates were centrifuged at 12000 x g for 15 minutes at 4ºC to precipitate cell debris.

3.6.2. Measurement of Protein Concentration

The protein content in cell lysates was analysed with Lowry Assay. A commercial kit by Bio-Rad in order to determine the protein concentration was utilized for this purpose. The Lowry assay contains two different reagents. The first one is reactive A (is an alkaline copper tartrate solution) and the other one is reactive B (is a diluted folin solution)

The Lowry assay was carried out on a 96-well plate. Different concentrations of inactivated BSA solutions were used to construct the standard curve (0.05 mg/mL, 0.25 mg/mL, 0.5

mg/mL and 0.75 mg/mL). Isolated protein samples were prepared in 1:10 dilutions and 5 µL of BSA samples and diluted protein samples were placed into 96 well plates. Into each well 25 µL of Reagent A solution was added. After mixing the Reagent A solution with the samples, 200 µL of Reagent B solution per well was added into the mixture. All samples were incubated at room temperature for 15 minutes and the absorbance was measured spectroscopically at 750 nm.

3.6.3. Sodium Dodecyl Sulfate-Polyacrylamide Gel Electrophoresis (SDS-PAGE)

Proteins in cell lysate samples were separated using SDS-PAGE analysis. For this experiment, protein samples of at least 50µg was mixed with 2x Laemmle buffer (4 percent SDS, 20 percent glycerol, 10 percent 2-mercaptoethanol, 0.004 percent bromophenol blue and 0.125 M Tris HCl with pH 6.8.) in a 1:1 ratio and denatured at 95^{o}C for 5 minutes to break down the disulphide bonds and linearize the proteins.

The SDS-PAGE method comprises of two different types of gels. The top of the gel has a stacking (top or loose) gel and possess wells to load samples. On the lower part of the gel is the separating (resolving, hard or bottom) gel, where the proteins act according to their molecular weight. The target proteins have different molecular weights so separating gels in different concentrations were used. For ITGβ-1, TG2 and β-actin proteins 8 percent, for Cycline E1, CDK-4 and CDK-2 proteins 12% and for Cycline D3 and p27 proteins 15 percent separating gels were prepared as described Table 3.4.

Table 3.4. Components of stacking and separating gel at different concentrations

Components of Gel Solution	Staking Gel Volumes	Separating Gel Volumes		
Per cent of Gel Solution	4%	8%	12%	15%
30% (w/v) acrylamide 0.8% bisacrylamide	0.65 mL	4 mL	6 mL	7.5 mL
0.5 M Tris-HCl with 0.4% (w/v) SDS, ph 6.8	1.25 mL	X	X	X
Distilled Water	3.05 mL	7.5 mL	5.5 mL	4 mL
1.5 M Tris-HCl with 0.4% (w/v) SDS, pH 8.8	X	3.75 mL	3.75 mL	3.75 mL
10 % (w/v) Ammonium persulphate (APS) in dH_2O	25 µL	50 µL	50 µL	50 µL
N, N, N, N' Tetramethylethylenediamine (TEMED)	5 µL	10 µL	10 µL	10 µL

Mini PROTEAN Tetra Cell Electrophoresis System of Bio-RAD was used for SDS-PAGE analysis. Gels were cast in 1 mm-thick glass, which was 60 mm long and 80 mm wide. After addition TEMED and APS into the mix (Table 3.4) separating gel was quickly poured into gel plate and 1 mL of isopropanol was added onto the separating gel to keep the gel smooth during the polymerization. Upon polymerization, isopropanol was removed, and the gel surface was gently washed with distilled water for 3 times. Excess water was removed with the help of napkin. The 4% stacking gel prepared according to Table 3.4 was poured immediately into the gel plate and 1mm combs were placed into the stacking gel before the gel polymerization began. Fifteen minutes later, the combs were removed from the polymerized gels and the wells were washed with dH_20 and then filled with running buffer. A maximum volume of 30 µL of sample were loaded into each well and gel plates cassettes

were placed in Mini PROTEAN Tetra Cell Electrophoresis system a filled with running buffer that is composed of 0.1 percent SDS (w/v), 0.192 M glycine and 0.025 M Tris pH 8.5. Stacking gel was run at 60 V for 20 minutes, and the separating gel was run at 90 V until the dye front reached the bottom of the gel plate.

3.6.4. Western Blot

Following the SDS-PAGE procedure described in Section 3.6.3, Western Blot technique was used to determine changes in the expression of target proteins and in protein-protein interactions in all groups of heMSCs and peMSCs. Upon completion of SDS-PAGE separation of proteins, gels were removed from the tank and incubated in the transfer buffer along with nitrocellulose membranes. PVDF membranes were soaked in 100 percent ethanol at room temperature for ten minutes to activate the chemical groups within the PVDF membrane to initiate protein-membrane interaction. 0.45 μm nitrocellulose membrane was used for the ITGβ-1 (121 kDa), TG2 (80 kDa) and β-actin (42 kDa) proteins while 0.22 μm PVDF membrane was used for Cycline E1 (48 kDa), CDK-4 (30 kDa), CDK-2 (33 kDa), Cycline D3 (31 kDa), p27 (22 kDa) and SDC-4 (21 kDa). After activation of the membrane, the Bio-Rad's Mini-Protean Tetra Trans-Blot system was assembled for wet transfer from two sponge pads, whatmann filter papers (42 X 125mm), SDS-PAGE and membrane, all equilibrated in the transfer buffer. The apparatus was assembled on the black cassette plate (cathode) in the order of the sponge pad followed by two filter papers, then the gel, membrane, two more filter papers, and the last sponge, respectively. The cassette was then locked and placed into the blotting module according to the color coding (black catode side of casettes facing the black catode side of the transfer module). Next, module was transferred into the tank filled with cold transfer buffer (0.025 M Tris-Base PH 8.3, 0.192 M glycine and 20 percent methanol), and transfer was performed at 175 mA for 90 minutes at 4^{o}C. During the transfer process, cell lysate proteins separated through SDS-PAGE were transferred to the membrane. After the disassembly of transfer module and membrane was rinsed in TBS-T wash buffer composed of 20 mM Tris, 150 mM NaCl and 0.01 percent

Tween-20 pH 7.4. The next step is blocking, which is performed to eliminate nonspecific binding between the membrane and the antibody of the target protein. For blockage, the membrane was incubated with 5% BSA or non-fat milk powder in TBS-T pH 7.4 for 1 hour at room temperature. Next, membranes were washed three times for 5 minutes with TBS-T pH 7.4 and then subsequently was incubated with antibodies in the blocking buffer (*for TG2 CUB 7402 and β-actin 1: 100000, for ITGβ-1 and SDC-4 1:1000 and for Cyclin E1, CDK-4, CDK-2, Cyclin D3, p27 1:500 diluted in blocking solution in a total volume*) overnight at +4ºC on a rocking platform. The next day, the membranes were rinsed three times for 5 minutes with TBS-T pH 7.4, and then treated with blocking solution for 30 minutes prior to the incubation with secondary anti-rabbit or secondary anti-mouse antibodies diluted in blocking buffer was specified in the Table 2.1. After the removal of secondary antibodies, membrane was washed three times for 5 minutes with TBS-T pH 7.4 and then transferred to the PBS pH 7.4 solution until the addition of HRP substrate Bio-Rad Clarity ECL substrates. Membranes were incubated with 1 mL of HRP substrate for 5 minutes, excess substrate was removed by gentle taping onto the filter paper. Images were captured by Bio-Rad Chemidoc XL. The intensities of the target proteins on the membrane images were analyzed using Image J program using the β-actin to verify equal loading.

Table 3.5. Summary of primary (1^0 Ig) and secondary (2^0 Ig) antibodies used in Western Blot. Solution, [Sol]: concentration, o/n: overnight, RT: room temperature

Target Protein	1^0 Ig	1^0 Ig [Sol]	Blocking [Sol]	1^0 Ig incubation conditions	2^0 Ig	2^0 Ig [Sol]	2^0 Ig incubation conditions
TG2	Anti-mouse Cub7 402	1 µL dilution in a total volume of 10 mL	5% Non-fat milk powder	+4ºC o/n	Goat anti-mouse-HRP	1 µL dilution in a total volume of 10 mL	RT for 2 hrs.

ITGβ-1	Anti-mouse ITGβ-1	1 µL dilution in a total volume of 1 mL	5% Non-fat milk powder	+4°C o/n	Goat anti-mouse-HRP	1 µL dilution in a total volume of 1 mL	RT for 2 hrs.
SDC-4	Anti-rabbit SDC-4	1 µL dilution in a total volume of 1 mL	5% Non-fat milk powder	+4°C o/n	Goat anti-rabbit - HRP	1 µL dilution in a total volume of 1 mL	RT for 2 hrs.
Cyclin E1	Anti-mouse Cycline E1	1 µL dilution in a total volume of 500 µL	5% Non-fat milk powder	+4°C o/n	Goat anti-mouse-HRP	1 µL dilution in a total volume of 500 µL	RT for 2 hrs.
CDK-4	Anti-rabbit CDK-4	1 µL dilution in a total volume of 500 µL	3% BSA in 1x TBS-T	+4°C o/n	Goat anti-rabbit - HRP	1 µL dilution in a total volume of 500 µL	RT for 2 hrs.
CDK-2	Anti-rabbit CDK-2	1 µL dilution in a total volume of 500 µL	3% BSA in 1x TBS-T	+4°C o/n	Goat anti-rabbit - HRP	1 µL dilution in a total volume of 500 µL	RT for 2 hrs.
Cyclin D3	Anti-rabbit Cycline D3	1 µL dilution in a total volume of 500 µL	3% BSA in 1x TBS-T	+4°C o/n	Goat anti-rabbit - HRP	1 µL dilution in a total volume of 500 µL	RT for 2 hrs.

p27	Anti-rabbit p27	1 µL dilution in a total volume of 500 µL	3% BSA in 1x TBS-T	+4°C o/n	Goat anti-rabbit - HRP	1 µL dilution in a total volume of 500 µL	RT for 2 hrs.
β-Actin	Anti-mouse β-Actin	1 µL dilution in a total volume of 10 mL	5% Non-fat milk powder	+4°C o/n	Goat anti-mouse-HRP	1 µL dilution in a total volume of 10 mL	RT for 2 hrs.

3.7. MESUARMENT OF TG2 CROSS-LINK ENZYME ACTIVTY BY BIOTIN-X CADAVERINE (BTC) ASSAY

96-well plates were coated with 10 µg/mL FN from human plasma (Sigma, USA) in 50 mM Tris-HCl, pH 7.4 for 16 hours at 4°C or 1 hour at 37°C and blocked with 3 percent (w/v) BSA in PBS, pH 7.4 for 30 minutes at 37°C. Wells were then gently washed three times with 50 mM Tris-HCl, pH 7.4 for 5 minutes on a shaker. eMSCs were trypsinized and resuspended in serum-free media. Cells were then counted and seeded on FN-coated plates at 20.000 cells/well density in serum-free media containing 0.132 mM Biotin cadaverine, trifluoroacetate salt (N-(5-aminopentyl) biotin amide, trifluoroacetic acid salt) (BTC) (Biotium, USA). FN-coated wells incubated only with serum-free media containing 0.132 mM BTC served as the negative background control. Following a three-hour incubation at 37°C, wells were rinsed twice with PBS, pH 7.4 and 100 µL of 0.1 percent (w/v) sodium deoxycholate, 2mM EDTA solution (pH 7.4) were placed into each well to dissolve cell membranes without damaging TG2-crosslinked BTC-FN matrix. After the incubation at room temperature for 10 minutes by gentle shaking, wells were washed three times for 5 minutes with 50 mM Tris-HCl, pH 7.4. In order to label FN crosslinked BTC, 100 µL of extravidin peroxidase (dissolved 1:1000 in 3 percent (w/v) BSA) were placed into each well

for 90 minutes at 37°C. Following three washing steps performed with 50 mM Tris-HCl, pH 7.4 for 5 minutes by gentle shaking, wells were equilibrated with the developing buffer containing 0.1 M NaOAc, pH 6, for 5 minutes. The reaction was then developed by the addition of 100 µL per well developing buffer containing 3,3',5,5'-tetramethyl benzidine (TMB), which is the substrate for extravidine peroxidase. Plate was then incubated at room temperature or 37°C for 15-30 minutes until blue colour formation occurred. The reaction was subsequently terminated by the addition of 50 µL of 2.5 M H_2SO_4 to each well, and the absorbance was measured at 450 nm using an ELISA plate reader.

3.8. CO-IMMUNOPRECIPITATION ASSAY

Cells (600.000 cells per well) seeded into six well plates for 16 hours were collected in 100µL of immunoprecipitation buffer (50 mM Tri-HCl pH 7.4, 0.25 percent sodium deoxycholate, 150 mM NaCl, 0.1 mM PMSF, 1 percent (v/v) protein inhibitor cocktail, and 50µM TG2-specific inhibitor (Z-DON). Cell lysates (300 µg/mL) were then incubated with 1 µg mouse IgG at 4ºC for an hour to eliminate proteins that were non-specifically bound to mouse IgGs by incubation with protein G-coated sepharose beads for an hour. Mouse IgG bound proteins were then removed from the slurry by centrifugation at 300xg. The pre-cleared cell lysate was then incubated with mouse SDC-4 (1.25 µg/mL) or ITGß-1 (0.5 µg/mL) antibodies at 4ºC for an hour. SDC-4 associated proteins bound to anti-SDC4 antibody were precipitated by incubation the slurry with protein G-coated sepharose beads for 90 minutes. Following precipitation of beads (300 x g 15 mins), the supernatant was discarded, and beads were resuspended in 2x Laemmli buffer to be separated by SDS-PAGE. The proteins were transferred onto a 45 µm nitrocellulose membrane by Western blotting and the membrane was incubated with TG2 CUB7402 antibody to detect if TG2 proteins have an interaction with SDC-4 or ITGß-1 [327]. The data were analyzed using Image J software.

3.9. GROWTH RATE AND CELL CYCLE ANALYSIS

3.9.1. WST-1

Colorimetric 2-[4-iodophenyl]-3-[4-nitrophenyl]-5-[2,4-disulfophenyl]-2H tetrazolium monosodium saltwater soluble tetrazolium (WST-1) assay were performed to determine the standard cell number and to test the viability and proliferation capacity of cells. In the working principle of WST-1 cell proliferation assay, mitochondrial activity of cells is measured. This assay is based on the reduction of tetrazolium salts catalysed by mitochondrial enzyme systems. Tetrazolium salts are usually colourless and mitochondrial activity in alive cells on tetrazolium results in coloured products. The WST-1 reagent is broken down into a formazan class dye by viable cells through the mitochondrial succinate-tetrazolium reductase enzyme [418].

In experimental set-up, 2000 eMSCs per well was seeded into a 96-well plate and incubated for 24, 48, 72 and 96 hours. For the preparation of a standard curve that relates absorbance values to cell number, early in the morning eMSCs were seeded into a 96-well plate at 2000, 5000, 10.000, 15.000 and 20.000 cells per well and allowed to attach for 12 hours. Next, 5 µL of WST-1 reagent were mixed with 45 µL of media, and the mix was placed to each well. After the addition of WST-1 reagent, the absorbance was measured after 1 hour at 420-480 nm (λ max 450 nm) wavelength.

3.9.2. Cytell Cell Imaging Analysis

The Cytell Reagent G Cell Cycle kit was used to determine the G0 / G1, S, G2 and M cell cycle phases in eMSCs. Cells were seeded into 96 well plate at a density of 5000 cells/ well for 6 hours in complete media and incubated at 37^{o}C and 5 percent CO_2 humidified air. At the of the 6th hour, the complete media were changed with 4 percent of FBS media and cells ere incubated for 16 hours. After this time point, the 4 percent of FBS media were removed and cells were washed with PBS pH 7.4. Then the cells were treatment with 4X of Reagent

G in 4 percent of FBS low glucose DMEM for 45 minutes at 4ºC. After the incubation, cell cycle checkpoints were analysed by Cell Cycle BioApp software of the Cytell Cell Image System.

3.10. ZYMOGRAPHY ASSAY

Changes in MMP activations of mesenchymal stem cells were determined by using the zymography method on cell culture media collected at the 48th hour. A zymography gel consists of resolving and stacking gels. The resolving gel was composed of 1mL of 5mg/mL gelatin dissolved in distilled water (Sigma-Aldrich 2 percent Gelatin solution Type B), 3.1 mL of H_2O, 2.5 mL of 1.5M Tris HCl pH 8.8, 3.33 mL of 29 percent acrylamide/1 percent N, N'-methylene bisacrylamide, 50 µl of 10 percent APS, and 10 µl of TEMED. Stacking gel contained 0.65 mL of 29 percent acrylamide/1 percent N, N'-methylene bisacrylamide, 3 mL of H_2O, 1.25mL of 0.5M Tris-HCl pH 6.8, 50 µl of 10 percent SDS, 25 µl of 10 percent APS, and 5µl of TEMED. Gels were casted as described before in Section 3.6.3 and 40 µl of non-denatured cell culture medium mixed with 4x loading buffer (0.25 M Tris-HCL pH 6.8, 40 percent glycerol, 8 percent SDS and 0.01 percent bromophenol blue) was loaded into the wells. After loading step, the gel was run in cold-running buffer (0.025 M Tris-Base pH 8.3, 0.192 M glycine and 0.1 percent SDS) for approximately 5 hours at 60 volts at 4 °C. After electrophoresis, the gel was washed twice with 2.5 percent Triton X-100 to remove SDS detergent and then incubated with the developing solution (100mM Tris-HCl pH 8, 5mM $CaCl_2$, 0.005 percent Brij-35, 1µM $ZnCl_2$ and 0.001 percent NaN_3) for 48 hours at 37ºC to activate MMPs. At the end of the incubation period, gel was washed twice with distilled water and stained with 0.2 percent Coomassie Brilliant Blue R-250 dissolved in 50 percent ethanol for two hours. Once to the lytic strips was observed, the excess dye was removed from the gel by treating the gel with 5-minute microwave irradiation in distilled water for three times. The active forms of enzymes on the gel were visualized with the BioRad ChemiDoc XRS + device in the form of lytic strips on the blue background. The

density of the lytic strips showing the MMP activities were determined by the Image J software.

3.11. COLONY FORMING UNIT ASSAY

Colony forming characteristics of eMSCs were tested by colony forming unit assay. For this purpose, eMSCs were seeded at a clonal density of 50 cells/ cm^2 onto gelatine, and fibronectin-coated 100-mm culture dishes and cultured in low glucose DMEM containing 20 percent (v/v) inactive FBS, 100 IU / mL penicillin, 100 μg / mL streptomycin and 1 percent NEAA for 21 day at 37ºC and 5 percent CO_2-humidified air. The media change was performed once a week. At the end of the 21 days, colonies were monitored microscopically to ensure they were derived from singe cells. Cells were then fixed with 3.7 percent (w/v) paraformaldehyde and stained with Giemsa G250 (Sigma Aldrich). Images of cells were captured with Leica stereo microscope at 4X and 10X magnification and quantified using the Image J software.

3.12. CELL MIGRATION ASSAY

All isolated cells were seed at the density of 300,000 cells/well in 24-well plates and incubated at 37ºC and 5 percent CO2-humidified air for 16 hours. At the end of the incubation, straight lines on cells attached to TCP as a single layer was drawn with the help of a six-comb SPL Scratcher. Following this procedure, the migration potential of the cells to the wound closure area was captured by Cytell Cell Imaging System and calculated using Image J software for the pictures taken at the 6^{th} and 12^{th} hours.

3.13. TRANSWELL INVATION ASSAY

Commercial 8 μm matrigel-coated transwell inserts were used from Corning for transwell migration assay. Matrigel-coated transwell maintained at -20ºC were transferred to sterile

24 well plates. inserts were separated two part by matrigel coated membrane. Fist, 750 µl complete medium was added to the bottom of 24 well plate inserts and 200 µl serum-free DMEM containing eMSCs at a density of $2.5x10^5$ cell/well was added to the upper part of inserts and incubated at 37°C and 5 percent CO_2-humidified air for 24 hours. At the end of the incubation period, the medium on the transwell was removed, and the insert was washed three times with PBS pH 7.4. Next, 3.7 percent paraformaldehyde in PBS pH 7.4 was used to fix the cells for 15 minutes at room temperature. Following the removal of paraformaldehyde, the insert was washed three times with PBS pH 7.4 and then, cells were treated with 0.1 percent of Triton X-100 in PBS pH 7.4 for 15 minutes at room temperature to achieve cell permeability. At the end of this period, Triton X-100 was removed by three PBS washes. Cells were stained with 0.5 percent crystalline viole in ethanol for 15 minutes at room temperature. Cells were finally washed 3 times with PBS pH 7.4 to remove excess dye in the background and then inserts were left to stand at room temperature for 30 minutes to dry. Images from five different areas from each insert were visualized with a Zeiss microscope on a 20x lens equipped with AxioCam ICc camera and then analysed by the image J software.

3.14. shRNA TRANSDUCTION

eMSCs were treated with shRNA, while healthy eMS cells were treated with control shRNA (scrambled). First of all, all healthy and patient eMSCs were seeded as 30.000 cells per well in 24 well tissue culture plate and incubated at 37°C and 5 percent CO_2-humidified air for overnight. At the end of the incubation time, cells were treated with 8 µg/mL protamine sulfate in low glucose DMEM with containing 4 percent FBS (v/v) and 1 percent P/S (v/v) for 12 hours. Following the protamine sulfate incubation, lentiviral particles were included to low glucose DMEM with containing 4 percent FBS (v/v) and 1 percent P/S (v/v) the growth media at the multiplicity of infection (MOI) of 2 for healthy eMSCs and 5 for patient eMSCs for 36 hours. Then, stable transduced cells were selected by the addition of 3 µg/mL puromycin in complete growth media, which was changed with fresh complete growth media

with 3 μg/mL puromycin every 2 day. At the end of the tenth day, cells when reached to 80 percent confluency, were transferred to T-75 cell culture flasks. The TG2 levels in eMS cells were determined by Western Blot and Q-PCR analysis prior to cryopreservation.

3.15. STATISTICAL ANALYSIS

GraphPad Prism 6 program was used for the graphs of all data analyses and after the parametric or non-parametric distribution of the data was determined, the data showing the parametric distribution were analyzed by the student-t test compared to the control. ANOVA and Mann-Whitney tests were used for non-parametric data. Each experiment was repeated at least 5 times.

4. RESULTS

4.1. CHARACTERIZATION OF eMSCs

4.1.1. Isolation of eMSCs with Non-Enzymatic Method

In the first stage of this thesis, mesenchymal stem cell isolation from five different healthy and five different endometriosis individuals was performed using the non-enzymatic method. The non-enzymatic method described in detail in Section 3.3.1 was applied to both samples taken from healthy tissue from individuals who were not diagnosed with endometriosis and to the biopsy samples from patients diagnosed with endometriosis. Migrated cells from the tissue were monitored at the end of day five (Figure 4.1.).

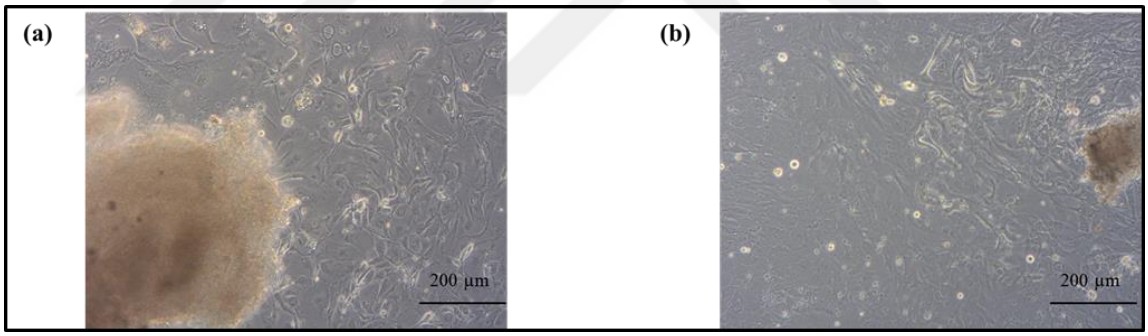

Figure 4. 1. Representative images for MSCs migrating from tissue explants. (a) Healthy tissue explant. (b) Patient tissue explant. Scale bar represents 200µm.

As seen in Figure 4.1, heMSCs and peMSCs were migrated from the minced biopsy samples by the end of the fifth day. All images were taken with the ZEISS microscope using a 10x objective.

4.1.2. Characterization of eMSCs by Flow Cytometric Analysis

heMSCs and peMSCs, which morphologically showed MSC appearance under the microscope, were subjected to the flow cytometric analysis as described in Section 3.4 for expression of stem cell markers. eMSCs seeded at 3x 10^5 cells per well in 6-well plates and incubated for 16 hours were probed for CD 146, PDGFR, W5C5, CD 44, CD 29, ITGB-1, CD 73, CD 90, CD 105, CD 14, CD 31, CD 34, CD 45.

The results of flow cytometric technique performed to determine the characterization of heMSCs and peMSCs samples in Group-1 were given in Figures 4.2 and 4.3.

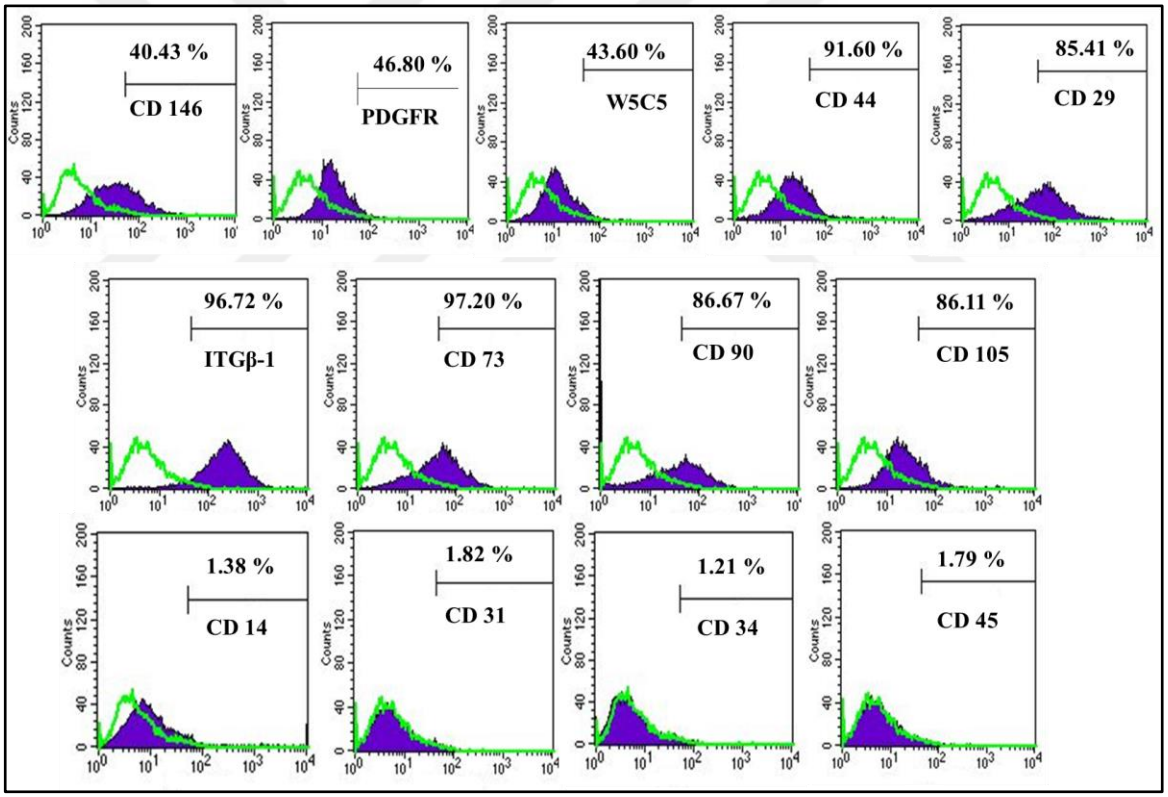

Figure 4. 2. Characterization of heMSCs isolated by non-enzymatic method by flow cytometry for Group-1. 1x 10^4 cells were read into the flow cytometer for each marker. Cells incubated with isotype IgG antibody was used as negative control (NC) and it was presented by green line.

heMSCs were isolated with non-enzymatic procedure at passage 3 were characterized using Flow Cytometry. The isolated heMSCs were tested positive for MSC markers including CD 146, PDGFR, W5C5, CD 44, CD 29, ITGβ-1, CD 73, CD 90, and CD 105 but negative for hematopoietic stem cell markers CD 14, CD 31, CD 34, and CD 45 (Figure 4.2). heMSCs expressed 40.43 percent CD146, 46.80 percent PDGFR, 43.60 percent W5C5, 91.60 percent CD 44, 85.41 percent CD 29, 96.72 percent ITGβ-1, 97.20 percent CD 73, 86.67 percent CD 90, 86.11 percent CD 105, 1.38 percent CD 14, 1.82 percent CD 31, 1.21 percent CD 34 and 1.79 percent CD 45 (Figure 4.2.).

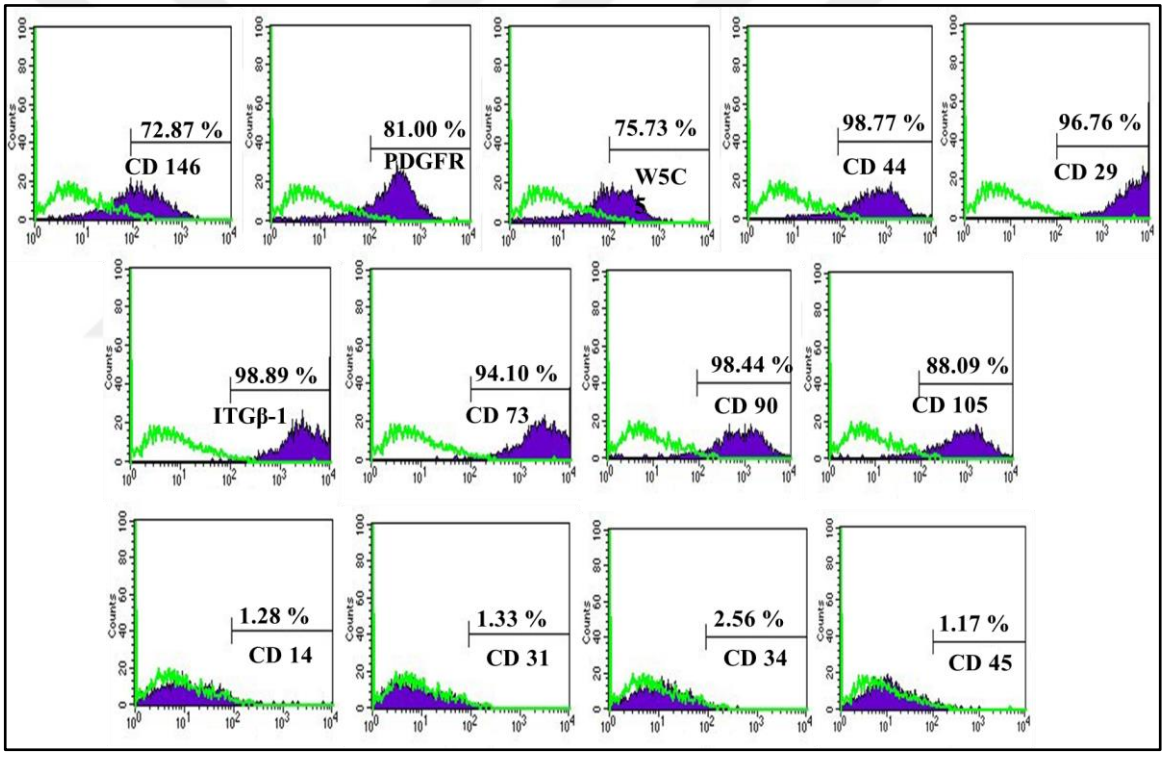

Figure 4.3. Characterization of peMSCs isolated by non-enzymatic method by flow cytometry for Group-1. 1x 10^4 cells were read into the flow cytometer for each marker. Cells incubated with isotype IgG antibody was used as negative control (NC) and it was presented by green line.

peMSCs were isolated with non-enzymatic procedure at passage 3 were characterized using Flow Cytometry. The isolated peMSCs were tested positive for MSC markers including CD

146, PDGFR, W5C5, CD 44, CD 29, ITGβ-1, CD 73, CD 90, and CD 105 but negative for hematopoietic stem cell markers CD 14, CD 31, CD 34, and CD 45 (Figure 4.3). peMSCs expressed 72.87 percent CD146, 81.00 percent PDGFR, 75.73 percent W5C5, 98.77 percent CD 44, 96.76 percent CD 29, 98.89 percent ITGβ-1, 94.10 percent CD 73, 98.44 percent CD 90, 88.09 percent CD 105, 1.28 percent CD 14, 1.31 percent CD 31, 2.56 percent CD 34 and 1.17 percent CD 45.

The results of flow cytometric technique performed to determine the characterization of heMSCs and peMSCs samples in Group-2 were given in Figures 4.4 and 4.5.

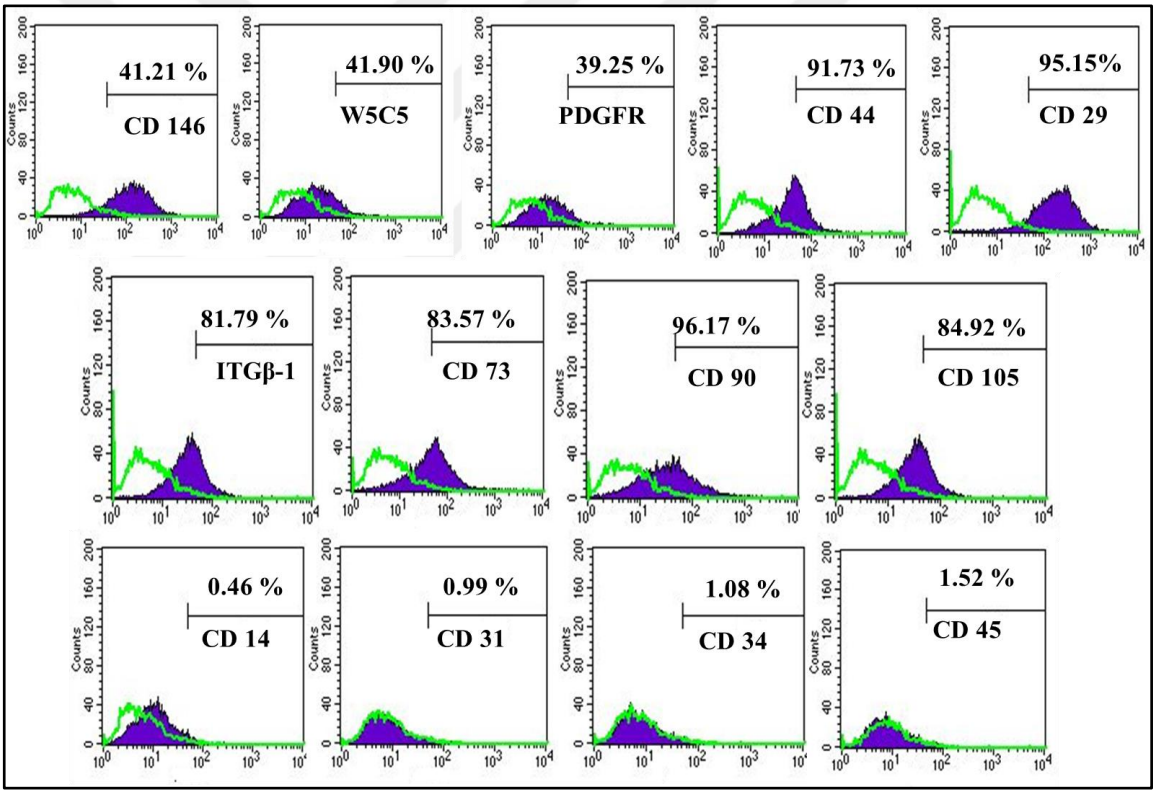

Figure 4.4. Characterization of heMSCs isolated by non-enzymatic method by flow cytometry for Group-2. 1x 10^4 cells were read into the flow cytometer for each marker. Cells incubated with isotype IgG antibody was used as negative control (NC) and it was presented by green line.

heMSCs were isolated with non-enzymatic procedure at passage 3 were characterized using Flow Cytometry. The isolated heMSCs were tested positive for MSC markers including CD 146, PDGFR, W5C5, CD 44, CD 29, ITGβ-1, CD 73, CD 90, and CD 105 but negative for hematopoietic stem cell markers CD 14, CD 31, CD 34, and CD 45 (Figure 4.4). heMSCs expressed 41.21 percent CD146, 41.90 percent W5C5, 39.25 percent PDGFR, 91.73 percent CD 44, 95.16 percent CD 29, 81.79 percent ITGβ-1, 93.57 percent CD 73, 96.17 percent CD 90, 84.92 percent CD 105, 0.46 percent CD 14, 0.99 percent CD 31, 1.08 percent CD 34 and 1.52 percent CD 45 in Figure 4.4.

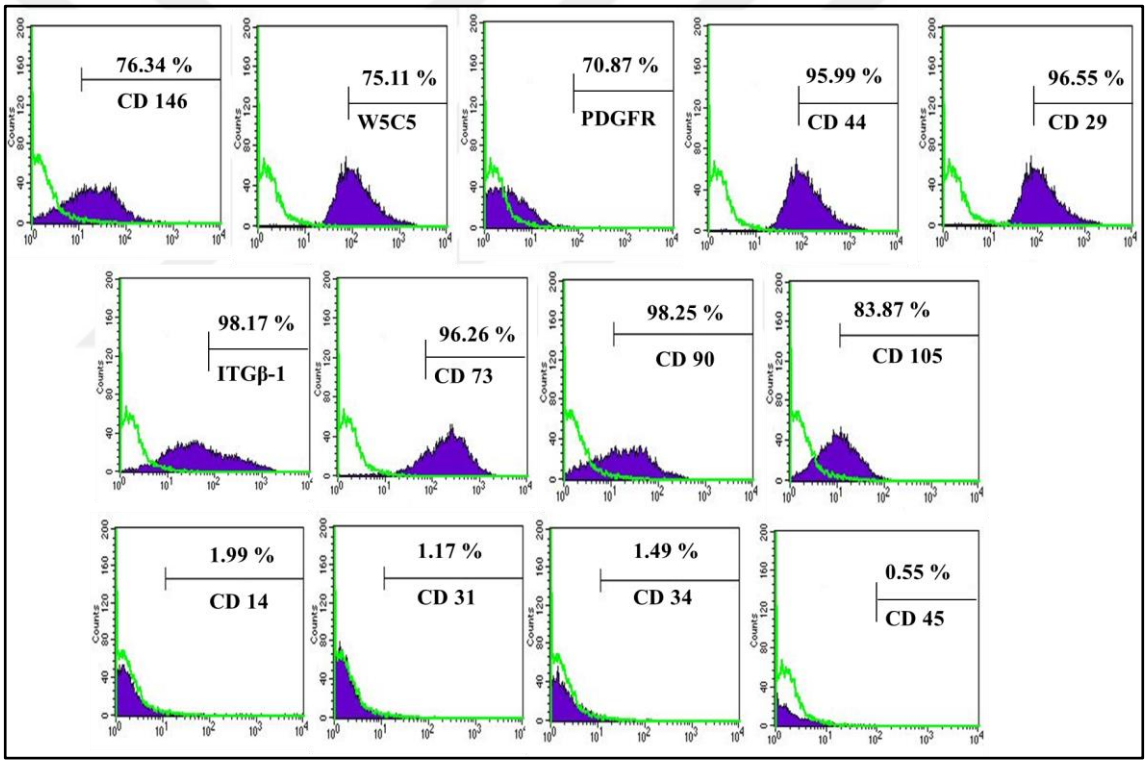

Figure 4.5. Characterization of peMSCs isolated by non-enzymatic method by flow cytometry for Group-2. 1x 10^4 cells were read into the flow cytometer for each marker. Cells incubated with isotype IgG antibody was used as negative control (NC) and it was presented by green line.

peMSCs were isolated with non-enzymatic procedure at passage 3 were characterized using Flow Cytometry. The isolated peMSCs were tested positive for MSC markers including CD

146, PDGFR, W5C5, CD 44, CD 29, ITGβ-1, CD 73, CD 90, and CD 105 but negative for hematopoietic stem cell markers CD 14, CD 31, CD 34, and CD 45 (Figure 4.5). peMSCs expressed 76.34 percent CD146, 75.11 percent W5C5, 70.84 percent PDGFR, 95.99 percent CD 44, 95.55 percent CD 29, 98.17 percent ITGβ-1, 96.26 percent CD 73, 98.25 percent CD 90, 83.87 percent CD 105, 1.99 percent CD 14, 1.17 percent CD 31, 1.49 percent CD 34 and 0.55 percent CD 45.

The results of flow cytometric technique performed to determine the characterization of heMSCs and peMSCs samples in Group-3 were given in Figures 4.6 and 4.7.

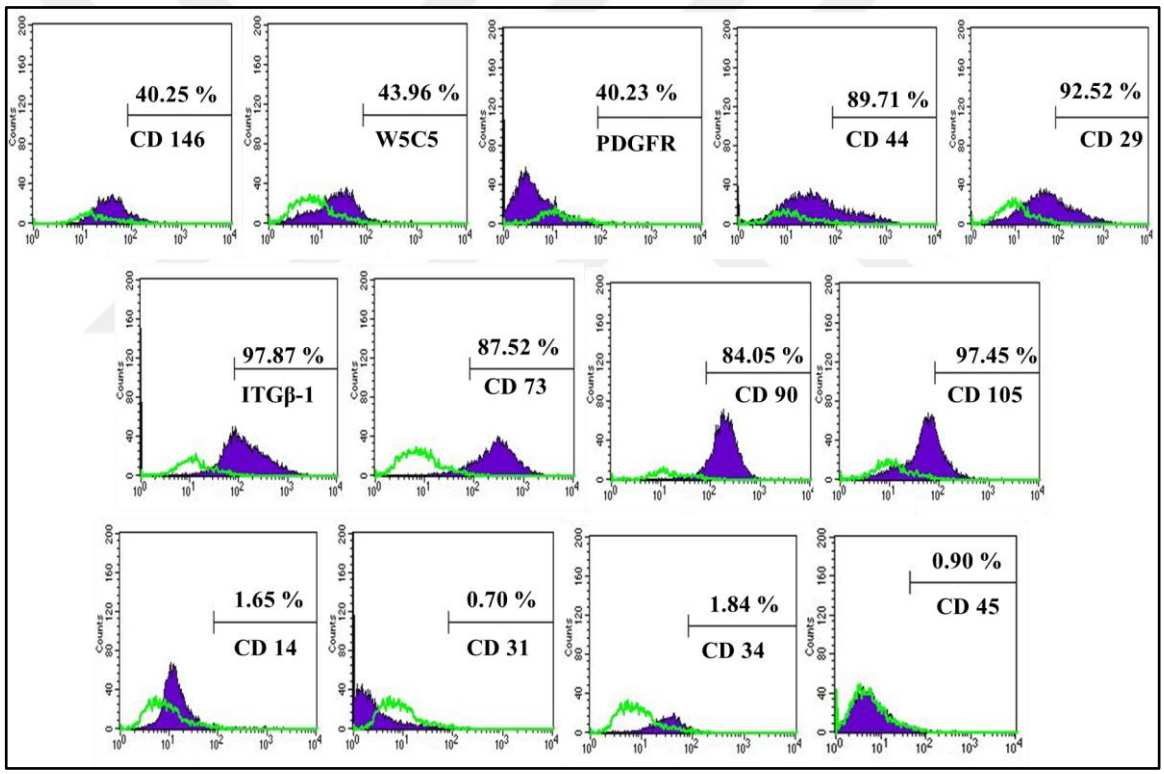

Figure 4.6. Characterization of heMSCs isolated by non-enzymatic method by flow cytometry for Group-3. 1x 10^4 cells were read into the flow cytometer for each marker. Cells incubated with isotype IgG antibody was used as negative control (NC) and it was presented by green line.

heMSCs were isolated with non-enzymatic procedure at passage 3 were characterized using Flow Cytometry. The isolated heMSCs were tested positive for MSC markers including CD 146, PDGFR, W5C5, CD 44, CD 29, ITGβ-1, CD 73, CD 90, and CD 105 but negative for

hematopoietic stem cell markers CD 14, CD 31, CD 34, and CD 45 (Figure 4.6). heMSCs expressed 40.25 percent CD146, 43.96 percent W5C5, 40.23 percent PDGFR, 89.71 percent CD44, 92,52 percent CD29, 97.87 percent Integrin β1, 87.52 percent CD73, 84.05 percent CD90, 97.45 percent CD105, 1.65 percent CD14, 0.70 percent CD31, 1.84 percent CD34, 0.90 percent CD45.

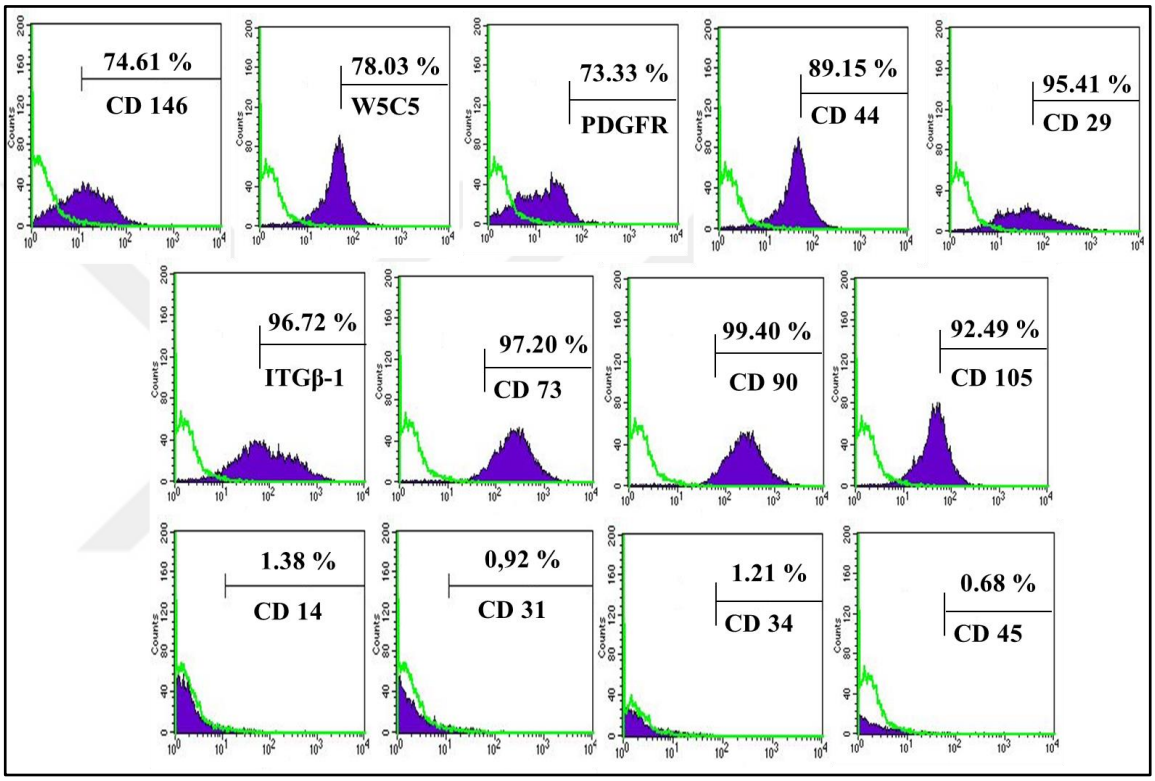

Figure 4.7. Characterization of peMSCs isolated by non-enzymatic method by flow cytometry for Group-3. 1x 10^4 cells were read into the flow cytometer for each marker. Cells incubated with isotype IgG antibody was used as negative control (NC) and it was presented by green line.

peMSCs were isolated with non-enzymatic procedure at passage 3 were characterized using Flow Cytometry. The isolated peMSCs were tested positive for MSC markers including CD 146, PDGFR, W5C5, CD 44, CD 29, ITGβ-1, CD 73, CD 90, and CD 105 but negative for hematopoietic stem cell markers CD 14, CD 31, CD 34, and CD 45 (Figure 4.7). peMSCs expressed 76.61 percent CD146, 78.03 percent W5C5, 73.33 percent PDGFR, 89.15 percent

CD44, 92,41 percent CD29, 96.72 percent Integrin β1, 97.20 percent CD73, 99.40 percent CD90, 92.49 percent CD105, 1.38 percent CD14, 0.92 percent CD31, 1.21 percent CD34, 0.68 percent CD45. Cells incubated with isotype IgG antibody was used as negative control (NC) in Figure 4.7.

The results of flow cytometric technique performed to determine the characterization of heMSCs and peMSCs samples in Group-4 were given in Figures 4.8 and 4.9.

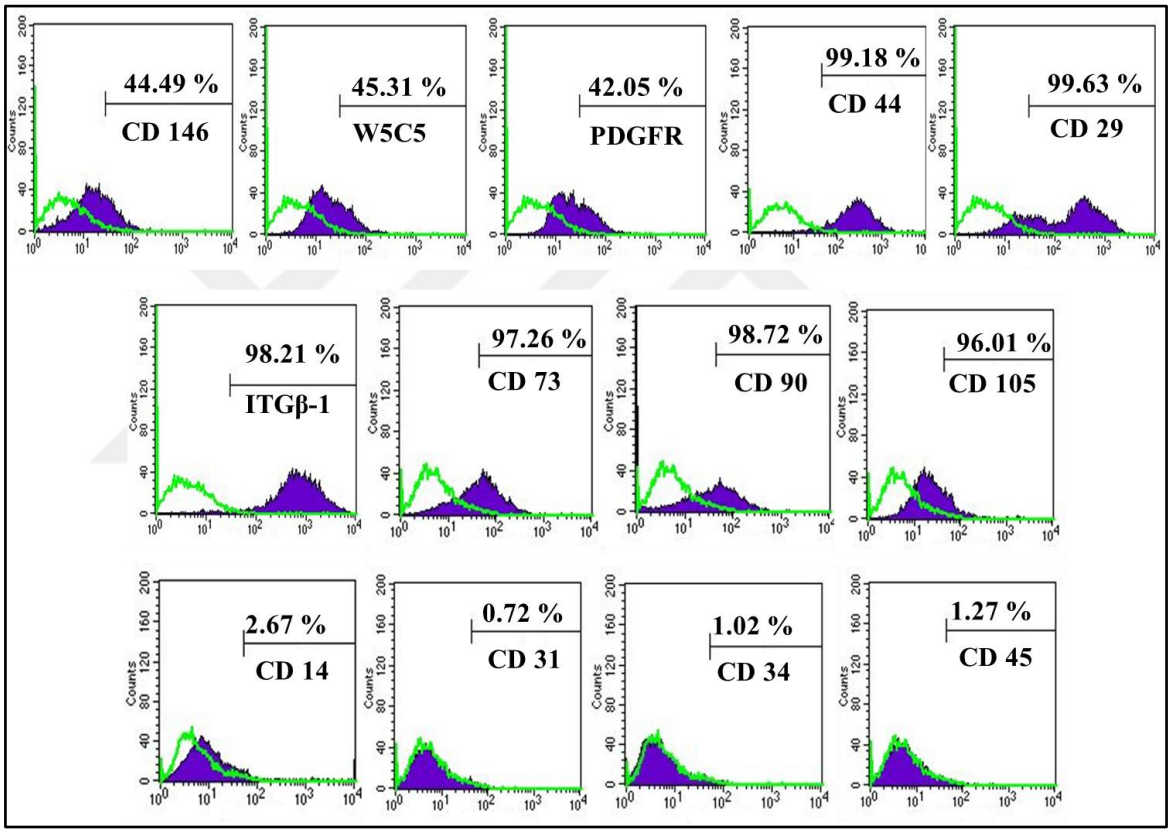

Figure 4.8. Characterization of heMSCs isolated by non-enzymatic method by flow cytometry for Group-4. 1x 10^4 cells were read into the flow cytometer for each marker. Cells incubated with isotype IgG antibody was used as negative control (NC) and it was presented by green line.

heMSCs were isolated with non-enzymatic procedure at passage 3 were characterized using Flow Cytometry. The isolated heMSCs were tested positive for MSC markers including CD 146, PDGFR, W5C5, CD 44, CD 29, ITGβ-1, CD 73, CD 90, and CD 105 but negative for hematopoietic stem cell markers CD 14, CD 31, CD 34, and CD 45 (Figure 4.8). heMSCs

expressed 44.49 percent CD146, 45.31 percent W5C5, 42.05 percent PDGFR, 99.18 percent CD44, 99.63 percent CD29, 98.21 percent Integrin β1, 97.26 percent CD73, 98.72 percent CD90, 99.01 percent CD105, 2.67 percent CD14, 0.72 percent CD31, 1.02 percent CD34, 1.27 percent CD45 (Figure 4.8).

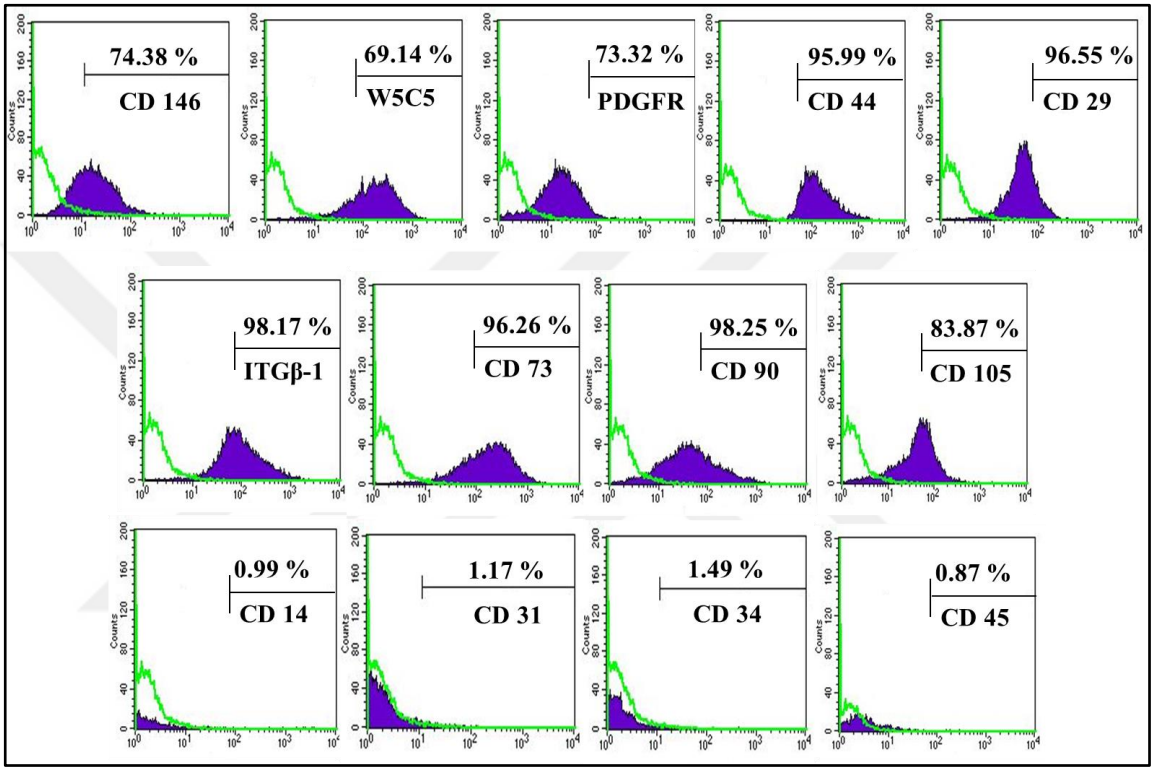

Figure 4.9. Characterization of peMSCs isolated by non-enzymatic method by flow cytometry for Group-4. 1x 10^4 cells were read into the flow cytometer for each marker. Cells incubated with isotype IgG antibody was used as negative control (NC) and it was presented by green line.

peMSCs were isolated with non-enzymatic procedure at passage 3 were characterized using Flow Cytometry. The isolated peMSCs were tested positive for MSC markers including CD 146, PDGFR, W5C5, CD 44, CD 29, ITGβ-1, CD 73, CD 90, and CD 105 but negative for hematopoietic stem cell markers CD 14, CD 31, CD 34, and CD 45 (Figure 4.9). peMSCs expressed 74.38 percent CD146, 69.14 percent W5C5, 73.32 percent PDGFR, 95.99 percent CD44, 96.55 percent CD29, 98.17 percent Integrin β1, 96.26 percent CD73, 98.25 percent

CD90, 83.87 percent CD105, 0.99 percent CD14, 1.17 percent CD31, 1.49 percent CD34, 0.87 percent CD45.

The results of flow cytometric technique performed to determine the characterization of heMSCs and peMSCs samples in Group-5 were given in Figures 4.10 and 4.11.

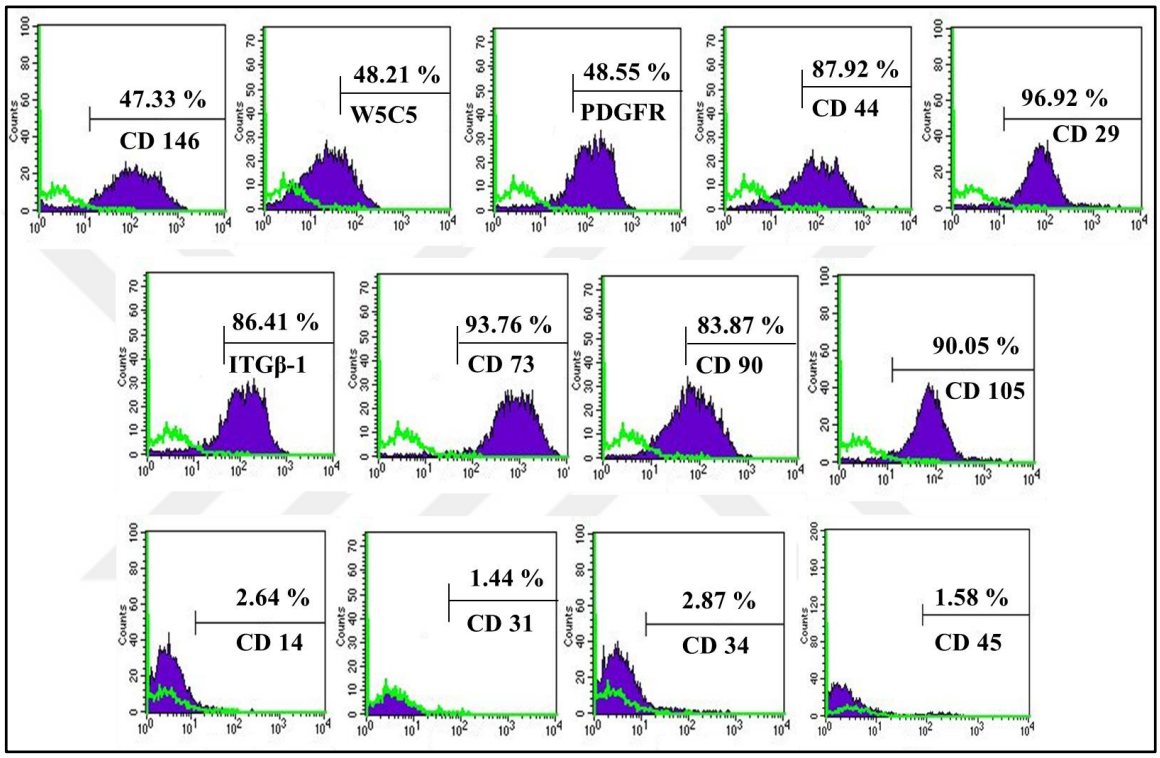

Figure 40. Characterization of heMSCs isolated by non-enzymatic method by flow cytometry for Group-5. 1x 10^4 cells were read into the flow cytometer for each marker. Cells incubated with isotype IgG antibody was used as negative control (NC) and it was presented by green line.

heMSCs were isolated with non-enzymatic procedure at passage 3 were characterized using Flow Cytometry. The isolated heMSCs were tested positive for MSC markers including CD 146, PDGFR, W5C5, CD 44, CD 29, ITGβ-1, CD 73, CD 90, and CD 105 but negative for hematopoietic stem cell markers CD 14, CD 31, CD 34, and CD 45 (Figure 4.10). heMSCs expressed 47.33 percent CD146, 48.21 percent W5C5, 48.55 percent PDGFR, 87.92 percent CD44, 96.92 percent CD29, 86.41 percent Integrin β1, 93.76 percent CD73, 83.87 percent

CD90, 90.05 percent CD105, 2.64 percent CD14, 1.44 percent CD31, 2.87 percent CD34, 1.58 percent CD45 (Figure 4.10).

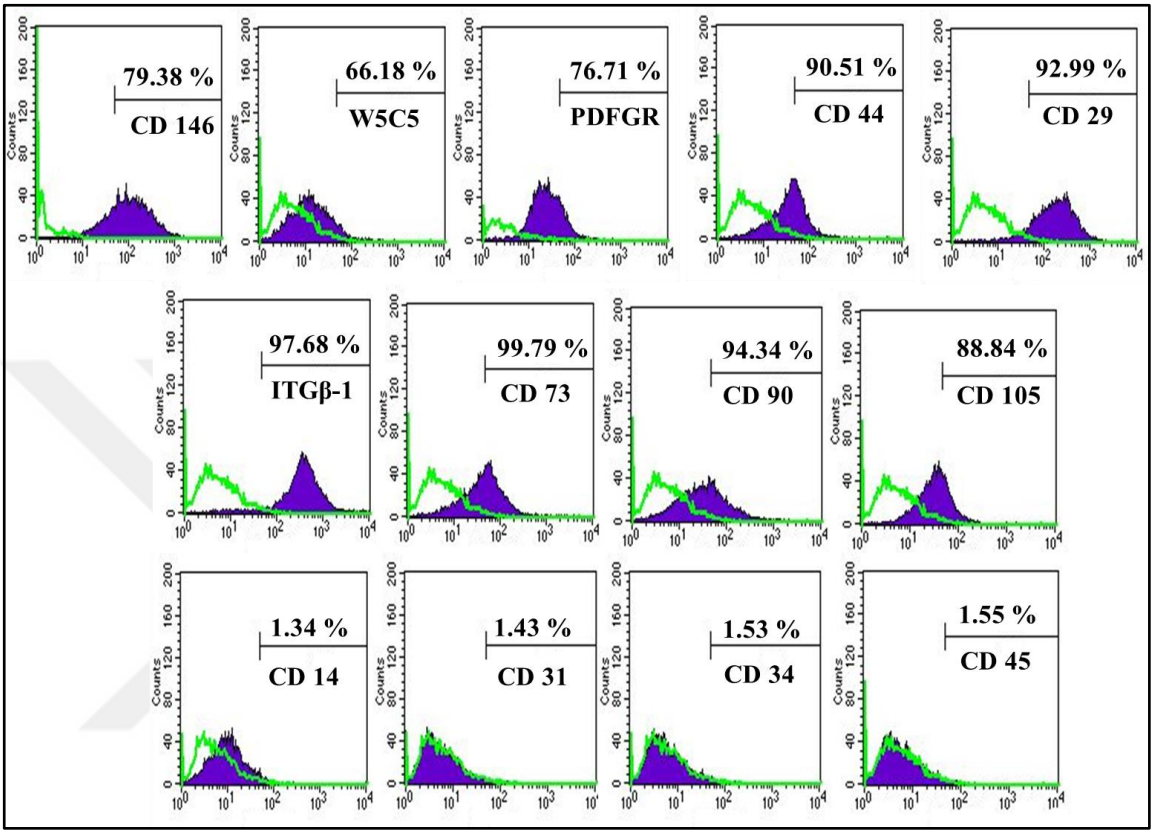

Figure 4.11. Characterization of peMSCs isolated by non-enzymatic method by flow cytometry for Group-5. 1x 10^4 cells were read into the flow cytometer for each marker. Cells incubated with isotype IgG antibody was used as negative control (NC) and it was presented by green line.

peMSCs were isolated with non-enzymatic procedure at passage 3 were characterized using Flow Cytometry. The isolated peMSCs were tested positive for MSC markers including CD 146, PDGFR, W5C5, CD 44, CD 29, ITGβ-1, CD 73, CD 90, and CD 105 but negative for hematopoietic stem cell markers CD 14, CD 31, CD 34, and CD 45 (Figure 4.11). peMSCs expressed 79.38 percent CD146, 66.18 percent W5C5, 76.71 percent PDGFR, 90.51 percent CD44, 92.99 percent CD29, 97.68 percent Integrin β1, 99.79 percent CD73, 94.34 percent CD90, 88.84 percent CD105, 1.34 percent CD14, 1.43 percent CD31, 1.53 percent CD34,

1.55 percent CD45. Cells incubated with isotype IgG antibody was used as negative control (NC) in Figure 4.11.

The mean values and standard deviations of eMSCs isolated from endometrium samples taken from five healthy volunteers and endometriosis patients are given in the Table 4.1.

Table 4.1. Average percentage of stem cells markers in five different heMSCs and peMSCs.

	heMSCs		**peMSCs**		
CD Markers Name	**%**	**± SD**	**%**	**± SD**	**p Value**
CD 146	42.74	3.08	75.52	2.49	****** (p< 0.0001)**
W5C5	44.6	2.36	73.99	6.29	****** (p< 0.0001)**
PDGFR	43.38	4.1	73.99	2.29	****** (p< 0.0001)**
CD 44	92.03	4.29	94.08	4.07	**ns**
CD 29	93.93	5.42	95.65	1.58	**ns**
ITGß-1	92.2	7.59	97.93	0.8	**ns**
CD 73	91.86	6.1	96.7	2.02	**ns**
CD 90	94.9	7.04	97.74	1.96	**ns**
CD 105	90.91	5.67	87.43	3.65	**ns**
CD 14	1.76	0.93	1.4	0.37	**ns**
CD 31	1.13	0.49	1.2	0.19	**ns**
CD 34	1.6	0.78	1.6	0.39	**ns**
CD 45	1.41	0.34	0.96	0.4	**ns**

Table 4.1. presents the average percentage values for stem cell markers from five different heMSCs and peMSCs. Standard deviations of five different cell samples were shown with ±. Results were statistically analysed in GraphPad Prism 6 software program by 2way ANOVA multiple comparisons.

4.2. TG2 EXPRESSION AND ACTIVITY PROFILE OF eMSCs

In this section, TG2 gene expression, protein level and enzyme activity of heMSCs and peMSCs in five different groups were investigated. For this purpose, 3 x 10^5 cells per well of a 6-well plate was seeded for 48 hours and cell lysates were collected to detect mRNA and protein levels.

4.2.1. Detection of TG2 Gene Expression with Real-Time PCR

Cells seeded was used to determine mRNA levels of TG2 in all groups of isolated eMSCs using RT-PCR. The primers to be used for RT-PCR were purchased from Qiagen, and the details of the method were described in Section 3.5. 18sRNA was used as housekeeping gene and loading control. Quantification of TG2/18mRNA was performed from quantitation cycle (Cq) values plotted against log of known cDNA concentration using random18S rRNA samples. Results of all healthy and patient samples were presented in Figure 4.12.

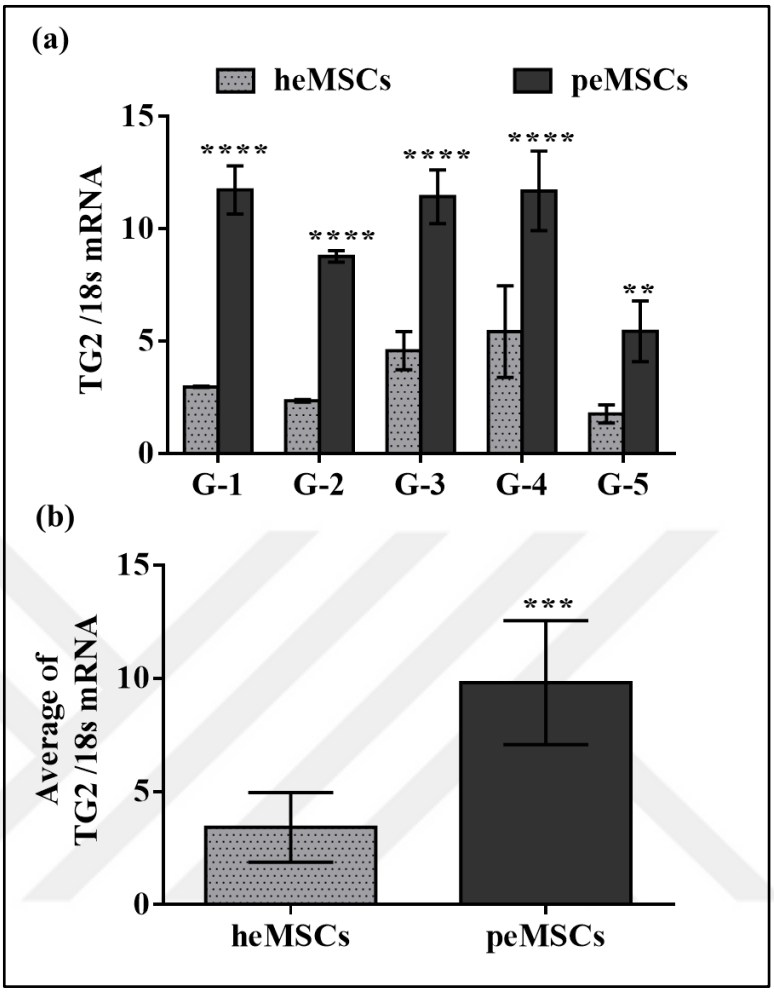

Figure 4.12. RT-PCR analysis of TG2 expressions in heMSCs and peMSCs. (a) Ratio of TG2 mRNA levels to 18srRNA in heMSCs and peMSCs of all groups (G-1 to G-5). (b) The average of TG2 mRNA levels versus 18srRNA for heMSCs and peMSCs of all groups. Results were statistically analysed in GraphPad Prism 6 software program by 2way ANOVA multiple comparisons for (a) and t test unpaired was used for (b). ** was used for $p<0.01$, *** was used for $p<0.001$ and **** was used for $p<0.0001$.

When samples of heMSCs in group-1 were compared with peMSCs (Figure 4.12.a.), peMSCs were found to express 4 times more TG2 genes compared to heMSCs. When similar comparisons were made for groups 2, 3, 4 and 5, peMSCs were shown to have 3.8, 2.5, 2.2 and 3.1 times more TG2 expression than heMSCs, respectively. Comparison of average of TG2 mRNA values for heMSCs and peMSCs samples in five different groups showed that peMSCs possessed 2.9 times more TG2 mRNA than heMSCs ($p<0.001$).

4.2.2. Analysis of TG2 Protein Levels by Western Blot

TG2 protein levels in cells was determined by performing Western Blot analysis (described in Section 3.6.4.) following the SDS–polyacrylamide gel electrophoresis (described in Section 3.6.3.) Separated proteins were probed for TG2 antigen using CUB 7402 antibody. In addition, β-actin antibody was used to determine the equal loading of proteins. Western Blot experiment was independently performed on five different groups consisting of five different heMSCs and peMSCs (Figure 4.13).

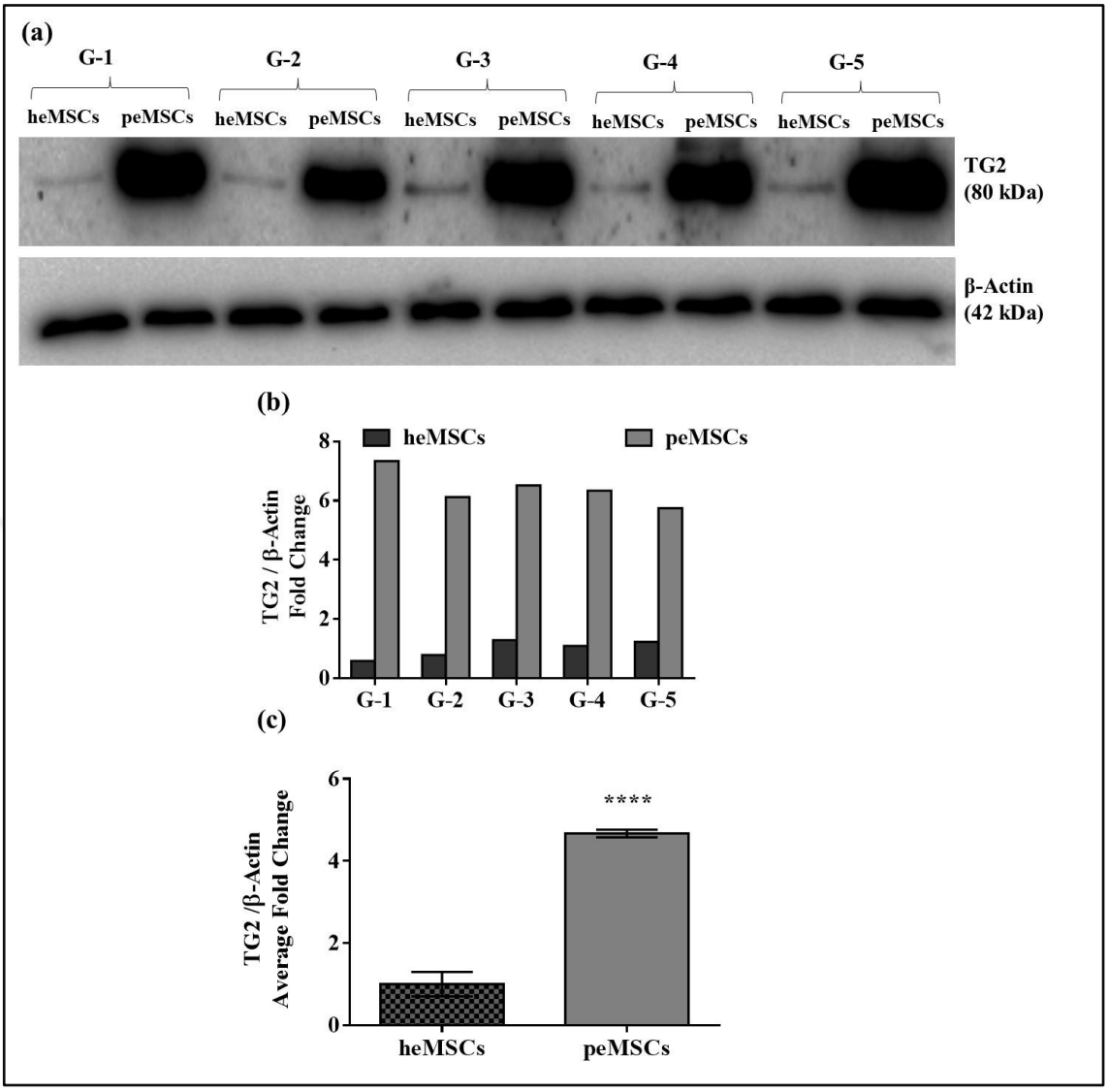

Figure 4.13. TG2 protein level in all isolated eMSCs. Cells used in all groups (G-1 to G-5) for this experiment was at passage 3. (a) Western Blot analysis of TG2 protein level in five different groups. Cell lysates were separated in an 8 percent SDS-PAGE gel and blotted on 0.45 μm nitrocellulose membrane. (b) Analysis of TG2 protein level in five different groups of heMSCs and peMSCs. Band intensities were quantified using Image J analysis. (c) Average TG2 protein levels for heMSC and peMSC of five different groups. Mean of TG2 / β-Actin values for each group member was used to construct the graph and the value of $p < 0.0001$ was symbolized by ****.

TG2 level in Group-1 peMSC was higher than heMSC by 7.4 folds. Group-2 peMSCs had 6.1 times higher TG2 protein levels compared to heMSCs. Similar results were also observed

in protein samples of peMSCs from Group 3, Group 4 and Group 5 by 6.5, 6.3, and 5.8 folds. In Figure 4.13.c., the mean value of TG2 protein level of all groups was calculated, and the statistical results were evaluated with the Oneway ANOVA test in GraphPad Prism 6. It was observed that peMSCs samples synthesized 4.7 times more TG2 protein than heMSCs samples ($p < 0.0001$).

4.2.3. TG2 Activity Levels in eMSCs by Biotin-X-Cadaverine Assay

The enzymatic activity of TG2 was determined by carrying out biotin-X-cadaverine (BTC) assay (Section 3.7). Assay principle relies on the incorporation of TG2 substrate BTC into fibronectin (FN) by the cell surface associated TG2. For this purpose, $0.3x10^5$ cells were seeded into each well of 96-well plates coated with FN in the presence of BTC. The amount of BTC cross-linked to FN by catalytically active cell surface TG2 was measured by extravidin-peroxide based assay. The BTC experiment was performed on heMSCs and peMSCs from five different groups (Figure 4.14).

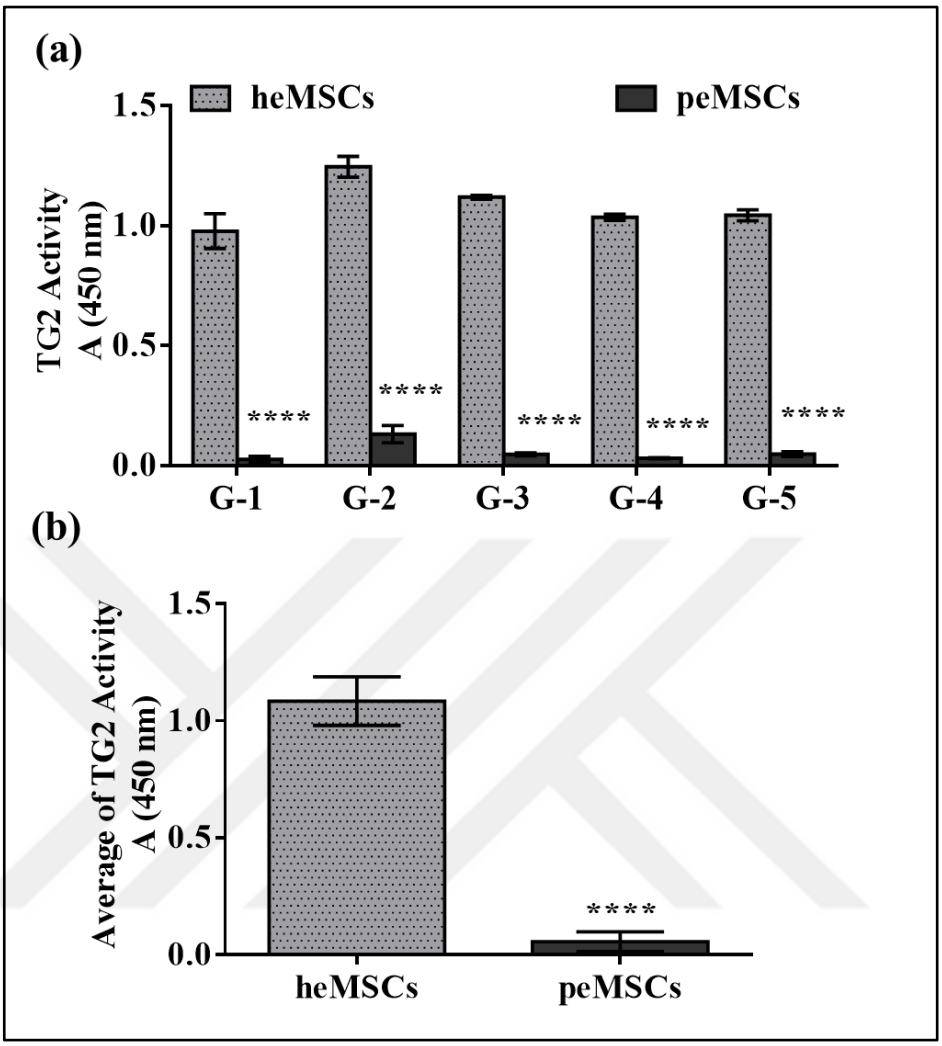

Figure 4.14. Analysis of TG2 activity in eMSCs for all groups (G-1 to G-5) by BTC assay. All eMSCs used in the experiments were at passage 3. (a) TG2 activity levels in individual heMSCs and peMSCs samples of five different groups. (b) Average of TG2 activity levels for heMSCs and peMSCs. Each data point represents mean absorbance value of five different groups ± STD. 2way ANOVA multiple comparisons (a) and t-test unpaired (b) from GraphPad Prism6 software program were used. The value of $p < 0.0001$ was symbolized by ****.

As shown in Figure 4.14.a, peMSC in group 1 had 36.7 times less TG2 activity than the group- 1 heMSCs. Similarly, there was a 9.5-fold decrease in TG2 activity of peMSCs when compared to heMSCs. TG2 enzyme activity was 24-fold, 32.2-fold and 21.6-fold less in eMSCs isolated from endometriotic tissue group 3, 4 and 5, respectively, in comparison to

heMSCs from corresponding groups. In the average, heMSCs had 19 times more TG2 activity than peMSCs with a significant difference of $p < 0.0001$.

4.3. ASSOCIATOIN OF TG2 WITH ITS BINDING PARTNERS ITGβ-1 AND SDC-4 IN eMSCs.

In this section, ITGβ1 and SDC4 gene expression levels and their interaction on the cell surface with TG2 in heMSCs and peMSCs in five different groups were investigated. For this purpose, 3×10^5 cells per well of a 6-well plate was seeded for 48 hours and cell lysates were collected to detect mRNA and protein levels. During the experiments, cells used were at third passage number.

4.3.1. Detection of ITGβ-1 and SDC-4 Gene Expression Levels in eMSCs by RT-PCR

Cells seeded was used to determine mRNA levels of ITGβ-1 and SDC-4 in all groups of isolated eMSCs using RT-PCR. The primers to be used for RT-PCR were purchased from Qiagen, and the details of the method were described in Section 3.5. 18sRNA was used as housekeeping gene and loading control. Quantification of ITGβ-1/18mRNA and SDC-4/18mRNA were performed from Cq values plotted against log of known cDNA concentration using random18S rRNA samples. Results of all healthy and patient samples are presented in Figure 4.15 and 4.16.

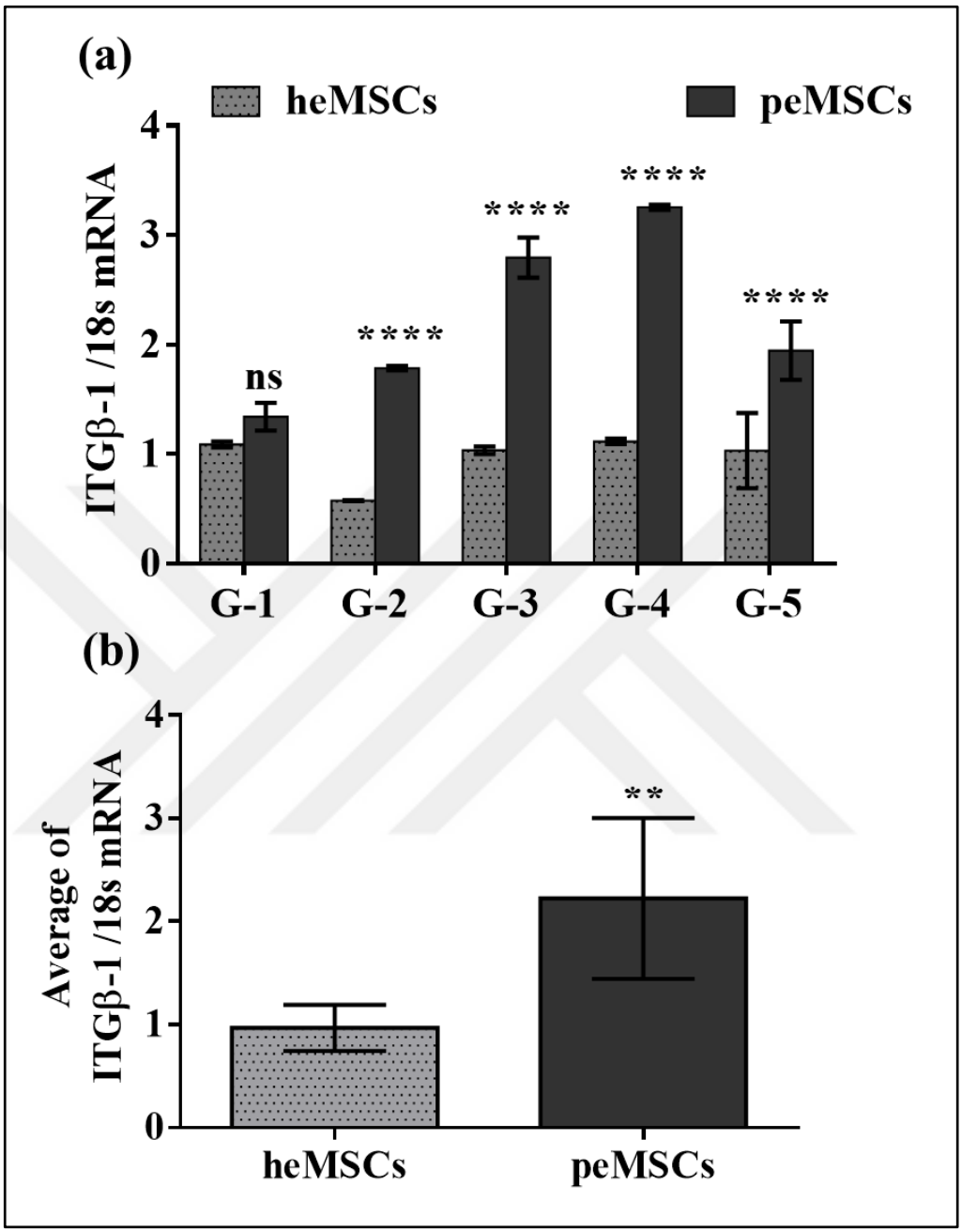

Figure 4.15. RT-PCR analysis of ITGβ-1 expressions in heMSCs and peMSCs. (a) Ratio of ITGβ-1 mRNA levels to 18srRNA in heMSCs and peMSCs of all groups (G-1 to G-5). (b) The average of ITGβ-1 mRNA levels versus 18srRNA for heMSCs and peMSCs of all groups. Results were statistically analysed in GraphPad Prism 6 software program by 2way ANOVA multiple comparisons for (a) and t test unpaired was used for (b). ns was used for non- significant, ** was used for $p<0.01$ and **** was used for $p<0.0001$.

ITGβ-1 levels expressed by each heMSCs and peMSCs samples from five different groups were normalized with 18srRNA (Figure 4.15.a.). According to the results of this analysis, no significant (ns) difference in ITGβ-1 expression was observed between heMSCs and peMSCs for group 1. When heMSCs samples of Group 2 were compared with peMSCs, it was found that peMSCs expressed 3.1 times more ITGβ-1 mRNA ($p<0.0001$). In Group 3 and 4, peMSCs expressed an average of 2.8-fold more ITGB1 than heMSCs samples, while peMSCs of group 5 showed 1.9 times more ITGB-1 expression ($p<0.0001$). When average ITGβ-1 expression values of heMSCs and peMSCs samples in five different groups were compared (Figure 4.15.b), ITGβ-1 gene expression was found to be higher in peMSCs than heMSCs by 2.3 folds ($p<0.01$).

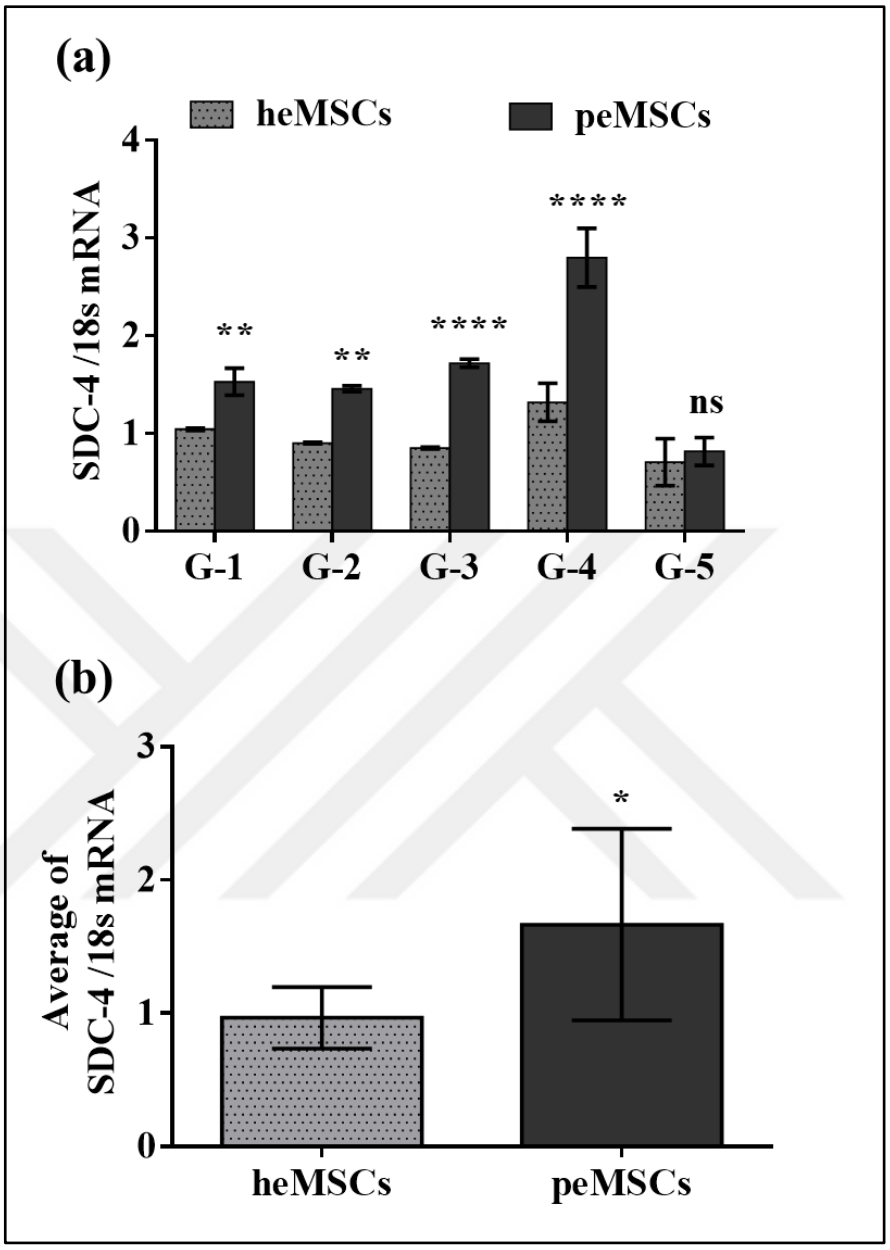

Figure 4.16. RT-PCR analysis of SDC-4 expressions in heMSCs and peMSCs. (a) Ratio of SDC-4 mRNA levels to 18srRNA in heMSCs and peMSCs of all groups (G-1 to G-5). (b) The average of SDC-4 mRNA levels versus 18srRNA for heMSCs and peMSCs of all groups. Results were statistically analysed in GraphPad Prism 6 software program by 2way ANOVA multiple comparisons for (a) and t test unpaired was used for (b). ns was used for non- significant, * was used for $p<0.05$, ** was used for $p<0.01$ and **** was used for $p<0.0001$.

SDC-4 levels expressed by each heMSCs and peMSCs samples from five different groups were normalized with 18srRNA (Figure 4.16.a.). According to the results of this analysis, when heMSCs samples were compared with peMSCs in group 1, it was found that peMSCs expressed 1.5 times ($p<0.01$) more SDC-4. Similar comparisons were performed for peMSCs samples in group 2, group 3, group 4 and group 5 and peMSCs were found to express 1.7 ($p<0.01$), 2.1 ($p<0.0001$), and 2.2 times ($p<0.0001$) more SDC-4, respectively. On the other hand, when the peMSCs in group 5 were compared with the heMSCs sample, no statistically significant difference was found between them. The average of SDC-4 expression values of heMSCs and peMSCs samples in five different groups are presented in Figure 4.16.b. When peMSCs samples were compared with heMSCs, it was found that heMSCs expressed approximately 1.8 times less SDC-4 gene expression ($p <0.05$).

4.3.2. CO-IP Results for eMSC

The association of novel cell adhesion and migration protein TG2 with ITGβ-1 and SDC-4 on the cell surface was determined using the immuno-precipitation method described in detail in Section 3.8 for five different groups of heMSCs and peMSCs. For this purpose, protein isolation was performed 48 hours after cells seeding and cell membrane lysates were pulled with anti- ITGβ-1 or –SDC-4 antibody, separated on the SDS-PAGE and then transferred to a nitrocellulose membrane to be probed with anti-TG2 CUB 7402 antibodies. In order to validate equal loading, whole cell lysates inputs were used for Western blot analysis for ITGβ-1 or SDC-4 expression.

In Figure 4.17.a, the whole cell lysate of five different heMSCs and peMSCs in all groups were firstly pull down with the ITGβ-1 antibody and then probed with the TG2 CUB 7402 antibody, so that complex formation between TG2 and ITGβ1 can be visualized.

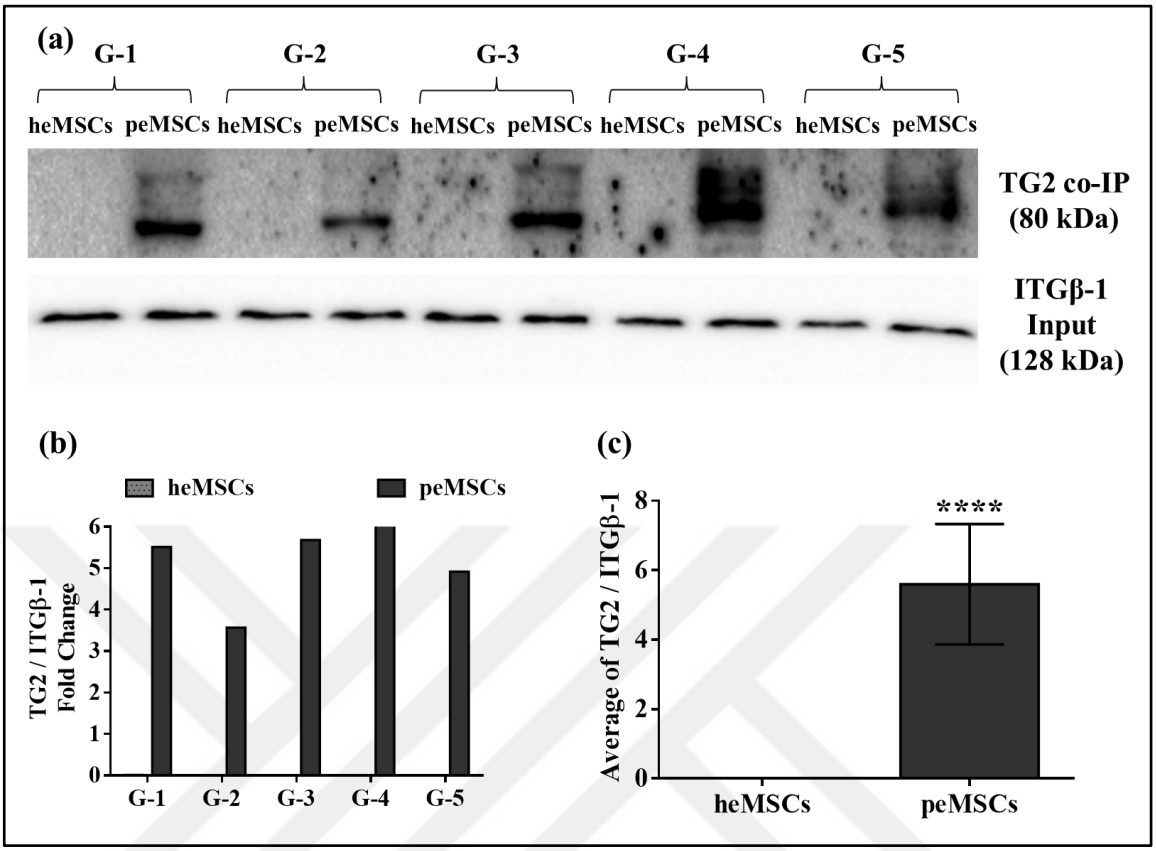

Figure 4.17. co-IP results of complex of TG2 with ITGβ-1 in eMSCs. (a) The membrane image of eMSCs membrane lysates probed with TG2 after pull-down with ITGβ-1. Band intensities were quantified using Image J analysis. (b) The results of the co-IP method for five different groups. (c) Mean values of co-IP results obtained for five different groups. The t-test unpaired tab of the GraphPad Prism 6 software program was used to determine the statistical significance value, and $p < 0.0001$ was indicated by ****.

In Figure 4.17.b, the fold changes of the co-IP results measured by Image J of the different heMSCs and peMSCs of five different groups showed that TG2 / ITGβ-1 complex formation for group 1 heMSCs was 5.5 times less than peMSCs. Similar results were obtained for groups 2, 3, 4 and 5, with 3.6-, 5.7-, 8.3- and 5-fold higher than TG2 / ITGβ-1 complex in peMSCs than heMSCs. Figure 4.17.c presenting the average band intensity obtained for TG2 of each heMSCs and peMSCs groups indicated that there was 5.6 times higher TG2 / ITGβ-1 complex formation on peMSCs cell surface than heMSCs ($p < 0.0001$).

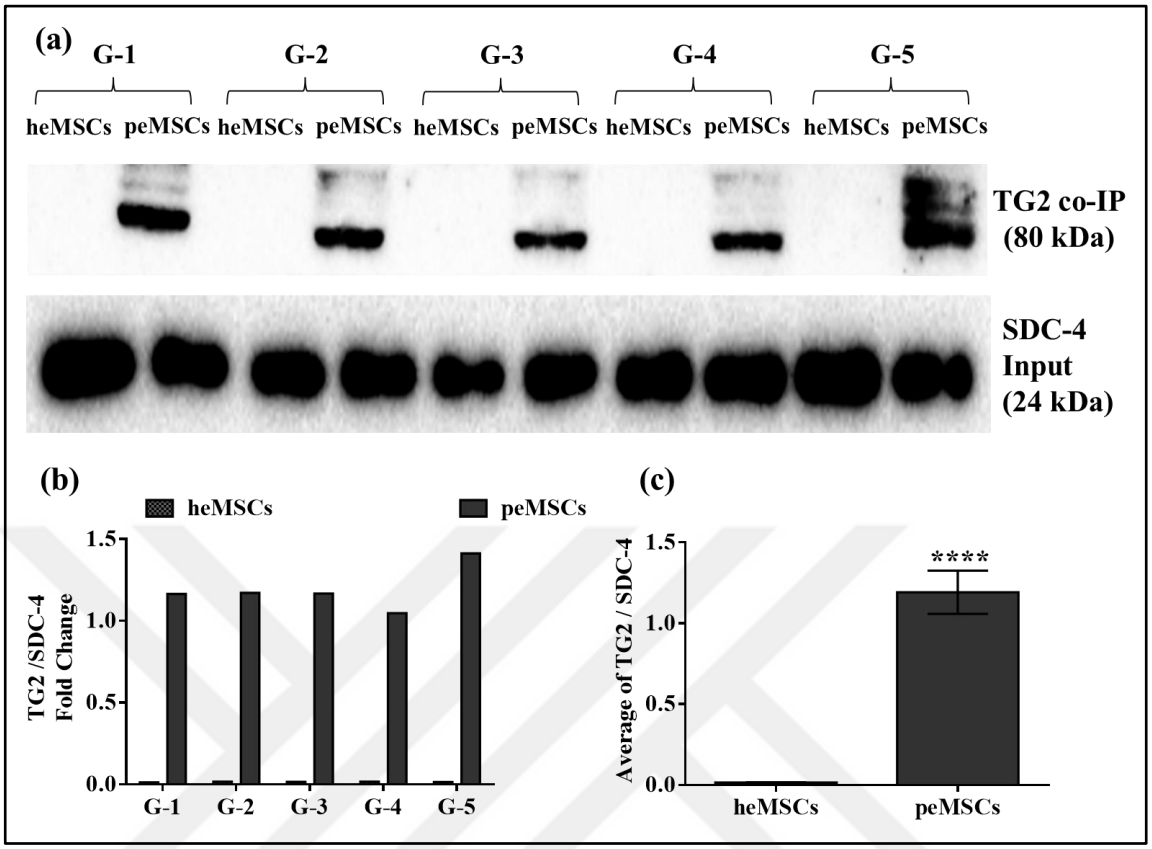

Figure 4.18. co-IP results of complex of TG2 with SDC-4 in eMSCs. (a) The membrane image of eMSCs protein lysates probed with TG2 after pull-down with SDC-4. Band intensities were quantified using Image J analysis. (b) The results of the co-IP method for five different groups. (c) Mean values of co-IP results obtained for five different groups. The t-test unpaired tab of the GraphPad Prism 6 software program was used to determine the statistical significance value, and $p < 0.0001$ was indicated by ****.

When level of TG2 in complex with SDC-4 in heMSCs and peMSCs of five different groups were compared (Figure 4.18.b.), TG2 band intensity of peMSCs was found to be 1.2-fold higher for Group 1-4 and 1.5-fold higher for Group 5. The average level of TG2 in complex with SDC-4 on peMSCs plasma membrane was 1.24 times more than heMSCs ($p < 0.0001$).

4.4. SILENCING OF TG2 in eMSCs

RT-PCR, Western Blot and BTC experiments were performed in order to determine the expression level of silencing of TG2 gene and to determine its protein levels and cross-linking enzyme activity in peMSCs samples, respectively.

4.4.1. Determination of TG2 Gene Expression in shRNA Lentivirus-Treated eMSCs Using Real-Time PCR

RT-PCR method described in Section 3.5. was applied to the five different groups of healthy and patient cell samples for determining the TG2 level of these samples, following the shRNA transduction detailed in Section 3.14. 48 hours after seeding, heMSCs and peMSCs samples at same passage number were used for RNA isolation. The assay setup includes samples of untreated heMSCs, scrambled shRNA-treated heMSCs (heMSCs + SCR), scrambled shRNA-treated peMSCs (peMSCs + SCR), and finally shRNA-treated (targeting TG2) peMSCs (peMSCs + shRNA). These experiments were performed in all healthy and patient cell samples, and the same experimental setup was used in further experiments to clarify the role of TG2 in the development of endometriosis. The primers to be used for RT-PCR were purchased from Qiagen, and the details of the method were described in Section 3.5. 18sRNA was used as housekeeping gene and loading control. Quantification of TG2/18mRNA was performed from quantitation cycle (Cq) values plotted against log of known cDNA concentration using random18S rRNA samples. Results of all healthy and patient samples were presented in Figure 4.19.

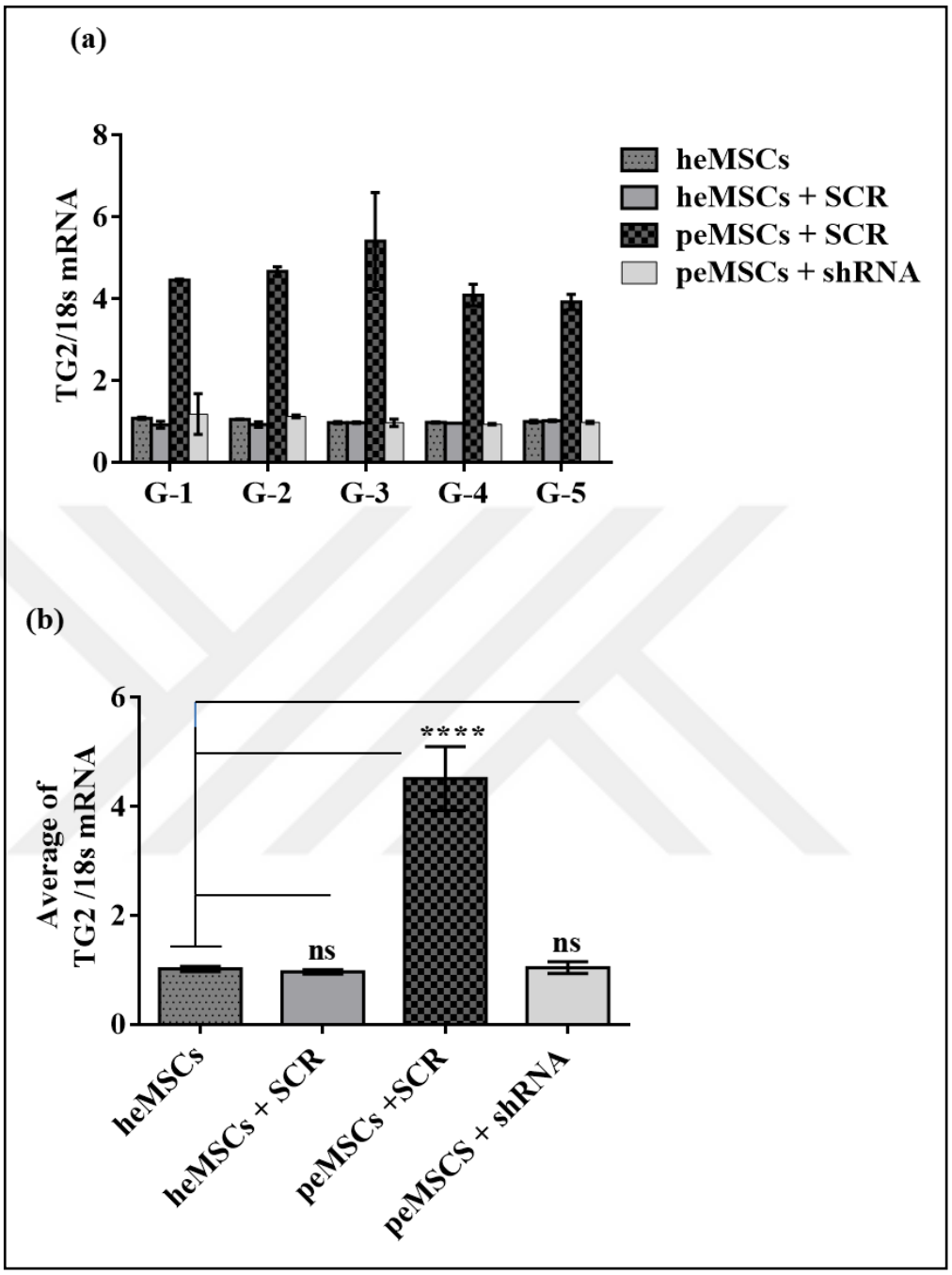

Figure 4.19. Determination of TG2 mRNA levels in eMSCs transduced with control scrambled (SCR) or TG2 targeting lentiviral shRNA (shRNA). (a) TG2 expression in five different eMSCs Groups (G-1 to G-5) following shRNA transduction. (b) The average of silenced TG2 expression values of all samples from five different groups. All statistical results were analysed in GraphPad Prism 6 software program by One-way ANOVA multiple comparisons. ns was used for non- significant, while **** was used for $p<0.0001$.

In Figure 4.19., changes in TG2 gene expression after shRNA lentivirus application to heMSCs and peMSCs samples were presented and results were obtained by comparing the samples in each group with the corresponding heMSCs. In this context, heMSCs samples for group 1 were compared with heMSCs + SCR, peMSCs + SCR and peMSCs + shRNA samples in the same group, and heMSCs were found to have the same TG2 expression level as heMSCs + SCR and peMSCs + shRNA samples. The treatment of G1 peMSCs with TG2 targeting shRNA lentiviral particles led to 3.75-fold decrease in TG2 expression. Similar results were found for groups 2,3,4 and 5 such as heMSCs samples in these groups were found to express TG2 at the same level as heMSCs + SCR and peMSCs + shRNA samples. Transduction of peMSCs with TG2-targeting shRNA-bearing viral particles (peMSCs + shRNA) resulted in a 4.2-fold decrease in Group 2, while this value was 5.5-fold for Group 3, 4.3-fold for Group 4 and 4-folds for group 5. In average, when the peMSCs + SCR samples were compared with the shRNA treated peMSCs, a 4.3-fold ($p<0.0001$) decrease in TG2 expression was detected in peMSCs + shRNA samples, after shRNA transduction (Figure 4.19.b).

4.4.2. Determination of TG2 Protein Level in shRNA Lentivirus-Treated eMSCs Using Western Blot

Following the shRNA silencing of TG2 in heMSCs, heMSCs + SCR, peMSCs + SCR, and peMSCs + shRNA, TG2 protein level was investigated using standard Western Blot and the results were presented in Figure 4.20. The band densities on the membrane were measured and quantified using the Image J software program and presented in Figure 4.21.a.

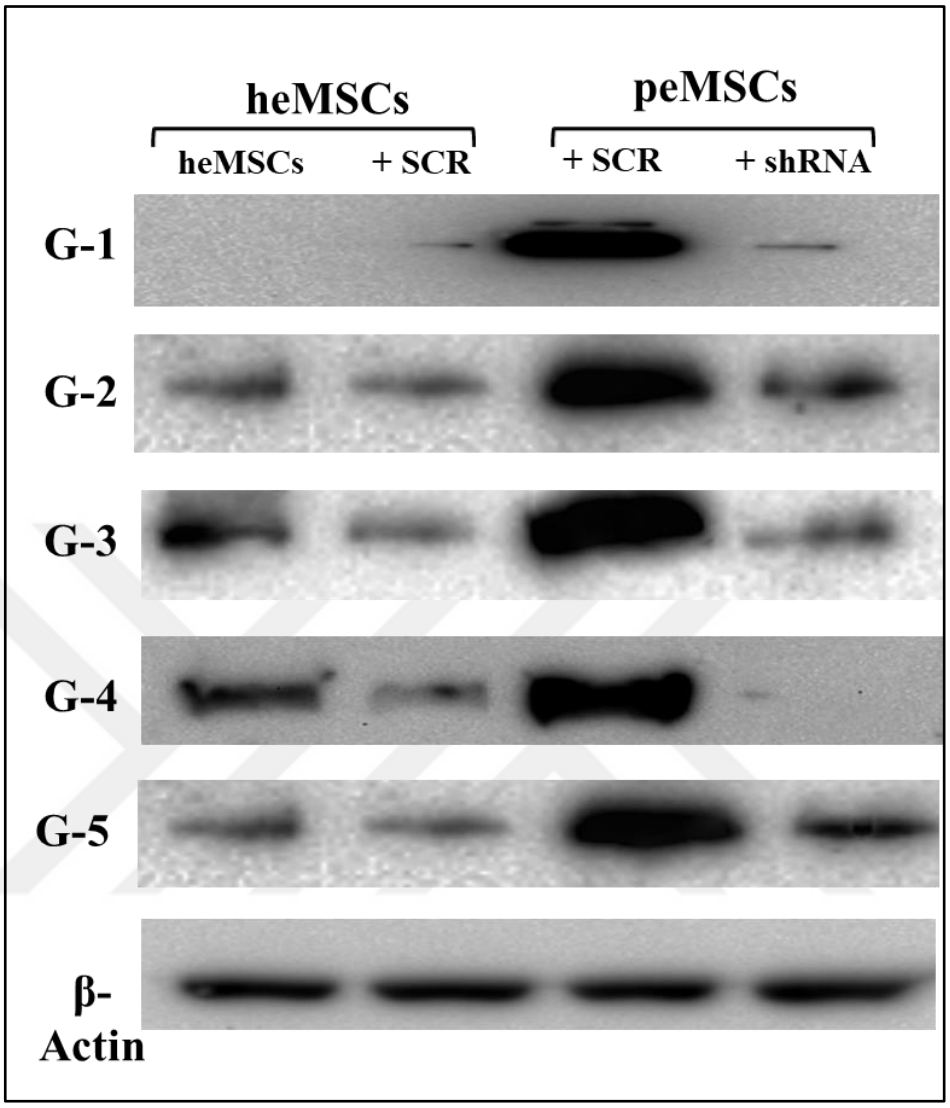

Figure 4.20. Determination of TG2 protein level in eMSCs transduced with control scrambled (SCR) or TG2 targeting lentiviral shRNA (shRNA) by Western Blot in five different groups. Cell lysates were separated in an 8 percent SDS-PAGE gel and blotted on 0.45 μm nitrocellulose membrane.

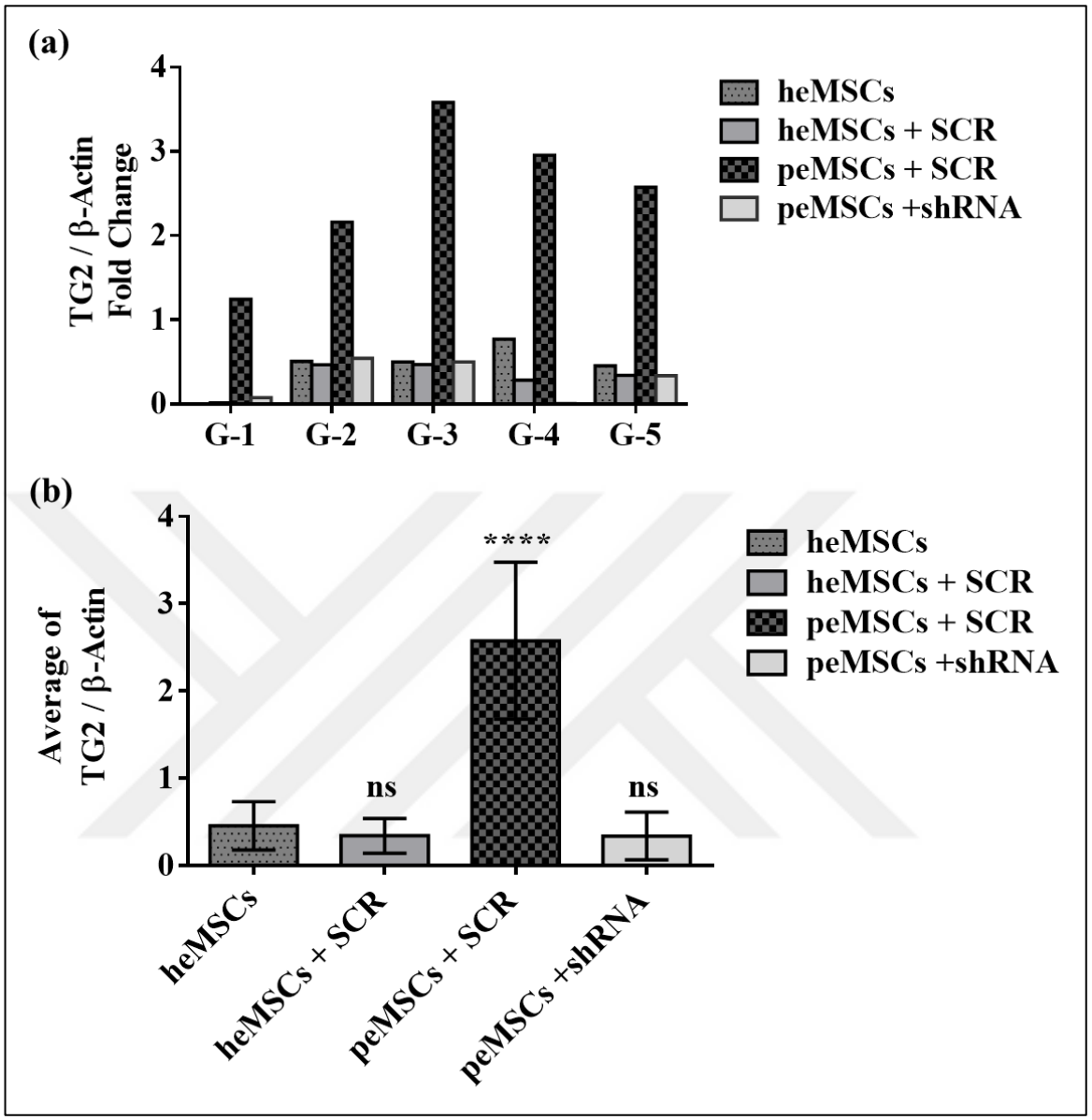

Figure 4.21. Determination of TG2 protein level in eMSCs transduced with control scrambled (SCR) or TG2 targeting lentiviral shRNA (shRNA). (a) TG2 protein level in five different eMSCs Groups (G-1 to G-5) following shRNA transduction. (b) The average of silenced TG2 protein level values of all samples from five different groups. All statistical results were analyzed in GraphPad Prism 6 software program by One-way ANOVA multiple comparisons. ns was used for non- significant, while **** was used for $p<0.0001$.

The quantitative results of the band densities in the membrane were determined using the Image J software program, and in Figure 4.21.a., the band densities were presented by adjusting the control load to β-actin.

Group 4 and 2.37 for Group 5. The reduction of TG2 expression in peMSCs by shRNA (peMSCs + shRNA) measured TG2 protein level was similar when compared with heMSCs and heMSCs + SCR (Figure 4.21.b). A similar comparison was made between the peMSCs samples and the peMSCs +shRNA samples on the same graph, peMSCs was observed to express 2.6 times more TG2 protein level than peMSCs + shRNA, and a significant $p<0.00001$ value was shown with ****.

4.4.3. Determination of TG2 Enzyme Activity in shRNA Lentivirus-Treated eMSCs Using BTC Assay

heMSCs and peMSCs cells treated with control shRNA (SCR) and shRNA particles were used in the biotin-X-cadaverine assay (Section 3.7) to measure cell surface TG2 enzyme activity. The passage number of all cells used in the BTC assay was three. Five different groups were established to be used for this experiment setup just as in the previous experiments. Each group was included heMSCs, heMSCs + SCR, peMSCs + SCR, and peMSCs + shRNA.

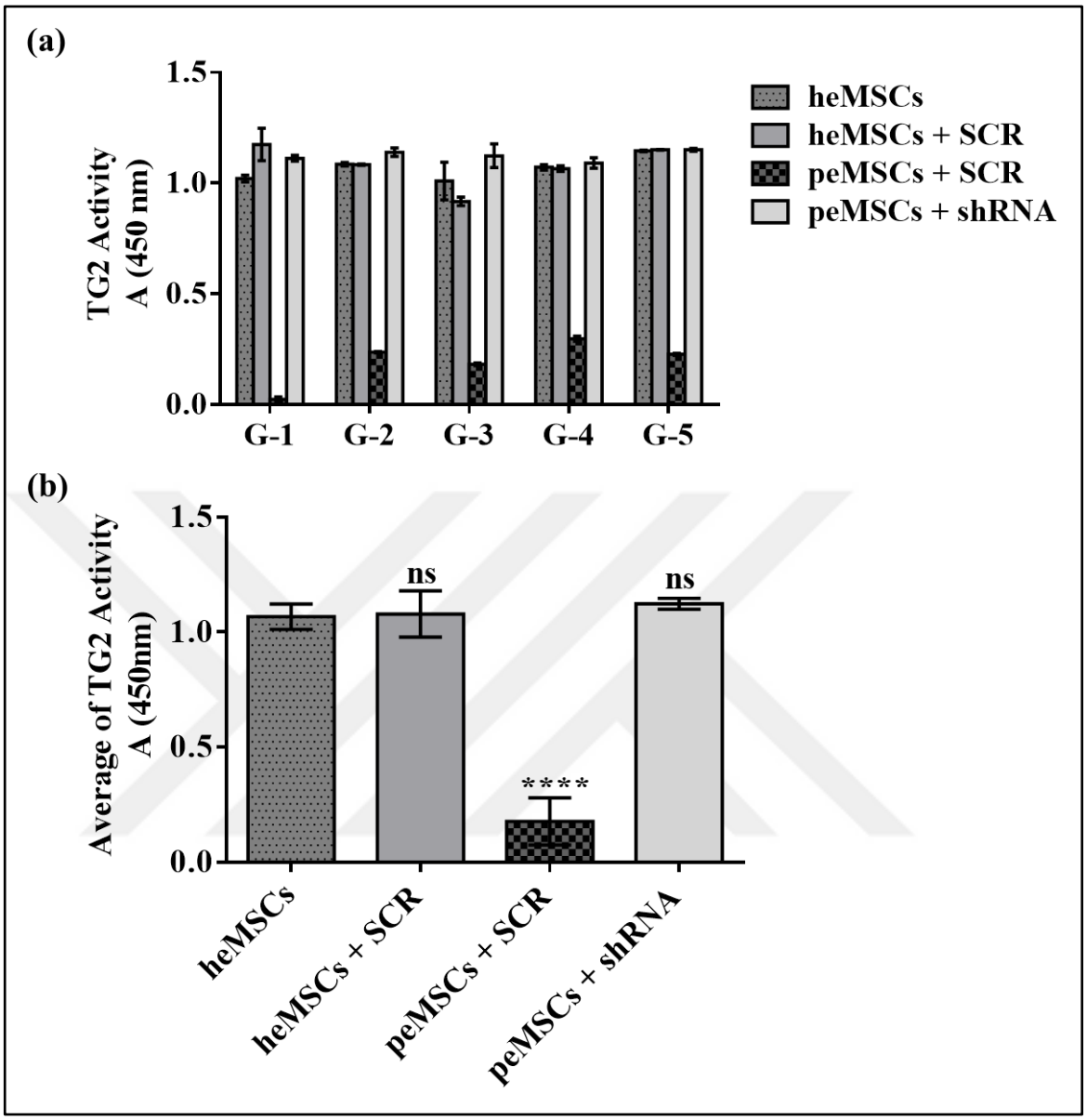

Figure 4.22. Determination of TG2 enzymatic activity in eMSCs transduced with control scrambled (SCR) or TG2 targeting lentiviral shRNA (shRNA). (a) TG2 enzymatic activity in five different eMSCs Groups (G-1 to G-5) following shRNA transduction. (b) The average of silenced TG2 enzymatic activity values of all samples from five different groups. All statistical results were analyzed in GraphPad Prism 6 software program by One-way ANOVA multiple comparisons. ns was used for non- significant, while **** was used for $p<0.0001$.

The biotin-x-cadaverine assay was performed to demonstrate the change in enzymatic activity of TG2 following shRNA transduction in five different groups as demonstrated in Figure 4.22.a. When heMSCs samples in Group-1 were compared with heMSCs + SCR, peMSCs + SCR and peMSCs + shRNA samples, TG2 enzyme activity were found to be the same in all samples. On the other hand, peMSCs + SCR sample in Group-1 had 4.9 times less TG2 enzyme compared to heMSCs sample. Similar comparisons were made with the samples of groups 2, 3, 4 and 5 showing that heMSCs, heMSCs + SCR, peMSCs + shRNA samples contained similar levels of TG2 enzyme activity with 1.01, 1.10 and 1.15 absorbance units (A_{450nm}), respectively. In addition, peMSCs + SCR samples in groups 2, 3, 4 and 5 were found to contain 4.8-, 6.5-, 4- and 5.2-times less TG2 enzyme, respectively, when compared to heMSCs samples. Figure 4.22.b which shows average TG2 enzyme activity for all SCR or shRNA treated samples in five different groups indicated that heMSCs, heMSCs + SCR, peMSCs + shRNA samples had similar TG2 enzyme in an average ratio of 1.1 absorbance unit (A_{450nm}). When the mean TG2 enzyme level of peMSCs + SCR samples in five different groups was compared with that of heMSCs samples, peMSCs + SCR samples demonstrated an average of 5 times ($p < 0.00001$) less TG2 enzyme activity.

4.5. EFFECT OF TG2 IN STEMNESS POTENTIAL OF eMSCs

After applying control shRNA (SCR) and TG2-targeted shRNA to eMSCs in five different groups, the change in stemness potentials were investigated by flow cytometry and Colony-Forming Unit (CFU) experiments. In the experiments, the passage number of the cells used was three.

4.5.1. Determination of Cell Surface Stem Cell markers in shRNA Lentivirus-Treated eMSCs using Flow Cytometry Analysis

Levels of cell surface stem cell markers after SCR or shRNA application to heMSCs and peMSCs samples in five different groups were determined by flow cytometry technique as described in detail in Section 3.4. eMSCs seeded at 3x 105 cells per well in 6-well plates and incubated for 16 hours were probed with anti-CD 146, -PDGFR, W5C5, -CD 44, -CD 29, -ITGB-1, -CD 73, -CD 90, -CD 105, -CD 14, -CD 31, -CD 34, and -CD 45 antibodies.

Flow cytometry analysis for expression of stem cell marker in heMSCs, heMSCs + SCR, peMSCs + SCR ve peMSCs +shRNA samples in Group-1 were given in Figures 4.23 and 4.24.

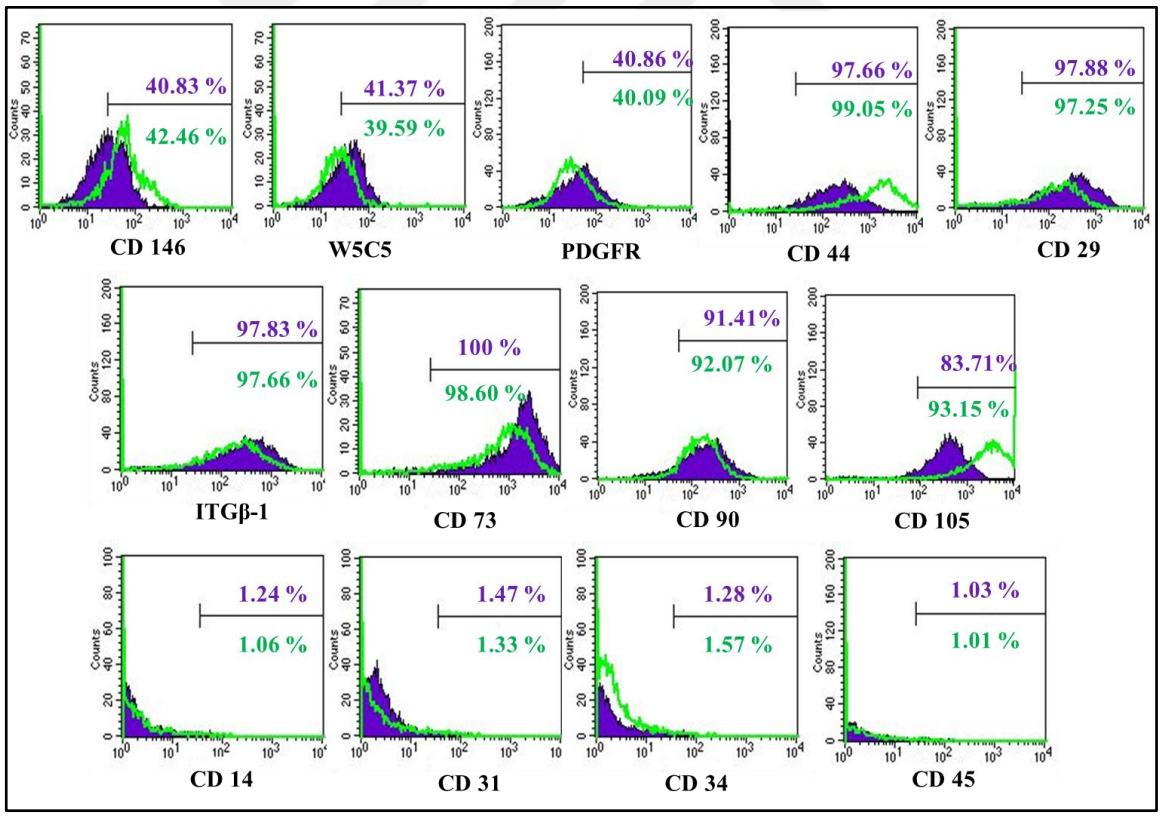

Figure 4.23. heMSCs and heMSCs + SCR samples in Group-1 are presented with overlapped forms of stem cell markers. heMSC samples are represented by a purple line while heMSCs + SCR samples are indicated by a green line.

heMSCs displayed 40.83 percent CD 146, 41.37 percent W5C5, 40.86 percent PDGFR, 97.66 percent CD 44, 97.80 percent CD 29, 97.83 percent ITGβ-1, 100 percent CD 73, 91.41 percent CD 90, 83.71 percent CD 105, 1.24 percent CD 14, 1.47 percent CD 31, 1.28 percent CD 34 and 1.03 percent CD 45 (Figure 4.23). heMSCs + SCR expressed 42.46 percent CD146, 39.59 percent W5C5, 40.09 percent PDGFR, 99.05 percent CD 44, 97.25 percent CD 29, 97.66 percent ITGβ-1, 98.60 percent CD 73, 92.07 percent CD 90, 93.15 percent CD 105, 1.06 percent CD 14, 1.33 percent CD 31, 1.57 percent CD 34 and 1.01 percent CD 45 (Figure 4.23).

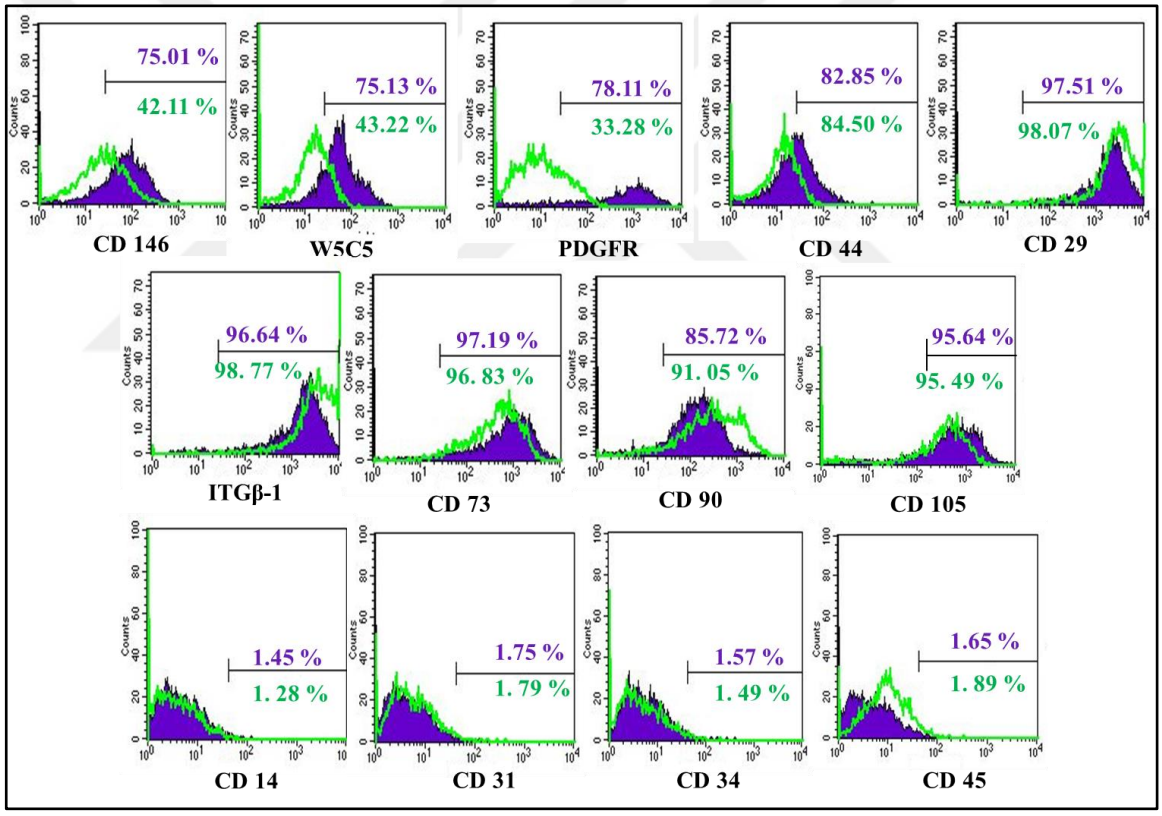

Figure 4.24. peMSCs + SCR and peMSCs + shRNA samples in Group-1 are presented with overlapped forms of stem cell markers. peMSCs samples are represented by a purple line while peMSCs + shRNA samples are indicated by a green line.

The peMSCs + SCR sample isolated by non-enzymatic method was peMSCs expressed 75.01 percent CD146, 75.1 percent W5C5C, 78.11 percent PDGFR, 82.85 percent CD 44, 97.51 percent CD 29, 96.64 percent ITGβ-1, 97.19 percent CD 73, 85.72 percent CD 90,

95.64 percent CD 105, 1.45 percent CD 14, 1.75 percent CD 31, 1.57 percent CD 34 and 1.65 percent CD 45 (Figure 4.24). peMSCs + shRNA expressed 42.11 percent CD146, 43.22 percent W5C5, 33.28 percent PDGFR, 84.50 percent CD 44, 98.70 percent CD 29, 98.77 percent ITGβ-1, 96.83 percent CD 73, 91.05 percent CD 90, 95.49 percent CD 105, 1.28 percent CD 14, 1.79 percent CD 31, 1.49 percent CD 34 and 1.89 percent CD 45 (Figure 4.24).

The results of flow cytometric technique performed to determine the silencing of TG2 in stemness potential of heMSCs, heMSCs + SCR, peMSCs + SCR ve peMSCs +shRNA samples in Group-2 were given in Figures 4.25 and 4.26.

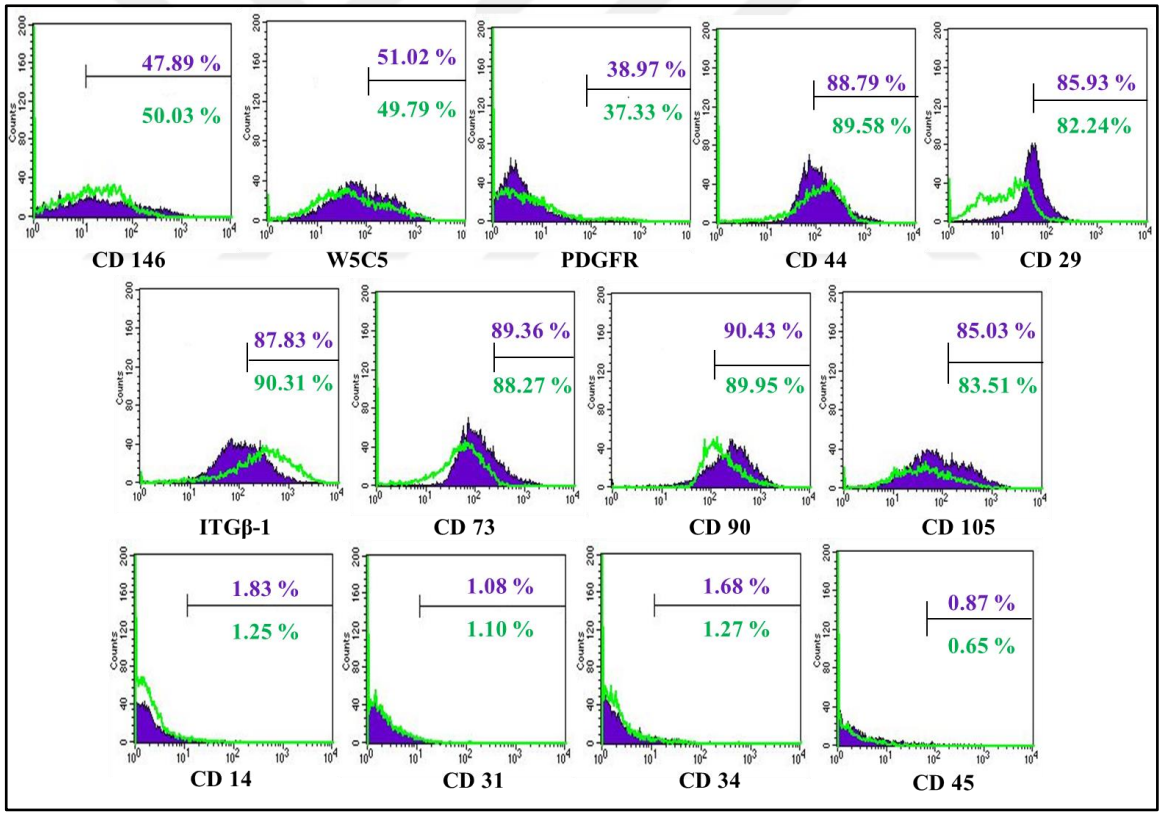

Figure 4.25. heMSCs and heMSCs + SCR samples in Group-2 are presented with overlapped forms of stem cell markers. heMSC samples are represented by a purple line while heMSCs + SCR samples are indicated by a green line.

The heMSCs isolated by non-enzymatic method heMSCs expressed 47.89 percent CD146, 51.02 percent W5C5, 38.97 percent PDGFR, 88.79 percent CD 44, 85.93 percent CD 29, 87.83 percent ITGβ-1, 89.6 percent CD 73, 90.43 percent CD 90 , 85.03 percent CD 105, 1.83 percent CD 14, 1.08 percent CD 31, 1.68 percent CD 34 and 0.87 percent CD 45 (Figure 4.25). heMSCs + SCR expressed 50.03 percent CD146, 49.79 percent W5C5, 37.33 percent PDGFR, 89.58 percent CD 44, 82.24 percent CD 29, 90.31 percent ITGβ-1, 88.27 percent CD 73, 89.95 percent CD 90, 83.51 percent CD 105, 1.25 percent CD 14, 1.10 percent CD 31, 1.27 percent CD 34 and 0.65 percent CD 45 (Figure 4.25).

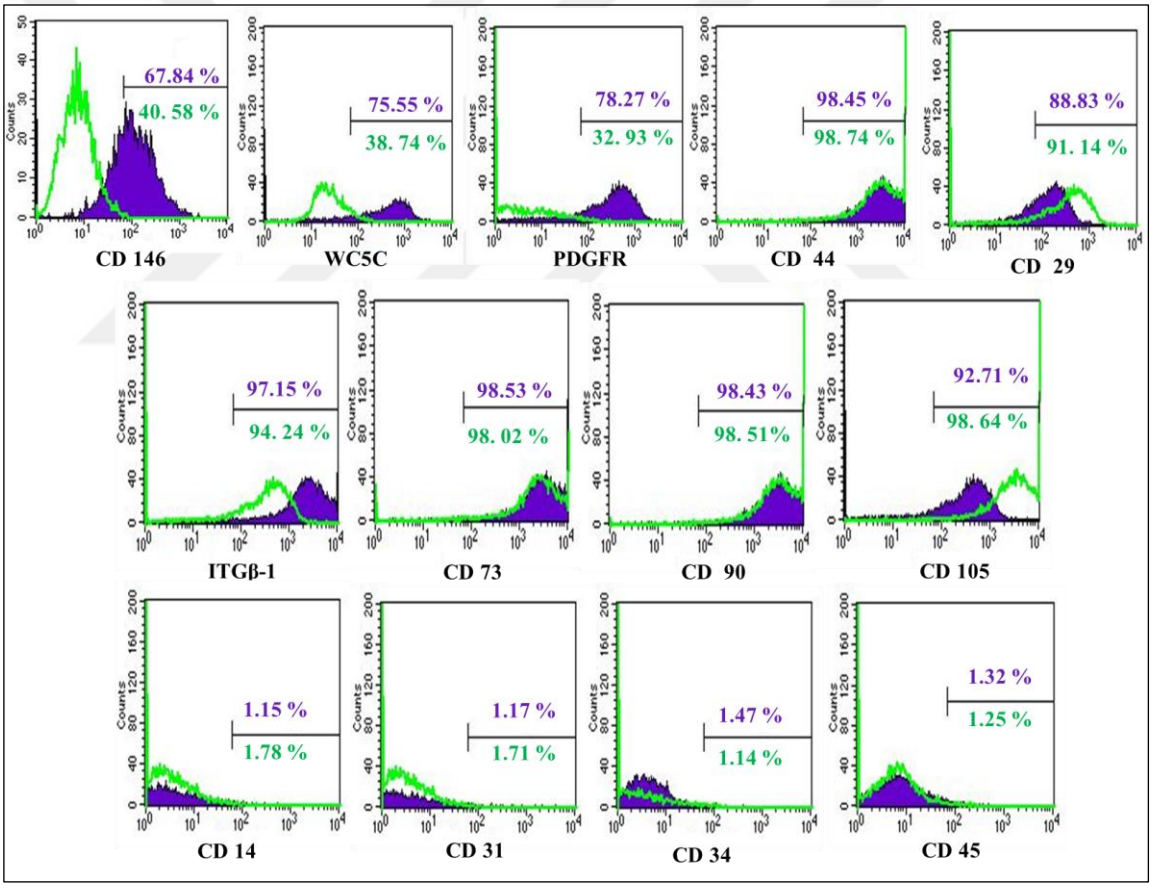

Figure 4.26. peMSCs + SCR and peMSCs + shRNA samples in group-2 are presented as overlapped forms of stem cell markers. The peMSCs + SCR sample is indicated by the purple line, while the peMSCs + shRNA sample is indicated by the green line.

The peMSCs + SCR sample isolated by non-enzymatic method was peMSCs + SCR expressed 67.84 percent CD146, 75.55 percent W5C5, 78.27 percent PDGFR, 98.45 percent CD 44, 88.83 percent CD 29, 97.15 percent ITGβ-1, 98.53 percent CD 73, 98.43 percent CD 90, 92.71 percent CD 105, 1.15 percent CD 14, 1.17 percent CD 31, 1.47 percent CD 34 and 1.32 percent CD 45 (Figure 4.26). peMSCs + shRNA expressed 40.58 percent CD146, 38.74 percent W5C5, 32.93 percent PDGFR, 98.74 percent CD 44, 91.14 percent CD 29, 94.24 percent ITGβ-1, 98.02 percent CD 73, 98.51 percent CD 90, 98.64 percent CD 105, 1.15 percent CD 14, 1.17 percent CD 31, 1.47 percent CD 34 and 1.32 percent CD 45 (Figure 4.26).

The results of flow cytometric technique performed to determine the silencing of TG2 in stemness potential of heMSCs, heMSCs + SCR, peMSCs + SCR ve peMSCs +shRNA samples in Group-3 were given in Figures 4.27 and 4.28.

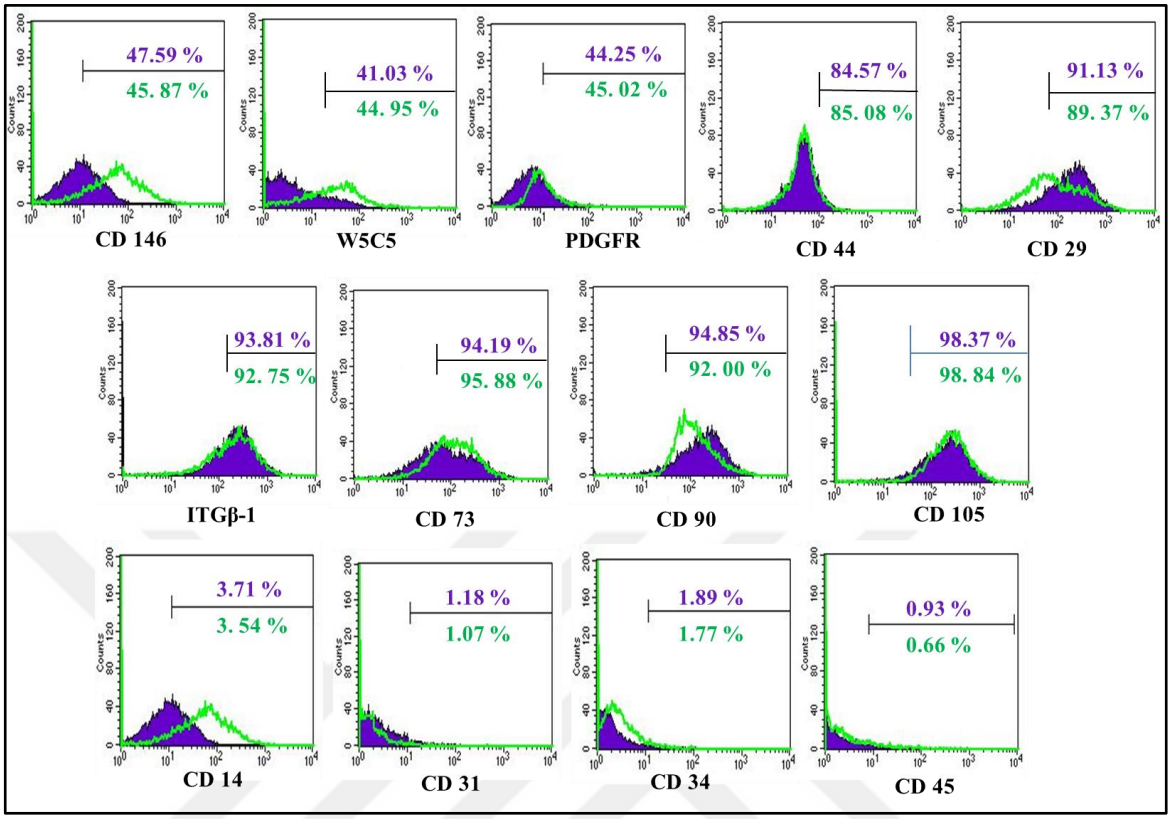

Figure 4.27. heMSCs and heMSCs + SCR samples in Group-3 are presented with overlapped forms of stem cell markers. heMSCs samples are represented by a purple line while heMSCs + SCR samples are indicated by a green line.

heMSCs isolated by non-enzymatic method heMSCs expressed 47.59 percent CD146, 41.03 percent W5C5, 44.25 percent PDGFR, 84.57 percent CD 44, 91.13 percent CD 29, 93.18 percent ITGβ-1, 94.19 percent CD 73, 94.85 percent CD 90 , 98.37 percent CD 105, 3.71 percent CD 14, 1.18 percent CD 31, 1.89 percent CD 34 and 0.93 percent CD 45 (Figure 4.27). heMSCs + SCR expressed 45.87 percent CD146, 44.95 percent W5C5, 45.02 percent PGDFR, 85.08 percent CD 44, 89.37 percent CD 29, 92.75 percent ITGβ-1, 95.88 percent CD 73, 92.00 percent CD 90, 98.84 percent CD 105, 3.54 percent CD 14, 1.07 percent CD 31, 1.77 percent CD 34 and 0.66 percent CD 45 (Figure 4.27).

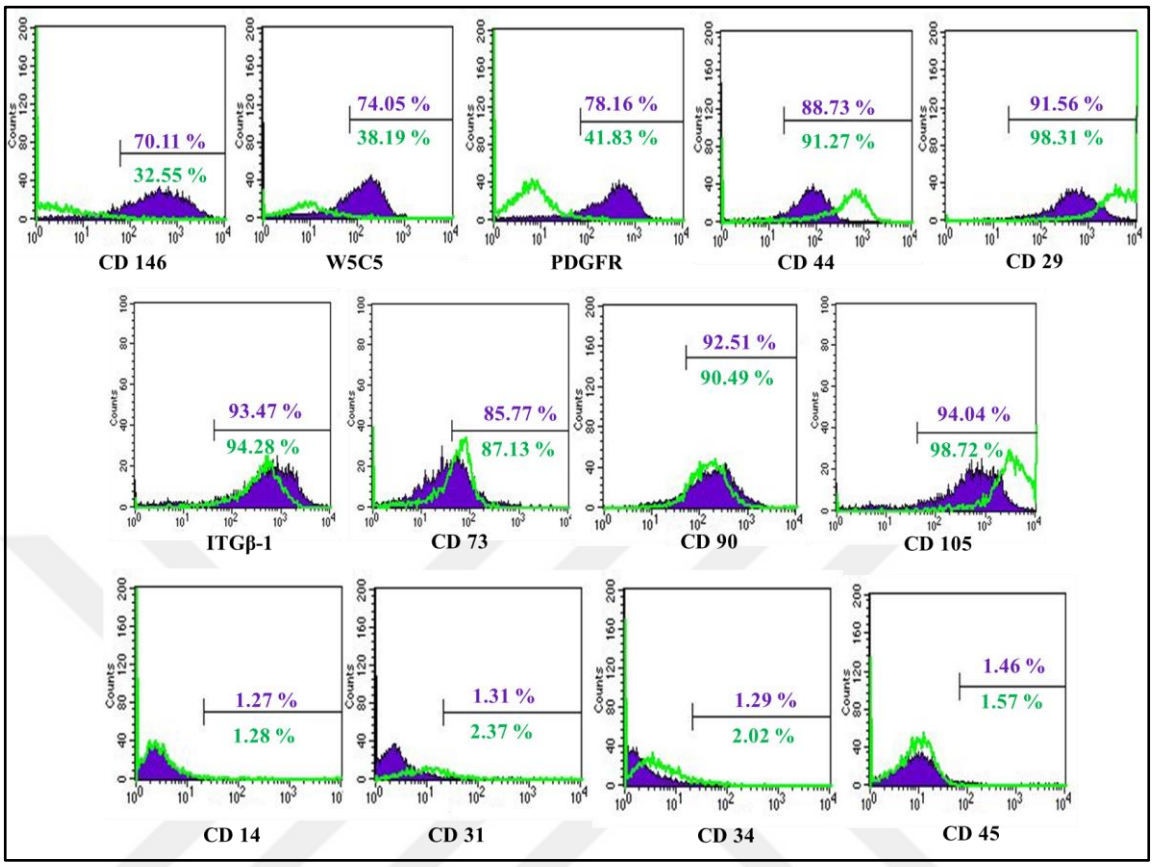

Figure 4.28. peMSCs + SCR and peMSCs + shRNA samples in Group-3 are presented as overlapped forms of stem cell markers. The peMSCs + SCR sample is indicated by the purple line, while the peMSCs + shRNA sample is indicated by the green line.

The peMSCs + SCR sample isolated by non-enzymatic method was peMSCs + SCR expressed 70.11 percent CD146, 74.05 percent W5C5, 78.16 percent PDGFR, 88.73 percent CD 44, 91.56 percent CD 29, 93.47 percent ITGβ-1, 85.77 percent CD 73, 92.51 percent CD 90, 94.04 percent CD 105, 1.27 percent CD 14, 1.31 percent CD 31, 1.29 percent CD 34 and 1.46 percent CD 45 (Figure 4.28). peMSCs + shRNA expressed 32.55 percent CD146, 39.19 percent W5C5, 41.83 percent PDGFR, 91.27 percent CD 44, 98.31 percent CD 29, 94.28 percent ITGβ-1, 83.13 percent CD 73, 90.49 percent CD 90, 98.72 percent CD 105, 1.28 percent CD 14, 2.37 percent CD 31, 2.02 percent CD 34 and 1.57 percent CD 45 (Figure 4.28).

The results of flow cytometric technique performed to determine the silencing of TG2 in stemness potential of heMSCs, heMSCs + SCR, peMSCs + SCR and peMSCs +shRNA samples in Group-4 were given in Figures 4.29 and 4.30.

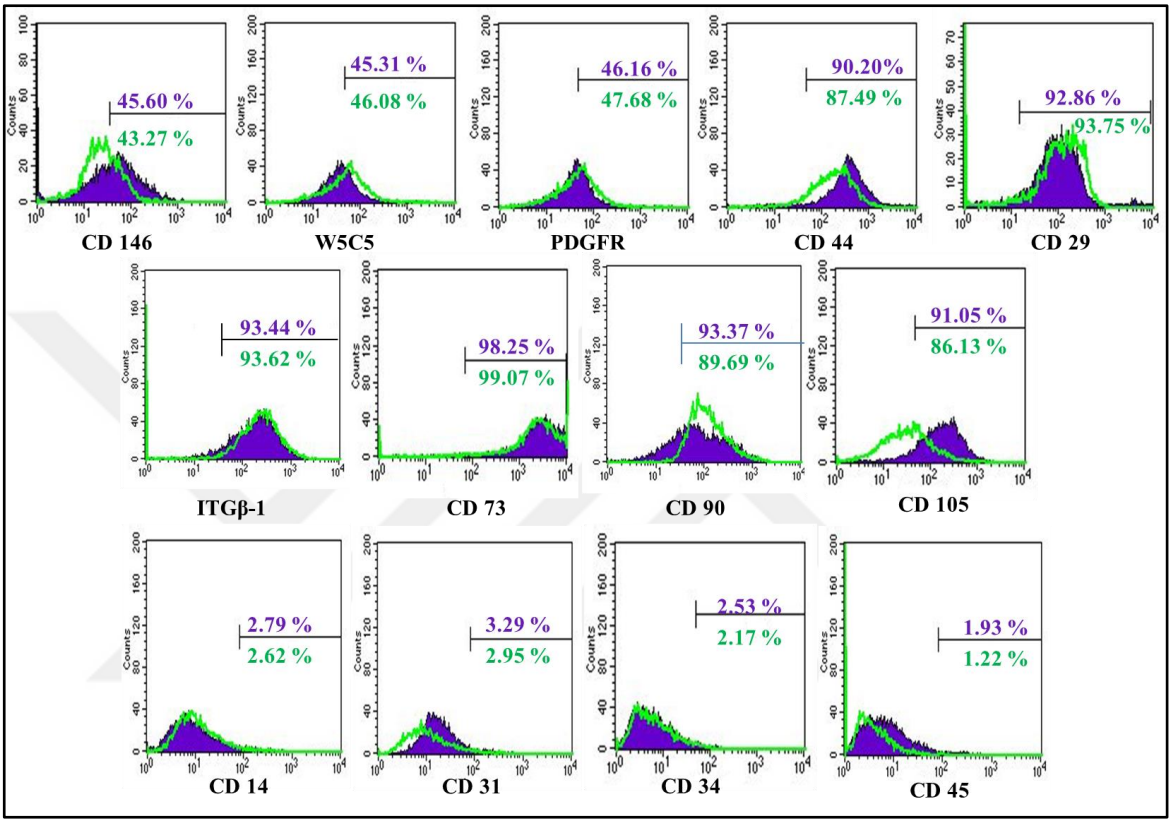

Figure 4.29. heMSCs and heMSCs + SCR samples in Group-4 are presented with overlapped forms of stem cell markers. heMSC samples are represented by a purple line while heMSCs + SCR samples are indicated by a green line.

heMSCs isolated by non-enzymatic method heMSCs expressed 45.60 percent CD146, 45.31 percent W5C5, 46.16 percent W5C5, 90.20 percent CD 44, 92.86 percent CD 29, 93.44 percent ITGβ-1, 98.25 percent CD 73, 93.37 percent CD 90 , 91.05 percent CD 105, 2.79 percent CD 14, 3.29 percent CD 31, 2.53 percent CD 34 and 1.93 percent CD 45 (Figure 4.29). heMSCs + SCR expressed 43.27 percent CD146, 46.08 percent W5C5, 47.68 percent PDGFR, 87.49 percent CD 44, 9.75 percent CD 29, 93.62 percent ITGβ-1, 99.07 percent CD 73, 89.69 percent CD 90, 86.13 percent CD 105, 2.62 percent CD 14, 2.95 percent CD 31, 2.17 percent CD 34 and 1.22 percent CD 45 (Figure 4.29).

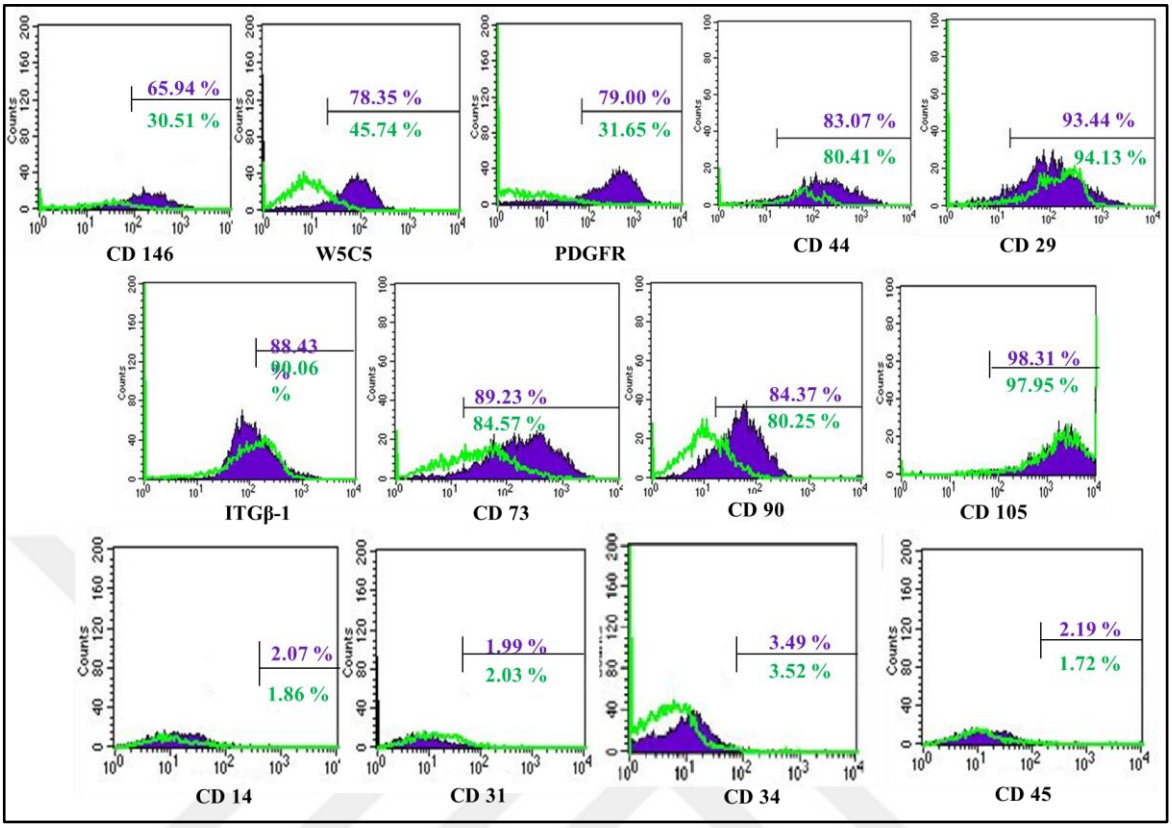

Figure 4.30. peMSCs + SCR and peMSCs + shRNA samples in Group-4 are presented as overlapped forms of stem cell markers. The peMSCs + SCR sample is indicated by the purple line, while the peMSCs + shRNA sample is indicated by the green line.

In this context, the peMSCs + SCR sample isolated by non-enzymatic method was peMSCs + SCR expressed 65.94 percent CD146, 78.35 percent W5C5, 79.00 percent PDGFR, 83.07 percent CD 44, 93.44 percent CD 29, 88.43 percent ITGβ-1, 89.23 percent CD 73, 84.37 percent CD 90, 98.31 percent CD 105, 2.07 percent CD 14, 1.99 percent CD 31, 3.49 percent CD 34 and 2.19 percent CD 45 (Figure 4.30). peMSCs + shRNA expressed 30.51 percent CD146, 45.74 percent W5C5, 31.65 percent PDGFR, 80.41 percent CD 44, 94.13 percent CD 29, 90.06 percent ITGβ-1, 84.57 percent CD 73, 80.25 percent CD 90, 97.95 percent CD 105, 1.86 percent CD 14, 2.03 percent CD 31, 3.52 percent CD 34 and 1.72 percent CD 45 (Figure 4.30).

The results of flow cytometric technique performed to determine the silencing of TG2 in stemness potential of heMSCs, heMSCs + SCR, peMSCs + SCR and peMSCs +shRNA samples in Group-5 were given in Figures 4.31 and 4.32.

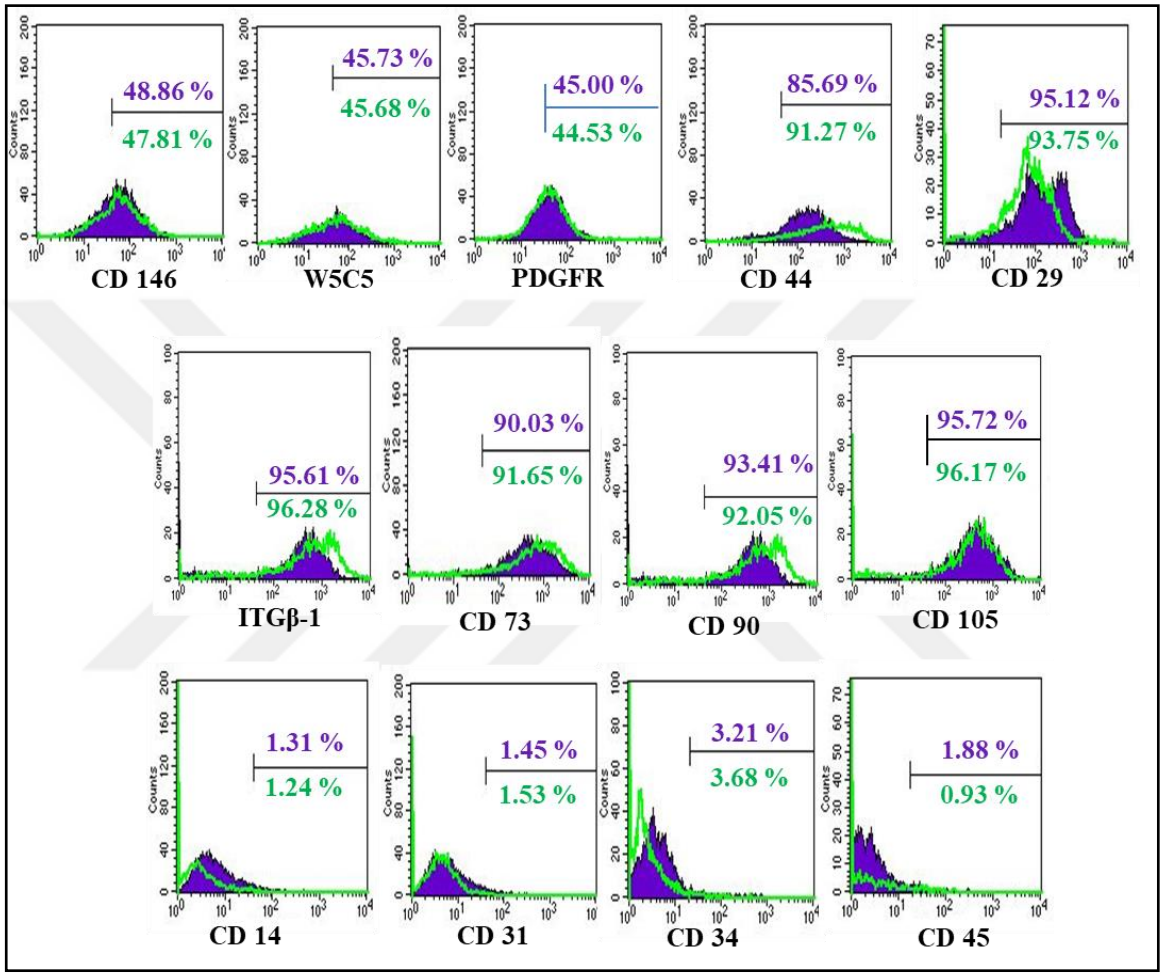

Figure 4.31. heMSCs and heMSCs + SCR samples in Group-5 are presented with overlapped forms of stem cell markers. heMSC samples are represented by a purple line while heMSCs + SCR samples are indicated by a green line.

heMSCs isolated by non-enzymatic method heMSCs expressed 48.86 percent CD146, 45.73 percent W5C5, 45.00 percent PDGFR, 85.59 percent CD 44, 95.12 percent CD 29, 95.61 percent ITGβ-1, 90.03 percent CD 73, 93.41 percent CD 90 , 95.72 percent CD 105, 1.31 percent CD 14, 1.45 percent CD 31, .21 percent CD 34 and 1.88 percent CD 45 (Figure 4.31). heMSCs + SCR expressed 47.81 percent CD146, 45.68 percent W5C5, 44.53 percent

PDGFR, 91.27 percent CD 44, 93.75 percent CD 29, 96.28 percent ITGβ-1, 91.65 percent CD 73, 92.05 percent CD 90, 96.17 percent CD 105, 1.24 percent CD 14, 1.53 percent CD 31, .68 percent CD 34 and 0.93 percent CD 45 (Figure 4.31).

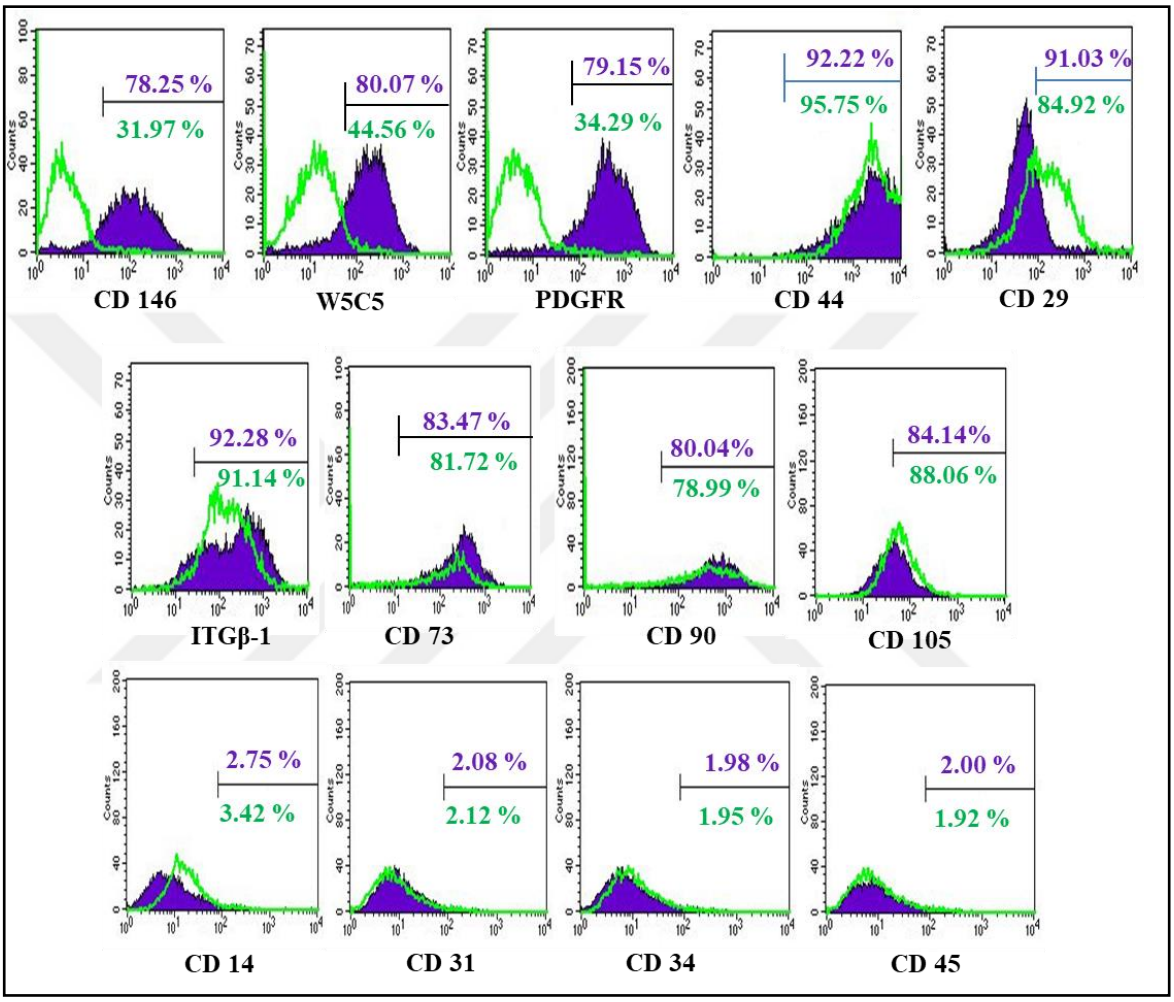

Figure 4.32. peMSCs + SCR and peMSCs + shRNA samples in Group-5 are presented as overlapped forms of stem cell markers. The peMSCs + SCR sample is indicated by the purple line, while the peMSCs + shRNA sample is indicated by the green line.

The peMSCs + SCR sample isolated by non-enzymatic method was peMSCs + SCR expressed 78.25 percent CD146, 80.07 percent W5C5, 79.15 percent PDGFR, 92.22 percent CD 44, 91.03 percent CD 29, 92.28 percent ITGβ-1, 83.47 percent CD 73, 80.04 percent CD 90, 84.14 percent CD 105, 2.75 percent CD 14, 2.08 percent CD 31, 1.98 percent CD 34 and 2.00 percent CD 45 (Figure 4.32). peMSCs + shRNA expressed 31.97 percent CD146, 44.56

percent W5C5, 34.29 percent PDGFR, 95.75 percent CD 44, 84.92 percent CD 29, 91.14 percent ITGβ-1, 81.72 percent CD 73, 78.99 percent CD 90, 86.06 percent CD 105, 3.42 percent CD 14, 2.12 percent CD 31, 1.95 percent CD 34 and 1.92 percent CD 45 (Figure 4.32).

Table 4.2. Average of intensity of different stem cells markers in five different heMSCs and heMSCs treated with control shRNA (heMSCs + SCR).

	heMSCs		**heMSCs + SCR**		
CD Markers Name	**%**	**± SD**	**%**	**± SD**	**p Value**
CD 146	46.15	3.2	45.89	3.14	**ns**
W5C5	44.89	4.05	45.22	3.66	**ns**
PDGFR	43.05	3.01	42.93	4.15	**ns**
CD 44	89.38	5.16	90.49	5.31	**ns**
CD 29	92.58	4.5	91.27	5.77	**ns**
ITGß-1	94.2	2.79	94.12	2.91	**ns**
CD 73	94.37	4.76	94.69	4.65	**ns**
CD 90	92.69	1.76	91.15	1.22	**ns**
CD 105	90.78	6.43	91.56	6.54	**ns**
CD 14	2.18	1.06	1.94	1.09	**ns**
CD 31	1.69	0.91	1.6	0.78	**ns**
CD 34	2.12	0.76	2.09	0.95	**ns**
CD 45	1.33	0.53	0.89	0.24	**ns**

Table 4.2. was presented the average of flow cytometry analysis percentage values of five different heMSCs and five different control shRNA applied heMSCs (heMSCs +SCR). Standard deviations of five different cell samples were expressed with ±. Results were statistically analysed in GraphPad Prism 6 software program by 2way ANOVA multiple

comparisons. As a result of the analysis, no significant (ns) changes were detected in CD markers when heMSCs samples were compared with heMSCs + SCR samples.

Table 4.3. Average of intensity of different stem cells markers in five different peMSCs treated with control shRNA (peMSCs + SCR) and peMSCs treated with TG2 targeting shRNA (peMSCs + SCR).

	peMSCs + SCR		**peMSCs + shRNA**		
CD Markers Name	**%**	**± SD**	**%**	**± SD**	**p Value**
CD 146	71.43	5.1	35.54	5.37	**** **(p< 0.0001)**
W5C5	76.63	2.49	42.09	3.43	**** **(p< 0.0001)**
PDGFR	78.54	0.5	34.8	4.04	**** **(p< 0.0001)**
CD 44	89.06	6.57	90.13	7.64	**ns**
CD 29	92.47	3.26	93.31	5.55	**ns**
ITGß-1	93.59	3.55	93.7	3.4	**ns**
CD 73	90.84	6.75	89.65	7.36	**ns**
CD 90	88.21	7.26	87.86	8.17	**ns**
CD 105	92.97	5.36	95.77	4.51	**ns**
CD 14	1.74	0.67	1.92	0.88	**ns**
CD 31	1.66	0.4	2	0.26	**ns**
CD 34	1.96	0.89	2.02	0.91	**ns**
CD 45	1.72	0.36	1.67	0.27	**ns**

Table 4.3. presents the average of flow cytometry analysis percentage values of five different peMSCs and TG2 targeting shRNA applied peMSCs (peMSCs + shRNA) samples. Standard deviations of five different cell samples were symbolized with ±. Results were statistically analysed in GraphPad Prism 6 software program by 2way ANOVA multiple comparisons.

Significant changes ($p < 0,0001$) were detected only for CD146, W5C5 and PDGFR surface markers amonf peMSCs samples and peMSCs + shRNA samples.

4.5.2. Determination of Colony Forming Units for Control and shRNA Transduced eMSCs

The colony-forming potentials (CFU) of the eMSCs were tested by the CFU method as described in Section 3.11. One of the characteristic features of mesenchymal cells is their potential to form colonies [76, 415, 419, 420, 421, 422] therefore, CFU potentials of heMSCs, heMSCs + SCR, peMSCs, peMSCs + SCR and peMSCs + shRNA samples were determined using the CFU method. For this purpose, cells were seeded in 60mm cell plates at 50 cells/cm^2 and allowed to colonize in the cell culture cabinet at 37^oC for 21 days at their growth medium [415, 420]. Colonies were imaged by stereomicroscopy and colony-forming potentials of eMSCs were analyzed using Image J program. For quantitative evaluation, five randomly selected eMSCs images having at least 5 colonies were captured and the number of cells in each colony were counted using the Image J program's “cell counter notice” option. Percentage CFU potential was calculated by accepting total number of cells counted for the peMSCs samples as 100 percent (Figure 4.33.).

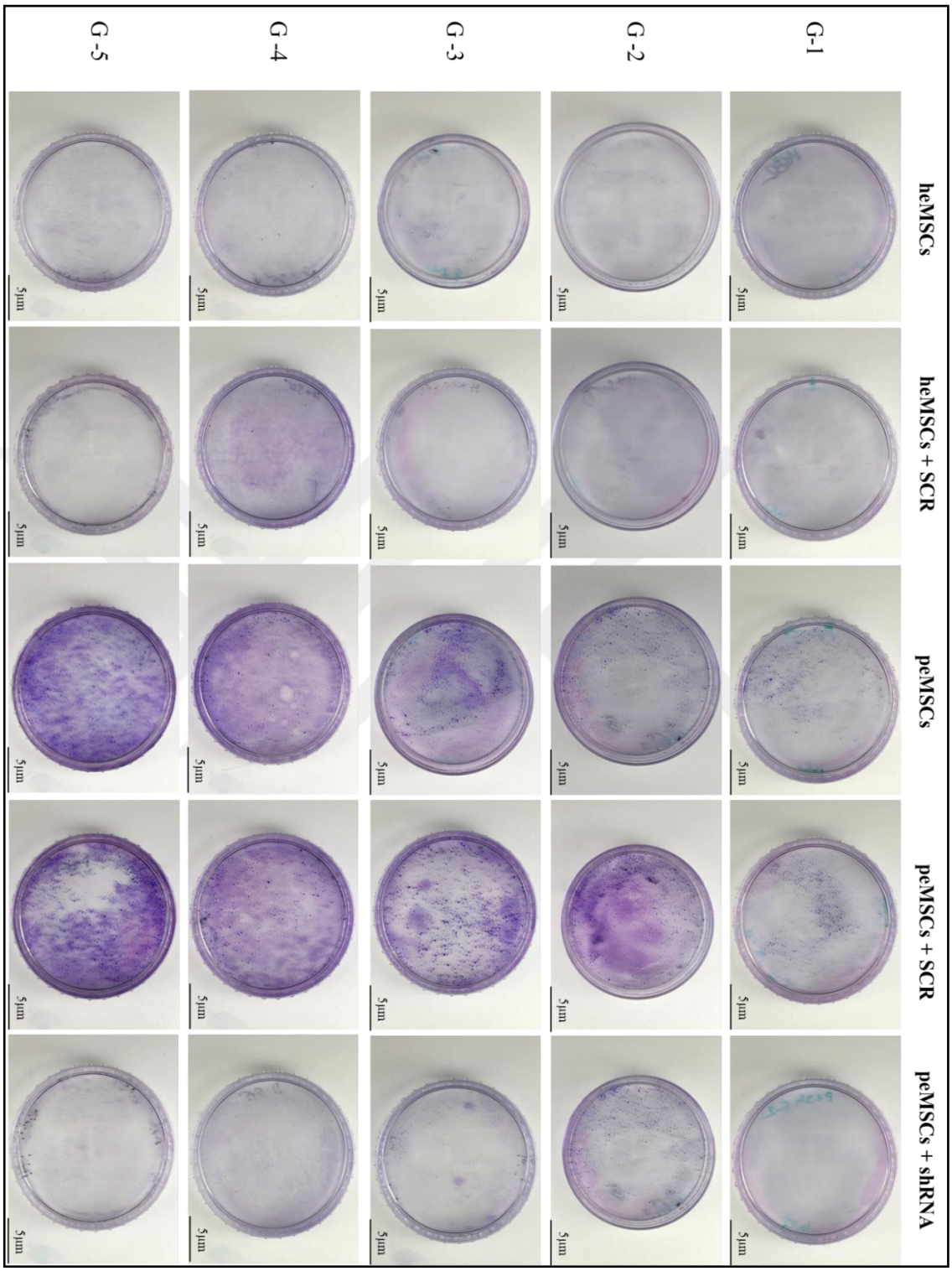

Figure 4.33. Images of colony formation ability of eMSCs transduced with control scrambled (SCR) or TG2 targeting lentiviral shRNA (shRNA). Photographs of five different groups of eMSCs samples were taken at the end of day 21 with a 1X stereo microscope. 5µm scale bar was used for 1x objective.

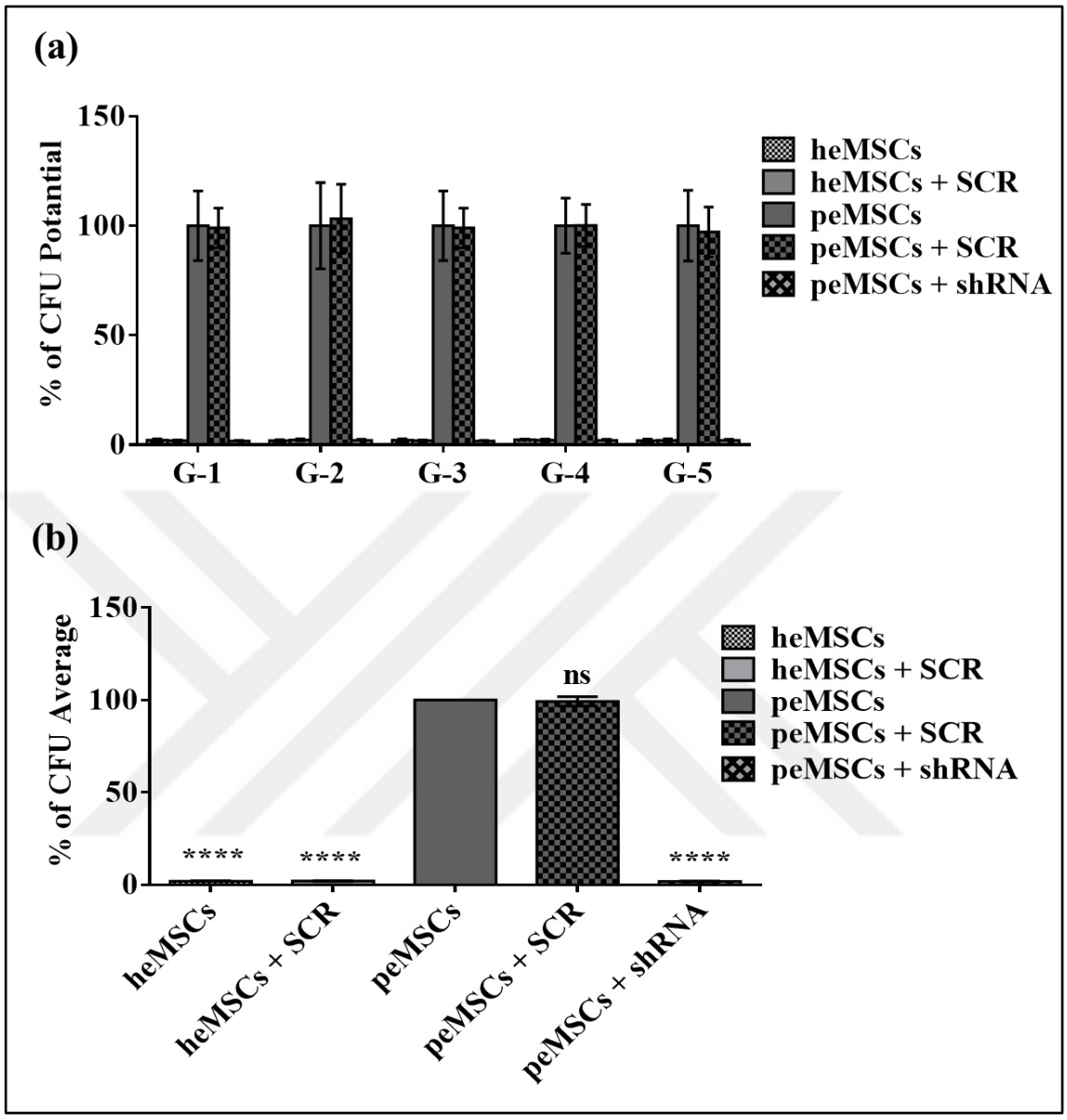

Figure 4.34. Determination of colony formation ability of eMSCs transduced with control scrambled (SCR) or TG2 targeting lentiviral shRNA (shRNA). (a) Analysis of the % colony forming unit (CFU) potential for eMSCs samples in five different groups. (b) Statistical analysis for the average % CFU of the eMSCs samples in five different groups. GraphPad Prism 6 ONEway ANOVA multiple comparison program was used in statistical analysis results for % CFU. $p < 0.00001$ value was symbolized by *****.

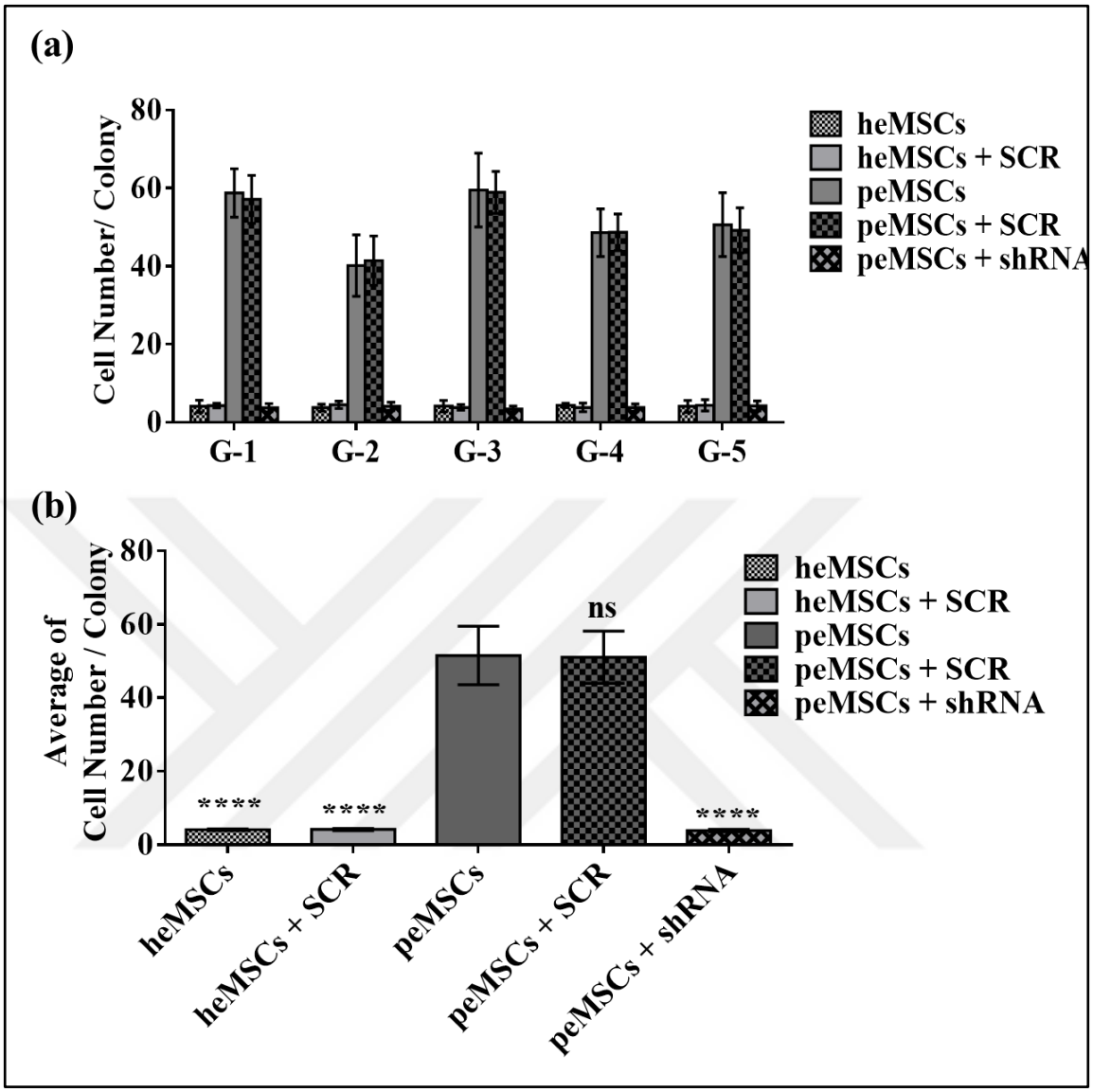

Figure 4.35. Determination of cell number /colony formation ability of eMSCs transduced with control scrambled (SCR) or TG2 targeting lentiviral shRNA (shRNA). (a) Analysis of the cell number /colony formation ability of eMSCs samples in five different groups (G-1 to G-5). (b) Analysis of the average cell number /colony formation ability of the eMSCs samples in five different groups. GraphPad Prism 6 One-way ANOVA multiple comparison program was used in statistical analysis results for% CFU and $p < 0.00001$ value was symbolized by *****.

In Group-1 when compared to peMSCs, percentage CFU potential for peMSCs + SCR was found similar with 97.2 percent, while the percentage CFU potential for peMSCs + shRNA

was found as 1.58 percent. As expected, there was a non-significant difference among the percentage CFU potentials of heMSCs and heMSCs + SCR with 1.88 and 1.80 percent, respectively. Similarly, percentage CFU potential in Group-2, was found as 1.90 percent for heMSCs samples, 2.24 percent for heMSCs + SCR, 103 percent for peMSCs + SCR, 2 percent for peMSCs + shRNA. These values were determined as 2.05 percent for heMSCs, 1.89 percent for heMSCs + SCR, 98.9 percent for peMSCs + SCR, 1.7 percent for peMSCs + shRNA in in Group-3. Percentage CFU potential was determined as 2.3 percent for heMSCs, 2.05 percent for heMSCs + SCR, 100 percent for peMSCs + SCR, and 2.03 percent for peMSCs + shRNA in Group-4. In Group-5, CFU potential for heMSCs, heMSCs + SCR, and peMSCs + shRNA was around 2 percent, while peMSCs + SCR cells displayed a 97.13 percent CFU potential. In the light of these results, when the average percentage CFU potentials of 5 different eMSCs samples in five different groups were analyzed (Figure 4.34.b), percentage CFU potential of heMSCs and heMSCs + SCR was 98 percent lower ($p < 0.00001$) than that of peMSCs and peMSCs + SCR cells, while peMSCs + shRNA showed an average of 1.86 percent CFU potential ($p < 0.00001$).

In order to evaluate efficiency of the colonies formed by eMSCs the cell number per colony was determined by dividing the total number of cells to the total number of colonies (Figure 4.35.). The number of cells per colony for heMSCs were calculated as 4.1, 3.8, 4.2, 4.3, 4.1 for Group-1 to -5 respectively. Similar values were obtained for heMSCs + SCR samples (Figure 4.35.a.). The colony efficiency for peMSCs and peMSCs + SCR was found similar with 58.8, 40.5, 59.5, 48.7, and 58.5 cell per colony for Group-1 to -5, respectively. However, the silencing of TG2 with shRNA led to a significant decrease in the number of cells per colonies, which was comparable to heMSCs. The comparison of average colony efficiencies among eMSCs samples shown that the number of cells per colonies was 4.1 for heMSCs, 4.2 for heMSCs + SCR, 51.6 for peMSCs, 51.1 for peMSCs + SCR and 3.9 for peMSCs + shRNA (Figure 4.35.b.).

4.6. ROLE OF TG2 ON PROLIFERATION OF eMSCs

4.6.1. Characterization of Cell Proliferation Profile in heMSCs and peMSCs by WST-1

In order to determine the cell proliferation potential of heMSCs and peMSCs samples in five different groups, the WST-1 method described in detail in Section 3.9.1. was applied to the cells for 24, 48, 72 and 96 hours. In order to convert absorbance values to cell numbers, 2000, 5000, 10000, 15000, and 20000 cell per well was seeded for five different heMSCs and peMSCs and allowed to attach for 16 hours prior to addition of WST-1 reagent. The absorbance values corresponding to cell numbers were used to plot the standard curve which gave a linear equation that was used to convert absorbance values to cell numbers. In order to eliminate the effect of senescence all cells used in this experiment was at the passage number of three.

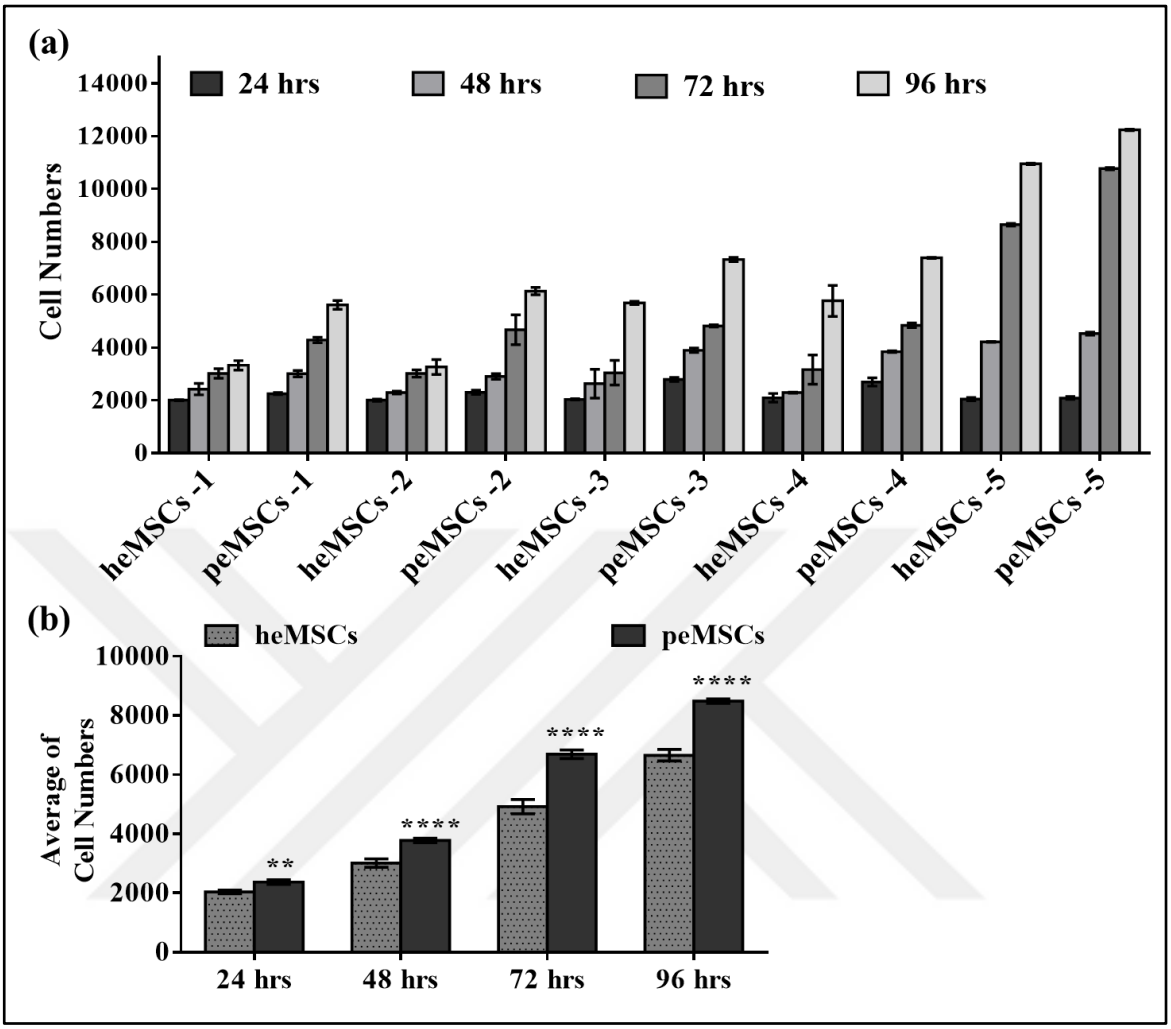

Figure 4.36. Determination of cell proliferation profile in heMSCs and peMSCs. (a) The cell numbers of five different groups of heMSCs (1-5) and peMSCs (1-5) samples at 24, 48,72 and 96 hours. (b. The average of cell numbers for five different groups of heMSCs (1-5) and peMSCs (1-5) samples at 24, 48,72 and 96 hours. GraphPad Prism 6 2way ANOVA multiple comparison program was used to determine the statistical analysis results. ** was used for $p < 0.01$, **** was used for $p < 0.00001$.

The cell numbers of heMSCs and peMSCs samples in five different groups at four different time points (24, 48, 72 and 96 hours) were presented in Figure 4.36.a. When cell number for peMSCs at 24, 48, 72 and 96 hours were compared to that of heMSCs, it was observed that peMSCs in Group 1 multiplied by 1.1, 1.2, 1.4, and 1.7 times more than heMSCs at 24, 48 hours, 72 hours and 96 hours, respectively. Similar ratios of cell proliferation were obtained

for Group-2 to 5 for peMSCs and heMSCs (Figure 4.36.a.). In addition to these values, when the average cell numbers of heMSCs and peMSCs samples in five different groups were compared for 24, 48, 72 and 96 hours, peMSCs samples were able to proliferate 1.16 times ($p < 0.01$) , 1.26 times ($p < 0.00001$), 1.36 times ($p < 0.00001$) and 1.27 times ($p < 0.00001$) faster, respectively (Figure 4.36.b.).

4.6.2. Effect of TG2 Silencing on peMSCs Proliferation

To determine the effect of controlled silencing TG2 on cell proliferation after SCR or shRNA treatment of heMSCs and peMSCs samples in five different groups, the WST-1 assay was applied on heMSCs, heMSCs + SCR, peMSCs, peMSCs + SCR, and peMSCs + shRNA cells at passage 3 from five different groups for 24, 48, 72, and 96-hours (Figure 4.37 to Figure 4.39).

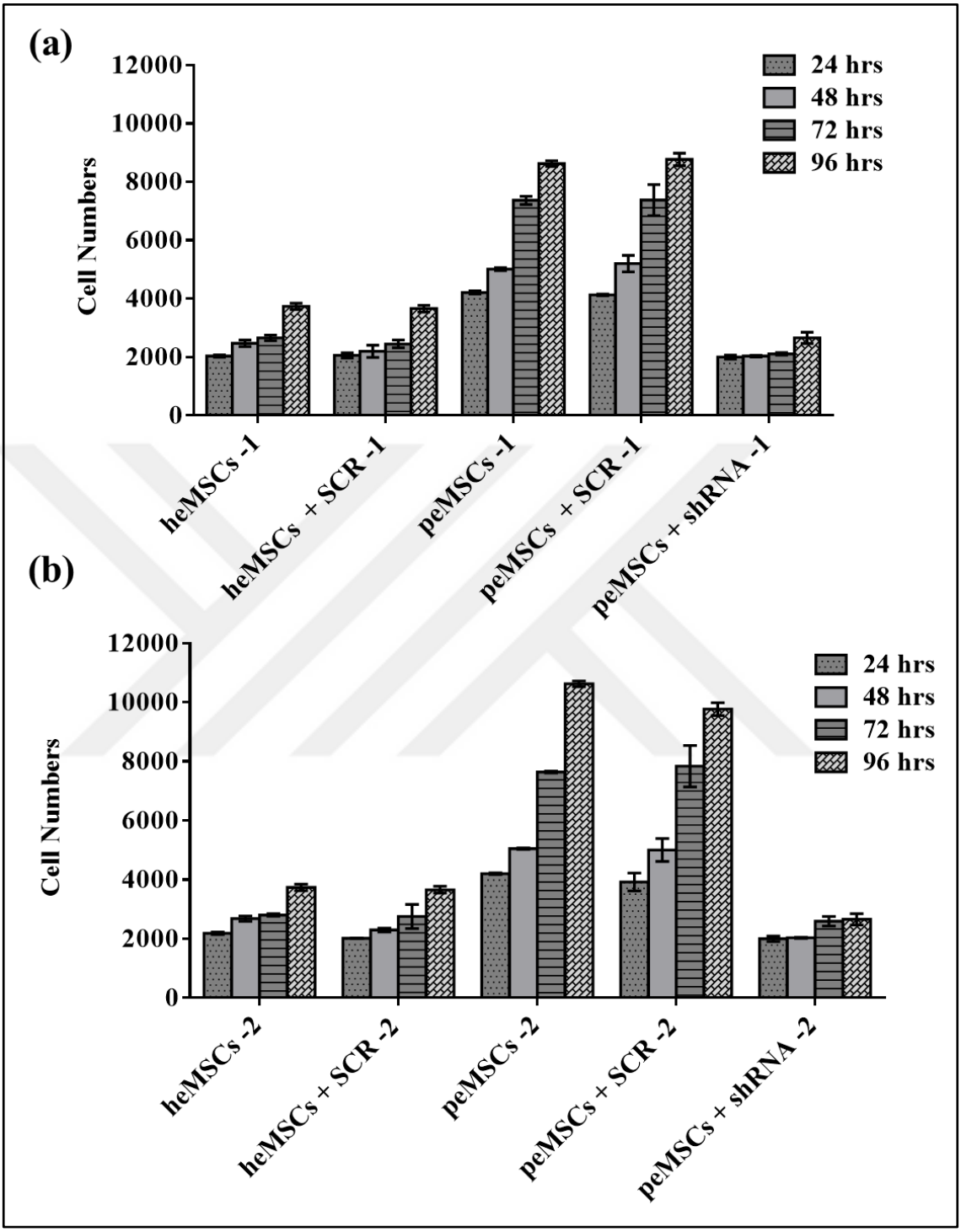

Figure 4.37. Effect of TG2 silencing on peMSCs proliferation for Group-1 to Group-2. (a) Effect of silenced TG2 on cell growth in eMSCs in Group-1. (b) Effect of silenced TG2 on cell growth in eMSCs in Group-2.

Among themselves, heMSCs, heMSCs + SCR and TG2 targeted shRNA-treated peMSCs + shRNA samples in Group-1 had similar proliferation ability at 24, 48, 72 and 96 hours. However, when peMSCs and peMSCs + SCR cell proliferation rate in the same group were compared with heMSCs samples, it was observed that cell proliferation in peMSCs was 2.07 times higher than heMSCs while cell proliferation of peMSCs + SCR was 2.03 times higher than heMSCs at the end of 24 hours. This 2-fold increase in proliferation ability of peMSCs and peMSCs + SCR cells was valid for the following 48, 72 and 96 hours. When the comparisons made for Group-1 were performed in Group-2, heMSCs, heMSCs + SCR and TG2-targeted shRNA-treated peMSCs + shRNA samples again showed similar number of cell growth (Figure 4.37.b.) at all time points. At 24 and 48 hours, peMSCs and peMSCs + SCR samples in Group-2 increased 1.92 and 1.86 times more than heMSCs, respectively. This rate was increased to 2.8-fold for peMSCs and peMSCs + SCR at 72 and 92 hours.

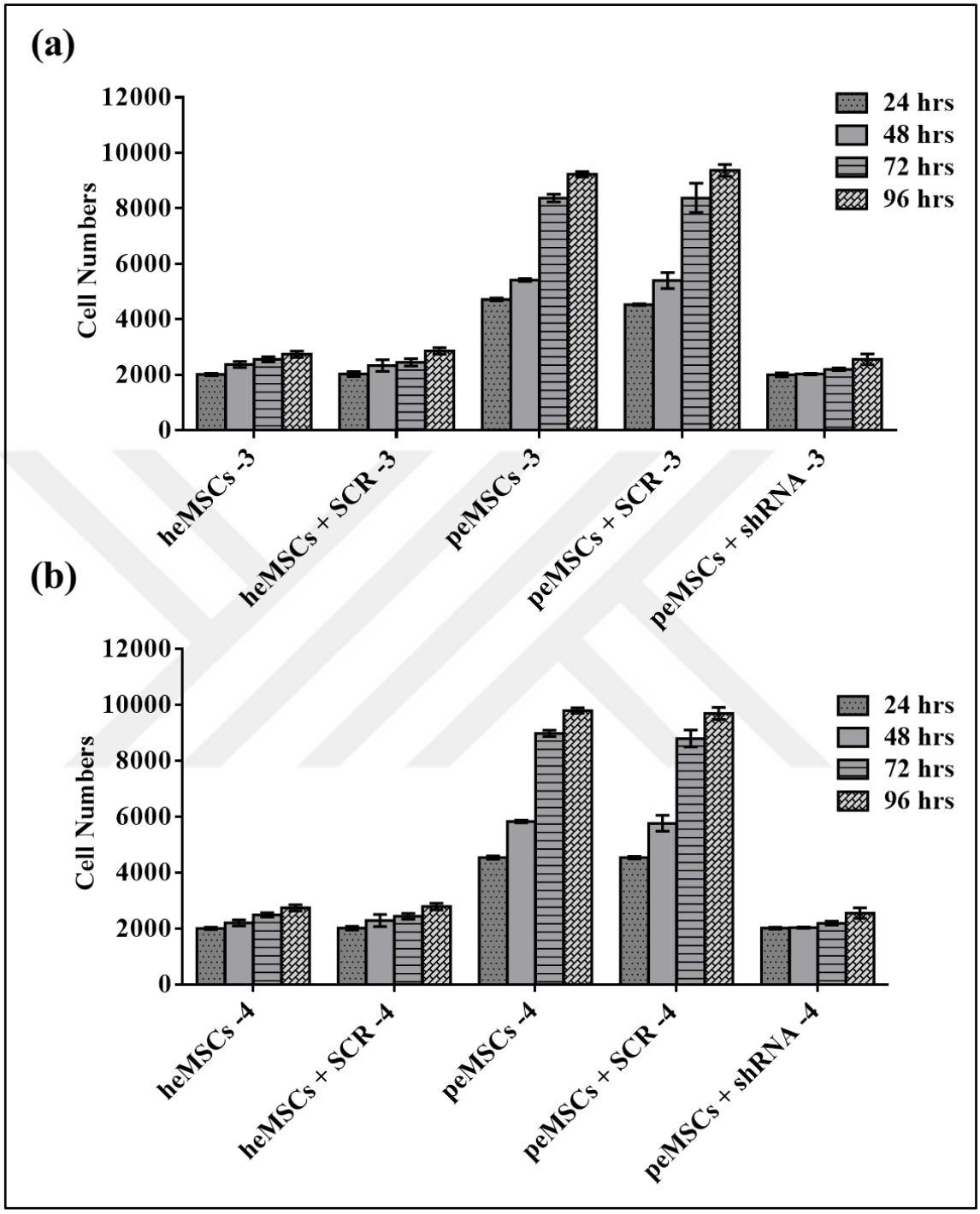

Figure 4.38. Effect of TG2 silencing on peMSCs proliferation for Group-3 to Group-4. (a) Effect of silenced TG2 on cell growth in eMSCs samples in Group-3. (b) Effect of silenced TG2 on cell growth in eMSCs samples in Group-4.

Cell numbers of heMSCs, heMSCs + SCR, peMSCs, peMSCs + SCR and peMSCs + shRNA samples in Groups-3 and -4 at 24, 48, 72 and 96 hours were depicted in Figure 4.38.a. and

b. The cell numbers recorded for heMSCs, heMSCs + SCR and TG2-targeted shRNA-treated peMSCs + shRNA samples at 24, 48, 72 and 96 hours were found similar (Figure 4.38.a.). The cell proliferation rate and the trend at 24 and 48 hours for peMSCs and peMSCs + SCR cells were also 2.3-fold higher than heMSCs in Group-3. This difference was further increased to 3.3-fold within 92 hours. In Group-4, the silencing of TG2 in peMSCs also resulted in the loss of increased proliferative rate and these cells (peMSCs + shRNA) displayed similar growth rate with heMSCs and heMSCs + SCR at all four time points (Figure 4.38.b). When peMSCs and peMSCs + SCR in the same group were compared with heMSCs, it was observed that the peMSCs and peMSCs + SCR cells displayed a respective 2.3, and 2.6 increase in their proliferation at 24 and 48 hours, and 3.6-fold increase in 72 and 92 hours.

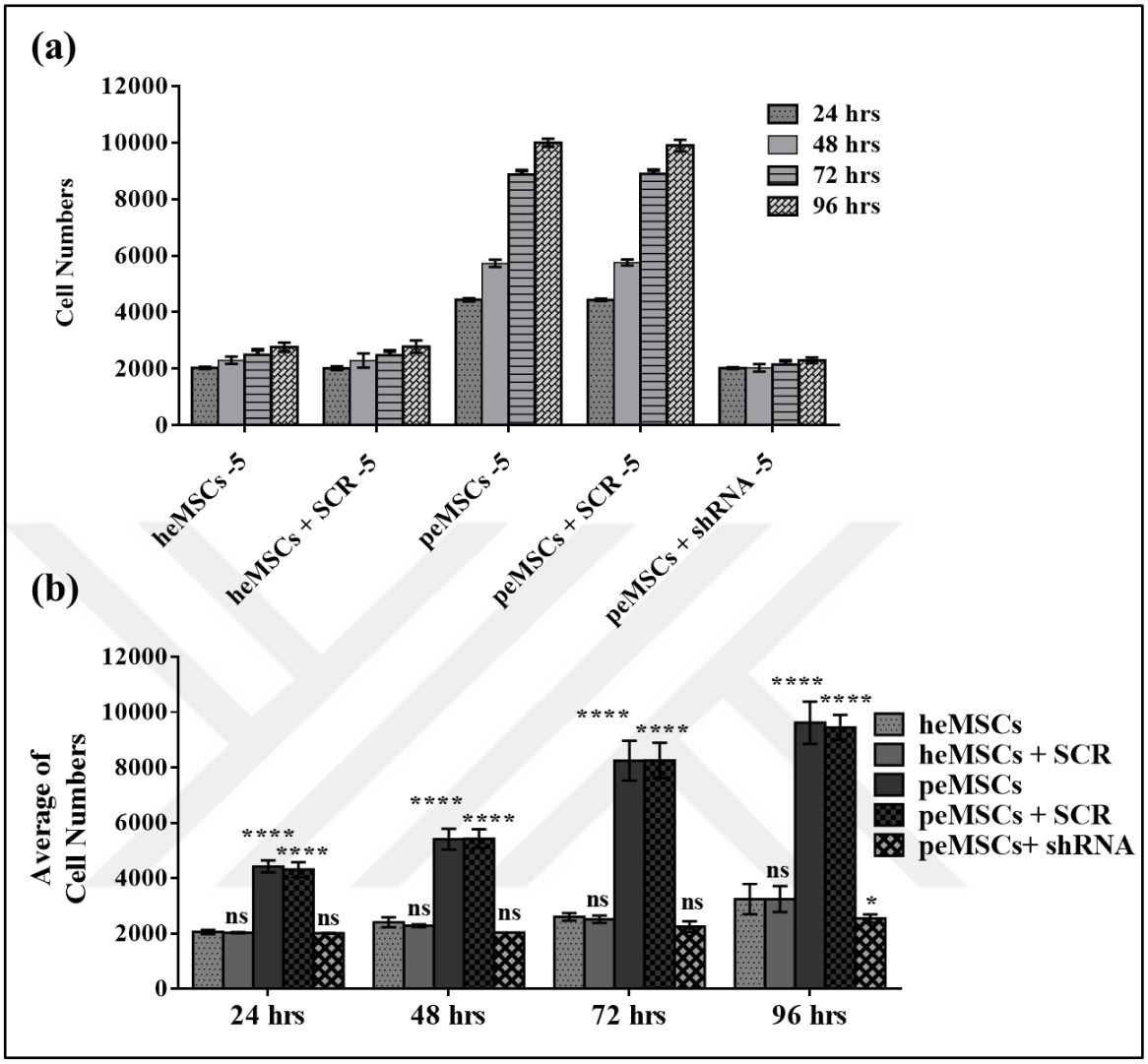

Figure 4.39. Effect of TG2 silencing on peMSCs proliferation Group-5 and average of eMSCs cell growth. (a) Effect of silenced TG2 on cell growth in eMSCs samples in Group-5. (b) Effect of silenced TG2 on average cell growth in eMSCs samples in five different groups. GraphPad Prism 6 2way ANOVA multiple comparison program was used to determine the statistical analysis results. “ns” was used for non-significant p value, * was used for $p < 0.05$, **** was used for $p < 0.00001$.

In Group-5, cell number recorded for heMSCs, heMSCs + SCR and peMSCs + shRNA samples at 24, 48, 72 and 96 hours were similar among themselves, while cell proliferation of peMSCs and peMSCs + SCRs were 2.18 times and 2.50 times higher than heMSCs after 24 and 48 hours, respectively (Figure 4.39.a). This rate was further increased to 3.55 and

3.62 times for peMSCs and peMSCs + SCR samples at 72 and 92 hours (Figure 4.39.a.). To sum up, the average cell numbers of heMSCs, heMSCs + SCR, peMSCs, peMSCs + SCR and peMSCs + shRNA cell samples at the end of 24, 48, 72 and 96 hours in five different groups (G-1 to G-5) was presented in Figure 4.39.b. At the end of 24, 48, 72 and 96 hours heMSCs, heMSCs + SCR and peMSCs + shRNA samples all showed to have similar numbers of cells. At the end of 24 and 48 hours, peMSCs and peMSCs + SCR samples were found to have an average number of 2.1 and 2.3 times more cells compared to heMSCs, while 72 and 96 hours the proliferation rate was inclined to 3.2 and 3.0 times, respectively.

4.7. REGULATION OF CELL CYCLE in eMSCs by TG2

4.7.1. Analysis of Cell Cycle Progression in heMSCs and peMSCs

The effect of TG2 on cell cycle in heMSCs and peMSCs sample from five different groups was determined by Western Blot analysis of Cyclin E1, CDK-4, CDK-2, Cyclin D3 and p27 protein levels as described (Section 3.6.4.).

4.7.1.1. Determination of Cell Cycle Progression in heMSCs and peMSCs by Western Blot

Cellular functions such as cell proliferation, cell differentiation, and apoptosis are controlled by the cell cycle. Cell cycle plays a key role for viability. In this process, cells undergo many biochemical, morphological, and genetic changes. After the cells receive the cleavage signal, the cells enter the active cell G1, G2, S and M phases, which can be detected by analysis of key regulators of cell cycle and molecular labelling of cellular DNA context, the potential role of TG2 on the regulation of cell cycle was analyzed by measuring the changes in the levels of Cyclin E1, CDK-4, CDK-2, Cyclin D3 and p27 proteins in heMSCs and peMSCs cells following SCR and TG2 targeting shRNA transduction.

The cell cycle is controlled by some specific proteins in the cycle. Examples of such proteins are; Cyclins, Cyclin-Dependent serine/threonine protein Kinases (CDKs), and cyclin-dependent kinase inhibitors (called CDIs, CKIs or CDKIs). In this context, the technique presented in Section 3.6.4 was used for the determination levels of Cyclin E1, CDK-4, CDK-2, Cyclin D3 and p27 proteins involved in determining the cell cycle of heMSCs and peMSCs samples.

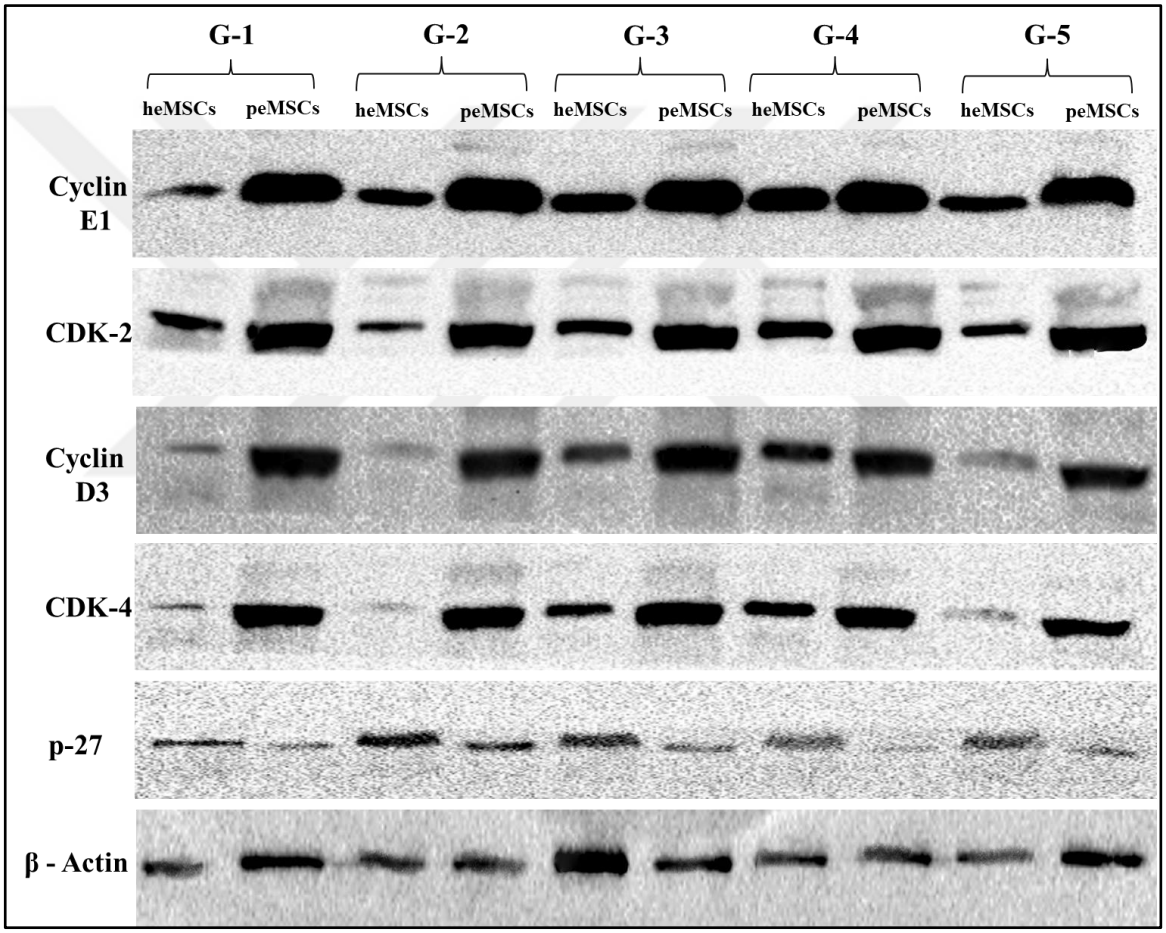

Figure 4.40. Determination of cell cycle progression in five different heMSCs and peMSCs (G-1 to G-5) by Western Blot. Band intensities were quantified using Image J analysis and β-actin was used for equal loading control.

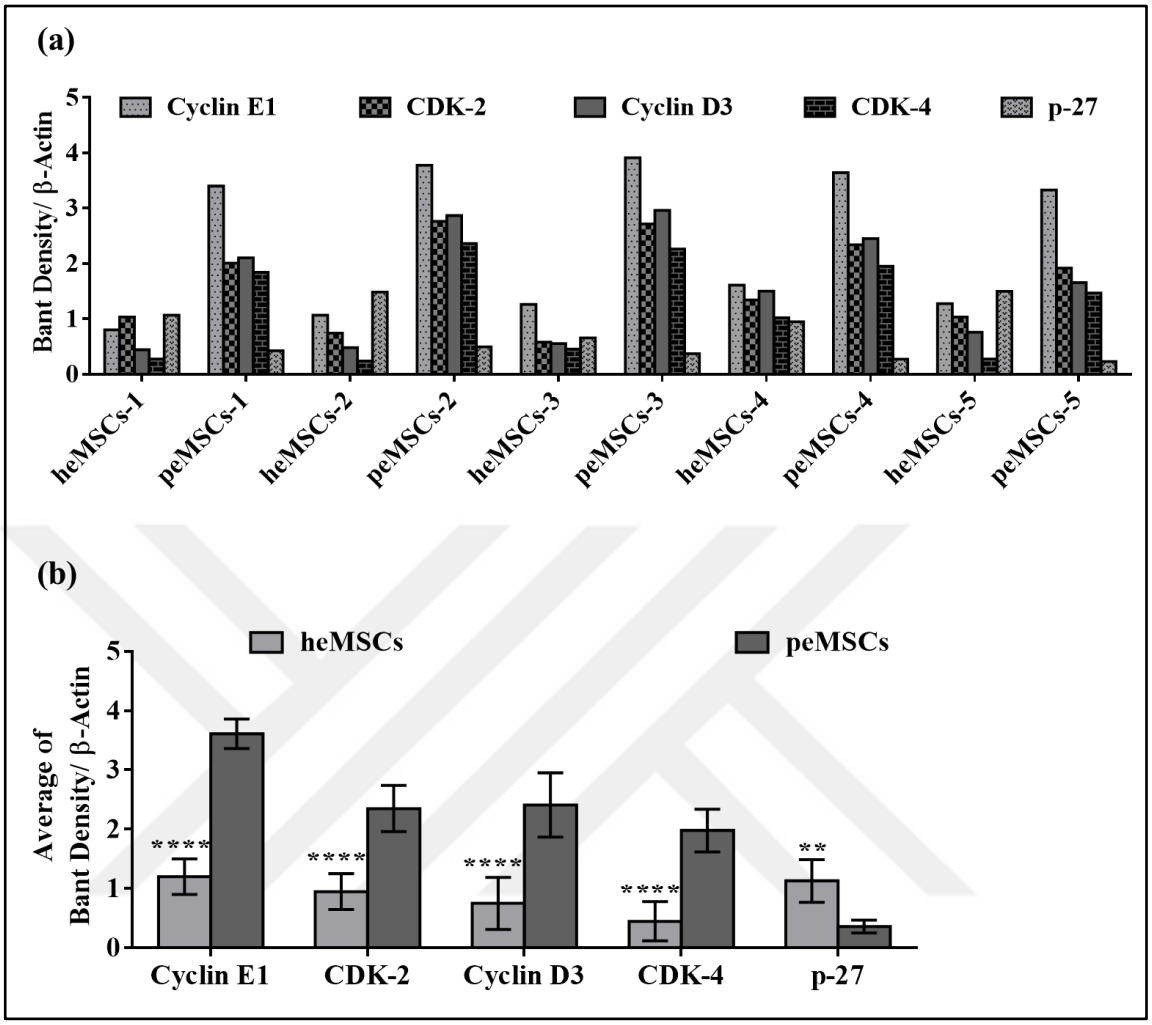

Figure 4.41. Quantification of cell cycle proteins in heMSCs and peMSCs samples in five different groups. (a) Quantification of cell cycle proteins in heMSCs and peMSCs samples in five different groups compared to B-Actin loading control. (b) Determination of the average synthesis amount of cell cycle proteins in heMSCs and peMSCs samples in five different groups compared to B-Actin loading control. Band density was determined by Image J program. GraphPad Prism 6 2way ANOVA multiple comparison program was used to determine the statistical analysis results. “ns” was used for non-significant p value, ** was used for p <0.01, **** was used for p <0.00001.

As a result of the membrane images in Figure 4.40., the amounts of cell cycle proteins of Cyclin E1, CDK2, Cyclin D3, CDK4, and p27 respectively in the heMSCs, heMSCs + SCR, peMSCs, peMSCs + SCR and peMSCs + shRNA samples in five different groups,

respectively, they were calculated by ratio to β-actin value (Figure 4.41.a.). The heMSCs sample in Group-1 was observed to have protein levels of 4.25 times less for Cyclin E1, 1.95 times less for CDK-2, 4.73 times less for Cyclin D3, and 6.65 times less for CDK-4, respectively, when compared to peMSCs in the same group. heMSCs were found to synthesize p-27 protein 2.50 times more than peMSCs. The heMSCs sample in Group -2 was found to synthesize 3.53 times less for Cyclin E1, 3.72 times less for CDK-2, 5.72 times less for Cyclin D3, and 9.91 times less for CDK-4, respectively, compared to peMSCs in the same group. heMSCs were found to synthesize p-27 protein 3.02 times more than peMSCs in Group-2. Similar comparisons were performed for Group-3, -4 and -5, respectively. As a result, it was found that heMSCs sample in Group -3 synthesized Cyclin E1 protein 3.10 times, CDK-2 4.69 times, Cyclin D3 5.33 times, CDK-4 4.99 times less and it was found that heMSCs in the same group synthesized p-27 protein 1.76 times more than peMSCs. The heMSCs sample in Group -4 was found to synthesize Cyclin E1 protein by 2.26 times, CDK-2 by 1.74 times, Cyclin D3 by 1.97 times, and CDK-4 by 2.07 times less. It was found that heMSCs in the same group contained 3.45 times more p-27 protein than peMSCs. In Group-5, heMSCs sample had 2.61-fold low protein levels for Cyclin E1, 1.85-fold low for CDK-2, 2.18-fold low for Cyclin D3, and 5.26-fold low for CDK-4, respectively, compared to the peMSCs in the same group. Western Blot results have shown that heMSCs had 6.43 times more p-27 protein level than peMSCs (Figure 4.41.a.). When the average synthesis amount of cell cycle proteins in heMSCs and peMSCs samples in five different groups were compared, heMSCs samples were 3.0 times less for Cyclin E1, 2.48 times less for CDK-2, 3.43 times less for CDK-4, and 4.43 times less for CDK-4, respectively and it was observed that heMSCs synthesized p-27 protein on average 3.14 times more than peMSCs (Figure 4.41.b.).

4.7.2. Determination of Cell Cycle Rate in TG2 Silenced peMSCs

After applying control shRNA (SCR) and TG2-targeted shRNA to eMSCs in five different groups, the change in cell cycle rates were investigated by the Cyclin E1, CDK4, CDK2, Cyclin D3 and p27 antibodies used in the Western Blot technique described in detail in Section 3.6.4. Moreover, Western Blot results were confirmed using the Cytell Cell Imaging System described in detail in Section 3.9.2. In the experiments, the passage number of the cells used was three.

4.7.2.1. Determination of Cell Cycle Rate in TG2 Silenced peMSCs by Western Blot

In order to determine the effect of TG2silencing on cell cycle in heMSCs, heMSCs + SCR, peMSCs, peMSCs + SCR and peMSCs + shRNA samples in five different groups, Western Blot technique was applied. In this context, the technique presented in Section 3.6.4 was used for the determination levels of Cyclin E1, CDK-2, Cyclin D3, CDK-4 and p-27 proteins involved in determining the cell cycles of five different groups with TG2 silenced (Figure 4.42 to Figure 4.46).

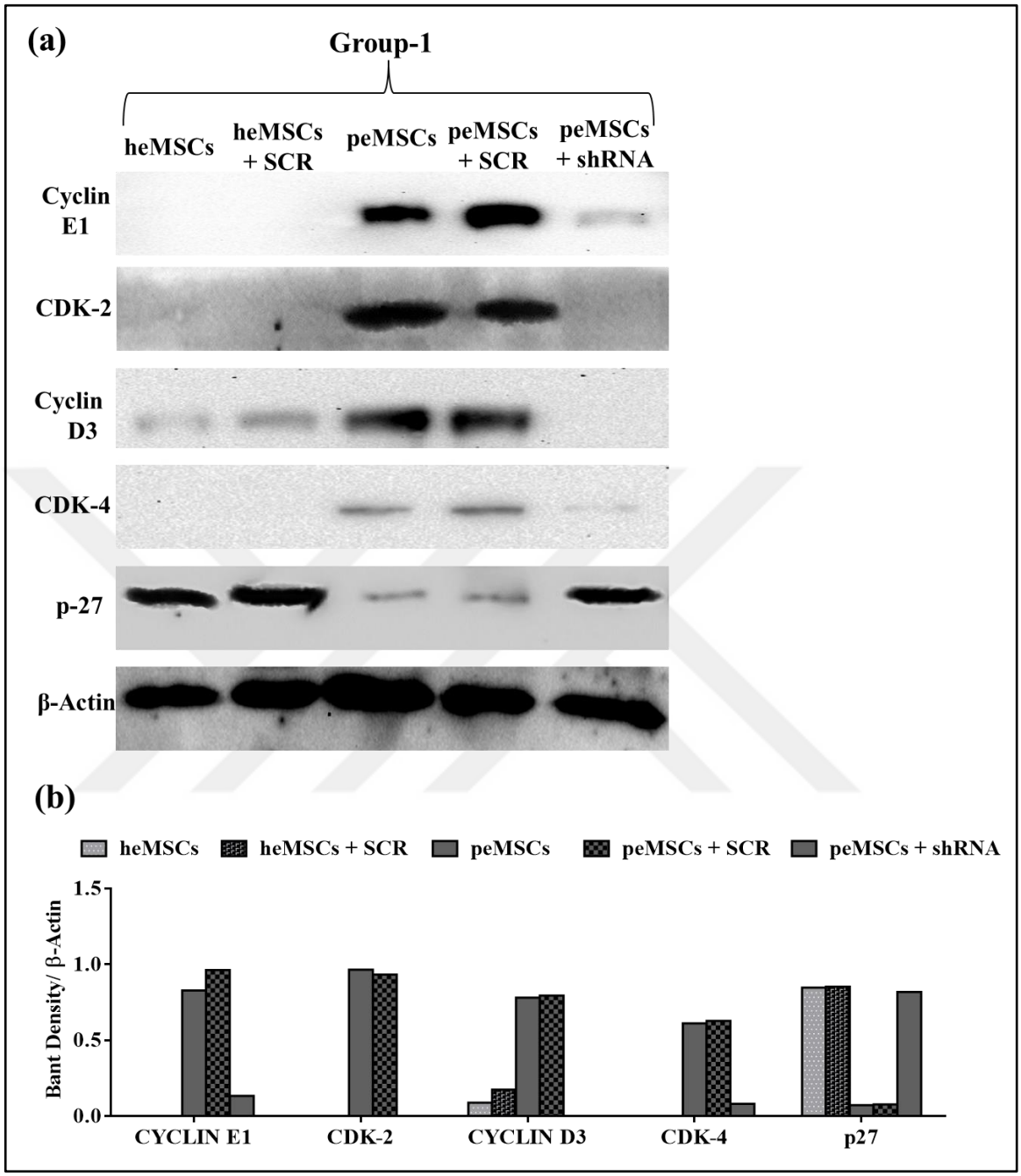

Figure 4.42. Determination of cell cycle proteins level in eMSCs transduced with control scrambled (SCR) or TG2 targeting lentiviral shRNA (shRNA) for Group-1. (a) Images of cell cycle and loading control β-Actin protein levels in Group-1 following shRNA transduction at 0.22 μm nitrocellulose membrane. (b) Quantification of cell cycle proteins adjusted to loading control β-Actin protein using the Image J program for Group-1.

To determine the levels of cell cycle proteins in heMSCs, heMSCs + SCR, peMSCs, peMSCs + SCR and peMSCs + shRNA samples in Group-1, Western Blot technique was applied, and β-actin loading control was selected to ensure that an equal amount of protein was loaded into the wells (Figure 4.42.a.). For the determination of the protein level of each sample, the band densities were proportional to the β-actin band density and Image J program was used for quantitative analysis (Figure 4.42.b.). In this context, it was determined that heMSCs and heMSCs + SCR samples in Group-1 did not synthesize Cyclin E1, CDK-2 and CDK-4 proteins, whereas they synthesized Cyclin D3 protein 8.85 and 4.49 times less than peMSCs sample in the same group, respectively. On the other hand, when a similar comparison was made for another cell cycle protein p-27, it was found that heMSCs and heMSCs + SCR samples were synthesized in equal amounts by 11.80 times more p-27. When the peMSCs sample was compared to the peMSCs + SCR sample in the same group, it was observed that they contained an equal amount of cell cycle proteins. In Group-1, the peMSCs treated with TG2 targeting lentiviral shRNA (peMSCs + shRNA), cell cycle protein results were similar to heMSCs and heMSCs + SCR samples. The peMSCs + shRNA sample synthesized Cyclin E1 protein 6.23 times less compared to peMSCs, while the p-27 protein expressed 11.30 times more. On the other hand, CDK-2, Cyclin D3 and CDK-4 proteins were not synthesized in peMSCs + shRNA sample.

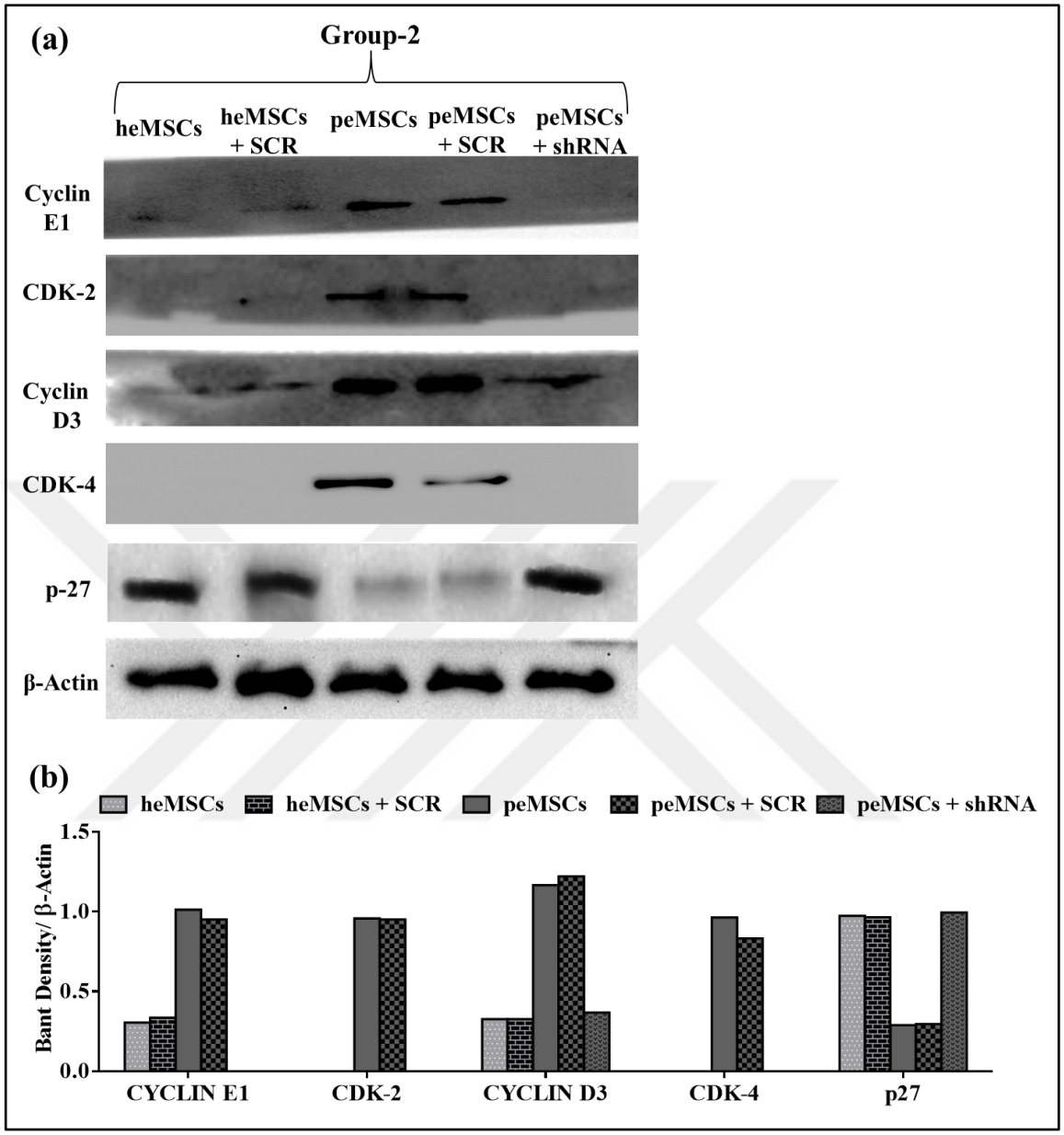

Figure 4.43. Determination of cell cycle proteins level in eMSCs transduced with control scrambled (SCR) or TG2 targeting lentiviral shRNA (shRNA) for Group-2. (a) Images of cell cycle and loading control β-Actin protein levels in Group-2 following shRNA transduction at 0.22 μm nitrocellulose membrane. (b) Quantification of cell cycle proteins adjusted to loading control β-Actin protein using the Image J program for Group-2.

The analysis performed in Group-1 for quantification was also applied to the samples in Group-2 (Figure 4.43.). heMSCs and heMSCs + SCR samples in Group-2 did not synthesize Cyclin E1, CDK-2 and CDK-4 proteins, whereas they synthesized Cyclin D3 protein 15.43

and 16 times less than peMSCs sample in the same group, respectively. On the other hand, when a similar comparison was made for another cell cycle protein p-27, it was found that heMSCs and heMSCs + SCR samples were synthesized in equal amounts by 3.68 times more p-27. When the peMSCs sample was compared to the peMSCs + SCR sample in the same group, it was observed that they contained an equal amount of cell cycle proteins. In Group-2, the peMSCs treated with TG2 targeting lentiviral shRNA (peMSCs + shRNA), cell cycle protein results were similar to heMSCs and heMSCs + SCR samples. The peMSCs + shRNA sample synthesized Cyclin D3 protein 8.47 times less compared to peMSCs, while the p27 protein expressed 3.86 times more. On the other hand, Cyclin E1, CDK2, and CDK4 proteins were not synthesized in peMSCs + shRNA sample (Figure 4.43.b.).

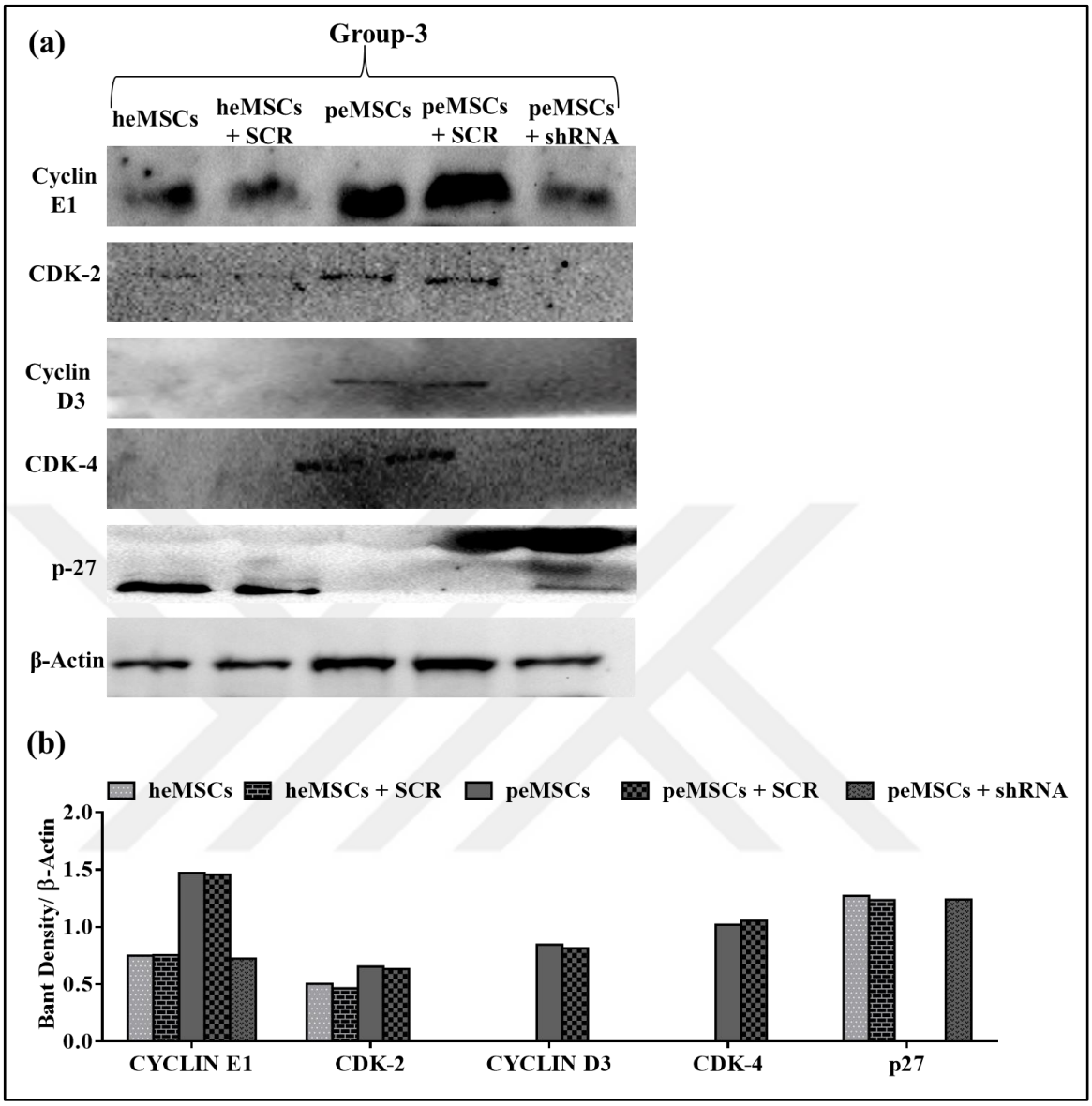

Figure 4.44. Determination of cell cycle proteins level in eMSCs transduced with control scrambled (SCR) or TG2 targeting lentiviral shRNA (shRNA) for Group-3. (a) Images of cell cycle and loading control β-Actin protein levels in Group-3 following shRNA transduction at 0.22 μm nitrocellulose membrane. (b) Quantification of cell cycle proteins adjusted to loading control β-Actin protein using the Image J program for Group-3.

In Group-3 (Figure 4.44.), heMSCs and heMSCs + SCR samples did not synthesize Cyclin D3 and CDK-4 proteins, whereas they synthesized Cyclin E1 protein 2 times less than peMSCs sample in the same group and the CDK-2 protein was synthesized 1.3 times less for heMSCs and 1.4 times less for heMSCs + SCR, respectively. On the other hand, when a

similar comparison was made for another cell cycle protein p27, it was found that heMSCs and heMSCs + SCR samples were synthesized in equal amounts by 1.28 times more p27. When the peMSCs sample was compared to the peMSCs + SCR sample in the same group, it was observed that they contained an equal amount of cell cycle proteins. In Group-3, the peMSCs treated with TG2 targeting lentiviral shRNA (peMSCs + shRNA), cell cycle protein results were similar to heMSCs and heMSCs + SCR samples. The peMSCs + shRNA sample synthesized Cyclin E1 protein 2 times less compared to peMSCs, while the p27 protein expressed 1.24 times more. On the other hand, CDK-2, Cyclin D3, and CDK-4 proteins were not synthesized in peMSCs + shRNA sample (Figure 4.44.b.).

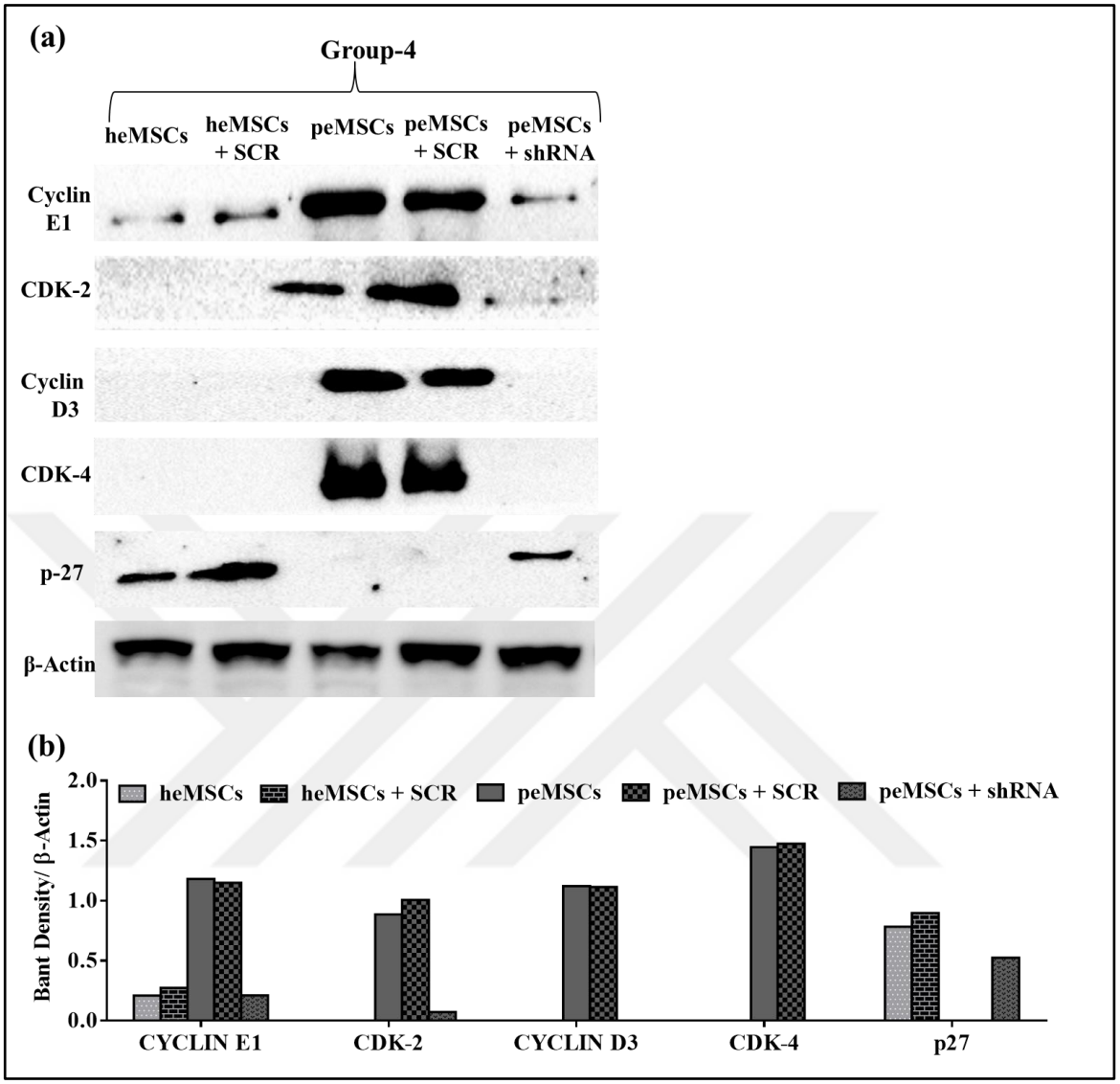

Figure 4.45. Determination of cell cycle proteins level in eMSCs transduced with control scrambled (SCR) or TG2 targeting lentiviral shRNA (shRNA) for Group-4. (a) Images of cell cycle and loading control β-Actin protein levels in Group-4 following shRNA transduction at 0.22 μm nitrocellulose membrane. (b) Quantification of cell cycle proteins adjusted to loading control β-Actin protein using the Image J program for Group-4.

In Group-4 (Figure 4.45.), heMSCs and heMSCs + SCR samples did not synthesize CDK-2, Cyclin D3 and CDK-4 proteins, whereas they synthesized Cyclin E1 protein 5.63 and 4.32 times less than peMSCs sample in the same group, respectively. On the other hand, when a similar comparison was made for another cell cycle protein p-27, it was found that heMSCs and heMSCs + SCR samples were synthesized in equal amounts by 0.9 and 1.09 times more

p-27. When the peMSCs sample was compared to the peMSCs + SCR sample in the same group, it was observed that they contained an equal amount of cell cycle proteins. In Group-4, the peMSCs treated with TG2 targeting lentiviral shRNA (peMSCs + shRNA), cell cycle protein results were similar to heMSCs and heMSCs + SCR samples. The peMSCs + shRNA sample synthesized Cyclin E1 protein 5.62 times less compared to peMSCs, while the p-27 protein expressed 0.99 times more. On the other hand, CDK-2 was synthesized 12.14-fold less than peMSCs sample and Cyclin D3, and CDK-4 proteins were not synthesized in peMSCs + shRNA sample (Figure 4.45.b.).

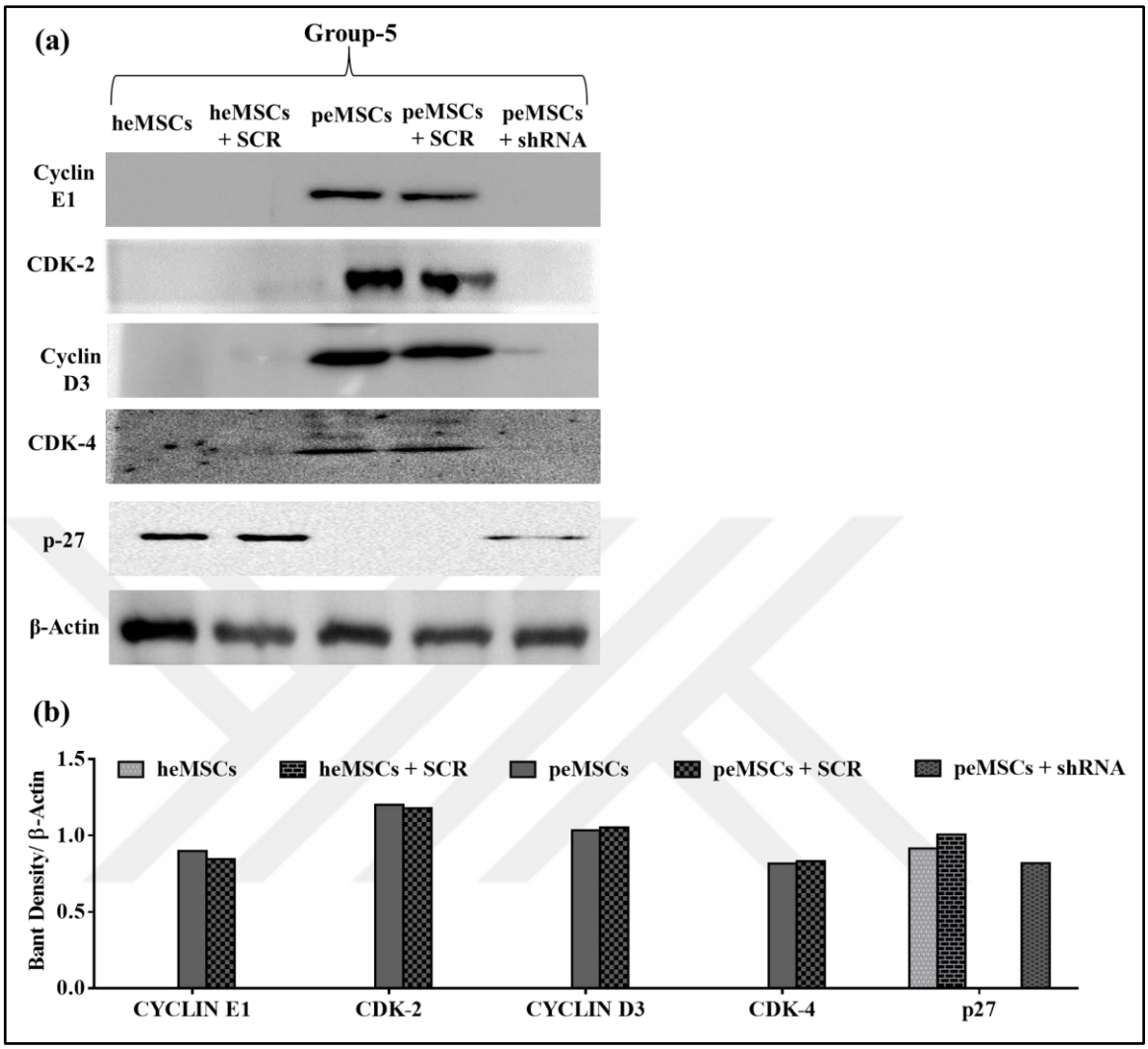

Figure 4.46. Determination of cell cycle proteins level in eMSCs transduced with control scrambled (SCR) or TG2 targeting lentiviral shRNA (shRNA) for Group-5. (a) Images of cell cycle and loading control β-Actin protein levels in Group-5 following shRNA transduction at 0.22 μm nitrocellulose membrane. (b) Quantification of cell cycle proteins adjusted to loading control β-Actin protein using the Image J program for Group-5.

In Group-5 (Figure 4.46.), heMSCs, heMSCs + SCR and peMSCs samples did not synthesize Cyclin E1, CDK2, Cyclin D3, and CDK4 proteins. On the other hand, when a similar comparison was performed for another cell cycle protein p-27, it was found that heMSCs, heMSCs + SCR and peMSCs samples were synthesized in equal amounts by 0.9, 1.1 and 0.80 times more p-27, respectively.

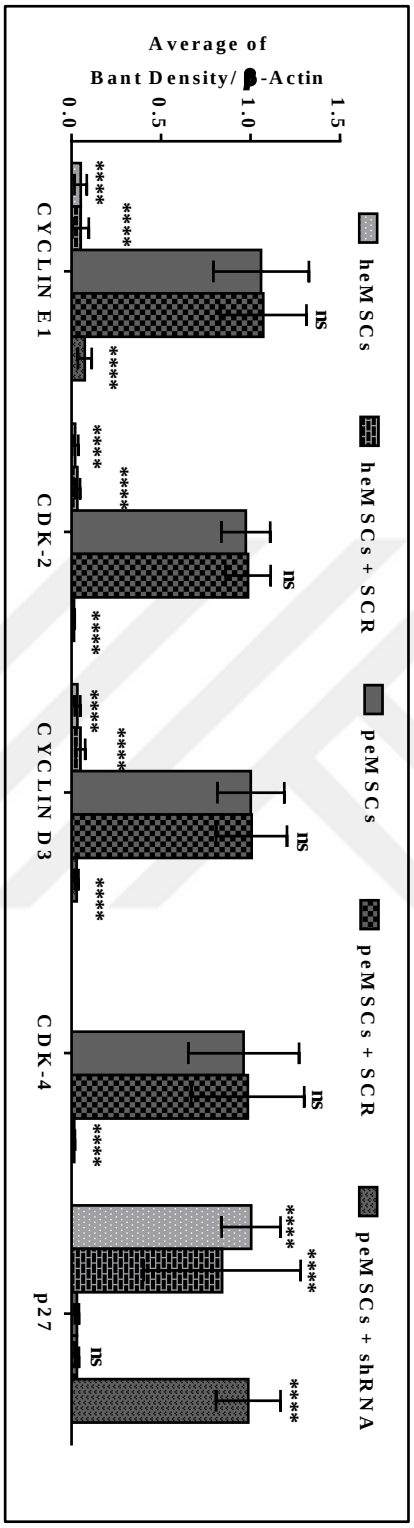

Figure 4.47. Determination of average of cell cycle proteins level in five different eMSCs transduced with control scrambled (SCR) or TG2 targeting lentiviral shRNA (shRNA). All statistical results were analyzed in GraphPad Prism 6 software program by 2way ANOVA multiple comparisons. ns was used for non- significant, while **** was used for $p<0.0001$.

In Figure 4.47., Western Blot technique was used to determine the average levels of cell cycle proteins in heMSCs, heMSCs + SCR, peMSCs, peMSCs + SCR and peMSCs + shRNA samples in five different groups. As a result of the analysis, heMSCs, heMSCs + SCR and peMSCs + shRNA samples were found to synthesize Cyclin E1, CDK-2, Cyclin D3 and CDK-4 proteins by 1.05, 0.97, 1.02 and 0.96 times respectively when compared to peMSCs samples ($p < 0.0001$). The peMSCs and peMSCs + SCR samples synthesized cell cycle proteins in equal amounts, and no statistical difference was observed between them (ns). On the other hand, the average p-27 value of heMSCs, heMSCs + SCR and peMSCs + shRNA samples were found to be similar, and this value was 0.98 times higher than the peMSCs sample ($p < 0.0001$).

4.7.2.2. Determination of Cell Cycle Rate in TG2 Silenced peMSCs by Cytell

In order to determine the effect of TG2 silencing on cell cycle progression of heMSCs, heMSCs + SCR, peMSCs, peMSCs + SCR and peMSCs + shRNA samples in five different groups, cells were stained using Reagent G, and the phases of cell cycle was determined at Cytell Imaging System using Cell Cycle program tab. In this context, the protocol presented in Section 3.9.2. was used for the determination of different phases of cell cycle (G0/G1 (%), S (%), G2/M (%) and >4n (Mitosis) in five different groups.

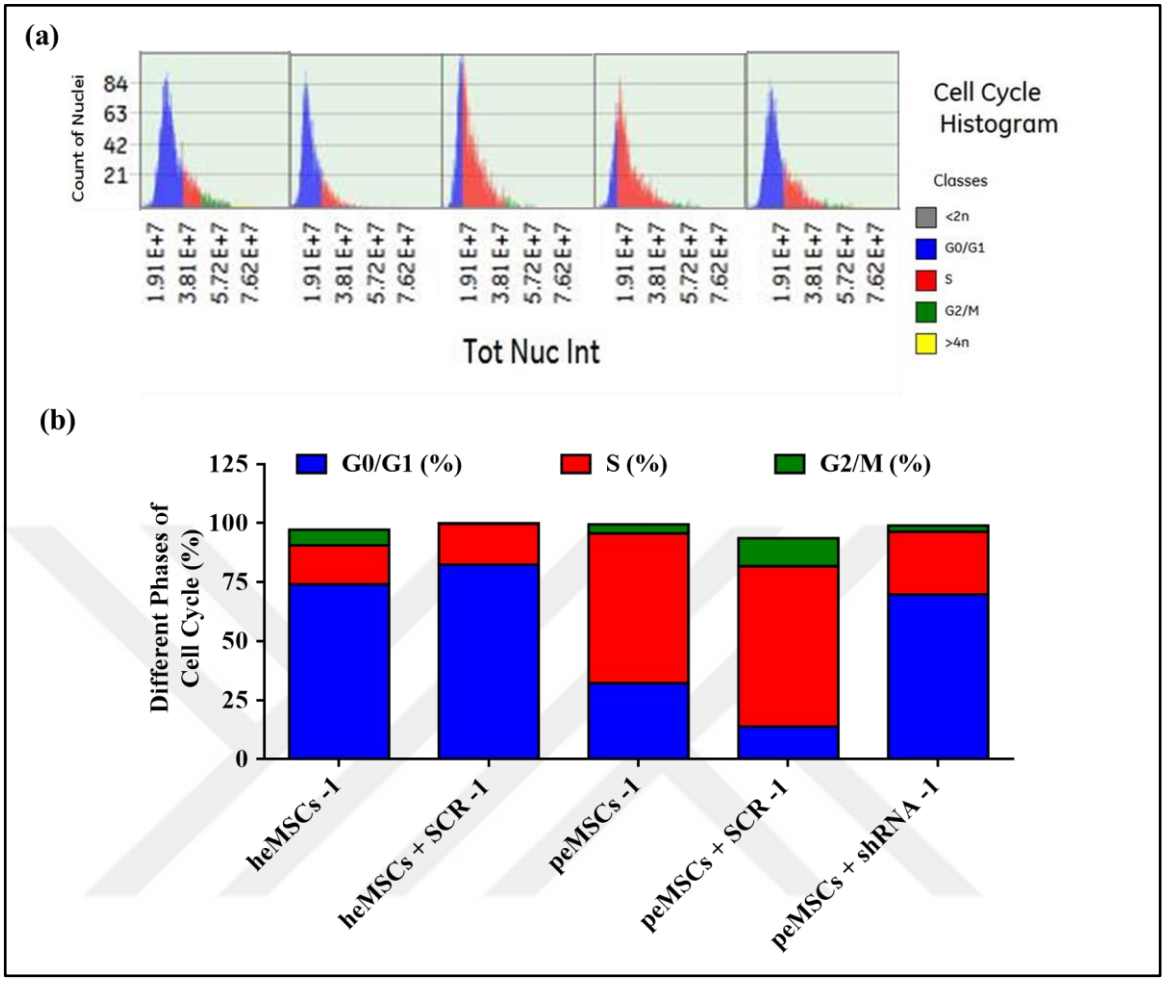

Figure 4.48. Cell cycle analysis for healthy (heMSC) and patient eMSCs (peMSC) transduced with control scrambled (SCR) or TG2 targeting lentiviral shRNA (shRNA) for Group-1. (a) Analysis of cell cycle by Cytell™ Cell Imaging System. (b) Distrubition of cell cycle phases in eMSCs for Group-1.

A commercially available Cytell Cell Cycle Kit was used. The kit contains a DNA binding dye called Reagent G. Reagent G binds to the total DNA content of living cells and positively stained cells as well as staining intensity was determined by cell cycle program of Cytell™ Cell Imaging System (Figure 4.48.a.). In Figure 4.46.b., the percentage value of each cell cycle phase was determined and presented for each sample. The heMSCs sample in Group-1 was found to be 74.10 percent in G0/G1 phase, 16.50 percent in S phase and 6.59 percent in G2/M phase. heMSCs + SCR was found to be 82.4 percent in G0/G1 phase, 17.4 percent in S phase and 0.18 percent in G2/M phase. peMSCs was found to be 32.2 percent in G0/G1

phase, 63.5 percent in S phase and 3.77 percent in G2/M phase. peMSCs + SCR was found to be 13.9 percent in G0/G1 phase, 67.9 percent in S phase and 11.8 percent in G2/M phase. peMSCs + shRNA was found to be 69.7 percent in G0/G1 phase, 26.7 percent in S phase and 2.63 percent in G2/M phase (Figure 4.48.b.). The silencing of TG2 resulted in a 2.34-fold reduction in S phase while a parallel increase G0 / G1 phase cells was detected. In other words, the percentage of peMSCs + shRNA in G0 / G1 phase was found to be similar to that of heMSCs and heMSCs + SCR samples. Control shRNA (scrambled) applied to heMSCs and peMSCs cells had no effect on cell cycle phases.

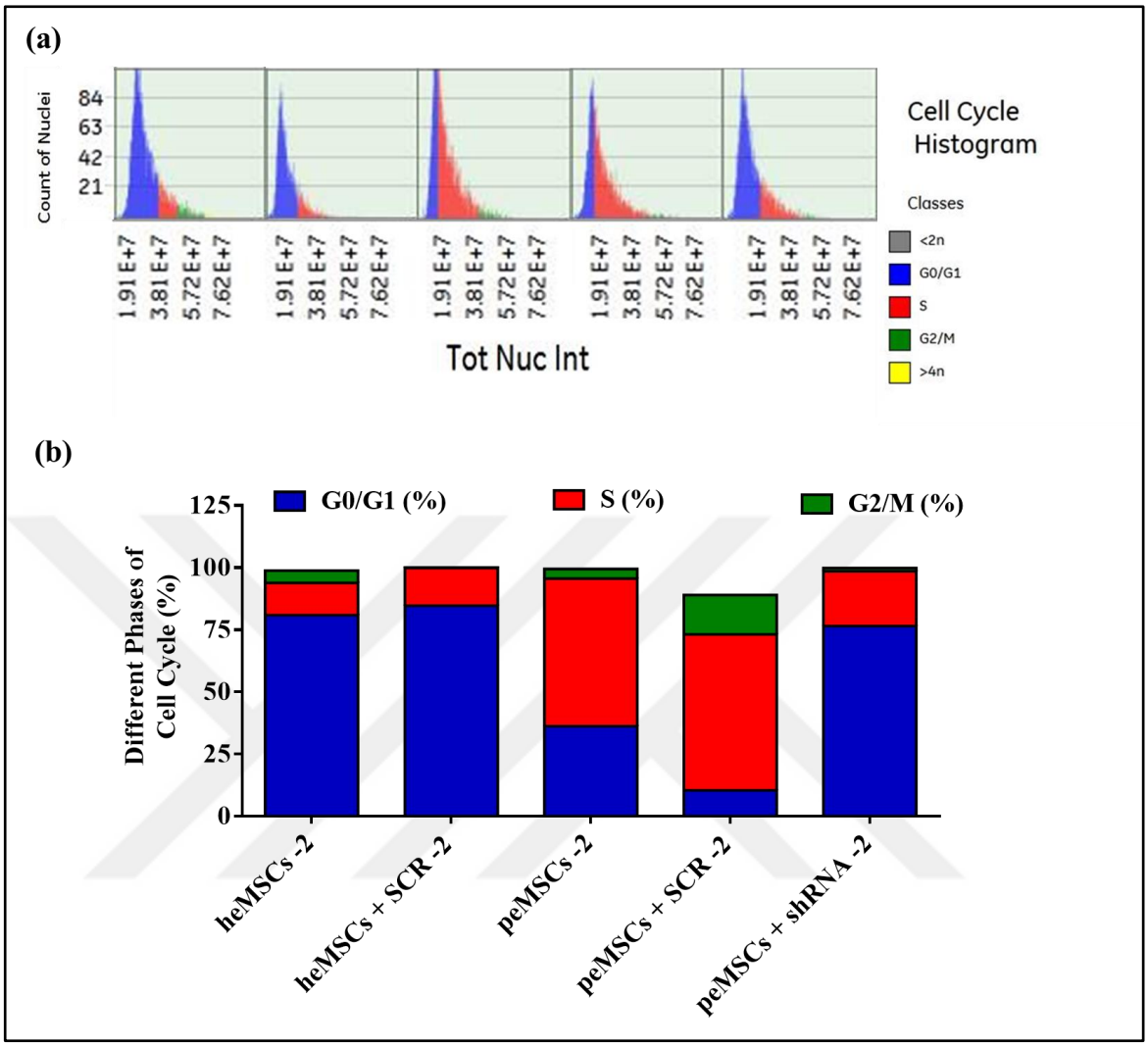

Figure 4.49. Cell cycle analysis for healthy (heMSC) and patient eMSCs (peMSC) transduced with control scrambled (SCR) or TG2 targeting lentiviral shRNA (shRNA) for Group-2. (a) Analysis of cell cycle by Cytell™ Cell Imaging System. (b) Distrubition of cell cycle phases in eMSCs for Group-2.

Analysis of cell cycle phases for the eMSCs of Group-2 (Figure 4.49) showed that while 80.90 percent of heMSCs was in G0/G1 phase, 12.90 percent and 5.01 percent was at S phase and G2/M phase, respectively. heMSCs + SCR was found to be 84.7 percent in G0/G1 phase, 15.1 percent in S phase and 0.18 percent in G2/M phase. peMSCs was found to be 36.2 percent in G0/G1 phase, 59.4 percent in S phase and 3.84 percent in G2/M phase. peMSCs + SCR was found to be 10.4 percent in G0/G1 phase, 62.7 percent in S phase and 15.9

percent in G2/M phase. peMSCs + shRNA was found to be 76.5 percent in G0/G1 phase, 22 percent in S phase and 1.34 percent in G2/M phase (Figure 4.49.b.). Application of TG2-targeted shRNA to peMSCs cells resulted in a 2.7-fold decrease in S phase and a 2.11-fold increase in G0 / G1 phase when compared to peMSCs and peMSCs + SCR.

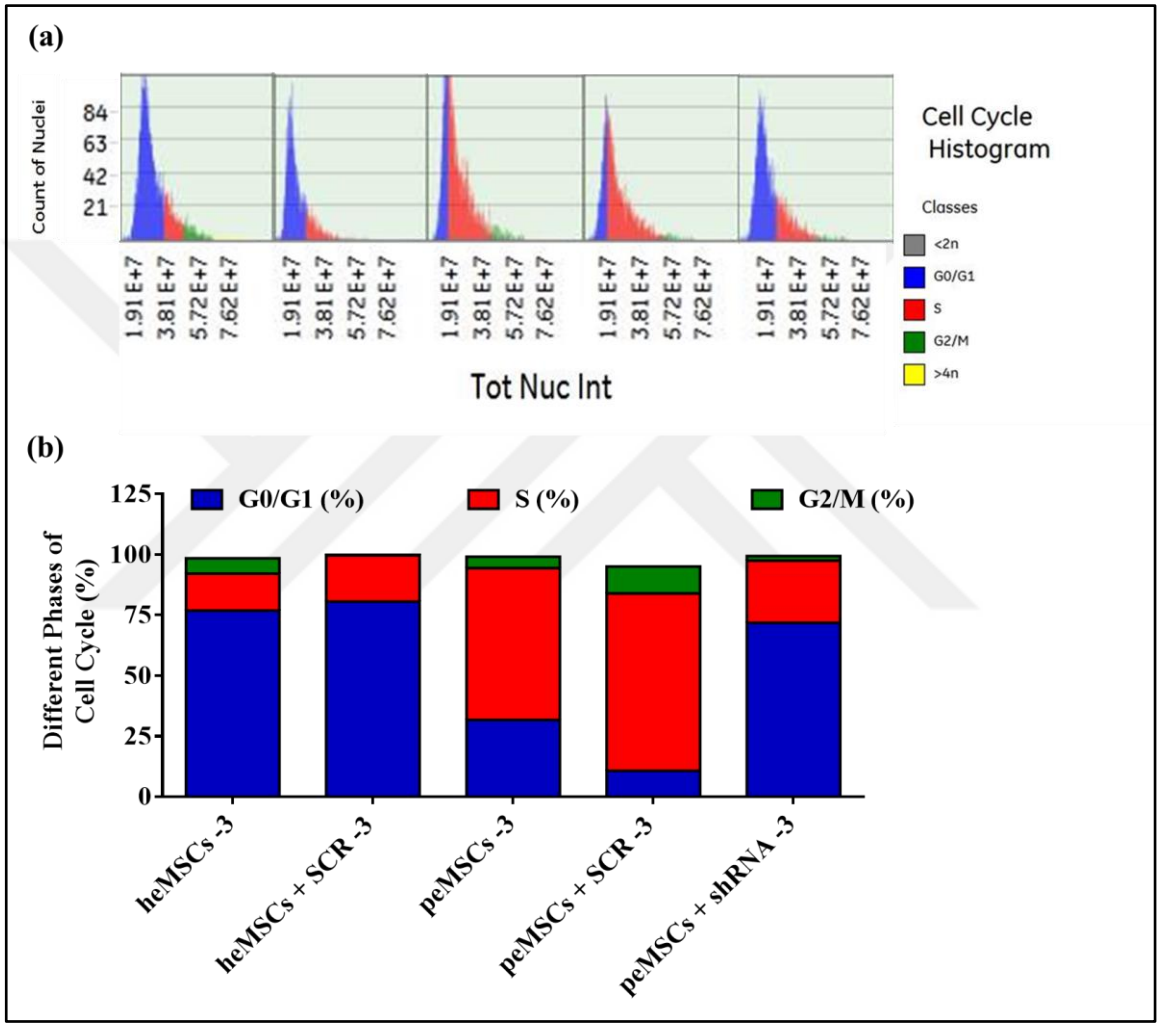

Figure 4.50. Cell cycle analysis for healthy (heMSC) and patient eMSCs (peMSC) transduced with control scrambled (SCR) or TG2 targeting lentiviral shRNA (shRNA) for Group-3. (a) Analysis of cell cycle by Cytell™ Cell Imaging System. (b) Distrubition of cell cycle phases in eMSCs for Group-3.

In Figure 4.50.a., the percentage histogram of the total amount of DNA stained by Reagent G is presented for each sample of Group-3. The heMSCs was found to be 76.90 percent in

G0/G1 phase, 15.20 percent in S phase and 6.34 percent in G2/M phase. heMSCs + SCR was found to be 80.6 percent in G0/G1 phase, 19.1 percent in S phase and 0.22 percent in G2/M phase. peMSCs was found to be 31.7 percent in G0/G1 phase, 62.7 percent in S phase and 4.73 percent in G2/M phase. peMSCs + SCR was found to be 10.7 percent in G0/G1 phase, 73.3 percent in S phase and 11.1 percent in G2/M phase. peMSCs + shRNA was found to be 71.9 percent in G0/G1 phase, 25.6 percent in S phase and 1.95 percent in G2/M phase (Figure 4.50.b.). Reduction of TG2 level in peMSCs + shRNA samples by shRNA application resulted in a 2.45-fold reduction in S phase cells, while a 3-fold increase in G0 / G1 phase was detected. heMSCs and peMSCs samples transduced with control scrambled did show a difference in the distribution of cell cycle phases.

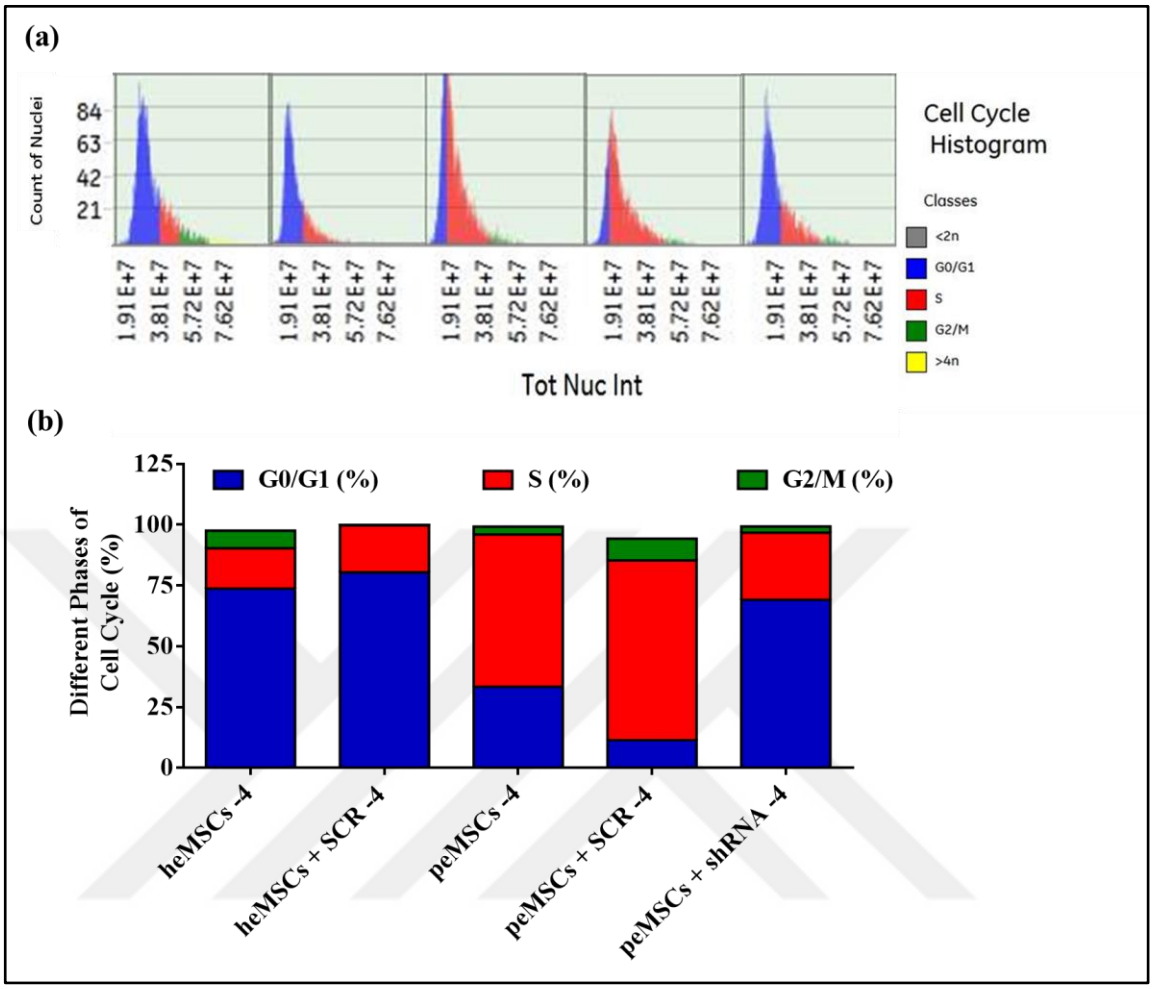

Figure 4.51. Cell cycle analysis for healthy (heMSC) and patient eMSCs (peMSC) transduced with control scrambled (SCR) or TG2 targeting lentiviral shRNA (shRNA) for Group-4. (a) Analysis of cell cycle by Cytell™ Cell Imaging System. (b) Distrubition of cell cycle phases in eMSCs for Group-4.

Distribution of eMSCs into cell cycle phases was detected using Reagent G for Group-4 healthy and patient samples as shown in Figure 4.51. 73.70 percent of heMSCs was found to be in G0/G1 phase, 16.60 percent in S phase and 7.24 percent in G2/M phase. heMSCs + SCR was found to be 80.4 percent in G0/G1 phase, 19.3 percent in S phase and 0.2 percent in G2/M phase. peMSCs was found to be 33.3 percent in G0/G1 phase, 62.7 percent in S phase and 3.2 percent in G2/M phase. peMSCs + SCR was found to be 11.4 percent in G0/G1 phase, 73.9 percent in S phase and 8.94 percent in G2/M phase. peMSCs + shRNA was found to be 69.1 percent in G0/G1 phase, 27.6 percent in S phase and 2.58 percent in G2/M

phase (Figure 4.51.b.). Silencing of TG2 in peMSCs resulted in a 2.27-fold increase in S phase in peMSCs + shRNA samples compared to peMSCs samples while a 2.08-fold increase in G0 / G1 phase was recorded. Scramble shRNA containing control lentiviral particles did not affect cell cycle phases in heMSCs and peMSCs samples.

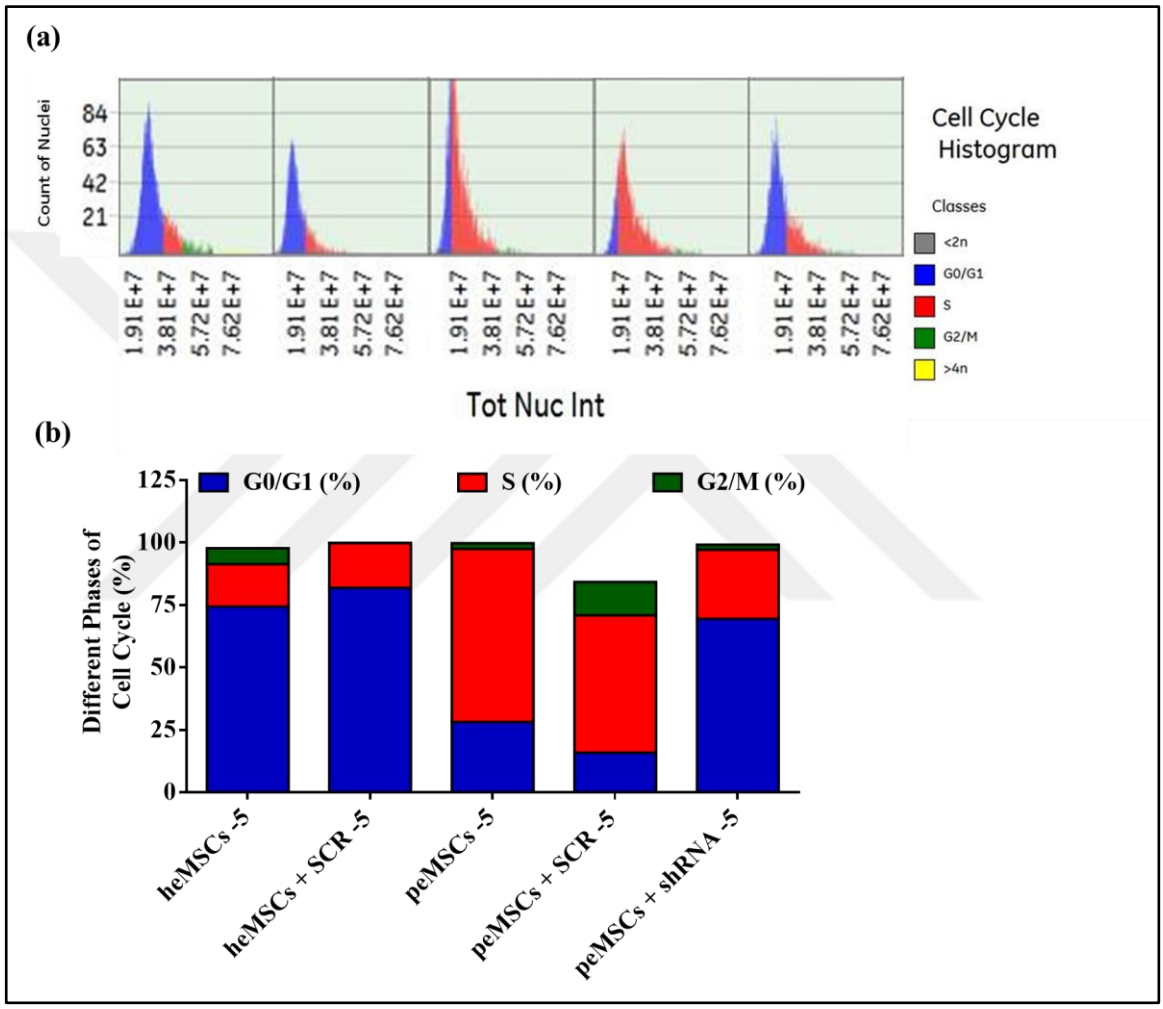

Figure 4.52. Cell cycle analysis for healthy (heMSC) and patient eMSCs (peMSC) transduced with control scrambled (SCR) or TG2 targeting lentiviral shRNA (shRNA) for Group-5. (a) Analysis of cell cycle by Cytell™ Cell Imaging System. (b) Distrubition of cell cycle phases in eMSCs for Group-5.

Analysis of cell cycle phases for Group-5 eMSCs showed a similar pattern with the rest of the groups (Figure 4.52), in that, the percentage of peMSCs was at least 55 percent more

than heMSCs. heMSCs was found to be 74.30 percent in G0/G1 phase, 17 percent in S phase and 6.40 percent in G2/M phase. heMSCs + SCR was found to be 81.8 percent in G0/G1 phase, 18 percent in S phase and 0.08 percent in G2/M phase. peMSCs was found to be 28.1 percent in G0/G1 phase, 69.3 percent in S phase and 2.26 percent in G2/M phase. peMSCs + SCR was found to be 15.8 percent in G0/G1 phase, 55 percent in S phase and 13.4 percent in G2/M phase. peMSCs + shRNA was found to be 69.4 percent in G0/G1 phase, 27.7 percent in S phase and 1.97 percent in G2/M phase (Figure 4.52.b.). The silencing of TG2 resulted in a 2.5-fold reduction in S phase, while a parallel increase in G0/G1 phase was detected for peMSCs + shRNA cells. Control shRNA (scrambled) applied to heMSCs and peMSCs cells had no effect on cell cycle phases.

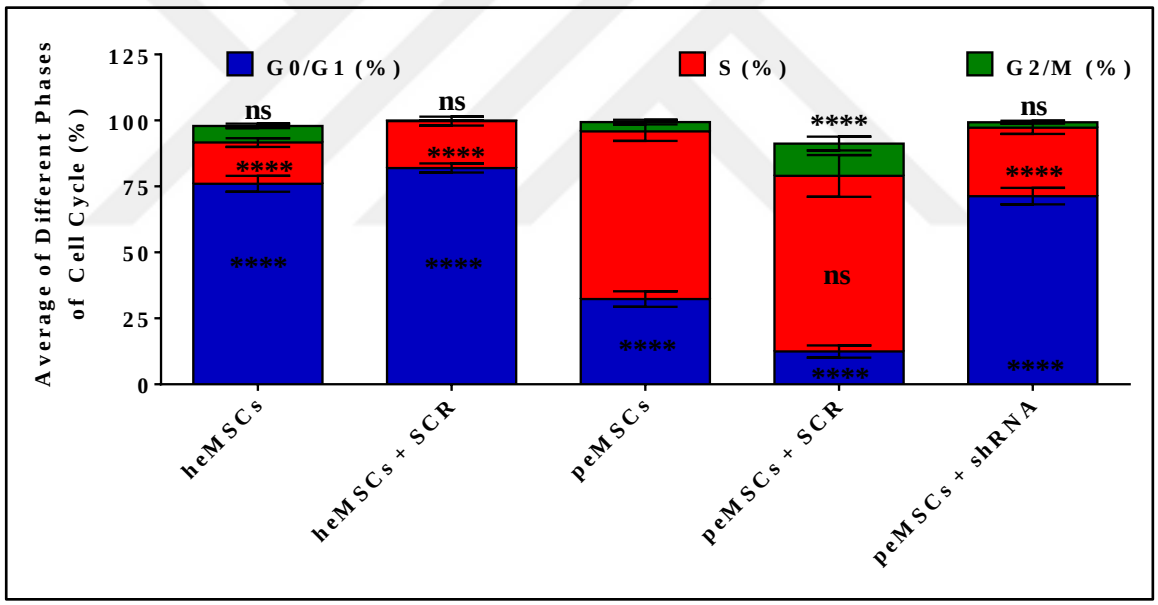

Figure 4.53. Determination of average of cell cycle phases in five different eMSCs transduced with control scrambled (SCR) or TG2 targeting lentiviral shRNA (shRNA).

Average values of cell percentage detected for each cell cycle phase in the heMSCs, heMSCs + SCR, peMSCs, peMSCs + SCR and peMSCs + shRNA samples of five different groups were presented in Figure 4.53. heMSCs and peMSCs samples transduced with control scrambled did not show a statically significance for distribution of cells on cell cycle phases, when compared to their non-transduced counterparts. On average, heMSCs samples were

found to be 75.98 percent in G0/G1 phase, 15.64 percent in S phase, 6.32 percent in G2/M phase. Similarly, heMSCs + SCR samples were found to be 81.98 percent in G0/G1 phase, 17.78 percent in S phase, 0.17 percent in G2/M phase. peMSCs samples were found to be 32.30 percent in G0/G1 phase, 63.52 percent in S phase, 3.56 percent in G2/M phase. peMSCs + SCR samples were found to be 12.44 percent in G0/G1 phase, 66.56 percent in S phase, 12.23 percent in G2/M phase. peMSCs + shRNA samples were found to be 71.32 percent in G0/G1 phase, 25.92 percent in S phase, 2.09 percent in G2/M phase. G0/G1 heMSC population was 2.3 folds more than peMSCs ($p<0.0001$), while there was 4-fold more cells in S phase for peMSCs than heMSCs ($p<0.0001$). No significant difference in the percentage G2/M phase cell population was detected bewteen peMSCs and heMSCs. Reduction of TG2 expression in peMSCs + shRNA samples by shRNA application resulted in a 2.45-fold reduction in S phase cell population, while a 2.20-fold increase in G0/G1 phase was observed.

4.8. EFFECT OF TG2 ON MIGRATON POTENTIAL OF eMSCs

The scratch assay protocol as described in Section 3.12 was applied to determine the cell migration potential of heMSCs, heMSCs + SCR, peMSCs, peMSCs + SCR and peMSCs + shRNA samples in five different groups. For this purpose, after the cells of the same passage number (passage 3) were plated into 6-well plates at a density of 300,000 cells per well, the cell monolayer was scratched with SLP scratcher. Wound beds were imaged immediately and then followed with imaging at 6 and 12 hours under the Cytell Imaging System using auto-imaging option (Figure 4.54. to Figure 4.59.). Percentage wound closure was analyzed using MRI_Wound_Healing_Tool in Image J program. The wound closure potential was calculated by normalizing the wound area value obtained for peMSCs at 12^{th} hour to 100 percent.

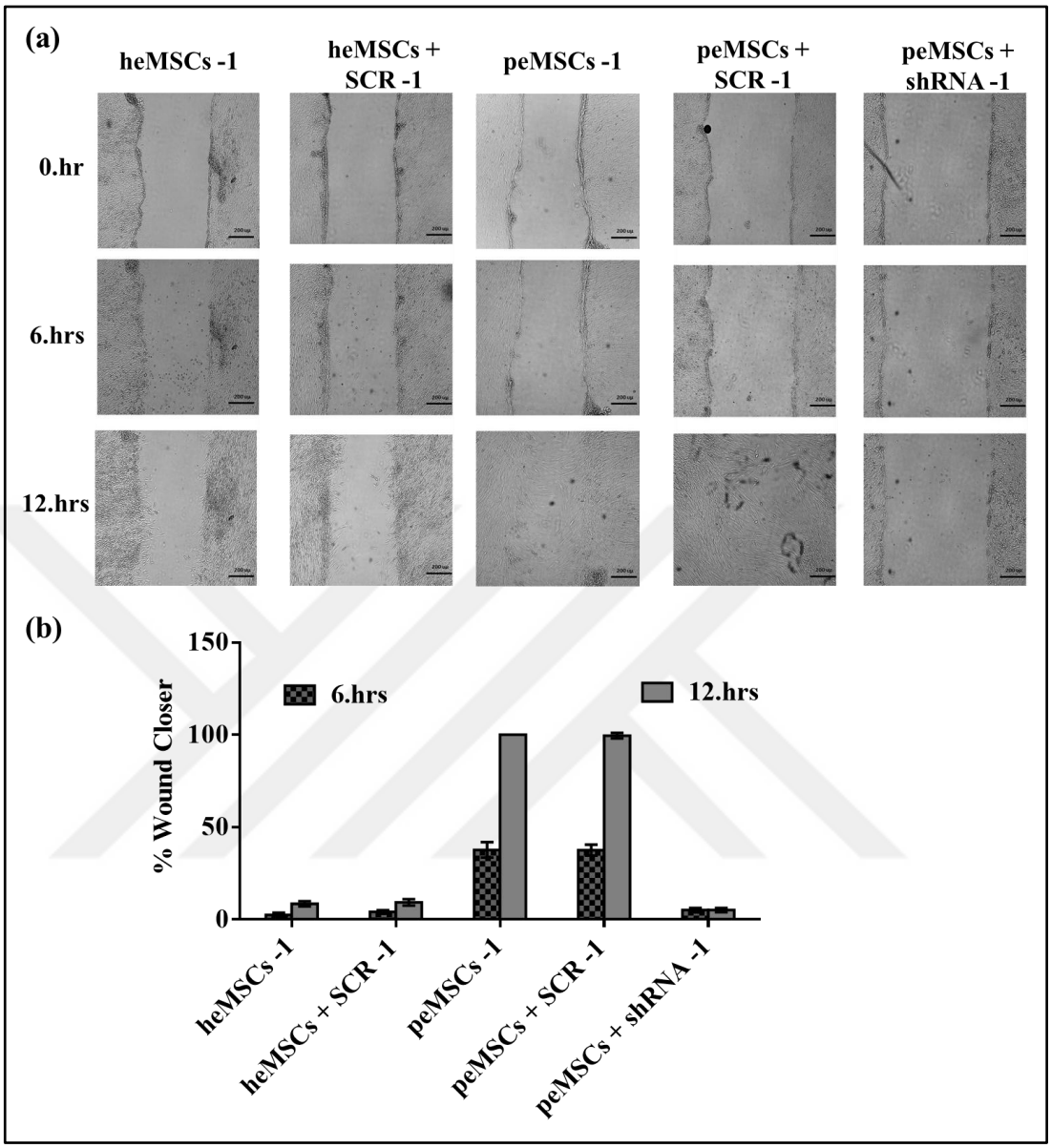

Figure 4.54. Effect of TG2 silencing on migratory potential of Group-1 eMSCs by wound scratch assay. (a) Representative photographs for heMSCs, heMSCs + SCR, peMSCs, peMSCs + SCR, peMSCs + shRNA in Group-1 were captured by 20x objective at 0, 6 and 12 hours. (b) Evaluation of percentage wound closure for eMSCs by measuring the wound bed area in Image J program. Area values were expressed as percentage of peMSCs wound closure, which represents 100 percent. Scale bar was 200 μm.

Results were first evaluated independently for each cell treatment in Group-1, and the representative photographs reflecting the results were shown in Figure 4.54.a. At 6th hour,

heMSCs, and heMSCs + SCR were able to migrate by 2.6 percent and 4.16 percent, respectively, while wound closing capacity of peMSCs and peMSCs + SCR samples were found as 37 percent. However, when TG2 was silenced by shRNA transduction in peMSCs the migratory potential of these cells was dropped to 5.15 percent. By 12^{th} hour, heMSCs and heMSCs + SCR in Group-1 showed a 3.32 percent migration potential, when compared to peMSCs with 100 percent wound closure rate and the peMSCs + SCR sample with 99 percent cell migration potential. Silencing of TG2 still impaired the migration of peMSCs + shRNA as percentage wound closure rate did not change and was still 5.15 percent.

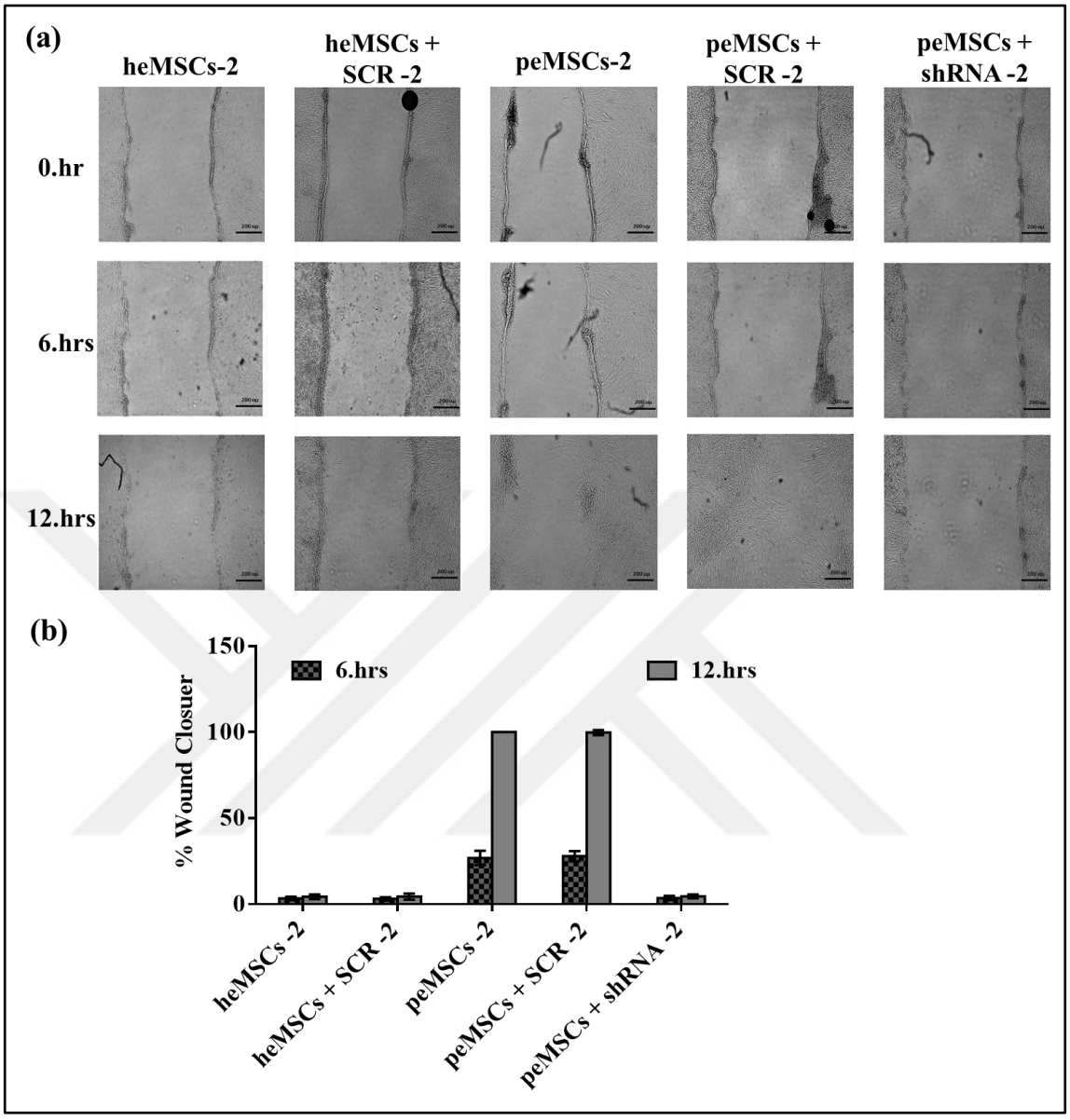

Figure 4.55. Effect of TG2 silencing on migratory potential of Group-2 eMSCs by wound scratch assay. (a) Representative photographs for heMSCs, heMSCs + SCR, peMSCs, peMSCs + SCR, peMSCs + shRNA in Group-2 were captured by 20x objective at 0, 6 and 12 hours. (b) Evaluation of percentage wound closure for eMSCs by measuring the wound bed area in Image J program. Area values were expressed as percentage of peMSCs wound closure, which represents 100 percent. Scale bar was 200 μm. The representative photographs in Figure 4.55.a. were captured using a 20x lens, and the scale bar was 200 μm.

The results were tested independently for each cell in Group-2, and the representative photographs reflecting the results were included. The peMSCs sample in Group-2 was considered to be 100% wound closure at the end of the 12th hours and all values at the other time point were compared with the peMSCs value to obtain results. When the heMSCs, heMSCs + SCR and peMSCs + shRNA samples at the 6th hour was compared with the peMSCs samples, it was found that they had similar migration potential at 3.30 percent. When the migration potential of peMSCs and peMSCs + SCR at the end of the 6th hour was compared, it was found that approximately 27.8 percent of them closed the wound bed. At the end of the 12th hour, heMSCs, heMSCs + SCR and peMSCs + shRNA samples had the potential to migrate to the wound bed at a rate of 4.56 percent, while this rate was 99.75 percent for the peMSCs + SCR sample.

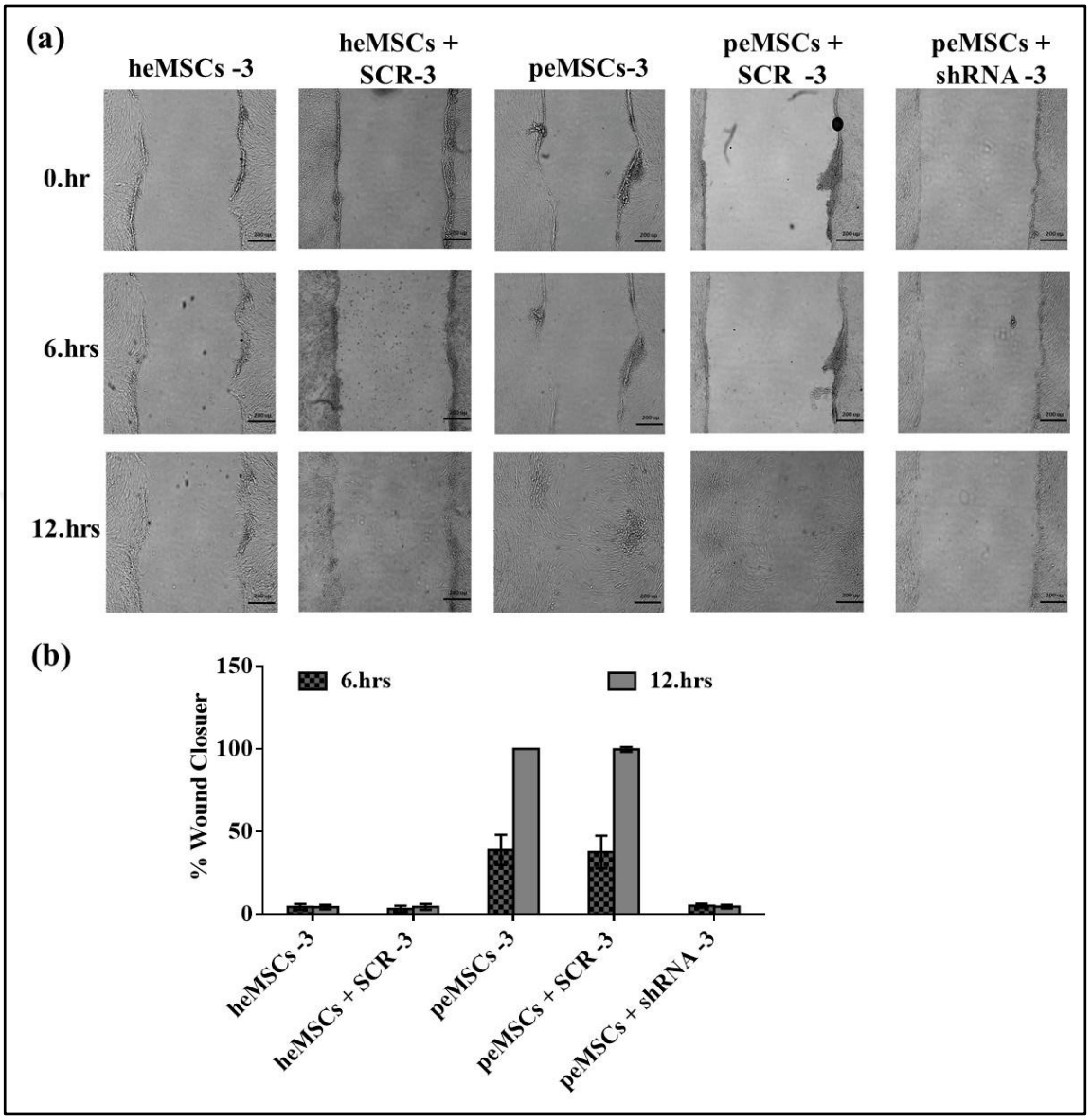

Figure 4.56. Effect of TG2 silencing on migratory potential of Group-3 eMSCs by wound scratch assay. (a) Representative photographs for heMSCs, heMSCs + SCR, peMSCs, peMSCs + SCR, peMSCs + shRNA in Group-3 were captured by 20x objective at 0, 6 and 12 hours. (b) Evaluation of percentage wound closure for eMSCs by measuring the wound bed area in Image J program. Area values were expressed as percentage of peMSCs wound closure, which represents 100 percent. Scale bar was 200 μm. The representative photographs in Figure 4.56.a. were captured using a 20x lens, and the scale bar was 200 μm.

The representative photographs in Figure 4.56.a. were captured using a 20x lens, and the scale bar was 200 μm. The results were tested independently for each cell in Group-3, and the representative photographs reflecting the results were included. The peMSCs sample in Group-3 was considered to be 100% wound closure at the end of the 12th hours and all values at the other time point were compared with the peMSCs value to obtain results. When the heMSCs, heMSCs + SCR and peMSCs + shRNA samples at the 6th hour was compared with the peMSCs samples, it was found that they had similar migration potential at 4.40 percent. When the migration potential of peMSCs and peMSCs + SCR at the end of the 6th hour was compared, it was found that approximately 38.87 percent of them closed the wound bed. At the end of the 12th hour, heMSCs, heMSCs + SCR and peMSCs + shRNA samples had the potential to migrate to the wound bed at a rate of 6.80 percent, while this rate was 98.8 percent for the peMSCs + SCR sample.

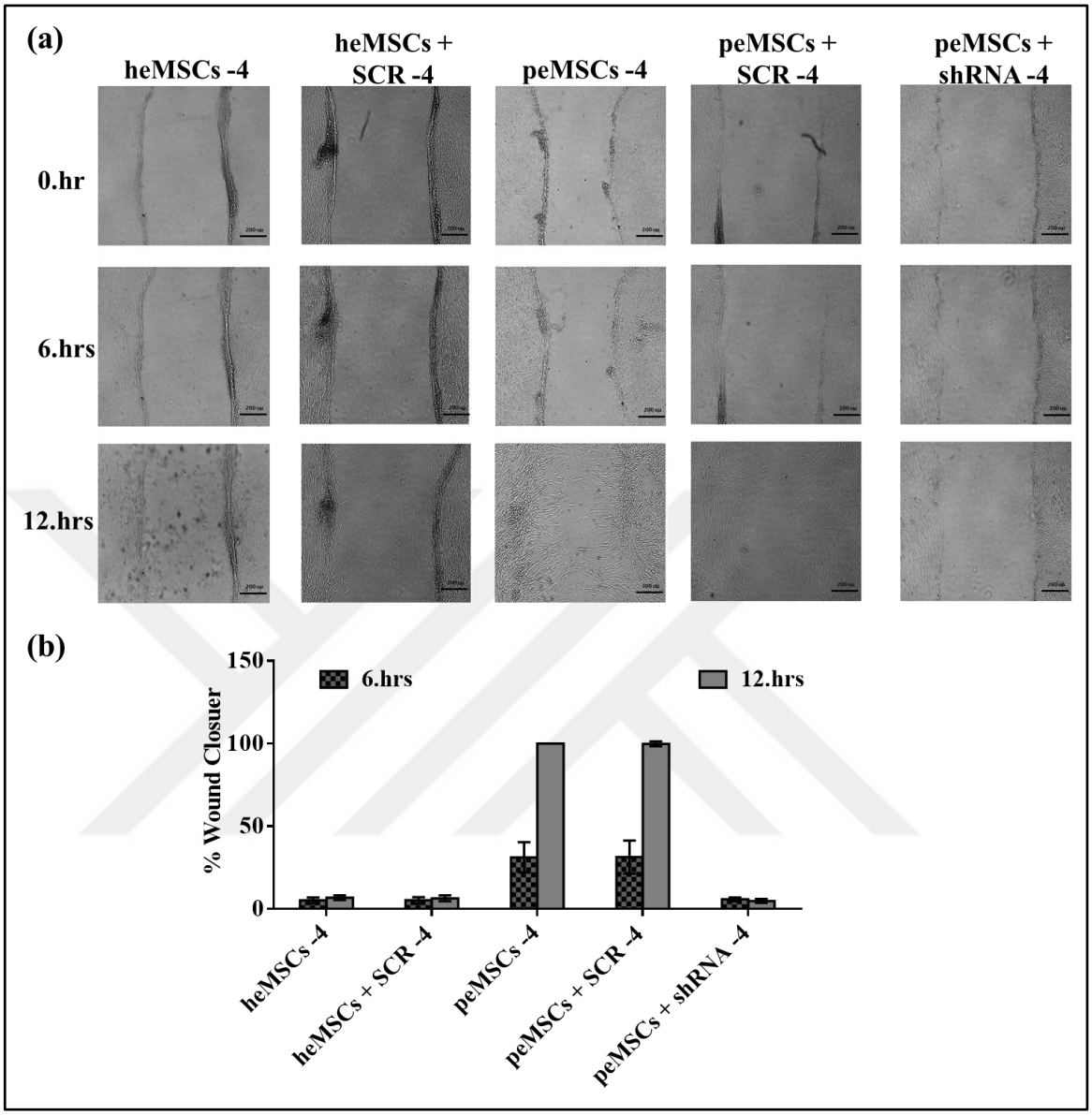

Figure 4.57. Effect of TG2 silencing on migratory potential of Group-4 eMSCs by wound scratch assay. (a) Representative photographs for heMSCs, heMSCs + SCR, peMSCs, peMSCs + SCR, peMSCs + shRNA in Group-4 were captured by 20x objective at 0, 6 and 12 hours. (b) Evaluation of percentage wound closure for eMSCs by measuring the wound bed area in Image J program. Area values were expressed as percentage of peMSCs wound closure, which represents 100 percent. Scale bar was 200 μm. The representative photographs in Figure 4.57.a. were captured using a 20x lens, and the scale bar was 200 μm.

The representative photographs in Figure 4.57.a. were captured using a 20x lens, and the scale bar was 200 μm. The results were tested independently for each cell in Group-4, and the representative photographs reflecting the results were included. The peMSCs sample in Group-4 was considered to be 100% wound closure at the end of the 12th hours and all values at the other time point were compared with the peMSCs value to obtain results. When the heMSCs, heMSCs + SCR and peMSCs + shRNA samples at the 6th hour was compared with the peMSCs samples, it was found that they had similar migration potential at 5.20 percent. When the migration potential of peMSCs and peMSCs + SCR at the end of the 6th hour was compared, it was found that approximately 31.22 percent of them closed the wound bed. At the end of the 12th hour, heMSCs, heMSCs + SCR and peMSCs + shRNA samples had the potential to migrate to the wound bed at a rate of 6.40 percent, while this rate was 99.86 percent for the peMSCs + SCR sample.

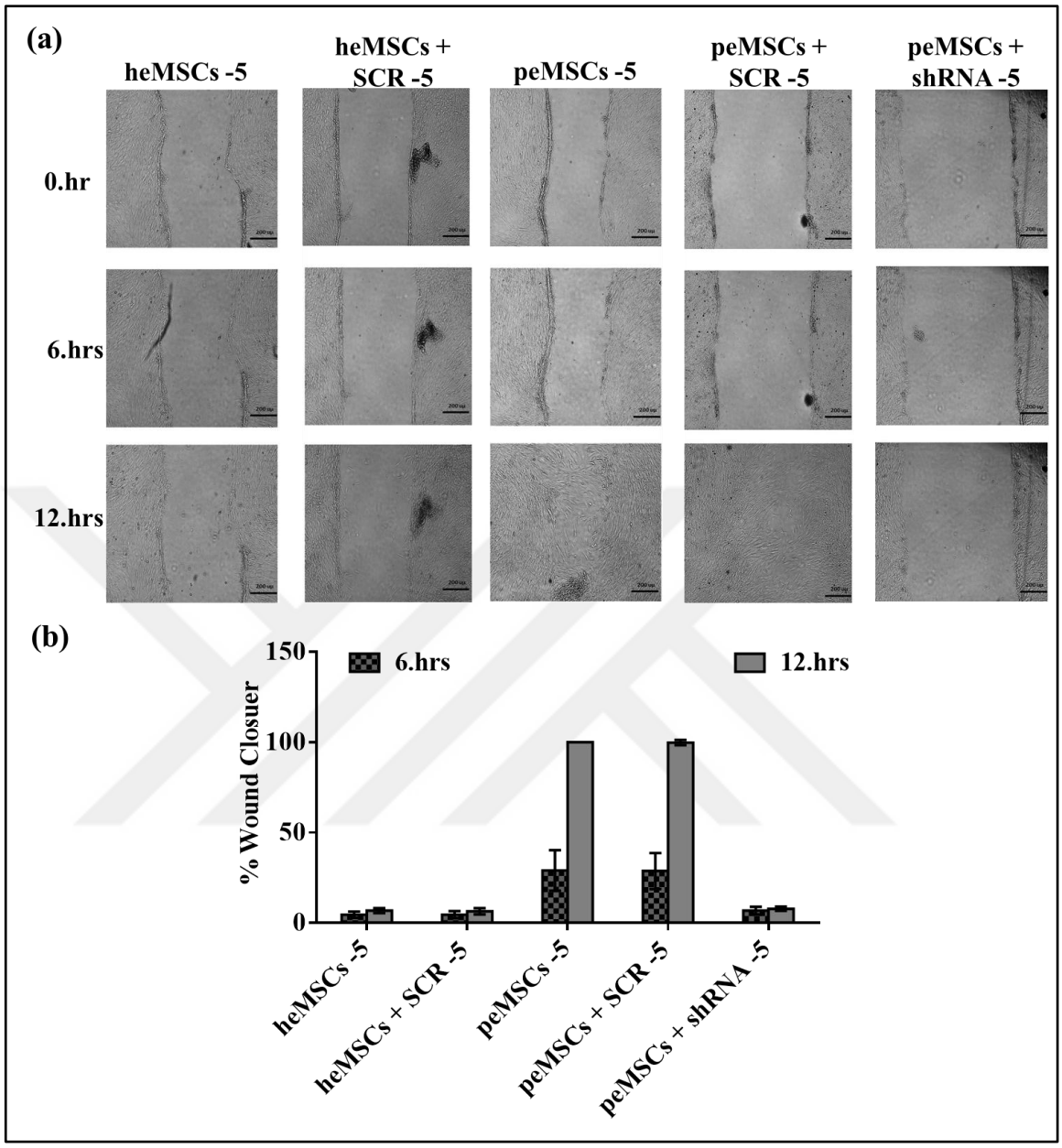

Figure 4.58. Effect of TG2 silencing on migratory potential of Group-5 eMSCs by wound scratch assay. (a) Representative photographs for heMSCs, heMSCs + SCR, peMSCs, peMSCs + SCR, peMSCs + shRNA in Group-5 were captured by 20x objective at 0, 6 and 12 hours. (b) Evaluation of percentage wound closure for eMSCs by measuring the wound bed area in Image J program. Area values were expressed as percentage of peMSCs wound closure, which represents 100 percent. Scale bar was 200 μm. The representative photographs in Figure 4.58.a. were captured using a 20x lens, and the scale bar was 200 μm.

The representative photographs in Figure 4.58.a. were captured using a 20x lens, and the scale bar was 200 μm. The results were tested independently for each cell in Group-5, and the representative photographs reflecting the results were included. The peMSCs sample in Group-5 was considered to be 100% wound closure at the end of the 12th hours and all values at the other time point were compared with the peMSCs value to obtain results. When the heMSCs, heMSCs + SCR and peMSCs + shRNA samples at the 6th hour was compared with the peMSCs samples, it was found that they had similar migration potential at 4.60 percent. When the migration potential of peMSCs and peMSCs + SCR at the end of the 6th hour was compared, it was found that approximately 29.01 percent of them closed the wound bed. At the end of the 12th hour, heMSCs, heMSCs + SCR and peMSCs + shRNA samples had the potential to migrate to the wound bed at a rate of 5.04 percent, while this rate was 99.85 percent for the peMSCs + SCR sample in Figure 4.58.b.

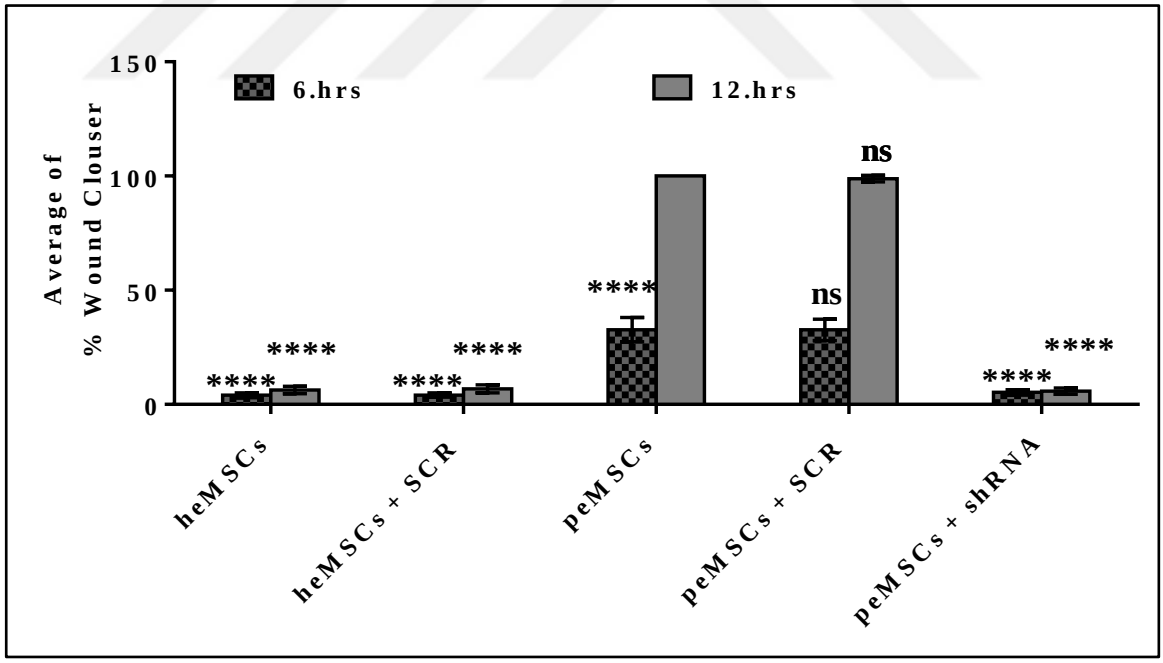

Figure 4.59. Average of the effect of shRNA silenced TG2 on cell migration by wound scratch for five different group (G-1 to G-5) at 6 and 12 hours. GraphPad Prism 6 2way ANOVA multiple comparison program was used to determine the statistical analysis results. ns was used for non-significant p value, **** was used for p <0.00001.

In Figure 4.59., the average wound bed closure potential of eMSCs samples in five different groups with control shRNA (SCR) and TG2-targeted shRNA was calculated. The average wound bed closure value of the peMSCs with or without SCR shRNA transduction was 32.65 percent at the 6th hour, while that of heMSCs and heMSCs + SCR was calculated as 4.14 percent. peMSCs + shRNA was able to close the wound bed by 5.28 at 6th hour, which was not significantly improved by 12th hour as wound closure rate was determined to be 5.81 percent.

4.9. ROLE OF TG2 ON INVASION ABILITES OF eMSCs

The transwell method described in Section 3.13 was used to determine the invasion potential of heMSCs, heMSCs + SCR, peMSCs, peMSCs + SCR and peMSCs + shRNA in five different groups. Cell migration through 8μm -matrigel coated commercial transwells were imaged with 20x objective of Zess microscope at 16 hours. For the quantitative analysis of the images obtained from five different random images, Image J program “cell counter” tab was used. Findings obtained at the end of the method were presented in Figure 4.60 and Figure 4.61.

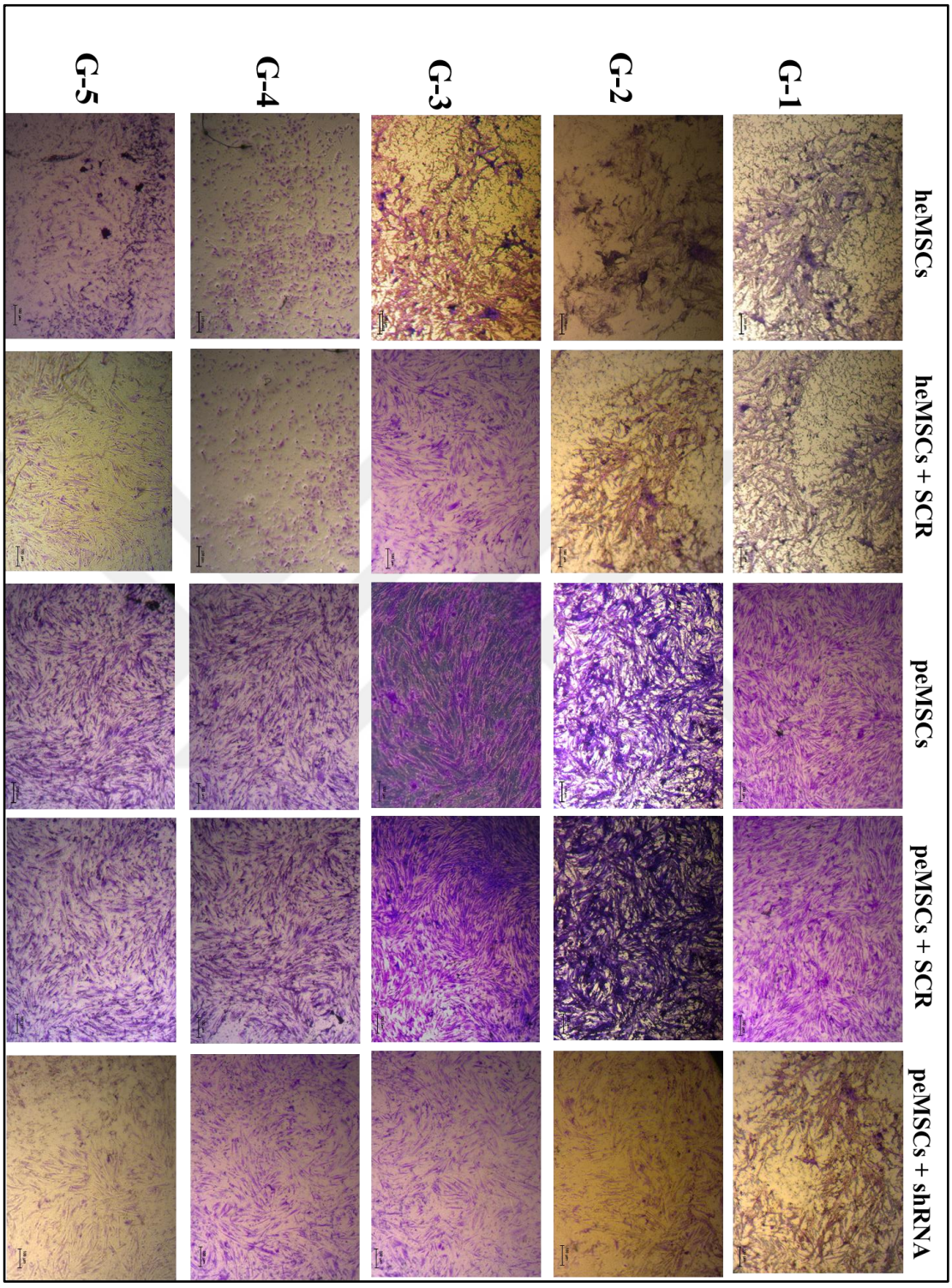

Figure 4.60. Effect of TG2 silencing on invasion potential of eMSCs by transwell invasion assay. Representative photographs for heMSCs, heMSCs + SCR, peMSCs, peMSCs + SCR, peMSCs + shRNA in Group-1 were captured by 20x objective 16 hours after seeding. Scale bar was set to 100µm.

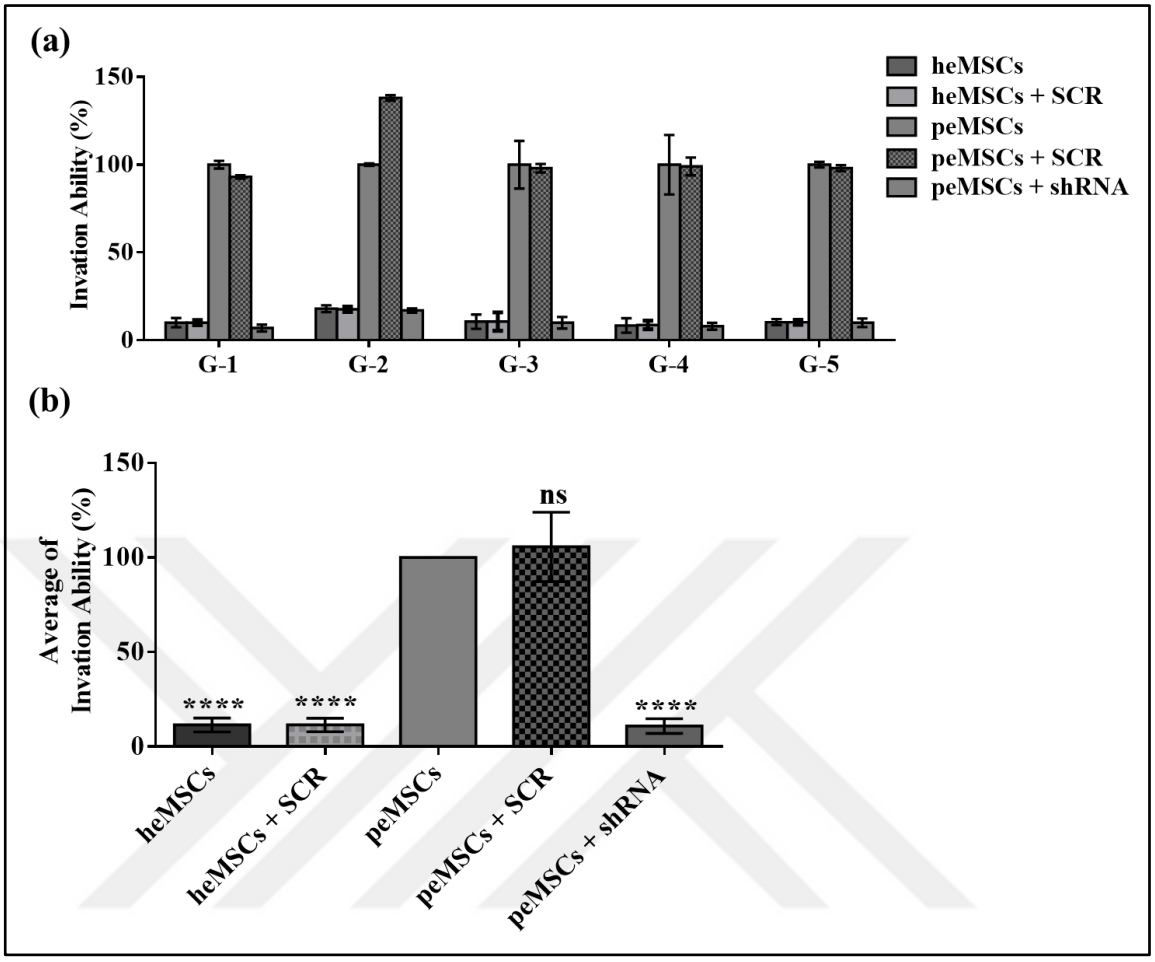

Figure 4.61. Quantification of transwell migration assay to determine percentage invasion ratios in eMSCs in five different groups (G-1 to G-5). (a) Quantitative analyses of invasion potentials of heMSCs, heMSCs + SCR, peMSCs, peMSCs + SCR and peMSCs + shRNA cells in five different groups. (b) Quantitative analyses of average of invasion potentials of heMSCs, heMSCs + SCR, peMSCs, peMSCs + SCR and peMSCs + shRNA cells in five different groups. All cells used in the experiments belonged to the 3rd passage number, and the ns used for non-significant results and statistical significance was $p<0.00001$ with *****.

In Figure 4.61.a., invasion ratios were calculated in terms of percentage values that was obtained by adjusting the total cell number in the lower chamber for peMSCs to 100 percent in each group. Cell numbers obtained for the other samples were expressed according to this percentage. In Group-1, 10.11 percent invasion ability was determined for heMSCs and

heMSCs + SCR cells. When peMSCs + shRNA samples in the same group were compared with peMSCs, the invasion potential of 7.61 percent was found in peMSCs + shRNA. When similar comparisons were made for heMSCs, heMSCs + SCR and peMSCs + shRNA in Group-2, it was observed that these samples were capable of invasion at the same rate of 18.01 percent. When peMSCs samples in Group-2 were compared with peMSCs + SCR, peMSCs + SCR had 38 percent more invasion potential than peMSCs. In Group-3, the invasion potential for heMSCs, heMSCs + SCR and peMSCs + shRNA were determined to be 10.66 percent, whereas this ratio was determined as 98.43 in peMSCs + SCR samples. Similar results were observed in Group-5, while heMSCs, heMSCs + SCR and peMSCs + shRNA samples in Group-4 showed approximately 8.42 percent invasion potential, peMSCs + SCR demonstrated 98 percent invasive capacity. The mean percentage invasion potential of heMSCs, heMSCs + SCR, peMSCs, peMSCs + SCR and peMSCs + shRNA samples in five different groups were presented in Figure 4.61.b. As a result of similar comparisons made assuming the invasion potential of peMSCs samples to be 100 percent, heMSCs and heMSCs + SCR samples had an average invasion potential of 11.51 percent ($p<0.00001$). When peMSCs samples were compared with peMSCs + SCR samples, they showed similar invasion potential and no statistical difference (ns). On the other hand, when peMSCs samples were compared with peMSCs + shRNA samples, it was found that peMSCs + shRNA samples had 10.89 percent invasion potential ($p<0.00001$).

4.10. SIGNIFICANCE OF TG2 EXPRESSION ON MMPs BIOSYNTHESS AND ACTIVITY IN eMSCs

4.10.1. MMPs Expression and Activity Profile of eMSCs

RT-PCR and zymography methods was used to determine MMP-2 and MMP-9 expression and activity levels in heMSCs and peMSCs samples in five different groups. The passage numbers of the cells used during the experiments were three.

4.10.1.1. Determination of MMPs Expression Profile of eMSCs by RT-PCR

Cells seeded in 6-well plates were used to determine mRNA levels of MMP-2 and MMP-9 in all groups of isolated eMSCs using RT-PCR. The primers to be used for RT-PCR were purchased from Qiagen, and the details of the method were described in Section 3.5. 18sRNA was used as housekeeping gene and loading control. Quantification of MMP-2/18mRNA and MMP-9/18mRNA were performed from quantitation cycle (Cq) values plotted against log of known cDNA concentration using random18S rRNA samples. Results of all healthy and patient groups were presented in Figure 4.62 and Figure 4.63.

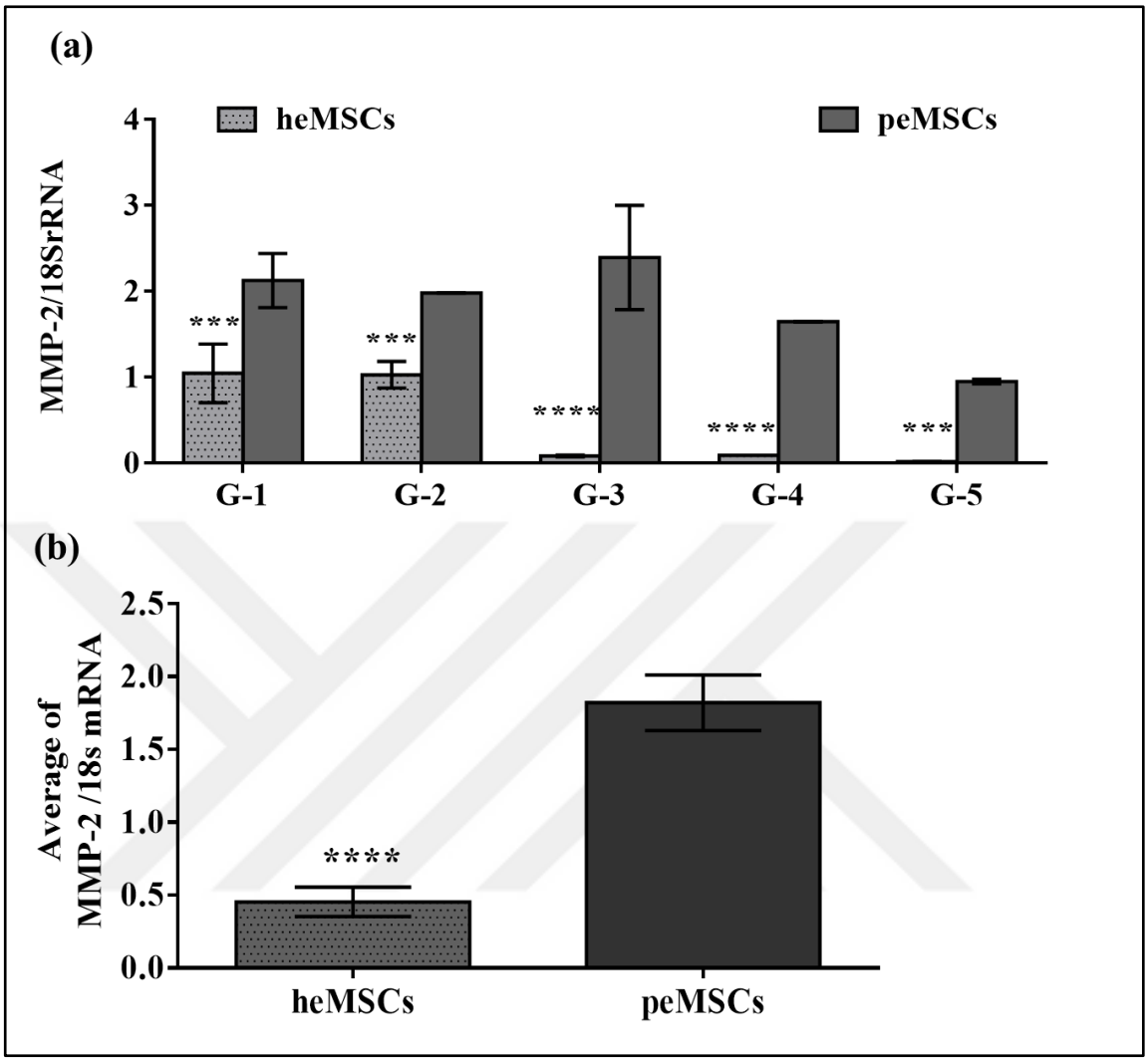

Figure 4.62. RT-PCR analysis of MMP-2 expressions in heMSCs and peMSCs. (a) Ratio of MMP-2 mRNA levels to 18srRNA in heMSCs and peMSCs of all groups (G-1 to G-5). (b) The average of MMP-2 mRNA levels versus 18srRNA for heMSCs and peMSCs of all groups. Results were statistically analyzed in GraphPad Prism 6 software program by 2way ANOVA multiple comparisons. *** was used for $p<0.001$ and **** was used for $p<0.0001$.

When samples of heMSCs in Group-1and Group-2 were compared with peMSCs (Figure 4.62.a.), peMSCs were found to express 2 times more MMP-2 gene compared to heMSCs for each group. When similar comparisons were made for groups 3, 4 and 5, peMSCs were shown to have 2.4, 1.65 and 1 times more MMP-2 levels than heMSCs, respectively.

Comparison of average MMP-2 mRNA values for heMSCs and peMSCs samples in five different groups showed that peMSCs possessed 1.81 times more MMP-2 mRNA than heMSCs ($p<0.0001$).

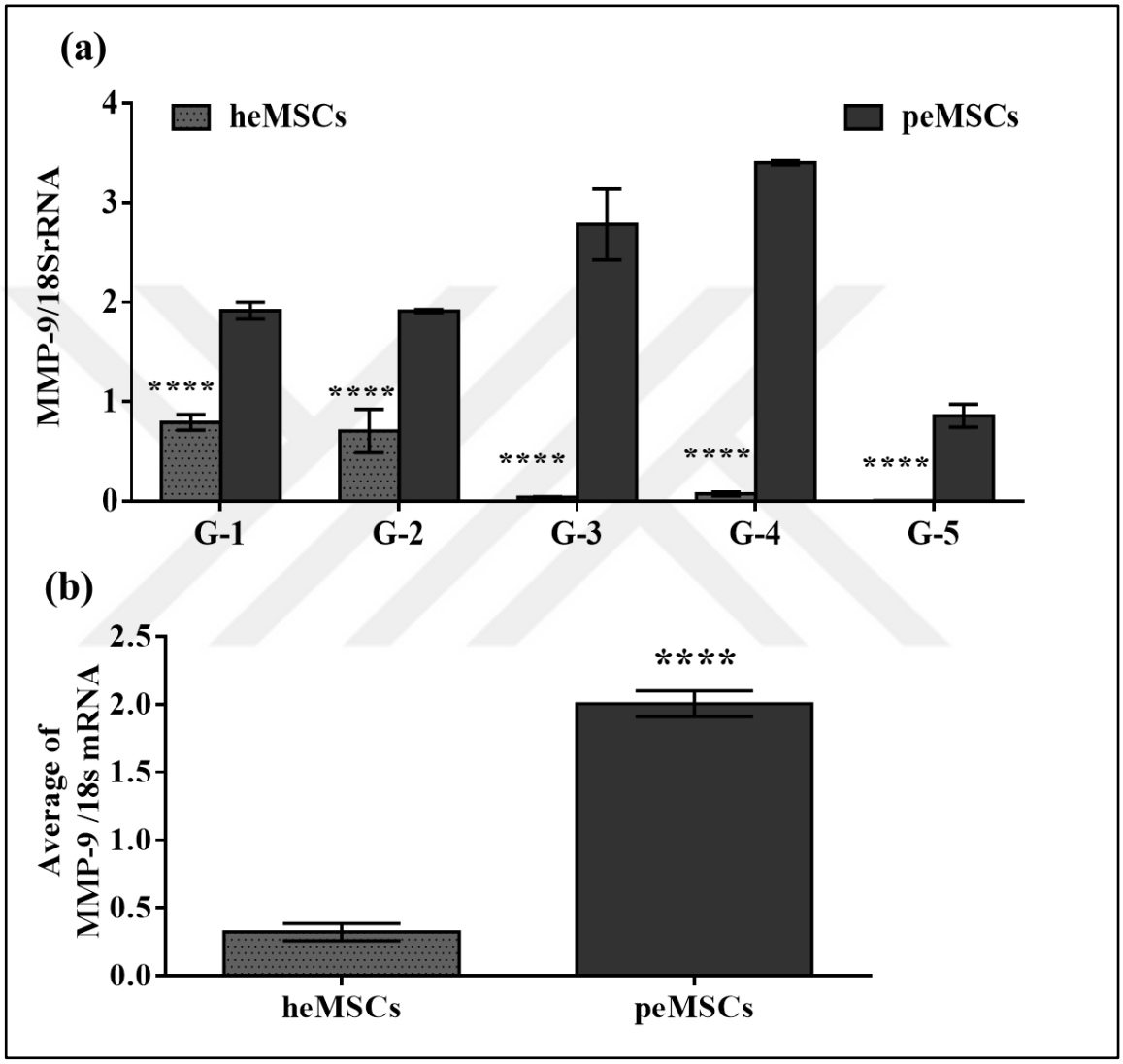

Figure 4.63. RT-PCR analysis of MMP-9 expressions in heMSCs and peMSCs. (a) Ratio of MMP-9 mRNA levels to 18srRNA in heMSCs and peMSCs of all groups (G-1 to G-5). (b) The average of MMP-9 mRNA levels versus 18srRNA for heMSCs and peMSCs of all groups. Results were statistically analyzed in GraphPad Prism 6 software program by 2way ANOVA multiple comparisons. **** was used for $p<0.0001$.

When MMP-9 expression for heMSCs in Group-1 and Group-2 were compared with peMSCs (Figure 4.63.a.), the MMP-9 mRNA level was recorded to be 2.71 more in peMSCs in comparison to heMSCs. Consistently, peMSCs were shown to have a respective 2.78, 3.4 and 0.9 times more MMP-9 expression than heMSCs for groups 3, 4 and 5. Comparison of average MMP-9 mRNA values for heMSCs and peMSCs samples in five different groups showed that peMSCs possessed 2.44 times more MMP-9 mRNA than heMSCs ($p<0.0001$).

4.10.1.2. Determination of MMPs Activity Profile of eMSCs by Zymography

For the determination of enzyme activities of MMP-2 and -9 in eMSCs isolated from five healthy and five different patient volunteer donors, the zymography technique detailed in Section 3.10 was used. The cells were plated to six-well plates 300,000 cells/well; the cells' medium was collected after 48 hours. An equal volume of 4x SDS-free loading buffer mixed cells medium was loaded into each well, and samples were run with the cold running buffer on a gelatin-containing separating gel. After these processes, in the samples where the enzymes MMP-2 and -9 were active, the lytic zones were seen as white bands in Coomassie brilliant blue stained gel, and these white lytic areas were photographed with ChemiDOC (Figure 4.64.). The densities of the band images presented in Figure 4.64. were measured using the Image J program. Since MMP-2 and MMP-9 enzymes used gelatine, which is a similar substrate for these MMPs, enzyme activities were determined by gelatine zymography method. In order to standardize band densities, the heMSCs of all cell samples in each group were accepted as one-fold, and the graph in Figure 4.64.b. for MMP-2 and the graph in Figure 4.64.c. for MMP-9 were generated. On the other hand, mean value of MMP-2 and MMP-9 enzyme activities for heMSCs and peMSCs samples of five different groups are presented in Figure 4.64.d., to analyse activity change in MMP-2 and MMP-9 enzyme in endometriosis ($p<0.0001$).

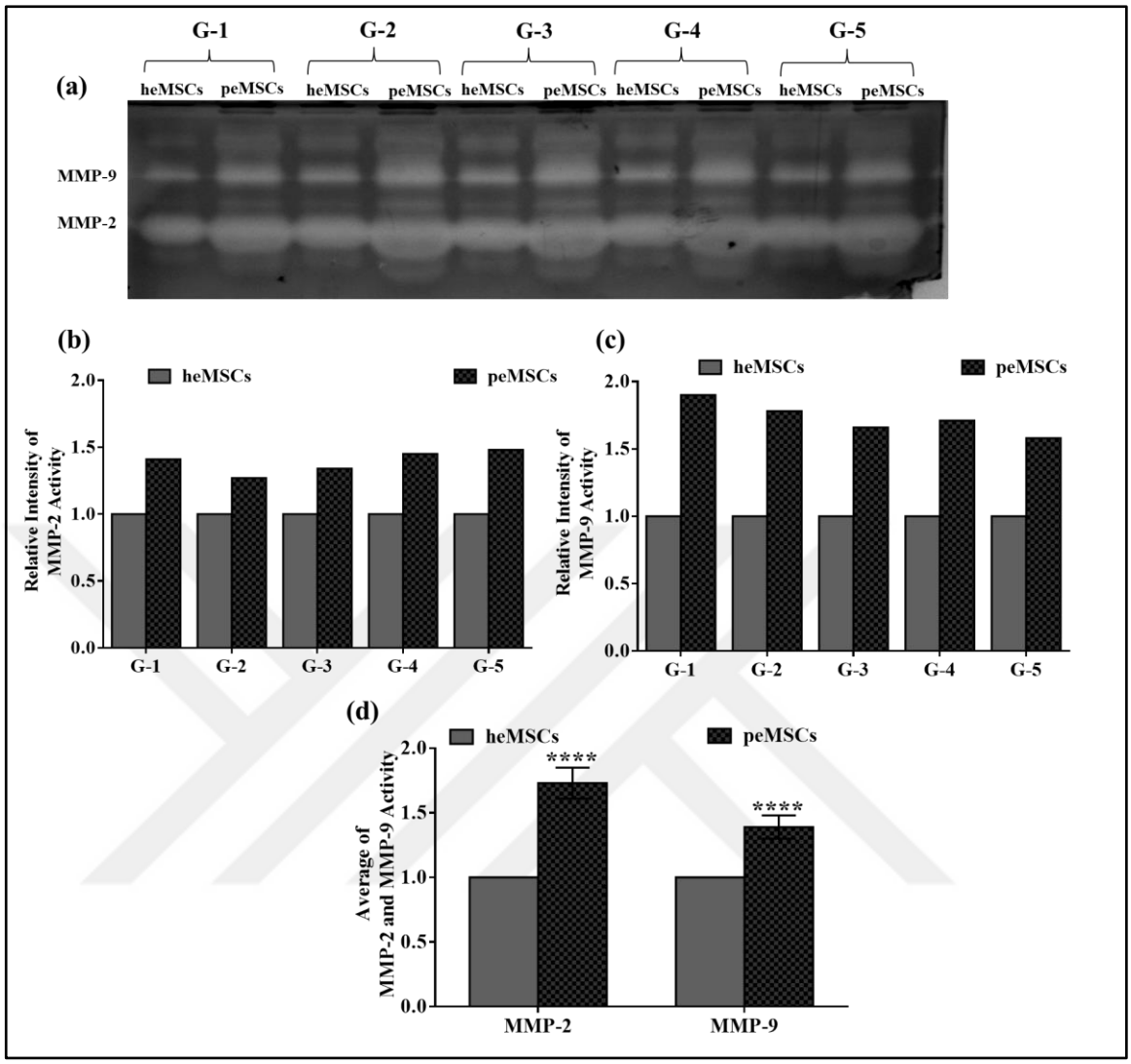

Figure 4.64. Activity analysis of MMP-2 and -9 in heMSCs and peMSCs. (a) Lytic band images of gelatin zymography gel showing active MMP-2 and MMP-9 enzyme for heMSCs and peMSCs of all groups (G-1 to G-5). (b) Relative MMP-2 activity levels in heMSCs and peMSCs of all groups (G-1 to G-5. (c) Relative MMP-9 activity levels in heMSCs and peMSCs of all groups (G-1 to G-5). (d) Average of MMP-2 and -9 activity level for heMSCs and peMSCs of all groups. Results were statistically analyzed in GraphPad Prism 6 software program by 2way ANOVA multiple comparisons. **** was used for $p<0.0001$.

Analysis of band densities using Image J program showed that the peMSCs sample in Group-1 possessed 1.41 times more active MMP-2 than heMSCs. When similar comparisons were

made for Group-2, -3, -4, and -5, peMSCs samples were found to comprise a respective 1.27, 1.34, 1.45 and 1.48 times more MMP-2 activity than heMSCs (Figure 4.64.b.). A similar trend was detected for the MMP-9 enzyme activity (Figure 4.64.c.), in that the MMP-9 enzyme activity of peMSCs was 1.9-, 1.66-fold, 1.71-fold, and 1.58-fold more than heMSCs in Group-1 to 5, respectively.

When the average enzyme activity of MMP-2 and MMP-9 for heMSCs and peMSCs was calculated for all groups (Figure 4.64.d), an average of 1.4 times more active MMP-2 was detected for patient samples, while a 1.7-fold increase for MMP-9 was evident in peMSCs in comparison to heMSCs samples.

4.10.2. MMPs Regulation of peMSCs by Silenced TG2

Following the shRNA silencing of TG2 in heMSCs, heMSCs + SCR, peMSCs + SCR, and peMSCs + shRNA, MMP-2 and MMP-9 genes expression level and enzyme activity were investigated using RT-PCR and zymography assay, respectively.

4.10.2.1. Determination of MMPs Expression Profile of TG2 Silenced eMSCs by RT-PCR

heMSCs and peMSCs cells transduced with control scrambled (SCR) or TG2 targeting lentiviral shRNA (shRNA) particles were used to measure the change in MMP-2 and MMP-9 gene expression. As before, RNA samples isolated from heMSCs, heMSCs + SCR, peMSCs + SCR, and peMSCs + shRNA cells (at passage three) of five group was used in RT-PCR (Section 3.5) reactions. Gene expression of MMP-2 and MMP-9 was normalized against 18s mRNA used as housekeeping gene and relative expression ratios were constructed using known cDNA concentration as described (Section 4.10.1)

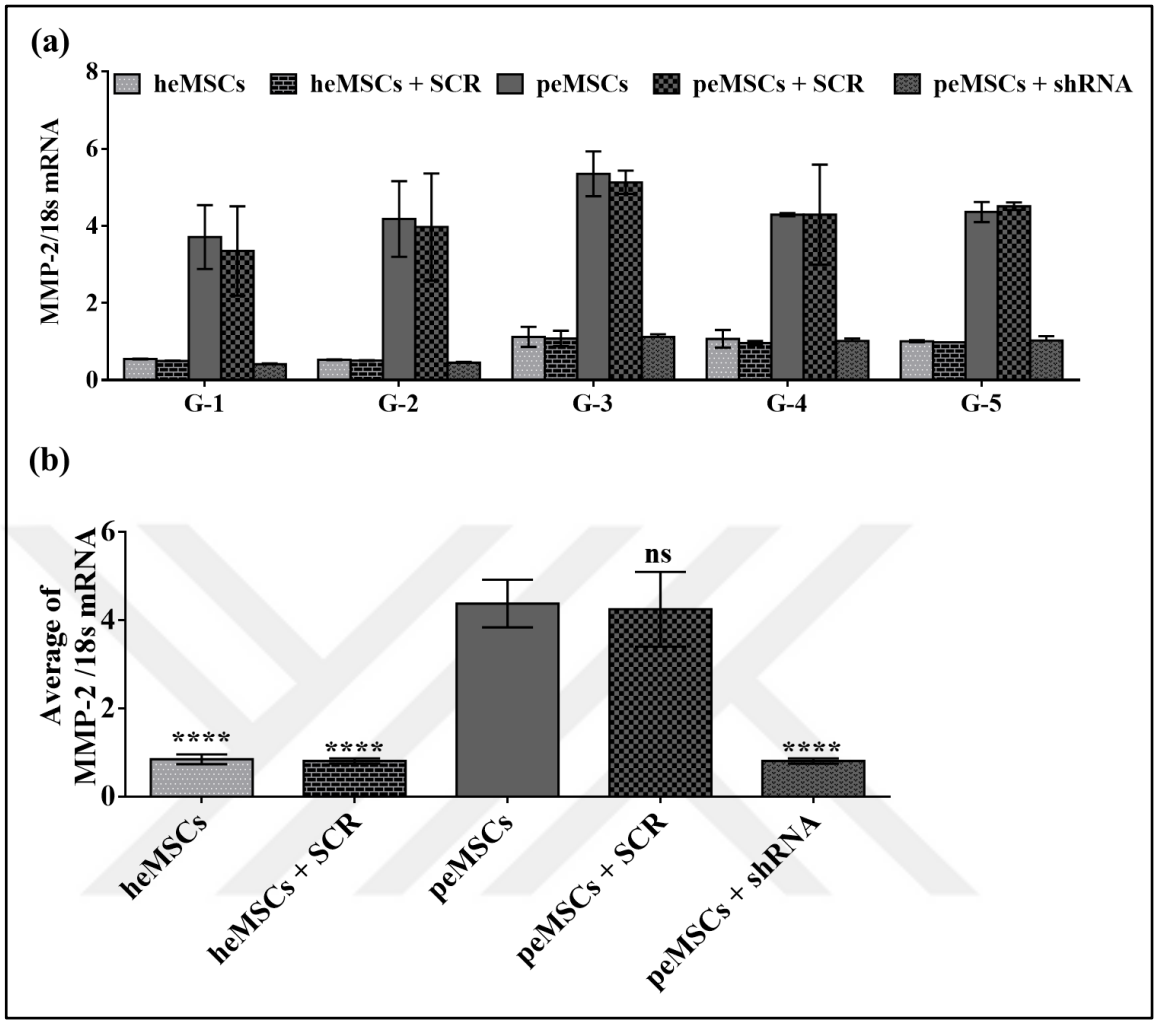

Figure 4.65. Determination of MMP-2 mRNA levels in eMSCs transduced with control scrambled (SCR) or TG2 targeting lentiviral shRNA (shRNA). (a) MMP-2 expression in five different eMSCs Groups (G-1 to G-5) following shRNA transduction. (b) The average of MMP-2 expression values of all transduced samples from five different groups. All statistical results were analyzed in GraphPad Prism 6 software program by One-way ANOVA multiple comparisons. ns was used for non- significant, while **** was used for $p<0.0001$.

Comparison of peMSCs samples in each group with heMSCs and heMSCs + SCR samples showed that MMP-2 expression levels (Figure 4.65.a.) was respectively, 6.8-, 7.9-, 4.8-, 4.1, and 4.4- fold more in peMSCs for Group-1 to -5. On the other hand, when the MMP-2 levels of peMSCs was compared to peMSCs + shRNA, there was a 9.1-, 9.3-, 4.8-, 4.2-, and 4.3-

fold decrease in MMP-2 expression of peMSCs + shRNA for Group-1 to -5, respectively. Analysis of average MMP-2 gene expression levels (Figure 4.65.b) showed that peMSCs samples expressed 5.13 times more MMP-2 than heMSCs and heMSCs + SCR ($p<0.0001$), while there was no detectable difference (ns) between peMSCs and the peMSCs + SCR for level of MMP-2 mRNA. On the other hand, when the average MMP-2 gene levels of peMSCs samples were compared with peMSCs + shRNA, it was seen that MMP-2 gene expression was decreased by 5.43-fold in peMSCs following TG2 targeting lentiviral shRNA transduction ($p<0.0001$).

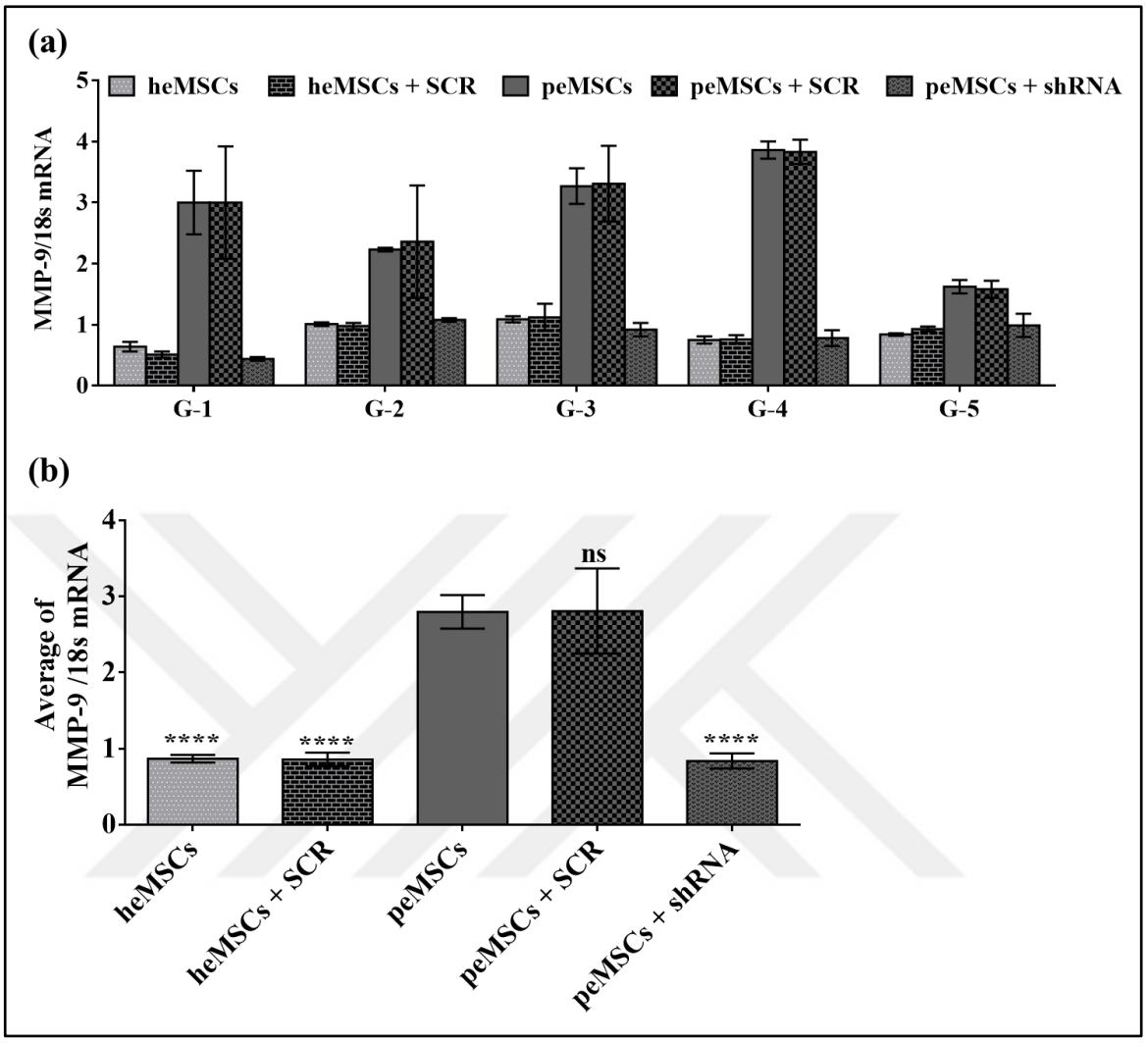

Figure 4.66. Determination of MMP-9 mRNA levels in eMSCs transduced with control scrambled (SCR) or TG2 targeting lentiviral shRNA (shRNA). (a) MMP-9 expression in five different eMSCs Groups (G-1 to G-5) following shRNA transduction. (b) The average of MMP-9 expression values of all transduced samples from five different groups. All statistical results were analyzed in GraphPad Prism 6 software program by One-way ANOVA multiple comparisons. ns was used for non- significant, while **** was used for $p<0.0001$.

After applying control shRNA (SCR) and TG2-targeted shRNA to eMSCs in five different groups, the change in the MMP-9 gene expression level was investigated by RT-PCR and results were presented in Figure 4.66. peMSCs samples in each group were compared with

heMSCs, heMSCs + SCR, peMSCs + SCR and peMSCs + shRNA samples, respectively. In this context, MMP-2 expression levels in heMSCs and heMSCs + SCR samples in Group-1 were similar and were 4.66 times lower than peMSCs. peMSCs in the same group were observed to express MMP-9 at the same level compared to control shRNA (SCR) treated peMSCs (peMSCs + SCR). However, the TG2-targeted shRNA (peMSCs + shRNA) was demonstrated to express 5.83 times less MMP-9 than the peMSCs. When similar statistical comparisons were applied to the samples in Group -2, -3, -4 and -5, respectively, it was determined that heMSCs and heMSCs + SCR samples in all groups expressed similar levels of the MMP-9 gene. peMSCs in Group-2 represented 2.21 times more MMP-9 gene expression, while peMSCs + shRNA of Group-2 expressed 2.40 times less MMP-9 gene in comparison to peMSCs. When the heMSCs + SCR samples having the same MMP-9 gene level and heMSCs in Group-3, -4 and -5 were compared with peMSCs samples, 2.99, 5.11, 1.92 times less MMP-2 gene expression was detected in heMSCs, respectively. When peMSCs samples in Group-3, -4 and -5 were compared with transduced peMSCs + shRNA, a respective 2.94, 5.03, and 1.69 times less MMP-9 gene expression was detected for peMSCs + shRNA of Group-3, -4 and -5. Comparison of average MMP-9 gene expression levels of all groups revealed (Figure 4.66.b), MMP-9 expression was 3.22 times more in peMSCs and peMSCs + SCR with respect to heMSCs and heMSCs + SCR samples, while peMSCs + shRNA samples possessed 3.26 times less MMP-9 expression than peMSCs ($p<0.0001$).

4.10.2.2. Determination of MMPs Activity Profile of TG2 Silenced eMSCs by Zymography

heMSCs and peMSCs cells transduced with control scrambled (SCR) or TG2 targeting lentiviral shRNA (shRNA) particles were used in the zymography (Section 3.10) to measure the MMP-2 and MMP-9 enzyme activity levels. Five different groups were established to be used for this experiment setup just as in the previous experiments. Each group was included

heMSCs, heMSCs + SCR, peMSCs + SCR, and peMSCs + shRNA. The passage number of all cells used in the zymography technic was three. The cells were plated to six-well plates 300,000 cells/well; the cells' medium was collected after 48 hours. An equal volume of 4x SDS-free loading buffer mixed cells medium was loaded into each well, and samples were run with the cold running buffer on a gelatin-containing separating gel. After these processes, in the samples where the enzymes MMP-2 and -9 were active, the lytic zones were seen as white bands in Coomassie brilliant blue stained gel, and gel images were photographed with ChemiDOC in Figure 4.67. In order to standardize band densities, the heMSCs of all cell samples in each group were accepted as one-fold, and the graph in Figure 4.68 for MMP-2 and the graph in Figure 4.63 for MMP-9. After applying control shRNA (SCR) and TG2-targeted shRNA to eMSCs in five different groups (G-1 to G-5), the MMP-2 and -9 activity levels of the heMSCs, heMSCs + SCR, peMSCs, peMSCs + SCR and peMSCs + shRNA samples were presented in Figure 4.67.

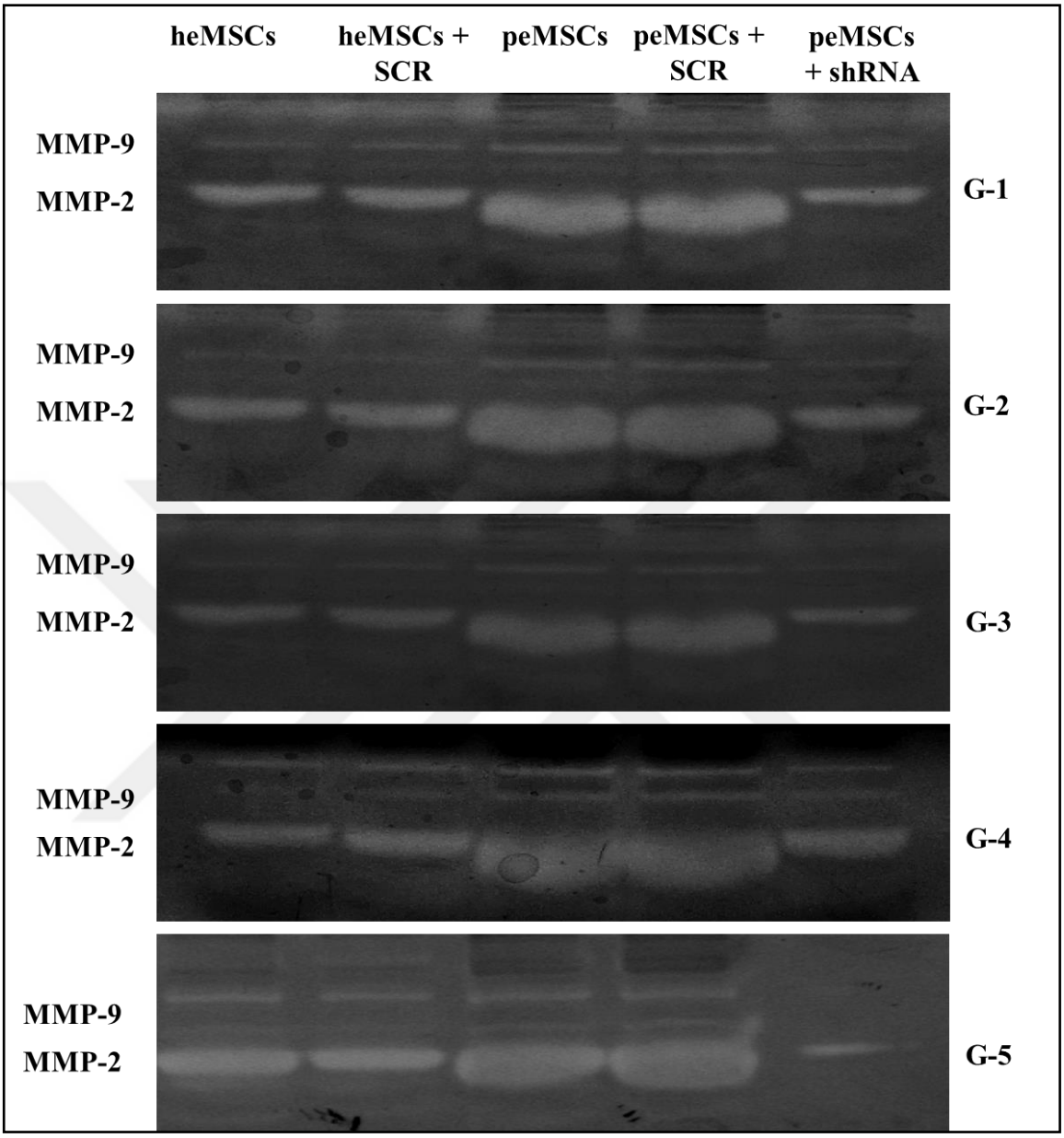

Figure 4.67. Activity analysis of MMP-2 and -9 in analysis in eMSCs transduced with control scrambled (SCR) or TG2 targeting lentiviral shRNA (shRNA) (G-1 to G-5). Zymography gel images were captured by ChemiDOC.

Gelatin zymography images of the MMP-2 and MMP-9 activities of heMSCs, heMSCs + SCR, peMSCs, peMSCs + SCR and peMSCs + shRNA samples in five different groups (G-1 to G-5) are presented in Figure 4.67. Images were captured by Bio-Rad Chemidoc XL.

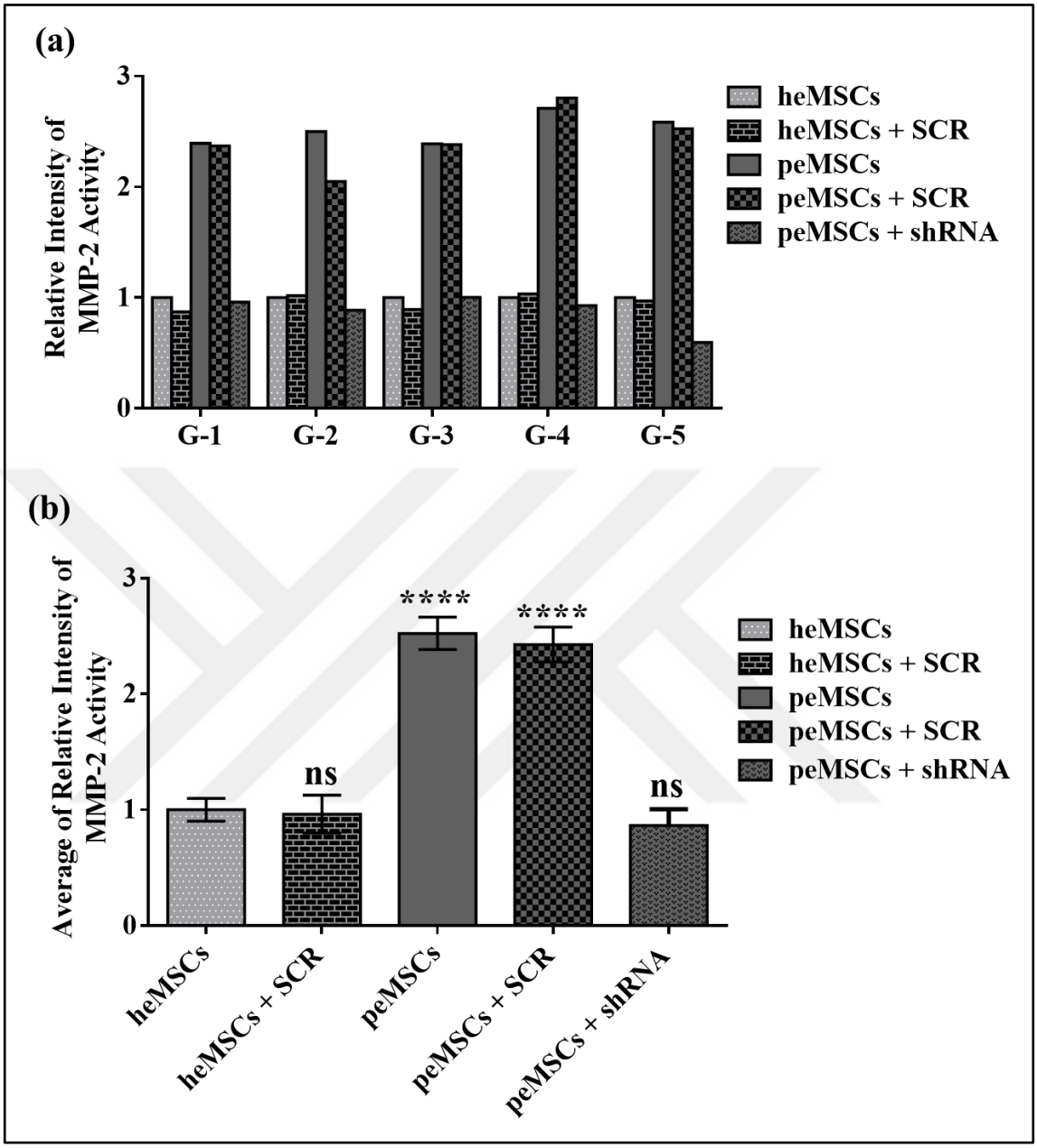

Figure 4.68. Activity analysis of MMP-2 in eMSCs transduced with control scrambled (SCR) or TG2 targeting lentiviral shRNA (shRNA) (G-1 to G-5). (a) Analysis of band intensities for MMP-2 enzyme activity on gelatine zymography gel in all transduced eMSCs groups (G-1 to G-5). (b) Average of MMP-2 activity levels for heMSCs and peMSCs of all transduced groups. Results were statistically analyzed in GraphPad Prism 6 software program by 2way ANOVA multiple comparisons. ns was used for non-significant, **** was used for $p<0.0001$.

The densities of the band images presented in Figure 4.68 were measured using the Image J program. Since MMP-2 and MMP-9 enzymes used gelatine, which is a similar substrate for these MMPs, enzyme activities were determined by gelatine zymography method. In order to standardize band densities, the heMSCs of all cell samples in each transduced group were accepted as one-fold, and the graph in Figure 4.68.a for MMP-2 was created. In this context, MMP-2 activity levels in heMSCs and heMSCs + SCR samples in Group-1 were found to be similar, however, peMSCs and peMSCs + SCR had 2.4 times MMP-2 activity than heMSCs. Similar results were found for the comparisons of control heMSCs and peMSCs samples for the remaining groups , in that, peMSCs and peMSCs + SCR of Group-2 to -5 respectively showed 2.5, 2.4, 2.71, 2.6 and 2.5 more MMP-2 activity when compared to that of heMSCs and heMSCs + SCR samples. In agreement with the qPCR results, silencing of TG2 in peMSCs led to a significant 0.98, 0.89, 1, 0.93 and 0.6-fold decrease in MMP-2 levels of peMSCs + shRNA cells of Group-1 to -5, respectively.

As before, when the results from all five groups were taken to reach average MMP-2 activity level, (Figure 4.68.b), peMSCs and peMSCs + SCR samples displayed approximately 2.5 times more MMP-2 activity than heMSCs and heMSCs + SCR samples ($p<0.0001$), which statistically similar level of MMP-2 activity (ns). On the other hand, when the average MMP-2 activity levels of peMSCs samples were compared with peMSCs + shRNA, it was seen that peMSCs + shRNA samples possessed 2.9 less MMP-2 activity on average, in that there was no significant difference between the average MMP-2 activity recorded for heMSCs and peMSCs + shRNA samples.

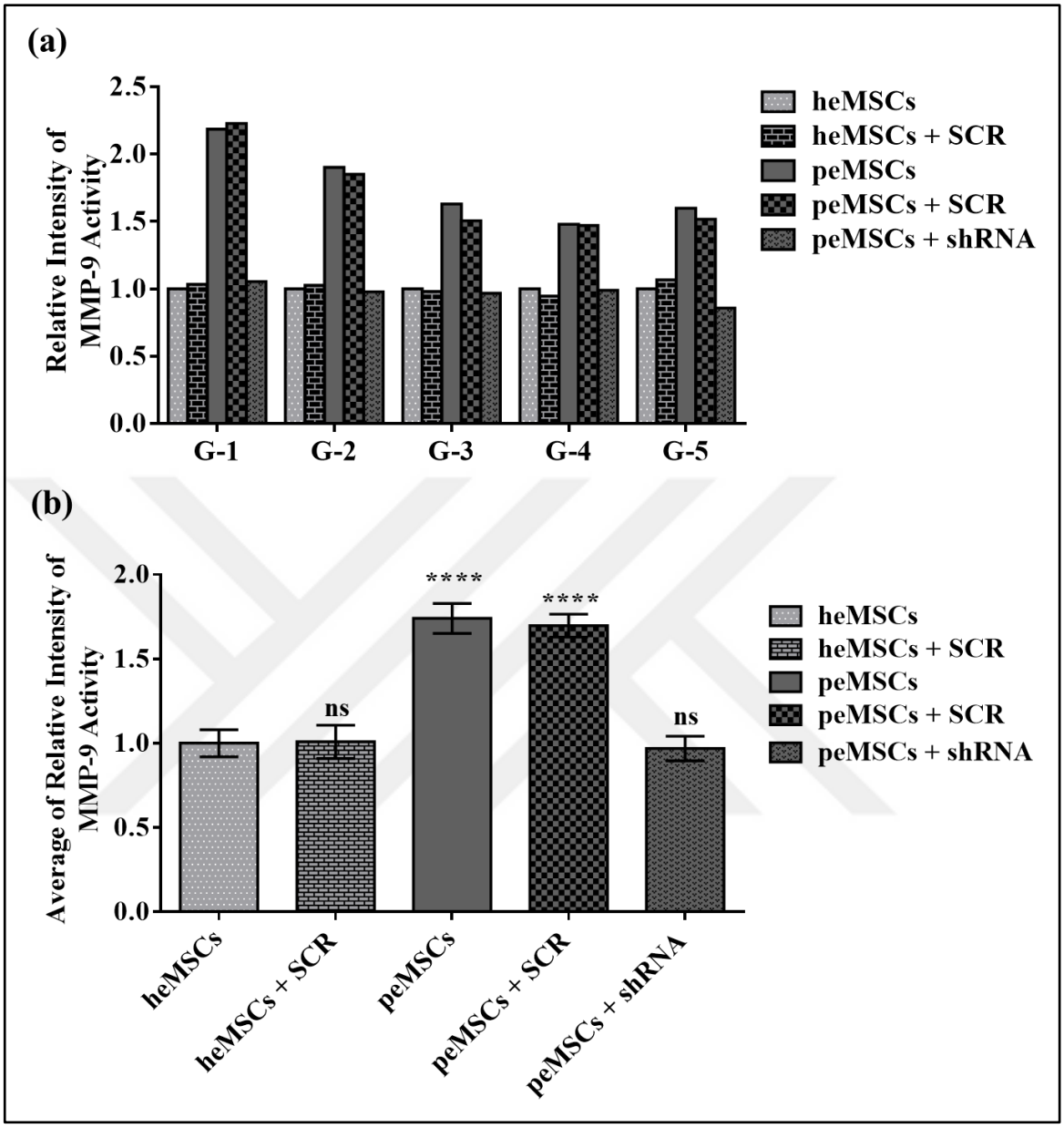

Figure 4.69. Activity analysis of MMP-9 in eMSCs transduced with control scrambled (SCR) or TG2 targeting lentiviral shRNA (shRNA) (G-1 to G-5). (a) Lytic band images of analysis of MMP-9 enzyme activity on gelatine zymography gel in all transduced groups (G-1 to G-5). (b) The average of MMP-9tivity levels for heMSCs and peMSCs of all transduced groups. Results were statistically analyzed in GraphPad Prism 6 software program by 2way ANOVA multiple comparisons. ns was used for non- significant, **** was used for $p<0.0001$.

The analysis of MMP-9 activity from gel images depicted in Figure 4.69.a revealed that MMP-9 activity levels in heMSCs and heMSCs + SCR samples in Group-1 were similar, while peMSCs and peMSCs + SCR were observed to have 2.2 times more MMP-9 activity than heMSCs. On the other hand, peMSCs + shRNA showed similar activity with heMSCs. For samples in Group -2, -3, -4 and -5, it was determined that heMSCs and heMSCs + SCR samples in all groups expressed similar ratios of the MMP-9 enzyme activity as well as peMSCs and peMSCs + SCR which sahred similar MMP-9 activity levels between themselves. When heMSCs samples were compared with peMSCs and peMSCs + SCR, it was determined that peMSCs and peMSCs + SCR of Group-2 to -5 showed 1.90, 1.6, 1.5, 1.6, and 1.7 times more MMP-9 activity, respectively. When heMSCs samples in Group-3, -4 and -5 were compared with peMSCs + shRNA, the similar MMP-9 activity was detected with heMSCs. Average MMP-9 activity level of all groups (Figure 4.69.b) indicated that peMSCs, peMSCs + SCR demonstrated 1.7 times more MMP-9 activity in comparison to heMSCs, heMSCs + SCR, while peMSCs + shRNA sample contained statistically similar (ns) average level of MMP-9 activity with the heMSCs, heMSCs + SCR.

5. DISCUSSON

Endometriosis was first described in the literature by Sampson in 1927 [2] as a benign gynecological problem that is defined by the presence of endometrial tissues in areas outside the uterine borders in reproductively active women [2, 4, 117]. Displaced endometrial tissue can be implanted to the pelvic surface, ovaries, peritoneum, abdominal wall and sometimes even to the brain [423, 424]. Approximately 10 to 20 percent of women in reproductive age are diagnosed with endometriosis, and of those 30-50 percent are diagnosed with endometriosis associated infertility [130, 425]. Accordingly, the prevalence of this disease is high in the female population with nearly 200 million women in the world [426]. Endometriosis is characterized by fatigue, unhappiness, irritable bowel syndrome, pain in sexual life, chronic pelvic pain, fibromyalgia as well as infertility [427], all of which decrease the quality of life. Although endometriosis is so widespread, there is still no clear diagnosis/treatment and the cost of existing methods has led to the research for alternative routes [428]. The budget for the treatment of endometriosis in the USA alone is $ 22 billion a year [429].

There are many theories about the development of endometriosis in the literature [430]. The most widely accepted and popular one of these theories is Sampson Retrograde theory [2, 430]. In the light of several scientific studies by Sampson, he explained that menstruation blood at times passes into the peritoneal cavity as backflow from the uterus through the tubes, from the tubal mucosa itself, resulting in the perforation of an endometrial hematoma of the ovary and possible implantation of endometrial tissue on peritoneal surfaces [2, 431, 432]. Sampson wanted to show the existence of living cells in the menstrual blood [41, 76, 419], and explain the endometriosis formation by the migration and implantation of these cells to areas outside the uterus [433,2]. These implanted cells formed endometrial focuses and caused the development of endometriosis due to their enhanced mobility [2] Sampson's work is still popular and accepted today and his thoughts have survived for generations

without being altered by gynecologists and other scientists [11]. At the time Sampson's theory was put forward, the presence of stem cells in the menstrual blood was yet to be discovered. Today, living cells in the menstrual blood whose reflux was associated with the endometriosis are suggested to be newly identified stem cells of endometrium [76, 79, 434, 68, 75, 77, 80]. In this context, scientific studies have proved the presence of stem/progenitor cells localized in the basal layer of the endometrium and showed that these cells have been shown to play an important role in the remodelling of the endometrium [434, 68, 75, 77, 80]. Chan et al. have shown that the endometrium and menstrual blood are a rich source of mesenchymal stem cells [76]. In other studies, they were determined that the cells isolated from endometrial tissue from women diagnosed with and without endometriosis had stem cell characterization [68, 435]. In follow-up studies, Garget group suggested that perivascular localization of eMSCs in menstrual blood through retrograde reflux into the peritoneal cavity may be the cause of endometriosis [422]. However, these studies did not answer why eMSCs in menstrual blood rooted in retrograde reflux can migrate and colonize outside of uterus in some individuals causing endometriosis and why not in others. In order to analyze the difference in invasive potential of eMSCs from healthy and endometriosis patients, molecular biomarkers associated with high migratory capacity was investigated in this thesis. In this context, the possibility of TG2 to induce enhanced cell adhesion and migration associated with invasive potential in eMSCs was determined in these cells isolated from endometrium of five healthy volunteers and endometriosis patients. Although there is no study on eMSCs showing the pros and cons of isolation methods, studies on MSCs from other resources comparing enzymatic and non-enzymatic methods suggested that non-enzymatic method might be a better choice for preservation of ECM-cell surface interactions [436]. In addition, it has been shown that if the enzymatic method was used in primary cell isolation, the integrity of the ECM can be impaired by proteolytic degradation [436]. Given that, this thesis also set to investigate the importance for TG2 interaction with cell surface SDC-4 and ITGβ-1 on eMSCs adhesive phenotype, as well as biological activities of MMP-2 and -9 on eMSCs invasive ability, the use of non-enzymatic method for cell isolation was

chosen. Besides, the stem cell niche plays a vital role in the functionality of stem cells, and ECM is a crucial stem cell niche component [437]. Soluble and matrix-binding effector molecules of ECM interact with cells, and they regulate cell self-renewal, differentiation functions, and homeostasis [438]. Actually, extrinsic cues which are provided by the niches' unique microenvironment and supportive ECM, maintain stemness of stem cells, determine their proliferation rate and specify whether to divide asymmetrically or symmetrically [437]. In this case, any changes in ECM components, such as unstable proteolytic degradation, may affect stem cell potential due to the niche of stem cells [439]. In short, the use of non-enzymatic method reduces lytic stress in *in vitro* environment of isolated cells leaving the supportive functions of the extracellular matrix intact hence the growth factors released from the tissue explant are not affected [436]. As can be seen from the phase-contrast microscope images (Figure 4.1) eMSCs non-enzymatically isolated were successfully migrated out from the tissue at the end of the fifth day and exhibited the distinct feature different from hemopoietic stem cells, namely the capacity to adhere onto tissue culture plastic (TCP), as reported in the literature [440]. In that, hematopoietic stem cells were on the other hand identified as non-adherent cells hence did not adhere to the TCP when cultured [440].When the morphology of eMSCs were compared to the properties of other mesenchymal cells in the literature, they were found to not be only TCP-adherent but also to exhibit spindle morphology [441, 41, 442], suggesting that the cells migrated out of endometrium biopsy explants (Figure 4.1) shared mesenchymal property with TCP adherence and spindle-shaped morphology [443, 444]. The molecular characterization of these cells by flow cytometry analysis showed CD44, CD29, CD73, ITGB-1, CD90, and CD105 positive profile for both heMSCs and peMSCs. These markers are known to be expressed by all MSCs [76, 445]. When heMSCs and peMSCs were stained for hematopoietic cell surface markers CD14, 31, 35 and CD45 [447], it was found that these cells were negative for these markers, confirming that the endometrium is a high source of mesenchymal stem cells. In addition to these markers, cells migrated out of biopsy explant were found to be positive for CD146, W5C5, and PDFG-R, which were previously shown to be specific for eMSCs [445] albeit with

significant difference in expression levels between healthy and patient groups. peMSCs exhibited significantly higher levels of CD146, W5C5, and PDFG-R when compared to heMSCs which may confer higher potential for cell migration, adhesion and invasion to peMSCs as these molecules were associated with these cellular functions [422, 445, 448, 449 450]. The W5C5 marker, which is highly expressed in our patient group and is unique to endometrial-derived MSCs, is commonly known as SUSD2 protein [422, 446, 448, 450]. Similar to CD146 and PDGF-R, W5C5 is also known to be expressed at the basal level in healthy endometrial mesenchymal stem cells [422, 448, 450]. In line with our results, W5C5 levels were also found to be overexpressed in endometrial stromal fibroblasts (eSFs) that originated from eMSCs in endometriosis patients [451], while eSFs from healthy controls were found to be negative for SUSD2 expression. Given that W5C5 expression is increased in the downstream of Notch signalling [451], overexpression of W5C5 might be due to overactivation of Notch pathway leading to increased stemness profile which might, in turn, may give rise to the increased number of eMSCs with high migratory potential [452] in menstrual blood. Apart from this marker, another marker which is found to be highly expressed in our patient group was MUC18 protein, commonly known as CD146 due to the clone of the antibody that reacts with the antigen [453]. Studies in the literature have shown that when overexpressed CD146, a member of the immunoglobulin superfamily (IgSF), was responsible from increased cell migration and invasion potential by acting as a cell adhesion molecule (CAM) [454, 455]. Immunohistochemistry analysis of endometrial fibrotic tissues showed high levels of CD146 staining [456] in comparison to healthy endometrium. In this context, high levels of CD 146 in eMSCs isolated from endometriosis patients may have provided these cells with the potential to migrate to other parts of the body outside the uterus, which is in line with the Sampson's theory. Another molecule found to be overexpressed by peMSCs was PDGF-R, which was previously shown to be highly expressed in ovarian [458, 459] and uterine cancers [457]. PDGF-R is essential in various cellular processes such as cell proliferation, migration, transformation, and survival of cells during the development and pathogenesis of various endometrial diseases [460]. Therefore, the fact that peMSCs

contained higher PDGFR explains why retrograde flux of peMSCs was successful in implantation outside of the uterus. It is quite possible that activation of PDGF-R pathway in peMSCs confer these cells with higher proliferative [461, 446] and invasive ability [446, 460, 461] when compared to heMSCs. In support of this, cell migration and invasive potential of peMSCs were found to be significantly higher than heMSCs (Figure 4.59 and 4.61).

As TG2 was a recently identified to mediate PDGF-R activation [462] and shown to be the orchestrator of mesenchymal phenotype [327] it was of interest to investigate the gene and protein levels as well as activity statue of TG2 in heMSCs and peMSCs. A previous study by Zemskov et al. demonstrated that cell surface TG2 interacts with PDGF-R and induce TG2-mediated PDGF-R-dependent cell adhesion in cooperation with integrins [462]. On the other hand, a recent study has shown that CD146 plays an essential role for the activation of PDGFR/PI3K pathway, which in turn mediates CD146-induced cell migration [463]. Therefore, it seems plausible that TG2 might also be cooperate with CD146 in the activation of PDGFR pathway provided that it is overexpressed in peMSCs samples.

TG2 is one of the nine transglutaminase members, mainly synthesized in the cytosol but also localized in plasma, mitochondria, nucleus membrane and ECM [194]. TG2 has also been shown to have many biological roles in the cell, including cell proliferation, migration, adhesion, invasion and cell cycle [208, 263]. The TG2 is a multi-site, multifunctional enzyme that in the presence of Ca^{2+} catalyses the formation of intermolecular and intramolecular isopeptide bonds [464, 207, 206] and thiol-dependent acyl transfer reactions [215, 465] between glutamine and lysine side chains of protein(s) [262, 466]. On the other hand, TG2 can change its confirmation and lose its cross-linking activity when bound to GTP [207, 235]. As a GTP-binding protein, TG2 takes part in the downstream signalling of α- adrenergic receptor signalling [268, 467] and plays an active role in epithelial-mesenchymal transition [194, 466]. As explained in the definition of endometriosis, endometriotic cells are able to migrate and adhere better than healthy cells [468]. The basis

of our hypothesis is that this ability of TG2 may confer peMSCs enhanced migration and invasion potential. In this context, the TG2 profile of heMSCs and peMSCs was determined at mRNA level by RT-PCR, protein level by Western blot and activity by BTC Assay. In support of our hypothesis, peMSCs samples expressed significantly more TG2 at mRNA and protein level in comparison to heMSCs samples. On the contrary to these results, activity assay showed that heMSCs comprised more active TG2 than peMSCs on the cell surface that cross-links BTC onto FN matrix. Although these results seem to be contradictory at first site, increased TG2-mediated cross-link activity fits well with the literature stating the importance of TG2 activity in the maintenance of ECM stability [254, 469]. As it is known, the ECM composition of the endometrial wall, which thickens every month and is destroyed by the menstural cycle and needs to be stable [470]. The ECM composition of the endometrial wall of healthy and reproductive age women is also essential for a successful implantation window [470]. The BTC results (Figure 4.14) suggests that this stable endometrial structure in heMSCs may be achieved by cross-linking activity of TG2. The higher TG2 activity of heMSCs samples indicates the presence of a healthy and stable. Thus, TG2 activity in heMSCs may result in the stabilization of ECM which would act as a physical barrier to eMSCs and prevent them from escaping of the endometrial tissue. Suppression of cross enzyme activity despite increased levels of TG2 protein and genes in peMSCs can be also explained by increased synthesis of eNOS and iNOS, which play an active role in eutopic and ectopic endometriosis formation in endometriosis patients. iNOS is important in the formation of endometriosis both in the endometrial glandular and luminal epithelium [471, 472] and stroma [473, 474]. The enzymes eNOS and iNOS synthesize nitric oxide (NO), an extracellular signaling molecule, which is involved in the nitrosylation of cysteine and tyrosine residues on proteins. It has been shown that 15 of the 18 cysteine residues in the structure of TG2 is nitrosylated by NO [475], causing a conformational change in TG2 and this change suppresses cross-linking activity of the enzyme [327]. Our group previously showed that the nitrosylation of TG2 renders the protein on the cell surface where it acts as a protein responsible for adhesion and migration [327]. Therefore, the lack of cross-linking

activity of TG2, which is highly expressed in peMSCs, can be explained by the high expression of eNOS and iNOS in these cells. However, iNOS and eNOS expression levels in peMSCs need to be determined in order to confirm this hypothesis. Taken together, differential activity and expression levels of TG2 between heMSCs and peMSCs suggests that by overexpressing TG2 independently from its cross-linking activity peMSCs might have gained ability to migrate out of uterus by losing ECM and implant into extra-uterian regions. This hypothesis is supported by the fact that TG2 can induce the adhesion and migration of cells by losing its Ca^{2+} -dependent transamidation activity [191, 401, 402] and associating with cell surface binding partners such as ITGβ-1 and SDC-4 [476, 327, 417]. Studies have shown that integrins are synthesized at basal levels on days 19-26 of the menstural cycle and integrins regulate uterine receptivity for a successful implantation window [477, 478]. However, in the pathological examination of endometriosis disease, over-synthesized integrins such as α2β1, α3β1, α4β1, α5β1 and α6β1 have been shown to play a potential role in the development of endometriotic lesions and endometriosis, and integrins are expressed in endometrial stromal cells [135]. These cell adhesion molecules have been found to play a role in the shedding of endometrial tissue during menstruation and in the migration and invasion of viable cells within endometrial tissue fragments to the peritoneum [135]. Syndecans have been found to play a role in the regulation and functionality of the endometrium during the menstural cycle in humans [479]. In animal experiments, it has been observed that SDC-1 is involved in blastocyte development and is synthesized by apical cells of endometrial tissue at basal level [480]. In another animal study, it was found that SDC-4 was synthesized in the subepithelial stroma in the early stage of pregnancy and involved in implantation of the embryo to the uterine wall [481]. In short, studies with human and animal models suggest that different types of syndecans are synthesized at the basal level, taking part in the menstrual cycle and embryo implantation [480, 481]. On the other hand, recent studies have shown that increased syndecan expression and synthesis play a role both in the development of endometriosis [482] and in the formation of endometrial cancer [483]. Consistently, both ITGβ-1 and SDC-4 mRNA levels was shown

to be significantly higher in peMSCs when compared to heMSCs (Figure 4.16 and 4.17). In addition to TG2, increased expression of ITGβ-1 and SDC-4 by peMSCs may also have provided these cells with the potential for adhesion and invasion during the formation of endometriotic lesions.

ITGβ-1 is known to have an active role in cell proliferation, differentiation, migration, adhesion, invasion and stemness potential [302, 337]. At the cell surface, TG2 has been shown to act as an integrin-binding adhesion co-receptor for FN and thereby regulate cell adhesion [13, 193, 194, 195, 257]. Another transmembrane protein that complexes with TG2 and takes part in cell adhesion and migration is SDC-4, a member of the cell surface heparan sulfate proteoglycan (HSPGs) family [279, 327, 329]. SDC-4 plays a role in cell-matrix interaction, cell proliferation, signal transduction, cell adhesion, and migration, respectively. Studies have shown that SDC-4 and TG2 can interact and participate in cell adhesion. In this context, the binding affinity of TG2 to heparin was demonstrated by *in vitro* experiments [279], followed by studies showing that SDC-4 binds to TG2 at the cell surface [327, 329, 345, 346, 347, 348].

In agreement with TG2's role as a binding partner to ITGβ-1 and SDC-4, co-IP results showed that in peMSCs TG2 protein was complex with ITGβ-1 and SDC-4 (Figure 4.18), which may enhance migration and invasion potentials of these cells. In order to understand whether TG2 plays a role on enhanced stemness of peMSCs endowing these cells with high migratory/invasive potential, the expression of TG2 level was silenced using shRNA technology. Silencing of TG2 in peMSCs (peMSCs + shRNA) was shown both in the gene and protein levels, while no change was evident for heMSCs (heMSCs + SCR) and peMSCs (peMSCs + SCR) transduced with scrambled shRNA. peMSCs + shRNA samples had similar enzyme activity to heMSCs samples in the BTC results and as expected SCR transduction did not cause any change in the level of enzyme activity in heMSCs and peMSCs. As mentioned above, TG2 was shown to be important in mesenchymal phenotype, downregulation of TG2 expression resulted in lower levels of MSC markers CD146, W5C5

and PDFGR in peMSCs + shRNA in comparison to peMSCs + SCR and peMSCs. The first findings of the presence of endometrial mesenchymal stem cells in human endometrium have been demonstrated by studies of colonization of single cell suspensions [76]. Later, small clonogenic cells in the endometrium of healthy women was shown to be responsible for the regeneration of the endometrium cycle and glands [76, 79, 422, 450]. These studies have shown that human endometrial cells can produce two types of CFU, large (> 50 cells) and small (<50 cells). It is observed that large CFUs are developed by stem / progenitor cells located at the base of the glands in the basal layer of the endometrium [79, 422, 450]. Small colonies have been shown to be localized in the functional layer and responsible for menstruation [79, 422, 450]. In the light of this information in the literature, the role of TG2 in enhanced stemness, colony-forming ability of heMSCs versus shRNA silenced and control peMSCs were investigated. As expected, peMSCs exhibited greater CFU potential than heMSCs, which was lost when TG2 was silenced (Figure 4.33). Application of SCR shRNA had no effect on CFU potential in heMSCs and peMSCs samples. In agreement with our results, $CD146^+$ $PDGF\text{-}R^+$ eMSCs showed to produce 8 times more CFU than eMSCs expressing low levels of CD146 and PDGF-R [79]. Taken together, when TG2 was downregulated by shRNA, peMSCs exhibited similar characteristics to heMSCs with low CD146, W5C5, PDGFR expression and low CFU potential.

Following the analysis of stemness, cell proliferation profiles of heMSCs, heMSCs + SCR, peMSCs, peMSCs + SCR and peMSCs + shRNA were tested by WST-1 (Section 3.9.1) experiments. When heMSCs samples were compared with peMSCs, it was found that the cell proliferation was higher in peMSCs cells. On the other hand, following administration of TG2-targeted lentiviral particulate shRNA to peMSCs samples (peMSCs + shRNA), cell proliferation decreases at designated time points comparable to the levels of heMSCs and heMSCs + SCR. Nikoo et al. have previously reported that stromal stem cells isolated from the menstural blood of healthy individuals showed lower cell proliferation capacity compared to that of endometriosis patients, but the reason for this difference was not

elucidated [484]. Our results suggest that TG2 expression could be the detrimental factor for the enhanced proliferative ability of peMSCs. Studies on the role of TG2 on cell proliferation revealed that TG2 is an important player in PDGFR and PI3K/Akt/mTOR pathway activation and when overexpressed, increase cell proliferation, mainly in cancer cells [485, 486, 487, 287, 286, 292]. Given that both TG2 and PDGFR levels are increased in peMSCs, the cell proliferation may be promoted due to overactivation of the PDGFR pathway. On the other hand, TG2 can lead to the activation of PI3K/AKT/mTOR pathway either through destabilization of the lipid phosphatase PTEN [277, 307] or forming a complex with Src and PI3K resulting in phosphorylation and activation of the PI3K signalling [308]. Therefore, it is also quite possible for TG2 to increase the growth of peMSCs by activating the PI3K/Akt/mTOR pathway. Another explanation for TG2-mediated enhanced peMSCs proliferation rate could be NF-$_K$β pathway activation. TG2 protein can induce cell proliferation through activation of the NF-$_K$β pathway by suppressing the of NF-κB inhibitor, PPAR-γ (peroxisome proliferator-activated receptor-γ) [313, 475, 319]. Many human and animal model studies of endometriosis have shown that PPAR- γ levels are reduced in endometriosis patients [488, 489, 490]. *In vitro* experiments on immortalized endometriotic epithelial cells and stromal cells showed that use of thiazolidinediones (TZDs), PPAR- γ activators, hinder the proliferation of these cells by deregulating cell cycle and apoptotic resistance [490]. In addition to these findings, inhibition of TG2 by siRNA silencing or R283 and KCC009 TG2 specific inhibitors led to decreased NF- κB activation in parallel with an increase in PPAR-γ activation [322]. Based on this information, it is tempted to speculate that increased TG2 levels in peMSCs may have led to decrease in PPAR-γ levels resulting in NF-κB activation and NF-κB–mediated cell proliferation.

In order to identify the molecular player in TG2-mediated cell proliferation in peMSCs cells, the levels of cyclin E1, CDK-2, cyclin D3, CDK-4 and p-27 proteins known to be involved in cell cycle checkpoints were determined by Western Blot analyis while G0 / G1, S and G2 / M cell cycle phases were analyzed using Cytell Imaging system. Cyclins, cyclin-dependent

kinases (CDK), and their inhibitors are involved in orderly progression of the cell cycle phases [491, 492]. Cyclins function in the cell cycle as regulators of CDK kinases and form complexes with CDKs. Each cycle interacts with specific CDKs at different checkpoints [491, 492]. Cyclin D3 is known to complex with CDK-4, which is necessary for the G1/S transition of the cell cycle [493]. Cyclin E1 regulates CDK-2 in the S phase of the cell cycle and forms an active complex with CDK2 [494]. The task of p-27 is to inhibit the Cyclin E-CDK-2 complex and regulate the checkpoint in G1 in healthy cells, [495]. In agreement with the WST-1 results, the percentage of S and G2/M phase cells were found to be higher for peMSCs and peMSCs + SRC. When the TG2 was down-regulated, the S-phase population was pulled backed to the levels of heMSCs and its scrambled control.

Compared to heMSCs, peMSCs exhibited high levels of Cyclin E1, CDK-2, Cyclin D3, and CDK-4 while the silencing of TG2 with shRNA hampered the levels of these proteins down to that of heMSCs. On the other hand, the levels of CKI inhibitor p-27 was lower in peMSCs compared to the levels found in peMSCs + shRNA and heMSCs samples.

In line with our results, epithelial cells and stromal cells isolated from endometriotic endometrium showed increased levels of Cyclin D3, CDK-4, Cyclin E1, and CDK-2 protein [312]. In another study with healthy, endometriosis patients with stage 1 or 2 and stage 3 or 4, it was observed that the p-27 level decreased significantly in patients with endometriosis compared to healthy samples [496].

So far, our results showed that increased TG2 expression accompanied by loss cross-linking activity confers eMSCs with enhanced cell proliferation and stemness capacity suggesting that TG2 overexpression might be the driving force in the development of endometriosis. As explained in the pathogenesis of endometriosis, endometriotic lesions are highly capable of migrating and adhering to tissues and organs in the regions out of uterine [497]. This led to the idea that the TG2 protein, which plays an active role in cell adhesion and migration, confers peMSCs the ability to migrate. The effect of TG2 on cell migration potential has been proven by a number of studies in the literature [256, 257, 260]. In order to elucidate

whether TG2 also play a role in migratory and invasive phenotype of peMSCs, which are the key process in the development of endometriosis, wound scratch and transwell experiments as well as analysis MMP profile were performed for peMSCs with or without TG2 silencing. peMSCs and peMSCs + SCR closed the wound bed faster than the heMSCs, heMSCs + SCR, while silencing of TG2 led to the loss of migratory phenotype in peMSCs + shRNA samples. Similarly, high invasive potential observed for peMSCs and peMSCs + SCRs was lost when these cells were transduced with targeting shRNA lentiviral particles. Recent studies showed that increase in TG2 protein expression in cancer cell lines leds to integrin β1 activation resulting in metaplastic properties and invasion potential [280, 302, 328]. TG2 does this task independently of crosslinking activity. Our results are consistent with literature in terms of increased TG2 expression in association with enhanced migratory and invasive capacity, albeit data from this thesis is the first to show this association in the context of endometriosis.

As regulation of invasive phenotype is governed by changes in MMP activity, effect of TG2 on the biosynthesis of MMP-2 and -9 was investigated in he- and pe-MSCs. Concisely with transwell assay results, MMP-2 and MMP-9 expression and activity levels were higher in peMSCs than heMSCs and peMSCs + shRNA. Although MMPs play an active role in the tissue hemostasis required for thickening, blood supply and fragmentation of the thickening wall in the menstrual cycle of a healthy woman [411, 498, 499], abnormal expression of MMPs results in reflux of menstrual fragments, thus assist the formation of endometriosis [500, 501, 502]. In human and animal endometriotic lesions, MMP expression has been shown to be increased while tissue MMP inhibitors TIMP-1 and TIMP-2 expressions were decreased [500, 501, 503, 504, 505]. Consistently, our results showed increased expression and activity for MMP-2 and -9 for peMSCs and revealed, for the first time in literature, that the high rate of MMP-2 and MMP-9 activation is TG2-driven in these cells.

6. CONCLUSION AND FUTURE PERSPECTIVE

Results from this thesis showed that eMSCs from the healthy tissue displayed lower TG2 protein levels with a high enzyme activity compared to peMSCs suggesting that the loss of TG2 cross-linking ability might favor the migration and invasion of peMSCs not only by destabilizing the extracellular matrix but also enhancing the cell migratory ability. The upregulation of TG2 was observed in peMSCs, which was possibly associated with an increase in the MMP-2 and -9 activity. The findings provide important information for the design and development of therapeutic chemicals that can be developed for the treatment of endometriosis by examining the formation of endometriosis from a molecular and mechanistic point of view. In the light of our results, a probability was revealed such as the inhibitors for TG2 that are currently in phase studies for cancer studies can also be used to prevent endometriosis.

Flow cytometric analysis showed that high expression of CD146, PDGF-R, and W5C5 in peMSCs were TG2 meadiated. The increased proliferation, migration and invasion in peMSCs may be due to this TG2-mediated CD146, PDGF-R, and W5C5 expression. In order to determine the individual contribution of these markers in cell proliferation, migration and invasion, shRNA sielencing can be used in the future experiments whereby the proliferative and invasive potential of peMSC is analysed in CD146, PDGF-R, and W5C5 silenced peMSCs.

As stated in our BTC and Western Blot results, the high TG2 cross-linking activity and low protein level in heMSCs samples can be explained by eNOs and iNOs levels. Previous studies have shown that increased eNOs and iNOs trigger the development of endometriosis [471, 472, 41, 473, 474]. However, no comment was made about the possible role of eNOs and iNOs on TG2 in endometriosis formation. We focus on the hypothesis that increased levels of eNOs and iNOs in endometriosis lead to conformational changes by nitrozilling TG2 and thus losing the crosslinking activity of TG2 in peMSCs samples and triggering cell

migration and adhesion. To strengthen our hypothesis, the amount of NOs can be determined by Griess Assay in heMSCs and peMSCs samples in the future experiment [506, 507]. On the other hand, the conformational change caused by increased NO in TG2 can be determined by decomposition under non-denaturing conditions [232]. In flow cytometric analysis, it was observed that peMSCs samples express high PDGF-R. Given that TG2 form a complex with PDGF-R [362] and PDGFR pathway may activate the cell migration along with proliferation, it is quite possible that the ability of peMSCs to migrate and invade is gained through this complex. In order to confirm this hypothesis, TG2/PDGFR interaction can be investigated by co-IP experiments in the future experiments using peMSCs and heMSCs.

In the literature, it has been suggested that increased eNOs and iNOs, which play an active role in the development of endometriosis [471, 472, 41, 473, 474] can increase NF-κβ activation and thus give endometriotic cell proliferation and invasion. Given the association of TG2 overexpression with the activation of NF-κβ pathway [277, 307, 313], the role of TG2 in the NF-κβ activation can be elucidated in peMSCs, peMSCs + SCR and peMSCs + shRNA versus heMSC using electro-mobility shift assay (EMSA).

In the discussion of WST-1 and cell cycle results, it was pointed out that PPAR-γ and PI3K /mTOR pathway may be responsible from the high proliferation and division rate in peMSCs samples. Although increased TG2 protein synthesis has been shown to inhibit proliferation of cells by inhibiting PPAR-γ [322], the prevelance of, TG2-related PPAR-γ inhibition has not been studied in patients with endometriosis. In this context, future studies can analyze PPAR-γ levels in peMSCs and peMSCs samples where TG2 is silenced using Western blot.

To further confirm thesis results suggesting TG2 as a paramount molecule involved in the development of endometriosis, animal model studies can be performed. In literature, endometriosis is known to occur in primates, elephants, mice, and some animal species, such as bats, besides humans [508, 509]. In animal model studies, female nude or scid mice that do not develop immune response can be be used [510, 511, 504, 509] to implant peMSCs,

peMSCs + SCR, peMSCs + shRNA and heMSC+ SCR into the peritoneal cavities of animals. For *in vivo* visualization (IVIS) of the lesion size that will occur after implantation of endometriotic and healthy cells, the cells can be be fluorescent or luminascently labelled using mammalian vector transfection [512, 513]. Following endometrial development in animals, the endometriotic fragments will be visualised by IVIS. Once the experimental model is set-up the efficiency of TG2 inhibitors can be analysed in animals peritoneally inoculated with heMSC and peMSC. Following scarification, pathologic analysis of endometriotic tissue samples can be performed along with molecular markers such as CD146, PDGF-R, W5C5, ITGB-1, SDC-4, MMP-2 & -9. Thereby, the role of TG2 in the development of endometriosis and the therapeutic potential of TG2 inhibitors in endometriosis can be elucidated.

REFERENCES

1. Ross MH, Pawlina W. *Histology: A text and atlas with correlated cell and molecular biology.* Philadelphia: Lippincott Williams & Wilkins Press; 2011.

2. Sampson JA. Peritoneal endometriosis due to the menstrual dissemination of endometrial tissue into the peritoneal cavity. *American Journal of Obstetrics & Gynecology*. 1927;1(4):422-25.

3. Leon S, Fritz MA. *Clinical gynecologic endocrinology and infertility*. Philadelphia: Lippincott Williams & Wilkins Publishing; 2007.

4. Houston DE, Noller K, Melton LJ and Selwin BJ. The epidemiology of endometriosis. *Clinical Obstetrics and Gynecology*. 1988;3(1):787-800.

5. Cramer DW, Missmer SA. The epidemiology of endometriosis. *Annals of the New York Academy of Sciences*. 2002;95(5):11-22.

6. Tietjen GE, Bushnell CD, Herial NA, Utley C, White L, Hafeez F. Endometriosis is associated with prevalence of comorbid conditions in migraine. *Headache.* 2007;4(7):1069-1078.

7. Pasoto SG, Abrao MS, Viana VS, Bueno C, Leon EP, Bonfa E. Endometriosis and systemic lupus erythematosus: a comparative evaluation of clinical manifestations and serological autoimmune phenomena. *American Journal of Reproductive Immunology*. 2005;5(3):85-93.

8. Sinaii N, Cleary SD, Ballweg ML, Nieman LK, Stratton P. High rates of autoimmune and endocrine disorders, fibromyalgia, chronic fatigue syndrome and atopic diseases among women with endometriosis: a survey analysis. *Human Reproduction*. 2002;1(7):2715-2724.

9. Lamb K, Nichols TR. Endometriosis: a comparison of associated disease histories. *American Journal of Preventive Medicine*. 1986;(2):324-329.

10. Mao AJ, Anastasi JK. Diagnosis and management of endometriosis: The role of the advanced practice nurce in primary care. *Journal of the American Academy of Nurse Practitioners*. 2010;2(2):109-116.

11. Brosens I, Pijnenborg R, Vercruysse L, Romero R. The great obstetrical syndromes are associated with disorders of deep placentation. *American Journal of Obstetrics and Gynecology*. 2011;204(3):193-201.

12. Makiyan Z. Endometriosis origin from primordial germ cells. *Organogenesis*. 2017;13(3):95-102.

13. Akimov SS, Krylov D, Fleischman LF, Belkin AM. Tissue transglutaminase is an integrin-binding adhesion coreceptor for fibronectin. *Journal of Cell Biology*. 2000;148(4):825-38.

14. Png E, Tong L. Transglutaminase-2 in cell adhesion: all roads lead to paxillin? *Cell Adhetion and Migration*. 2013;7(5):412–417.

15. Figueira PG, Abrão MS, Krikun G, Taylor HS. Stem cells in endometrium and their role in the pathogenesis of endometriosis. *Annals of the New York Academy of Sciences*. 2011;1226(1):10-17.

16. Puppo V. Embryology and anatomy of the vulva: the female orgasm and women's sexual health. *European Journal of Obstetrics & Gynecology and Reproductive Biology*. 2011;154(1):3–8.

17. Renner-Martin TF, Forstenpointner G, Weissengruber GE, Eberhardt L. Gross anatomy of the female genital organs of the domestic donkey. *Anatomia, Histologia, Embryologia*. 2009;38(2):133-138.

18. Gold JM, Shrimanker I. *Physiology: Vaginal*. London: StatPearls & Treasure Island Publishing; 2019.

19. Peate I, and Nair M. *Anatomy and Physiology for Nurses at a Glance*. West Sussex: John Wiley & Sons Press; 2015.

20. Heyden RJ. *Anatomy and physiology of the female reproductive system*. Texas: Tyler Junior College Press; 2016.

21. Agarwal N, Subramanian A. Endometriosis, morphology, clinical presentations and molecular pathology. *Journal of Laboratory Physicians*. 2010;2(1):1-9.

22. Devi KA, Damayanti N, Matum E. Histogenesis of uterus in human fetuses. *Journal of the Anatomical Society of India*. 2018;51(1):166-170.

23. Weiss S, Jaermann T, Schmid P, Staempfli P, Boesiger P, Niederer P, Caduff R, and Bajka M. Three-dimensional fiber architecture of the nonpregnant human uterus determined ex vivo using magnetic resonance diffusion tensor imaging. *The Anatomical Record*. 2006;28(8):84-90.

24. Jones RE, Lopez KH. *The menstrual cycle in human reproductive biology*. London: Academic Press; 2006.

25. Ferencyz A, and Bergeron C. Histology of the human endometrium: From birth to senescence. *Annals of the New York Academy of Sciences*. 1991;6(22):6-27.

26. Wynn RM. Histology and Ultrastructure of the Human Endometrium. *Biology of the Uterus*. 1977;2(4):85-90.

27. Brosens JJ, Pijnenborg R, Brosens IA. The myometrial junctional zone spiral arteries in normal and abnormal pregnancies. *American Journal of Obstetrics and Gynecology*. 2002;187(5):1416-1423.

28. Schwalm H, Dubrauszky V. The structure of the musculature of the human uterus--muscles and connective tissue. *American Journal of Obstetrics and Gynecology*. 1966;94(3):391-404.

29. Chibbar R, Miller FD, Mitchell BF. Synthesis of oxytocin in amnion, chorion, and decidua may influence the timing of human parturition. *The American Society for Clinical Investigation*. 1993;91(1):185-192.

30. Eşrefoğlu M. *Özel histoloji*. İstanbul: İstanbul Tıp Kitabevi, Publishing; 2016.

31. Junqueira LC, Carneiro J. *Basic histology text and atlas*. Fox: AJS Press; 2009.

32. Maybin JA, Critchley HO. Menstrual physiology: implications for endometrial pathology and beyond. *Human Reproduction Update*. 2015;21(6):748-61.

33. Segal JL, Vassallo BJ, Kleeman SD. Paravaginal defects: prevalence and accuracy of preoperative detection. *Urogynecol Journal Publishing*. 2004;15(6):378-83.

34. Fleming H. Structure and function of cultured endometrial epithelial cells. *Reproductive Endocrinology Journals*. 1999;17(1):93-106.

35. Sampson J. Perforating haemorrhagic (chocolate) cysts of the ovary. *The Archives of Surgery*. 1921;3(1):245-323.

36. Nezhat F, Nezhat C, Allan CJ, Metzger DA, Sears DL. Clinical and histologic classification of endometriomas. Implications for a mechanism of pathogenesis. *The Journal of Reproductive Medicine*. 1992;37(9):771-776.

37. Jain S, Dalton ME. Chocolate cysts from ovarian follicles. *Fertility and Sterility*. 1999;72(5):852–856.

38. Klemmt PAB, Starzinski-Powitz A. Molecular and cellular pathogenesis of endometriosis. *Current Women`s Health*. 2018;14(2):106-116.

39. Witz CA, Thomas MR, Montoya-Rodriguez IA, Nair AS, Centonze VE, Schenken RS. Short-term culture of peritoneum explants confirms attachment of endometrium to intact peritoneal mesothelium. *Fertility and Sterility.* 2001;75(2):385-390.

40. Groothius P, Koks CA, De Goeij AF. Adhesion of human endometrial fragments to peritoneum *in vitro*. *Fertility and Sterility.* 1999;71(8):1119-1124.

41. Schwab KE, Chan RW, Gargett CE. Putative stem cell activity of human endometrial epithelial and stromal cells during the menstrual cycle. *Fertility and Sterility.* 2005;84(2):1124-1130.

42. Friedenstein AJ. Osteogenic stem cells in bone marrow. *Bone and Mineral Research*. 1990;6(2):243-272.

43. Ben-Ami E, Berrih-Aknin S, Miller A. Mesenchymal stem cells as an immunomodulatory therapeutic strategy for autoimmune diseases. *Autoimmun*. 2011;10(7):410-415.

44. Eckfeldt CE, Mendenhall EM, Verfaillie CM. The molecular repertoire of the 'almighty' stem cell. *Nature Reviews Molecular Cell Biology*. 2005;6(9):726-737.

45. Ferrari G, Cusella-De Angelis G, Coletta M, Paolucci E, Stornaiuolo A, Cossu G. Muscle regeneration by bone marrow-derived myogenic progenitors. *Science*. 1998;2(3):1528-1530.

46. Becker AJ, McCulloch EA, Till JE. Cytological demonstration of the clonal nature of spleen colonies derived from transplanted mouse marrow cells. *Nature*. 1963;19(7):452-454.

47. Johnstone B, Yoo JU. Autologous mesenchymal progenitor cells in articular cartilage repair. *Clinical Orthopaedics and Related Research*. 1999;36(7):156-162.

48. Zuk PA, Zhu M, Mizuno H, Huang JI, Futrell WJ, Katz AJ, Benhaim P, Lorenz HP, Hedrick MH. Multilineage cells from human adipose tissue: implications for cell-based therapies. *Journal of Tissue Engineering*. 2001;7(1):211-226.

49. Seo BM, Sonoyama W, Yamaza T, Coppe C, Kikuiri T, Akiyama K. Shed repair critical size calvarial defects in mice. *Oral Diseases*. 2008;14(1):428-434.

50. Yin T, Li L. The stem cell niches in bone. *Journal of Clinical Investigation*. 2006;116(5):1195-1201.

51. Friedenstein AJ, Piatetzky-Shapiro II, Petrakova KV. Osteogenesis in transplants of bone marrow cells. *Journal of Embryology and Experimental Morphology*. 1966;16(3):381-390.

52. Ip JE, Wu Y, Huang J, Zhang L, Pratt RE, Dzau VJ. Mesenchymal stem cells use integrin beta1 not CXC chemokine receptor 4 for myocardial migration and engraftment. *Molecular Biology of the Cell*. 2007;18(8):2873-2882.

53. Ghannam S, Bouffi C, Djouad F, Jorgensen C, Noël D. Immunosuppression by mesenchymal stem cells: mechanisms and clinical applications. *Stem Cell Research & Therapy*. 2010;15(1):1-12.

54. Kyurkchiev D, Bochev I, Ivanova-Todorova E, et al. Secretion of immunoregulatory cytokines by mesenchymal stem cells. *World Journal of Stem Cells*. 2014;6(5):552-570.

55. Opitz CA, Litzenburger UM, Lutz C, Lanz TV, Tritschler I, Köppel A, et al. Toll-like receptor engagement enhances the immunosuppressive properties of human bone marrow-derived mesenchymal stem cells by inducing indoleamine-2,3-dioxygenase-1 via interferon-beta and protein kinase R. *Stem Cells*. 2009;27(5):909-919.

56. Waterman RS, Tomchuck SL, Henkle SL, Betancourt AM. A new mesenchymal stem

cell (MSC) paradigm: polarization into a pro-inflammatory MSC1 or an immunosuppressive MSC2 phenotype. *PLoS One*. 2010;5(1):100-118.

57. Oliveira-Bravo M, Sangiorgi BB, Schiavinato JL. LL-37 boosts immunosuppressive function of placenta-derived mesenchymal stromal cells. *Stem Cell Research & Therapy*. 2016;7(1):189-196.

58. Kocher AA, Schuster MD, Szabolcs MJ, Takuma S, Burkhoff D. Wang J, Itescu S. Neovascularization of ischemic myocardium by human bone-marrow–derived angioblasts prevents cardiomyocyte apoptosis, reduces remodeling and improves cardiac function. *Nature Medicine*. 2001;7(4):430–436.

59. Chen L, Tredget EE, Wu PY, Wu Y. Paracrine factors of mesenchymal stem cells recruit macrophages and endothelial lineage cells and enhance wound healing. *PLoS One*. 2008;3(4):1886-1899.

60. Ma S, Xie N, Li W, Yuan B, Shi Y, Wang Y. Immunobiology of mesenchymal stem cells. *Cell Death & Differentiation*. 2014;21(2):216-225.

61. Xu X, Zheng L, Yuan Q, Zhen G, Crane JL, Zhou X, Cao X. Transforming growth factor-β in stem cells and tissue homeostasis. *Bone Research*. 2018;6(1):31-52.

62. Gu C, Huang S, Gao D, Wu Y, Li J, Ma K, Wu X, and Fu X. Angiogenic effect of mesenchymal stem cells as a therapeutic target for enhancing diabetic wound healing. *The International Journal of Lower Extremity Wounds*. 2014;13(2):88-93.

63. Doorn J, Moll G, Le Blanc K, van Blitterswijk C, De Boer J. Therapeutic applications of mesenchymal stromal cells: paracrine effects and potential improvements. *Tissue Engineering*. 2012;18(2):101-115.

64. Lai RC, Chen TS, and Lim SK. Mesenchymal stem cell exosome: a novel stem cell-based therapy for cardiovascular disease. *Regenerative Medicine*. 2011;6(5):481-492.

65. Wang M, Yuan Q, Xie L. Mesenchymal stem cell-based immunomodulation: properties and clinical application. *Stem Cells International*. 2018;2(10):305-324.

66. Asari S, Itakura S, Ferreri K, et al. Mesenchymal stem cells suppress B-cell terminal differentiation. *Experimental Hematology*. 2009;37(5):604-615.

67. Starzinkski Powitz A, Zeitvogel A, Schreiner A. In search of pathogenic mechanims in endometriosis: the challenge for molecular cell biology. *Current Molecular Medicine*. 2001;1(5): 655-664.

68. Gargett CE. Uterine stem cells: What is the evidence? *Human Reproduction*. 2006;13(1):87-101.

69. Leyendecker G, Herbertz M, Kunz G. Endometriosis results from the dislocation of basal endometrium. *Human Reproduction*. 2002;17(1):2725-2736.

70. Sasson IE, Taylor HS. Stem cells and the pathogenesis of endometriosis. *Annals of the New York Academy of Sciences*. 2008;11(27):106-115.

71. Fazleabas AT, Brudney A, Gurates B. A modified baboon model for endometriosis. *Annals of the New York Academy of Sciences*. 2002;9(5):308-321.

72. Faramarzi H, Mehrabani D, Fard M. The potential of menstrual blood-derived stem cells in differentiation to epidermal lineage: A preliminary report. *World Journal of Plastic Surgery*. 2016;5(1):26-31.

73. Ulrich D, Muralitharan R, Gargett CE. Toward the use of endometrial and menstrual blood mesenchymal stem cells for cell-based therapies. *Expert Opinion on Biological Therapy*. 2013;13(10):1387-1400.

74. Deane JA, Gualano RC, Gargett CE. Regenerating endometrium from stem/progenitor cells: is it abnormal in endometriosis, Asherman's syndrome and

infertility? *Current Opinion in Obstetrics and Gynecology*.2013;4(25):193-200.

75. Gargett CE, Masuda H. Adult stem cells in the endometrium. *Molecular Human Reproduction*. 2010;16(3):818-834.

76. Chan RW, Schwab K, Gargett CE. Clonogenicity of human endometrial epithelial and stromal cells. *Biology of Reproduction*. 2004;70(6):1738-1750.

77. Gargett CE, Schwab KE, Zillwood RM, Nguyen HP, Wu D. Isolation and culture of epithelial progenitors and mesenchymal stem cells from human endometrium. *Biology of Reproduction*. 2009;80(6):1136-1145.

78. Spencer TE, Hayashi K, Hu J, Carpenter KD. Comparative developmental biology of the mammalian uterus. *Current Topics in Developmental Biology*. 2005;6(8):85-122.

79. Maruyama T, Masuda H, Ono M, Kajitani T, Yoshimura Y. Human uterine stem/progenitor cells: their possible role in uterine physiology and pathology. *Reproduction*. 2010;140(1):11-22.

80. Gargett CE, & Ye L. Endometrial reconstruction from stem cells. *Fertility and Sterility*. 2012;98(1):11–20.

81. Rajaraman G, White J, Tan KS, Ulrich D, Rosamilia A, Werkmeister J, Gargett CE. Optimization and scale-up culture of human endometrial multipotent mesenchymal stromal cells: potential for clinical application. *Tissue Engineering Methods*. 2012;19(12):80-92.

82. Viganq P, Parazzini F, Somigliana E. Endometriosis: epidemiology and aetiolo-gical factors. *Best Practice & Research Clinical Obstetrics & Gynaecology*. 2004;18(8):177-200.

83. Spaczynski RZ, Duleba AJ. Diagnosis of endometriosis. *Seminars in Reproductive*

Medicine. 2003;2(1):193-208.

84. Duleba AJ. Diagnosis of endometriosis. *Obstetrics and Gynecology Clinics of North America*. 1997;24(5):331-3346.

85. Kenney R.M., Ganjam V.K., Selected pathological changes of the mare uterus and ovary. *Journal of Reproduction Fertil Suppl*. 1975;3(7):335–339.

86. Campagnacci R, Perretta S, Guerrieri M, Paganini AM, De Sanctis A, Ciavattini A, Lezoche E. Laparoscopic colorectal resection for endometriosis. *Surgical Endoscopi*. 2005;19(1):662-664.

87. Rokitansky C. Uber uterus drüsenneu bildung. *Gesellsch Ärtzte*. 1860;3(16).577-582.

88. Eskenazi B, Warner ML. Epidemiology of endometriosis. *Obstetrics and Gynecology Clinics of North America*. 1997;24(1):235-258.

89. Vercellini P, Viganò P, Somigliana E, Fedele L. Endometriosis: pathogenesis and treatment. *Nature Reviews Endocrinology*. 2013;10(5):261–275.

90. Sampson JA. Ovarian hematomas of endometrial type (perforating hemorrhagic cysts of the ovary) and implantation adenomas of endometrial type. *Boston Medical Surgical Journal*. 1922;18(6):445-473.

91. Vignali M, Infantino M, Matrone R. Endometriosis: novel etiopathogenetic concepts and clinical perspectives. *Fertility and Sterility.* 2002;78(1):665-678.

92. Vinatier D, Dufour P, Oosterlynck D. Immunological aspects of endometriosis. *Human Reproductive Update*. 1996;2(6):371-384.

93. Somigliana E, Vercellini P, Gattei U. Bladder endometriosis: getting closer and closer to the unifying metastatic hypothesis. *Fertility and Sterility.* 2007;87(1):1287-1290.

94. Di W, Guo SW. The search for genetic variants predisposing women to endometriosis. *Current Opinion in Obstetrics and Gynecology*. 2007;19(6):395-401.

95. Kashima K, Ishimaru T, Okamura H. Familial risk among Japanese patients with endometriosis. *International Journal of Gynecology & Obstetrics*. 2004;84(1):61-64.

96. Ryer S, Foster W. Environmental dioxins and endometriosis. *Toxicological Sciences*. 2002;70(3):161-170.

97. Collins FS, McKusick VA. Implications of the Human Genome Project for medical science. *Jama Journal*. 2001;2(85):540-544.

98. Matarese G, De Placido G, Nikas Y, Alviggi C. Pathogenesis of endometriosis: natural immunity dysfunction or autoimmune disease? *Trends Molecular Medicine*. 2003;9(4):223-228.

99. Crow J, Amso NN, Levvin J. Morphology and ultrastructure of fallopian tube epithelium at different stages of the menstruel cycle and menapouse. *Human Reproduction*. 1994;9(1):2224-2233.

100. Matorras R, Ocerin I, Unamuno M, Nieto A, Peiró E, Burgos J. Prevalence of endometriosis in women with systemic lupus erythematosus and Sjogren's syndrome. *Lupus*. 2007;1(6):736-40.

101. Sampson JA. The escape of foreign material from the uterine cavity into the uterine veins. *American Journal of Obstetrics and Diseases of Women and Children*. 1918;78(3):161–175.

102. Sampson JA. Pelvic endometriosis and tubal fimbriae. *American Journal of Obstetrics and Gynecology*. 1932;24(1):497-542.

103. Sampson JA. Endometrial carcinoma of the ovary, arising in endometrial tıssue in that

organ. *Archives of Surgery*. 1925;10(1):1-5.

104. Sampson JA. Endometriosis of the sac of a right inguinal hernia, associated with a pelvic peritoneal endometriosis and an endometrial cyst of the ovary. *The American Journal of Surgery*. 1926;1(5):308-309.

105. Ferguson BR, Bennington JL, Haber SL. Histochemistry of mucosubstances and histology of mixed mullerian pelvic lymph node glandular inclusions. Evidence for histogenesis by mullerian metaplasia of coelomic epithelium. *Obstetrics and Gynecology*. 1969;33(5):617-625.

106. Macer ML, Taylor HS. Endometriosis and infertility: a review of the pathogenesis and treatment of endometriosis-associated infertility. *Obstetrics and Gynecology Clinics of North America*. 2012;39(4):535-549.

107. Berek JS. *Berek & Novak jinekoloji*. Ankara: Nobel Tıp Kitabevleri Press; 2007.

108. Missmer SA, Hankinson SE, Spiegelman D, Barbieri RL, Marshall LM, Hunter DJ. Incidence of laparoscopically confirmed endometriosis by demographic, anthropometric, and lifestyle factors. *American Journal of Epidemiology*. 2004;160(8):784–796.

109. Darrow SL, Vena JE, Batt RE, Zielezny MA, Michalek AM, Sharon S. Menstrual cycle characteristics and the risk of endometriosis. *Epidemiology*. 1993;4(2):135-142.

110. Matalliotakis I, Cakmak H, Fragouli Y, Goumenou A, Mahutte N, Arici A. Epidemiological characteristics in women with and without endometriosis in the Yale series. *Archives of Gynecology and Obstetrics*. 2008;277(5):389-393.

111. Missmer S, Hankinson S, Spiegelman D, Barbieri R, Malspeis S, Willett W, Hunter D. Reproductive history and endometriosis among premenopausal women. *Obstetrics and Gynecology*. 2004;104(5):965–974.

112. Signorello LB, Harlow BL, Cramer DW, Spiegelman D, Hill JA. Epidemiologic determinants of endometriosis: A hospital-based case-control study. *Annals of Epidemiology*. 1997;7(4):267–274.

113. Parasar P, Ozcan P, Terry KL. Endometriosis: Epidemiology, Diagnosis and Clinical Management. *Current Obstetrics and Gynecology Reports*. 2017;6(1):34–41.

114. Stilley JA, Birt JA, Sharpe-Timms KL. Cellular and molecular basis for endometriosis-associated infertility. *Cell and Tissue Research*. 2012;349(3):849–862.

115. Treloar SA, Wicks J, Nyholt DR et al. Genomewide linkage study in 1,176 affected sister pair families identifies a significant susceptibility locus for endometriosis on chromosome 10q26. *American Journal of Human Genetics*. 2005;77(1):365–376.

116. Jones RK, Searle R.F, Bulmer JN. Apoptosis and bcl-2 expression in normal human endometrium, endometriosis and adenomyosis. *Human Reproduction*. 1998;13(12):3496–3502.

117. Burney RO, Giudice LC. Pathogenesis and pathophysiology of endometriosis. *Fertility and Sterility* 2012;98(3):511-519.

118. Wingfield M, Macpherson A, Healy DL, Rogers PA. Cell proliferation is increased in the endometrium of women with endometriosis. *Fertility and Sterility*. 1995;64(2):340-346.

119. Sato N, Tsunoda H, Nishida M, Morishita Y, Takimoto Y, Kubo T. Loss of heterozygosity on 10q23.3 and mutation of the tumor suppressor gene PTEN in benign endometrial cyst of the ovary: possible sequence progression from benign endometrial cyst to endometrioid carcinoma and clear cell carcinoma of the ovary. *Cancer Research*. 2000;60(24):7052–7056.

120. Zhang X, Ho SM. Epigenetics meets endocrinology. *Journal of Molecular*

Endocrinology. 2011;46(1):11-32.

121. Houshdaran S, Zelenko Z, Tamaresis JS, Irwin JC, Giudice LC. Abnormal epigenetic signature in eutopic endometrium of subjects with severe endometriosis. *Reproductive Sciences*. 2011;18(3):191-208.

122. Guo SW. Epigenetics of endometriosis. *Molecular Human Reproductive*. 2009;1(5):587–607.

123. Nap AW, Groothuis PG, Demir AY, Maas JW, Dunselman GA, de Goeij AF. Tissue integrity is essential for ectopic implantation of human endometrium in the chicken chorioal lantoic membrane. *Human Reproductive*. 2003;1(8):30-40.

124. Oosterlynck DJ, Cornillie FJ, Waer M, Vandeputte M, Koninckx PR. Women with endometriosis show a defect in natural killer activity resulting in a decreased cytotoxicity to autologous endometrium. *Fertility and Sterility*. 1991;56(1):45-51.

125. Gerhard I, Becker T, Eggert-Kruse W, Klinga K, Runnebaum B. Thyroid and ovarian function in infertile women. *Human Reproductive*. 1991;6(1):338-345.

126. Poppe K, Glinoer D, Van Steirteghem A, Tournaye H, Devroey P, Schiettecatte J. Thyroid dysfunction and autoimmunity in infertile women. *Thyroid*. 2002;1(2):997-1001.

127. Lucidi RS, Witz CA, Chrisco M, Binkley PA, Shain SA, Schenken RS. A novel *in vitro* model of the early endometriotic lesion demonstrates that attachment of 38 endometrial cells to mesothelial cells is dependent on the source of endometrial cells. *Fertility and Sterility*. 2005;8(4):16–21.

128. Liu YG, Tekmal RR, Binkley PA, Nair HB, Schenken RS, Kirma NB. Induction of endometrial epithelial cell invasion and c-fms expression by transforming growth factor beta. *Molecular Human Reproductive*. 2009;1(5):665–673.

129. Britton JA, Westhoff C, Howe G and Gammon MD. Diet and benignovarian tumors. *Cancer Causes Control*. 2000;11(5):389-401.

130. Parazzini F. Selected food intake and risk of endometriosis. *Human Reproduction*. 2004;19(8):1755–1759.

131. Mehedintu C, Plotogea MN, Ionescu S, Antonovici M. Endometriosis still a challenge. *Journal of Medicine Life*. 2014;15(3):349-357

132. Jeong JW. In search of molecular mechanisms in endometriosis. *Endocrinology*. 2014;155(4):1178-1180.

133. Bouquet De Jolinière J, Ayoubi JM, Gianaroli L, Dubuisson JB, Gogusev J, Feki A. Endometriosis: a new cellular and molecular genetic approach for understanding the pathogenesis and evolutivity. *Frontiers in Surgery*. 2014;27(1):16-46.

134. Nisolle M, Donnez J. Peritoneal endometriosis, ovarian endometriosis, and adenomyotic nodules of the rectovaginal septum are three different entities. *Fertility and Sterility*. 1997;68(4):585–596.

135. Van der Linden PJQ, de Goeij AFPM, Dunselman GAJ, van der Linden EPM., Ramaekers FCS, Evers J L H. Expression of integrins E-cadherin in cells from menstrual effluent, endometrium, peritoneal fluid, peritoneum, endometriosis. *Fertility and Sterility*. 1994;61(1):85–90.

136. Hopwood D, Levison DA. Atrophy and apoptosis in the cyclical human endometrium. *Pathology*. 1976;11(9):159–166.

137. Akao Y, Otsuki Y, Kataoka S, Ito Y, Tsujimoto Y. Multiple subcellular localization of Bcl-2: Detection in nuclear outer membrane, endoplasmic reticulum membrane, and mitochondrial membranes. *Cancer Research*. 1994;54(1):2468-2471.

138. Otsuki Y, Misaki O, Sugimoto O. Cyclic bcl-2 gene expression in human uterine endometrium during menstrual cycle. *The Lancet*. 1994;34(4):28-39.

139. Sharpe-Timms KL. Endometrial anomalies in women with endometriosis. *Annals of the New York Academy of Sciences*. 2001;93(4):131-147.

140. Gebel HM, Braun DP, Tambur A, Frame D, Rana N, Dmowski WP. Spontaneous apoptosis of tissue is impaired in women with endometriosis. *Fertility and Sterility.* 1998;69(1):1042-1044.

141. Dmowski WP, Ding J, Shen J, Rana N, Fernandez BB, Braun DP. Apoptosis in endometrial glandular and stromal cells in women with and without endometriosis. *Human Reproduction*. 2001;16(9):1802-1808.

142. Fujishita A, Nakane PK, Koji T, Masuzaki H, Chavez RO, Yamabe T, Ishimaru T. Expression of estrogen and progesterone receptors in endometrium and peritoneal endometriosis: an immunohistochemical and in situ hybridization study. *Fertility and Sterility*. 1997;67(5):856-864.

143. Tao XJ, Tilly KI, Maravei DV, Shifren JL, Krajewski S, Reed JC, Isaacson KB. Differential expression of members of the Bcl-2 gene family in proliferative and secretory human endometrium: Glandular epithelial cell apoptosis is associated with increased expression of Bax-1. *The Journal of Clinical Endocrinology & Metabolism*. 1997;82(8):2738-2746.

144. Meresman GF, Vighi S, Buquet RA, Contreras-Ortiz O, Tesone M, & Rumi, L. S. Apoptosis and expression of Bcl-2 and Bax in eutopic endometrium from women with endometriosis. *Fertility and Sterility*. 2000;74(4):760-766.

145. Bilotas M, Barañao RI, Buquet R, Sueldo C, Tesone M, Meresman G. Effect of GnRH analogues on apoptosis and expression of Bcl-2, Bax, Fas and FasL proteins in

endometrial epithelial cell cultures from patients with endometriosis and controls. *Human Reproduction*. 2006;22(3):644-653.

146. Mirakhor Samani S, Ezazi Bojnordi T, Zarghampour M, Merat S, Fouladi DF. Expression of p53, Bcl-2 and Bax in endometrial carcinoma, endometrial hyperplasia and normal endometrium: A histopathological study. *Journal of Obstetrics and Gynaecology*. 2018;38(7):999-1004.

147. Rogers PAW, Lederman F, Plunkett D, Affandi B. Bcl-2, Fas and caspase 3 expression in endometrium from levonorgestrel implant users with and without breakthrough bleeding. *Human Reproduction*. 2000;15(3):152-161.

148. Wu L, Mao C, Ming, X. Modulation of Bcl-x Alternative Splicing Induces Apoptosis of Human Hepatic Stellate Cells. *BioMed Research International*. 2016;1(1):1-7.

149. Bielli P, Bordi M, Di Biasio V, Sette C. Regulation of BCL-X splicing reveals a role for the polypyrimidine tract binding protein (PTBP1/hnRNP I) in alternative 5′ splice site selection. *Nucleic Acids Research*. 2014;42(1):12070-12081.

150. Oltval ZN, Milliman CL, Korsmeyer SJ. Bcl-2 heterodimerizes *in vivo* with a conserved homolog, Bax, that accelerates programed cell death. *Cell*. 1993;74(4):609-619.

151. Yeramian A, Moreno-Bueno G, Dolcet X. Endometrial carcinoma: molecular alterations involved in tumor development and progression. *Oncogene*. 2013;32(1):403-413.

152. Braun DP, Ding J, Shaheen F, Willey JC, Rana N, Dmowski WP. (2007). Quantitative expression of apoptosis-regulating genes in endometrium from women with and without endometriosis. *Fertility and Sterility*. 2007;87(2):263-268.

153. Nagata S, Suda T. Fas and Fas ligand: lpr and gld mutations. *Immunology Today*.

1995;16(1):39–43.

154. Sbracia M, Valeri C, Antonini G, Biagiotti G, Pacchiarotti A, Pacchiarotti A. Fas and Fas-Ligand in eutopic and ectopic endometrium of women with endometriosis. *Reproductive Sciences*. 2015;23(1):81-86.

155. Gogacz M, Gałczyński K, Wojtaś M. Fas-related apoptosis of peritoneal fluid macrophages in endometriosis patients: Understanding the disease. *Journal of Immunology Research.* 2017;31(7):53-64.

156. Cheung LW, Hennessy BT, Li J, Yu S, Myers AP, Djordjevic B, Lu Y, Stemke-Hale K, Dyer MD, Zhang F, et al. High frequency of PIK3R1 and PIK3R2 mutations in endometrial cancer elucidates a novel mechanism for regulation of PTEN protein stability. *Cancer Discover*. 2011;1(1):170-185.

157. Le Du F, Eckhardt BL, Lim B, Litton JK, Moulder S, Meric-Bernstam F, Gonzalez-Angulo AM, Ueno NT. Is the future of personalized therapy in triple-negative breast cancer based on molecular subtype? *Oncotarget*. 2015;6(15):12890-12908.

158. Oda K, Stokoe D, Taketani Y, McCormick F. High frequency of coexistent mutations of PIK3CA and PTEN genes in endometrial carcinoma. *Cancer Research*. 2005;65(5):10669–10673.

159. Hayes MP, Wang H, Espinal-Witter R, Douglas W, Solomon GJ. PIK3CA and PTEN mutations in uterine endometrioid carcinoma and complex atypical hyperplasia. *Clincal Cancer Research*. 2006;12(7):5932-5935.

160. Bruhn MA, Pearson RB, Hannan RD, Sheppard KE. AKT-independent PI3-K signaling in cancer - emerging role for SGK3. *Cancer Managment Research*. 2013;5(3):281-292.

161. Samuels Y, Velculescu VE. Oncogenic mutations of PIK3CA in human cancers. *Cell*

Cycle. 2004;3(10):1221-1224.

162. Konopka B, Janiec-Jankowska A, Kwiatkowska E, Najmoła U, Bidziński M, Olszewski W, Goluda C. PIK3CA mutations and amplification in endometrioid endometrial carcinomas: relation to other genetic defects and clinicopathologic status of the tumors. *Human Pathology*. 2011;42(11):1710-1719.

163. Paplomata E, O'Regan R. The PI3K/AKT/mTOR pathway in breast cancer: targets, trials and biomarkers. *Therapeutic Advances in Medical Oncology*. 2014;6(4):154–166.

164. Cinar O, Seval Y, Uz YH, Cakmak H, Ulukus M, Kayisli UA, Arici A. Differential regulation of Akt phosphorylation in endometriosis. *Reproductive BioMedicine Online*. 2009;19(6):864–871.

165. Laudanski P, Szamatowicz J, Kowalczuk O, Kuźmicki M, Grabowicz M, Chyczewski L. Expression of selected tumor suppressor and oncogenes in endometrium of women with endometriosis. *Human Reproductive*. 2009;24(4):1880–1890.

166. Leconte M, Nicco C, Ngô C. The mTOR/AKT inhibitor temsirolimus prevents deep infiltrating endometriosis in mice. *The American Journal of Pathology*. 2011;179(2):880–889.

167. Arumugam K, Dip YC. Endometriosis and infertility: the role of exogenous lipid peroxides in the peritoneal fluid. *Fertility and Sterility.* 1995;63(1):198–199.

168. Jackson LW, Schisterman EF, Dey-Rao R, Browne R., Armstrong D. Oxidative stress and endometriosis. *Human Reproduction*. 2005;20(7):2014–2020.

169. Szczepanska M, Kozlik J, Skrzypczak J, Mikolajczyk M. Oxidative stress may be a piece in the endometriosis puzzle. *Fertility and Sterility.* 2003;79(6):1288–1293.

170. Ngô C, Chéreau C, Nicco C, Weill B, Chapron C, Batteux F. Reactive oxygen species controls endometriosis progression. *The American Journal of Pathology*. 2009;175(1):225–234.

171. Dalton TP, Shertzer HG, Puga A. Regulation of gene expression by reactive oxygen. *Annual Review of Pharmacology and Toxicology*. 1999;39(1):67–101.

172. Morel Y, Barouki R. Repression of gene expression by oxidative stress. *Biochemical Journal*. 1999;342(3):481–496.

173. Li W, Xu R, Jiang L, Shi J, Long X, Fan B. Expression of Cyclooxygenase-2 and Inducible Nitric Oxide Synthase Correlates with Tumor Angiogenesis in Endometrial *Carcinoma Medical Oncology*. 2005;22(1):063–070.

174. Lebovic DI, Mueller MD, Taylor RN. Immunobiology of endometriosis. *Fertility and Sterility*. 2001;75(1):1–10.

175. Lousse JC, Van Langendonckt A, González-Ramos R, Defrère S, Renkin E, Donnez J. Increased activation of nuclear factor-kappa B (NF-κB) in isolated peritoneal macrophages of patients with endometriosis. *Fertility and Sterility*. 2008;90(1):217-220.

176. Gupta S, Agarwal A, Sekhon L, Krajcir N, Cocuzza M, Falcone T. Serum and peritoneal abnormalities in endometriosis: potential use as diagnostic markers. *Minerva Ginecologica*. 2006;58(6):527-51.

177. Vercammen EE, D'Hooghe TM. Endometriosis and recurrent pregnancy loss. *Seminars in Reproductive Medicine*. 2000;18(04):363-368.

178. Tomassetti C, Meuleman C, Pexsters A, Mihalyi A, Kyama C, Simsa P, D'Hooghe T. Endometriosis, recurrent miscarriage and implantation failure: is there an immunological link? *Reproductive BioMedicine Online*. 2006;13(1):58-64.

179. Sinaii N, Plumb K, Cotton L, et al. Differences in characteristics among 1000 women with endometriosis based on extent of disease. *Fertility and Sterility*. 2008;89(3):538-545.

180. Marcoux S, Maheux R, Bérubé S. Laparoscopic surgery in infertile women with minimal or mild endometriosis. *New England Journal of Medicine*. 1997;337(4):217-222.

181. Alimi Y, Iwanaga J, Loukas M, Tubbs RS. The clinical anatomy of endometriosis. *Cureus*. 2018;10(9):3361-3370.

182. Barnhart K. Effect of endometriosis on *in vitro* fertilization. *Fertility and Sterility*. 2002;77(6):1148-1155.

183. De Hondt A, Peeraer K, Meuleman C, Meeuwis L, De Loecker P, D'Hooghe TM. Endometriosis and subfertility treatment. *Minerva Ginecologica*. 2005;57(3):257-267.

184. Omland AK, Åbyholm T, Fedorcsák P, Ertzeid G, Oldereid N B, Bjercke S, Tanbo T. Pregnancy outcome after IVF and ICSI in unexplained, endometriosis-associated and tubal factor infertility. *Human Reproduction*. 2005;20(3):722-727.

185. Gupta S, Goldberg JM, Aziz N, Goldberg E, Krajcir N, Agarwal A. Pathogenic mechanisms in endometriosis-associated infertility. *Fertility and Sterility*. 2008;90(2):247-257.

186. Fadhlaoui A, Bouquet de la Jolinière J, Feki A. Endometriosis and infertility: How and when to treat? *Frontierts in Surger*. 2014;1(1):24-35.

187. Mathur S P. Autoimmunity in Endometriosis. Relevance to Infertility. *American Journal of Reproductive Immunology*. 2000;44(2):89-95.

188. Prescott J, Farland LV, Tobias DK, Gaskins AJ, Spiegelman D, Chavarro JE, Missmer SA. A prospective cohort study of endometriosis and subsequent risk of infertility. *Human Reproduction*. 2006;31(7):1475-1482.

189. Mehta K. Mammalian transglutaminases: a family portrait. *Progress in Experimental Tumor Research*. 2005;38(1):1-18.

190. Thomas H, Beck K, Adamczyk M, Aeschlimann P, Langley M, Oita RC, Aeschlimann D. Transglutaminase 6: a protein associated with central nervous system development and motor function. *Amino Acids*. 2011;44(1):161-177.

191. Esposito C, Caputo I. Mammalian Transglutaminases: Identification of substrates as a key to physiological function physiopathological relevance. *The FEBS Journal*. 2005;272(3):615-631.

192. Odii BO, Coussons P. Biological functionalities of transglutaminase 2 and the possibility of its compensation by other members of the transglutaminase family. *Scientific World Journal*. 2014;20(14):7145-7161.

193. Akimov SS, Belkin AM. Cell-surface transglutaminase promotes fibronectin assembly via interaction with the gelatin-binding domain of fibronectin: a role in TGFbeta-dependent matrix deposition. *Journal of Cell Science*. 2001;114(16):2989-3000.

194. Eckert RL, Kaartinen MT, Nurminskaya M, Belkin AM, Colak G, Johnson GVW, Mehta K. Transglutaminase regulation of cell function. *Physiological Reviews*. 2014;94(5):383-417.

195. Gaudry CA, Verderio E, Jones RA, Smith C, Griffin M. Tissue transglutaminase is an important player at the surface of human endothelial cells: evidence for its externalization and its colocalization with the beta (1) integrin. *Experimental Cell*

Research. 1999;252(1):104-113.

196. Gaudry CA, Verderio E, Aeschlimann D, Cox A, Smith C, Griffin M. Cell surface localization of tissue transglutaminase is dependent on a fibronectin-binding site in its N-terminal beta-sandwich domain. *Journal of Biological Chemistry*. 1999;274(1):30707-30714.

197. Aeschlimann D, Paulsson M. Transglutaminases: Protein crosslinking enzymes in tissues and body fluids. *Thrombosis and Haemostasis*. 1994;71(1):402-415.

198. Grenard P, Bates MK, Aeschlimann D. Evolution of transglutaminase genes: Identification of a transglutaminase gene cluster on human chromosome 15q15. *Journal of Biological Chemistry*. 2001;276(35):33066-33078.

199. Rachel NM, Pelletier JN. Biotechnological applications of transglutaminases. *Biomolecules*. 2013;3(4):870-888.

200. Kieliszek M, Misiewicz A, Microbial transglutaminase and its application in the food industry. *Folia Microbiologica*. 2013;59(3):241-50.

201. Singh PK, Neeraj-Shrivastava BKO. Enzymes in the meat industry. *Enzymes in Food Biotechnology*. 2019;1(5):111-128.

202. Jaros D, Rohm H. Enzymes exogenous to milk in dairy technology: Transglutaminase. *Reference Module in Food Science*. 2016;12(7):297-300.

203. Sulic MA, Kurppa K, Rauhavirta T, Kaukinen K, Lindfors K. Transglutaminase as a therapeutic target for celiac disease. *Expert Opinion on Therapeutic Targets*. 2015;19(3):335-348.

204. Aeschlimann D, Thomazy V. Protein crosslinking in assembly and remodelling of extracellular matrices: the role of transglutaminases. *Connective Tissue Research*.

2000;41(1): 1-27.

205. Satchwell TJ, Shoemark DK, Sessions RB, Toye AM. Protein 4.2: a complex linker. *Blood Cells, Molecules and Diseases*. 2009;42(3):201-210.

206. Iismaa SE, Mearns BM, Lorand L, Graham RM. Transglutaminases and disease: lessons from genetically engineered mouse models and inherited disorders. *Physiological Reviews*. 2009;89(53):991-1023.

207. Lorand L, Graham RM. Transglutaminases: crosslinking enzymes with pleiotropic functions. *Nature Reviews Molecular Cell Biology*. 2003;4(15):140-156.

208. Klöck C, Diraimondo TR, Khosla C. Role of transglutaminase 2 in celiac disease pathogenesis. *Semin Immunopathology*. 2012;34(4):513-522.

209. Korsgren C, Cohen CM. Organization of the gene for human erythrocyte membrane protein 4.2: structural similarities with the gene for a subunit of factor XIII. *Proceedings of the National Academy of Sciences*. 1991;88(11):4840-4844.

210. Dubbink HJ, de Waal L van Haperen R, Verkaik NS, Trapman J, Romijn JC. The human prostate-specific transglutaminase gene (TGM4): genomic organization, tissue-specific expression, and promoter characterization. *Genomics*. 1998;51(3):434-44.

211. Polakowska RR, Eickbush T, Falciano V, Razvi R, Goldsmith LA. Organization and evolution of the human epidermal keratinocyte transglutaminase 1 gene. *Proceedings of the National Academy of Sciences*. 1992;89(11):4476-4480.

212. De Laurenzi V, Melino G. Gene disruption of tissue transglutaminase. *Molecular and Cellular Biology*. 2001;21(1):148-155.

213. Ichinose A, Bottenus RE, Davie EW. Structure of transglutaminases. *Journal of*

Biological Chemistry. 1990;265(23):13411-1344.

214. Abe H, Goto M, and Kamiya N. Protein lipidation catalyzed by microbial transglutaminase. *Chemistry: A European Journal*. 2011;17(2):14004-14008.

215. Fesus L, Piacentini M. Transglutaminase 2: an enigmatic enzyme with diverse functions. *Trends in Biochemical Sciences*. 2002;27(10):534-539.

216. Fraij BM, Gonzales RA. Organization and structure of the human tissue transglutaminase gene. *Biochimica et Biophysica Acta (BBA)-Molecular Cell Research*. 1997;1354(1):65-71.

217. Phatak VM, Croft SM, Rameshaiah-Setty SG, Scarpellini A, Hughes DC, Rees R, McArdle S, Verderio EA. Expression of transglutaminase-2 isoforms in normal human tissues and cancer cell lines: dysregulation of alternative splicing in cancer. *Amino Acids*. 2013;44(1):33-44.

218. Lai TS, Greenberg CS. TGM2 and implications for human disease: Role of alternative splicing. *Frontiers in Bioscience*. 2013;18(5):504-519.

219. Murthy SNP, Lomasney JW, Mak EC Lorand L. Interactions of Gh/transglutaminase with phospholipase Cδ1 and with GTP. *Proceedings of the National Academy of Sciences of the USA*. 1999;96(21):11815–11819.

220. Lu S, Saydak M, Gentile V, Stein JP, Davies PJ. Isolation and characterization of the human tissue transglutaminase gene promoter. *The Journal of Biological Chemistry*. 1995;270(17):9748-9756.

221. Shimada J, Suzuki Y, Kim SJ, Wang PC, Matsumura M, Kojima S. Transactivation via RAR/RXR-Sp1 interaction: characterization of binding between Sp1 and GC box motif. *Molecular Endocrinology*. 2001;15(10):1677-1692.

222. Mirza A, Liu SL, Frizell E, Zhu J, Maddukuri S, Martinez J, Davies P, Schwarting R, Norton P, Zern MA. A role for tissue transglutaminase in hepatic injury and fibrogenesis, and its regulation by NF-kappaB. *American Journal of Physiology*. 1997;272(1):281-288.

223. Brown KD. Transglutaminase 2 and NF-κB: an odd couple that shapes breast cancer phenotype. *Breast Cancer Research and Treatment*. 2013;137(2):329-336.

224. Murthy SNP, Iismaa S, Begg G, Freymann DM, Graham RM, Lorand L. Conserved tryptophan in the core domain of transglutaminase is essential for catalytic activity. *Proceedings of the National Academy of Sciences of the United States of America*. 2002;99(5):2738–2742.

225. Mehta K, Kumar A, Kim HI. Transglutaminase 2: A multi-tasking protein in the complex circuitry of inflammation and cancer. *Biochemical Pharmacology*. 2010;80(2):1921-1929.

226. Kiraly R, Dem MA. Protein transamidation by transglutaminase 2 in cells: a disputed Ca^{2+}-dependent action of a multifunctional protein. *The FEBS Journal*. 2011;278(24):4717–4739.

227. Iismaa SE, Chung L, Wu MJ, Teller DC, Yee VC, Graham RM. The core domain of the tissue transglutaminase Gh hydrolyzes GTP and ATP. *Biochemistry*. 1997;36(39):11655-1164.

228. Hwang KC, Gray CD, Sivasubramanian N, Im MJ. Interaction site of GTP binding Gh (transglutaminase II) with phospholipase C. *Journal of Biological Chemistry*. 1995;270(45):27058-2762.

229. Liu S, Cerione RA, Clardy J. Structural basis for the guanine nucleotide-binding activity of tissue transglutaminase and its regulation of transamidation activity.

Proceedings of the National Academy of Sciences of the United States of America. 2002;99(5):2743-2747.

230. Bergamini CM. GTP modulates calcium binding and cation-induced conformational changes in erythrocyte transglutaminase. *The FEBS Journal*. 1988;239(2):255–258.

231. Di Venere A, Rossi A, De Matteis F, Rosato N, Agrò AF, Mei G. Opposite Effects of Ca^{2+} and GTP Binding on Tissue Transglutaminase Tertiary Structure. *Journal of Biological Chemistry*. 2000;275(6):3915–3921.

232. Pinkas D, Mç-Strop P, Brunger AT, Khosla C. Transglutaminase 2 undergoes a large conformational change upon activation. *Plos Biology*. 2007;5(61):327-335.

233. Király R, Csősz É, Kurtán T, Antus S, Szigeti K, Simon-Vecsei Z, Fésüs, L. Functional significance of five noncanonical Ca2+-binding sites of human transglutaminase 2 characterized by site-directed mutagenesis. *The FEBS Journal*. 2009;276(23):7083–7096.

234. Beninati S, Piacentini M, Bergamini CM. Transglutaminase 2, a double face enzyme. *Amino Acids*. 2017;49(3):415-423.

235. Lai TS, Lin CJ, Wu YT, Wu CJ. Tissue transglutaminase (TG2) and mitochondrial function and dysfunction. *Frontiers in Bioscience*. 2017;1(22):1114-1137.

236. Casadio R, Polverini E, Mariani P, Spinozzi F, Carsughi F, Fontana A, Polverino de Laureto P, Matteucci G, Bergamini CM. The structural basis for the regulation of tissue transglutaminase by calcium ions. *European Journal of Biochemistry*. 1999;262(3):672-679.

237. Mariani P, Carsughi F, Spinozzi F, Romanzetti S, Meier G, Casadio R. Ligand-induced conformational changes in tissue transglutaminase: Monte Carlo analysis of small-angle scattering data. *Biophysical Journal*. 2000;78(7):3240–3251.

238. Nurminskaya MV, Belkin AM. Cellular functions of tissue transglutaminase. *International Review of Cell and Molecular Biology*. 2012;294(1):64-97.

239. Plugis NM, Palanski BA, Weng CH, Albertelli M, Khosla C. Thioredoxin-1 selectively activates transglutaminase 2 in the extracellular matrix of the small intestine: Implications for Celiac Disease. *Journal of Biological Chemistry*. 2017;292(5):2000-2008.

240. Jin X, Stamnaes J, Klöck C, DiRaimondo TR, Sollid LM, Khosla C. Activation of extracellular transglutaminase 2 by thioredoxin. *Journal of Biological Chemistry*. 2011;286(43):37866-37873.

241. Yi MC, Melkonian AV, OuseyJA, Khosla C. Endoplasmic reticulum–resident protein 57 (ERp57) oxidatively inactivates human transglutaminase 2. *Journal of Biological Chemistry*. 2018;293(8), 2640-2649.

242. Kuo TF, Tatsukawa H, Kojima S. New insights into the functions and localization of nuclear transglutaminase 2. *The FEBS Journal*. 2011;278(24):4756–4767.

243. Gundemir S, Johnson GVW. Intracellular localization and conformational state of transglutaminase 2: Implications for cell death. *Plos One*. 2009;4(7):6123-6151.

244. Upchurch HF, Conway E, Maxwell MD. Localization of cellular transglutaminase on the extracellular matrix after wounding: characteristics of the matrix-bound enzyme. *Journal of Cellular Physiology*. 1991;149(9):375-382.

245. Piacentini M, Farrace MG, Piredda L, Matarrese P, Ciccosanti F, Falasca L, Rodolfo C, Giammarioli AM, Verderio E, Griffin M, Malorni W. Transglutaminase overexpression sensitizes neuronal cell lines to apoptosis by increasing mitochondrial membrane potential and cellular oxidative stress. *Journal of Neurochemistry*. 2002;81(5):1061-1072.

246. Haddox MK, Russell DH. Increased nuclear conjugated polyamines and transglutaminase during liver regeneration. *Proceedings of the National Academy of Sciences of the United States of America*. 1981;78(3):1712-1716.

247. Tong L, Png E, Aihua H, Yong SS, Yeo HL, Riau A, Mendo E, Chaurasia SS, Lim CT, Yiu TW, Iismaa SE. Molecular mechanism of transglutaminase -2 in corneal epithelilal migration and adhesion. *Biochimica Biophysica Acta*. 2013;1833(6):1304-1315.

248. Elli L, Bergamini CM, Bardella MT, Schuppan D. Transglutaminases in inflammation and fibrosis of the gastrointestinal tract and the liver. *Digestive and Liver Disease.* 2009;41(8):541-550.

249. Mayerle J, Tilg H. Clinical update on inflammatory disorders of the gastrointestinal tract. *Frontiers of Gastrointestinal Research*. 2010;26(2):83-94.

250. Prydz K, Tveit H, Vedeler A, Saraste J. Arrivals and departures at the plasma membrane: directand indirect transport routes. *Cell and Tissue Research*. 2013; 352(1):5-20.

251. Van den Akker J, VanBavel E, Van Geel R, Matlung HL, Guvenc TB, Janssen GMC, Bakker EN. The redox state of transglutaminase 2 controls arterial remodeling. *Plos One*. 2011;6(8):23067-23080.

252. Ientile R, Caccamo D, Griffin M. Tissue transglutaminase and the stress response. *Amino Acids*. 2007;33(2):385-394.

253. Aeschlimann D, Paulsson M. Cross-linking of laminin-nidogen complexes by tissue transglutaminase. A novel mechanism for basement membrane stabilization. *Journal of Biological Chemistry*. 1991;26(6):15308-15317.

254. Belkin AM. Extracellular TG2: emerging functions and regulation. *The FEBS*

Journal. 2011;278(24):4704-4716.

255. Gentile V, Thomazy V, Piacentini M, Fesus L, Davies PJ. Expression of tissue transglutaminase in Balb-C 3T3 fibroblasts: effects on cell morphology and adhesion. *Journal of Biological Chemistry*. 1992;11(9):463-474.

256. Stephens P, Grenard P, Aeschlimann P, Langley M, Blain E, Errington R, Kipling D, Thomas D, Aeschlimann D. Crosslinking and G-protein functions of transglutaminase 2 contribute differentially to fibroblast wound healing responses. *Journal of Cell Science*. 2004;11(7):3389-3403.

257. Telci D, Griffin M. 2006. Tissue transglutaminase (TG2): a wound response enzyme. *Frontiers in Bioscience*. 2006;11(1):867-882.

258. Pardali E. Transforming growth factor-beta signaling and tumor angiogenesis. *Frontiers in Bioscience*. 2009;14(1):4848-4861.

259. Goumans MJ, Liu Z, Ten-Dijke P. TGF-beta signaling in vascular biology and dysfunction. *Cell Research*. 2009;19(1):116-127.

260. Wang Z, Perez M, Lee ES, Kojima S, Griffin M. The functional relationship between transglutaminase 2 and transforming growth factor β1 in the regulation of angiogenesis and endothelial-mesenchymal transition. *Cell Death Discovery*. 2017;8(9):3032-3054.

261. Aeschlimann D, Mosher D, Paulsson M. Tissue transglutaminase and factor XIII in cartilage and bone remodeling. *Seminars in Thrombosis and Hemostasis*. 1996;22(5):437-443.

262. Folk JE. Mechanism and basis for specificity of transglutaminase-catalyzed epsilon-(gamma-glutamyl) lysine bond formation. *Advances in Enzymology and Related Areas of Molecular Biology*. 1983;54(5):1-56.

263. Gundemir S, Colak G, Tucholski J, Johnson G V W. Transglutaminase 2: A molecular Swiss army knife, *Biochimica et Biophysica Acta*. 2012;1823(2):406–419.

264. Lee KN, Arnold SA, Birckbichler PJ, Patterson MK, Fraij BM, Takeuchi Y, Carter HA. Site-directed mutagenesis of human tissue transglutaminase. Cys-277 is essential for transglutaminase activity but not for GTPase activity. *Biochimica et Biophysica Acta*. 1993;1202(7):1–6.

265. Jeon JH, Kim CW, Shin DM, Kim K, Cho SY, Kwon JC, Choi KH, Kang HS, Kim IG. Differential incorporation of biotinylated polyamines by transglutaminase 2. *The FEBS Journal*. 2003;534(1):180-184.

266. Facchiano A, Facchiano F. Transglutaminases and their substrates in biology and human diseases: 50 years of growing. *Amino Acids*. 2009;36(9):599-614.

267. De Re V, Magris R, Cannizzaro R. New insights into the pathogenesis of celiac disease. *Frontiers in Medicine (Lausanne)*. 2017;31(4):137-148.

268. Nakaoka H, Perez DM, Baek KJ, Das T, Husain A, Misono K, Im MJ, Graham RM. Gh: a GTP-binding protein with transglutaminase activity and receptor signaling function. *Science*. 1994;264(4):1593-1596.

269. Hasegawa G, Suwa M, Ichikawa Y, Ohtsuka T, Kumagai S, Kikuchi M, Sato Y, Saito Y. A novel function of tissuetype transglutaminase: protein disulphide isomerase. *Biochem Journal*. 2003;373(3):793-803.

270. Mastroberardino PG, Farrace MG, Viti I, Pavone F, Fimia GM, Melino G, Piacentini M. Tissue transglutaminase contributes to the formation of disulphide bridges in proteins of mitochondrial respiratory complexes. *Biochimica et Biophysica Acta Bioenergetics*. 2006;1757(9):1357-1365.

271. Mishra S, Murphy LJ. Tissue transglutaminase has intrinsic kinase activity. *Journal*

of Biological Chemistry. 2004;279(23):23863–23868.

272. Mishra S, Saleh A, Espino PS, Davie JR, Murphy LJ. Phosphorylation of histones by tissue transglutaminase. *Journal of Biological Chemistry*. 2006;281(9):5532–5538.

273. Takeuchi Y, Ohashi H, Birckbichler PJ, Ikejima T. Nuclear translocation of tissue type transglutaminase during sphingosine-induced cell death: a novel aspect of the enzyme with DNA hydrolytic activity. *Journal of Biosciences*. 1998;53(7):352-358.

274. Tucholski J, Johnson GV. Tissue transglutaminase differentially modulates apoptosis in a stimuli-dependent manner. *Journal of Neurochemistry*. 2002;81(4):780-791.

275. Milakovic T, Tucholski J, McCoy E, Johnson GV. Intracellular localization and activity state of tissue transglutaminase differentially impacts cell death. *Journal of Biological Chemistry*. 2004;279(3):8715-8722.

276. Kim DS, Park SS, Nam BH, Kim IH, Kim SY. Reversal of drug resistance in breast cancer cells by transglutaminase 2 inhibition and nuclear factor-kappaB inactivation. *Cancer Research*. 2006;66(22):10936-43.

277. Verma A, Mehta K. Tissue transglutaminase-mediated chemoresistance in cancer cells. *Drug Resistance Updates*. 2007;10(4-5):144-151.

278. Balklava Z, Verderio E, Collighan R, Gross S, Adams J, Griffin M. (2002). Analysis of tissue transglutaminase in the migration of Swiss 3T3 fibroblasts: the active-state conformation of the enzyme does not affect cell motility, but it is important for its secretion. *Journal of Biological Chemistry*. 2002;277(13): 16567-16575.

279. Verderio EA, Telci D, Okoye A, Melino G, Griffin M. A novel RGD-independent cell adhesion pathway mediated by fibronectin-bound tissue transglutaminase rescues cells from anoikis. *Journal of Biological Chemistry*. 2003;278(3):42604-42614.

280. Mangala LS, Mehta K. Tissue transglutaminase (TG2) in cancer biology. *Progress in Experimental Tumor Research*. 2005;38(11):125-138.

281. Mangala LS, Fok JY, Zorrilla-Calancha IR, Verma A, Mehta K. Tissue transglutaminase expression promotes cell attachment, invasion and survival in breast cancer cells. *Oncogene*. 2007;26(17):2459-2470.

282. Ai L, Kim WJ, Demircan B, Dyer LM, Bray KJ, Skehan RR, Massoll NA, Brown KD. The transglutaminase 2 gene (TGM2), a potential molecular marker for chemotherapeutic drug sensitivity, is epigenetically silenced in breast cancer. *Carcinogenesis*. 2008;29(3):510-518.

283. Fesus L, Thomazy V, Falus A. Induction and activation of tissue transglutaminase during programmed cell death. *FEBS Letters*. 1987;224(2):104-108.

284. Piacentini M, Davies PJA. and Fesus L. Tissue transglutaminase in cells undergoing apoptosis. In: Apoptosis II. *The Molecular Basis of Apoptosis in Disease*. 1994;1(5):143-163.

285. Nicholas B, Smethurst P, Verderio E, Jones R, and Griffin M. Cross-linking of cellular proteins by tissue transglutaminase during necrotic cell death: a mechanism for maintaining tissue integrity. *Biochemical Journal*. 200;371(2):413-422.

286. Fesus, L., & Szondy, Z. Transglutaminase 2 in the balance of cell death and survival. *FEBS Letters*. 2005;579(15):3297-3302.

287. Autuori F, Farrace M, Oliverio S, Piredda L, Piacentini M. Tissue transglutaminase and apoptosis. *Advances in Biochemical Engineering/Biotechnology*. 1998;62(3):129-136.

288. Fok JY, Mehta K. Tissue transglutaminase induces the release of apoptosis inducing factor and results in apoptotic death of pancreatic cancer cells. *Apoptosis*.

2007;12(8):1455-1463.

289. Tabolacci C, De Martino A, Mischiati C, Feriotto G, Beninati S. The role of tissue transglutaminase in cancer cell initiation, survival and progression. *Medical Sciences Basel*. 2019;7(2):19-27.

290. Rodolfo C, Mormone E, Matarrese P, Ciccosanti F, Farrace MG, Garofano E, Piacentini M. Tissue transglutaminase is a multifunctional BH3-only protein. *Journal of Biological Chemistry*. 2004;279(52):54783-54792.

291. Falasca L, Farrace MG, Rinaldi A, Tuosto L, Melino G, Piacentini M. Transglutaminase type II is involved in the pathogenesis of endotoxic shock. *The Journal of Immunology*. 2008;180(4):2616-2624.

292. Piacentini M, D'Eletto M, Falasca L, Farrace MG, Rodolfo C. Transglutaminase 2 at the crossroads between cell death and survival. *Advances in Enzymology and Related Areas of Molecular Biology*. 2011;78(1):197-246.

293. Tatsukawa H, Furutani Y, Hitomi K, Kojima S. Transglutaminase 2 has opposing roles in the regulation of cellular functions as well as cell growth and death. *Cell Death Disease*. 2016;7(6):2244-2257.

294. Boehm JE, Singh U, Combs C, Antonyak MA, Cerione RA. Tissue transglutaminase protects against apoptosis by modifying the tumor suppressor protein p110 Rb. *The Journal of Biological Chemistry*. 2002;277(23):20127-20130.

295. Telci D, Wang Z, Li X, Verderio EA, Humphries MJ, Baccarini M, Basaga H, Griffin M. Fibronectin-tissue transglutaminase matrix rescues RGD-impaired cell adhesion through syndecan-4 and beta1 integrin co-signaling. *Journal of Biological Chemistry*. 2008;283(30):20937-20947.

296. Kim SJ, Kim KH, Ahn ER, Yoo BC, Kim SY. Depletion of cathepsin D by

transglutaminase 2 through protein cross-linking promotes cell survival. *Amino Acids*. 2011;44(1):73-80.

297. Guan JL. Role of focal adhesion kinase in integrin signalling. *International Journal of Biochemistry and Cell Biology*. 1997;29(1):1085-1096.

298. Eckert RL. Transglutaminase 2 takes center stage as a cancer cell survival factor and therapy target. *Molecular Carcinogenesis*. 2019;58(6):837-853.

299. Chhabra A, Verma A, Mehta K. Tissue transglutaminase promotes or suppresses tumors depending on cell context. *Anticancer Research*. 2009;29(6):1909-1919.

300. Tatsukawa H, Furutani Y, Hitomi K, Kojima S. Transglutaminase 2 has opposing roles in the regulation of cellular functions as well as cell growth and death. *Cell Death and Disease*. 2016;7(6):2244–2255.

301. Herman JF, Mangala LS, Mehta K. Implications of increased tissue transglutaminase (TG2) expression in drug-resistant breast cancer (MCF-7) cells. *Oncogene*. 2006;25(21): 3049–3058.

302. Erdem M, Erdem S, Sanli O, Sak H, Kilicaslan I, Sahin F, Telci D. Up-regulation of TGM2 with ITGB1 and SDC4 is important in the development and metastasis of renal cell carcinoma. *Urologic Oncology*. 2014;32(25):13-20.

303. Bihorac A. Role of Transglutaminase 2 in migration of tumor cells and how mouse models fit. *Medical Sciences*. 2018;6(3):70-78.

304. Verma A, Guha S, Diagaradjane P, Kunnumakkara AB, Sanguino AM, Lopez-Berestein G, Mehta K. Therapeutic significance of elevated tissue transglutaminase expression in pancreatic cancer. *Clinical Cancer Research*. 2008;14(8):2476-2483.

305. Huang L, Xu AM, Liu W. Transglutaminase 2 in cancer. *American Journal of Cancer*

Research. 2015;5(9):2756-2776.

306. Jang GY, Jeon JH, Cho SY, Shin DM, Kim CW, Jeong EM, Kim IG. Transglutaminase 2 suppresses apoptosis by modulating caspase 3 and NF-κB activity in hypoxic tumor cells. *Oncogene*. 2009;29(3):356-367.

307. Verma A, Guha S, Diagaradjane P, Kunnumakkara AB, Sanguino AM, Lopez-Berestein G, Mehta K. Therapeutic significance of elevated tissue transglutaminase expression in pancreatic cancer. *Clinical Cancer Research*. 2008;14(8):2476-2483.

308. Boroughs LK, Antonyak MA, Cerione RA. A novel mechanism by which tissue transglutaminase activates signaling events that promote cell survival. *Journal of Biological Chemistry*. 2014;289(14):10115-10125.

309. Antonyak MA, Boehm JE, Cerione RA. Phosphoinositide 3-kinase activity is required for retinoic acid-induced expression and activation of the tissue transglutaminase. *Journal of Biological Chemistry*. 2002;277(17):14712-147126.

310. Mian S, el Alaoui S, Lawry J, Gentile V, Davies PJ, Griffin M. The importance of the GTP-binding protein tissue transglutaminase in the regulation of cell cycle progression. *FEBS Letters*. 1995;370(2):27-31.

311. Nadalutti C, Viiri KM, Kaukinen K, Maki M, Lindfors K. Extracellular transglutaminase 2 has a role in cell adhesion, whereas intracellular transglutaminase 2 is involved in regulation of endothelial cell proliferation and apoptosis. *Cell Proliferation*. 2011;44(7):49-58.

312. Lee J, Banu SK, Rodriguez R, Starzinski-Powitz A, Arosh JA. Selective blockade of prostaglandin E2 receptors EP2 and EP4 signaling inhibits proliferation of human endometriotic epithelial cells and stromal cells through distinct cell cycle arrest. *Fertility and Sterility.* 2010;93(8):2498-506.

313. Mann AP, Verma A, Sethi G, et al. Overexpression of tissue transglutaminase leads to constitutive activation of nuclear factor-kappaB in cancer cells: delineation of a novel pathway. *Cancer Research*. 2006;66(8):8788-8795.

314. Kim DS, Choi YB, Han BG, Park SY, Jeon Y, Kim DH, Ahn ER, Shin JE, Lee BI, Lee H, Hong KM, Kim SY. Cancer cells promote survival through depletion of the von Hippel-Lindau tumor suppressor by protein crosslinking. *Oncogene*. 2011;30(48):4780-4790.

315. Yuen JSP, Cockman ME, Sullivan M, Protheroe A, Turner GDH, Roberts IS, Macaulay VM. The VHL tumor suppressor inhibits expression of the IGF1R and its loss induces IGF1R upregulation in human clear cell renal carcinoma. *Oncogene*. 2007;26(45):6499-6508.

316. Kaelin WG. Molecular basis of the VHL hereditary cancer syndrome. *Nature*. 2002;2(1) :673-682.

317. Cao L, Petrusca DN, Satpathy M, Nakshatri H, Petrache I, Matei D. Tissue transglutaminase protects epithelial ovarian cancer cells from cisplatin-induced apoptosis by promoting cell survival signaling. *Carcinogenesis*. 2008;29(5):1893-1900.

318. Patel NM, Nozaki S, Shortle NH, Bhat-Nakshatri P, Newton TR, Rice S, Nakshatri H. Paclitaxel sensitivity of breast cancer cells with constitutively active NF-κB is enhanced by IκBα super-repressor and parthenolide. *Oncogene*. 2000;19(36):4159-4169.

319. Park KS, Kim HK, Lee JH, Choi YB, Park SY. Transglutaminase 2 as a cisplatin resistance marker in non-small cell lung cancer. *Journal of Cancer Research and Clinical Oncology*. 2010;136(12):493-502.

320. Vanden-Berghe W, Vermeulen L, Delerive P, De Bosscher K, Staels B, Haegeman G. A paradigm for gene regulation: inflammation, NF-kappaB and PPAR. *Advances in Experimental Medicine and Biology*. 2003;544(1):181-196.

321. Remels AH, Langen RC, Gosker HR, Russell AP, Spaapen F, Voncken JW, Schrauwen P, Schols AM. PPARgamma inhibits NF-kappaB-dependent transcriptional activation in skeletal muscle. *American Journal of Physiology-Endocrinology and Metabolism*. 2009;297(1):174-183.

322. Maiuri L, Luciani A, Giardino I, Raia V, Villella VR, D'Apolito M, Quaratino S. Tissue transglutaminase activation modulates inflammation in cystic fibrosis via PPAR down-regulation. *The Journal of Immunology*. 2008;180(11):7697-7705.

323. Dhar SK and St Clair DK. Nucleophosmin blocks mitochondrial localization of p53 and apoptosis. *Journal of Biological Chemistry*. 2009;284(24):16409-16418.

324. Wang Z, Griffin M. TG2, a novel extracellular protein with multiple functions. *Amino Acids*. 2012;42(3):939-949.

325. Nezir AE, Ulukan B, Telci D. Transglutaminase 2: The maestro of the oncogenic mediators in renal cell carcinoma. *Medical Sciences*. 2019;7(2):24-39.

326. Zemskov EA, Janiak A, Hang J, Waghray A, Belkin AM. The role of tissue transglutaminase in cell-matrix interactions. *Frontiers in Bioscience*. 2006;1(11):1057-1076.

327. Telci D, Wang Z, Li X, Verderio EA, Humphries MJ, Baccarini M, Basaga H, Griffin M. Fibronectin-tissue transglutaminase matrix rescues RGD-impaired cell adhesion through syndecan-4 and beta1 integrin co-signaling. *Journal of Biological Chemistry*. 2008;283(30):20937-20947.

328. Wang Z, Collighan RJ, Gross SR, Danen EHJ, Orend G, Telci D, Griffin M. RGD-

independent Cell adhesion via a tissue transglutaminase-fibronectin matrix promotes fibronectin fibril deposition and requires syndecan-4/2 and α5β1 integrin co-signaling. *Journal of Biological Chemistry*. 2010;285(51):40212-40229.

329. Lortat-Jacob H, Burhan I, Scarpellini A, Thomas A, Imberty A, Vivès RR, Verderio EAM. Transglutaminase-2 interaction with heparin. *Journal of Biological Chemistry*. 2012;287(22):18005-18017.

330. Caswell PT, Norman JC. Integrin trafficking and the control of cell migration. *Traffic*. 2006;7(1):14-21.

331. Morgan MR, Humphries MJ, Bass MD. Synergistic control of cell adhesion by integrins and syndecans. *Nature Reviews Molecular Cell Biology*. 2007;8(12):957-969.

332. Berrier AL, Yamada KM. Cell–matrix adhesion. *Journal of Cellular Physiology*. 2007;213(3):565-573.

333. Janiak A, Zemskov E, Belkin AM. Cell surface transglutaminase promotes RhoA activation via integrin clustering and suppression of the Src-p190RhoGAP signaling pathway. *Molecular Biology of the Cell*. 2006;17(4):1606-1619.

334. Satpathy M, Cao L, Pincheira R, Emerson R, Bigsby R, Nakshatri H, Matei D. Enhanced peritoneal ovarian tumor dissemination by tissue transglutaminase. *Cancer Research*. 2007;67(15):7194-7202.

335. Tomar A, Lim ST, Lim Y, Schlaepfer DD. A FAK-p120RasGAP-p190RhoGAP complex regulates polarity in migrating cells. *Journal of Cell Science*. 2009;122(11):1852–1862.

336. Avizienyte E, Frame MC. Src and FAK signalling controls adhesion fate and the epithelial-to-mesenchymal transition. *Current Opinion in Cell Biology*.

2005;17(5):542-547.

337. Bagatur Y, Ilter-Akulke AZ, Bihorac A, Erdem M, Telci D. Tissue transglutaminase expression is necessary for adhesion, metastatic potential and cancer stemness of renal cell carcinoma. *Cell Adhesion and Migration*. 2018;12(2):138-151.

338. Bass MD, Morgan MR, Roadch KA, Settleman J, Goryachev AB, Humphries MJ p190RhoGAP is the convergence point of adhesion signals from α5β1 integrin and syndecan-4. *Journal of Cell Biology*. 2008;181(6):1013-1026.

339. Tkachenko E, Rhodes JM, Simons M. Syndecans: New kids on the signaling block. *Circulation Research*. 2005;96(5):488-500.

340. Helfrich MH, Stenbeck G, Nesbitt SA, Horton MA. Integrins and other cell surface attachment molecules of bone cells. *Principles of Bone Biology*. 2008;13(1)385-424.

341. Szatmári T, Dobra K. The role of syndecan-1 in cellular signaling and its effects on heparan sulfate biosynthesis in mesenchymal tumors. *Frontiers in Oncology*. 2013;19(3):310-323.

342. Fears CY, Gladson CL, Woods A. Syndecan-2 is expressed in the microvasculature of gliomas and regulates angiogenic processes in microvascular endothelial cells. *Journal of Biological Chemistry*. 2006;281(21):14533-14536.

343. Afratis NA, Nikitovic D, Multhaupt HAB, Theocharis AD, Couchman JR, Karamanos NK. Syndecans - key regulators of cell signaling and biological functions. *The FEBS Journal*. 2016;284(1):27–41.

344. Cardin AD, Jackson RL, Sparrow DA, Sparrow JT. Interaction of glycosaminoglycans with lipoproteins. *Annals of the New York Academy of Sciences*. 1989;556(1):186-193.

345. Scarpellini A, Germack R, Lortat-Jacob H, Muramatsu T, Billett E, Johnson T, Verderio EAM. Heparan sulfate proteoglycans are receptors for the cell-surface trafficking and biological activity of transglutaminase-2. *Journal of Biological Chemistry*. 2009;284(27):18411-18423.

346. Verderio EAM, Scarpellini A, Johnson TS. Novel interactions of TG2 with heparan sulfate proteoglycans: reflection on physiological implications. *Amino Acids*. 2008;36(4):671-677.

347. Verderio EAM, Scarpellini A. Significance of the syndecan-4-transglutaminase-2 interaction. *Scientific World Journal*. 2010;14(10):1073-1077.

348. Furini G, Verderio EAM. Spotlight on the Transglutaminase 2-Heparan Sulfate Interaction. *Medical Sciences*. 2019;7(1):5-12.

349. Barsigian C, Stern AM, Martinez J. Tissue (type II) transglutaminase covalently incorporates itself, fibrinogen, or fibronectin into high molecular weight complexes on the extracellular surface of isolated hepatocytes. Use of 2-[(2-oxopropyl)thio] imidazolium derivatives as cellular transglutaminase inactivators. *Journal of Biological Chemistry*. 1991;266(33):22501-22509.

350. Burhan I, Furini G, Lortat-Jacob H. Interplay between transglutaminases and heparan sulphate in progressive renal scarring. *Scientific Reports*. 2016;6(3):31343-31355.

351. Signorini M, Pasini F, Bonaccorsi G, Mollica G, Ferrari C, Bergamini C. Regulation of endometrial transglutaminase activity during the menstrual cycle. *Biochemistry International*. 1988;16(5):77-82.

352. Walter I, Handler J, Miller I, Aurich C. Matrix metalloproteinase 2 (MMP-2) and tissue transglutaminase (TG2) are expressed in periglandular fibrosis in horse mares with endometrosis. Histology and Histopathology. 2005;20(4):1105-1113.

353. Jackson KS, Hastings JM, Mavroganis PA, Bagchi I, Fazleabas AT. Alterations in the calcitonin and calcitonin modulated proteins, e-cadherin and the enzyme tissue transglutaminase ii during the window of implantation in a baboon model of endometriosis. *Journal of Endometriosis*. 2009;1(1):57-67.

354. Santoro L, Campo S, D'Onofrio F, Gallo A, Covino M, Campo V, Montalto M. Looking for celiac disease in italian women with endometriosis: a case control study. *BioMed Research International.* 2014;3(2):1-5.

355. Aguiar FM, Melo SBC, Galvão LC, Rosa-e-Silva JC, dos Reis RM, Ferriani RA. Serological testing for celiac disease in women with endometriosis. *Clinical and Experimental Obstetrics and Gynecology*. 2009;36(1):23-25.

356. Jones FS, Jones PL. The tenascin family of ECM glycoproteins: Structure, function, and regulation during embryonic development and tissue remodeling. *Developmental Dynamics*. 2000;218(2):235-259.

357. Hewitt R, Danø K. Stromal cell expression of components of matrix-degrading protease systems in human cancer. *Enzyme Protein*. 1996;49(3):163-173.

358. Matrisian LM. Metalloproteinases and their inhibitors in matrix remodeling. *Trends in Genetics*. 1990;6(4):121-125.

359. Massova I, Kotra LP, Fridman R, Mobashery S. Matrix metalloproteinases: Structures, evolution, and diversification. *The FASEB Journal*. 1998;12(12):1075-1095.

360. DeClerck YA, Imren S, Montgomery AMP, Mueller BM, Reisfeld RA, Laug WE. Proteases and protease inhibitors in tumor progression. *Advances in Experimental Medicine and Biology*. 1997;425(7): 89-97.

361. Jones GT. Matrix metalloproteinases in biologic samples. *Advances in Clinical*

Chemistry. 2014;65(1):199-219.

362. Gross J, Lapıere CM. Collagenolytic activity in amphibian tissues: a tissue culture assay. *Proceedings of the National Academy of Sciences of the United States of America*. 1962;48(6):1014-1022.

363. Birkedal-Hansen B, Moore WGI, Taylor RE, Bhown AS, Birkedal-Hansen H. Monoclonal antibodies to human fibroblast procollagenase. inhibition of enzymatic activity, affinity purification of the enzyme, and evidence for clustering of epiopes in the nh, -terminal end of the activated enzyme. *Biochemistry*. 1988;27(5):6751-6758.

364. Iyer RP, Patterson NL, Fields GB, Lindsey ML. The history of matrix metalloproteinases: milestones, myths, and misperceptions. *American Journal of Physiology-Heart and Circulatory Physiology*. 2012;303(8):919–H930.

365. Cerdà-Costa N, Xavier Gomis-Rüth F. Architecture and function of metallopeptidase catalytic domains. *Protein Science*. 2013;23(2):123-144.

366. Sternlicht MD, Werb Z. How matrix metalloproteinases regulate cell behavior. *Annual Review of Cell and Developmental Biology*. 2001;17(1):463-516.

367. Rundhaug JE. Matrix metalloproteinases and angiogenesis. *Journal of Cellular and Molecular Medicine*. 2005;9(2):267-285.

368. Bourboulia D, Stetler-Stevenson WG. Matrix metalloproteinases (MMPs) and tissue inhibitors of metalloproteinases (TIMPs): Positive and negative regulators in tumor cell adhesion. *Seminars in Cancer Biology*. 2010;20(3):161-168.

369. Sethı CS. Matrix metalloproteinase biology applied to vitreoretinal disorders. *British Journal of Ophthalmology*. 2000;84(6):654-666.

370. Overall CM, López-Otín C. Strategies for MMP inhibition in cancer: innovations for

the post-trial era. *Nature Reviews Cancer*. 2002;2(9):657-672.

371. Nagase H, Woessner JF. Matrix metalloproteinases. *Journal of Biological Chemistry*. 1999;274(31):21491-21494.

372. Medina C, Santana A, Paz MC, Díaz-Gonzalez F, Farre E, Salas A, Quintero E. Matrix metalloproteinase-9 modulates intestinal injury in rats with transmural colitis. *Journal of Leukocyte Biology*. 2006;79(5):954-962.

373. Medina C. Role of Matrix metalloproteinases in intestinal inflammation. *Journal of Pharmacology and Experimental Therapeutics*. 2006;318(3):933-938.

374. Arpino V, Brock M, Gill SE. The role of TIMPs in regulation of extracellular matrix proteolysis. *Matrix Biology*. 2015;44(46):247-254.

375. Curry TE Jr, Osteen KG. Cyclic changes in the matrix metalloproteinase system in the ovary and uterus. *Biology of Reproduction*. 2001;64(5):1285-1296.

376. Scuderi GJ, Hanna L. Alpha-2-macroglobulin: Protease inhibitor treatment (PRP Variant). *Advanced Procedures for Pain Management*. 2018;3(1):459-467.

377. Singh M, Tyagi SC. Metalloproteinases as mediators of inflammation and the eyes: molecular genetic underpinnings governing ocular pathophysiology. *Journal of Ophthalmology*. 2017;10(8):1308-1318.

378. Lambert E, Dassé E, Haye B, Petitfrère E. TIMPs as multifacial proteins. *Critical Reviews in Oncology/Hematology*. 2004;49(3):187-198.

379. Sorsa T, Tjäderhane L, Salo T. Matrix metalloproteinases (MMPs) in oral diseases. *Oral Diseases*. 2004;10(6):311-318.

380. Visse R. Matrix metalloproteinases and tissue inhibitors of metalloproteinases: Structure, function, and biochemistry. *Circulation Research*. 2003;92(8):827-839.

381. Malemud CJ. Matrix metalloproteinases (MMPs) in health and disease. *Frontiers in Bioscience*. 2006;1(11):1696-701.

382. Bałkowiec M, Maksym RB, Włodarski PK. The bimodal role of matrix metalloproteinases and their inhibitors in etiology and pathogenesis of endometriosis. *Molecular Medicine Reports*. 2018;18(3):3123-3136.

383. Jabłońska-Trypuć A, Matejczyk M, Rosochacki S. Matrix metalloproteinases (MMPs), the main extracellular matrix (ECM) enzymes in collagen degradation, as a target for anticancer drugs. *Journal of Enzyme Inhibition and Medicinal Chemistry*. 2016;31(1):177-183

384. Kapoor C, Vaidya S, Wadhwan V, Kaur G, Pathak A. Seesaw of matrix metalloproteinases (MMPs). *Journal of Cancer Research and Therapeutics*. 2016;12(1):28-35.

385. Iyer RP, Nicolle L, Gregg B, Merry L. The history of matrix metalloproteinases: milestones, myths, and misperceptions. *The American Journal of Physiology - Heart and Circulatory Physiology*. 2012;303(8):919-930.

386. Brinckerhoff CE, Matrisian LM. Matrix metalloproteinases: a tail of a frog that became a prince. *Nature Reviews Molecular Cell Biology*. 2002;3(3):207-214.

387. Ennis BW, Matrisian LM. Matrix degrading metalloproteinases. *Journal of Neuro-Oncology*. 1994;18(2):105-109.

388. Van Doren SR. Matrix metalloproteinase interactions with collagen and elastin. *Matrix Biology*. 2015;44(46):224–231.

389. Van Wart HE. Human neutrophil collagenase. *Matrix Supplement*. 1992;1(1):31-36.

390. Peppin GJ, Weiss SJ. Activation of the endogenous metalloproteinase, gelatinase, by

triggered human neutrophils. *Proceedings of the National Academy of Sciences of the United States of America*. 1986;83(1):4322–4326.

391. Fisher GJ, Choi HC, Bata-Csorgo Z, Shao Y, Datta S, Wang ZQ, Voorhees JJ. Ultraviolet irradiation increases Matrix metalloproteinase-8 protein in human skin *in vivo*. *Journal of Investigative Dermatology*. 2001;117(2):219-226.

392. Shimokawa KI, Katayama K, Matsuda M, Takahashi Y, Hara H, Sato I, Kaneko HS. Matrix metalloproteinase (MMP)-2 and MMP-9 activities in human seminal plasma. *Molecular Human Reproduction*. 2002;8(1):32-36.

393. Pittayapruek P, Meephansan J, Prapapan O, Komine M, Ohtsuki M. Role of matrix metalloproteinases in photoaging and photocarcinogenesis. *International Journal of Molecular Sciences*. 2016;17(6):868-880.

394. Kihira Y, Mori K, Miyazaki K, Matuo Y. (1996). Production of recombinant human matrix metalloproteinase 7 (Matrilysin) with potential role in tumor invasion by refolding from Escherichia coli inclusion bodies and development of sandwich ELISA of MMP-7. *Urologic Oncology Seminars and Original Investigations*. 1996;2(1):20-26.

395. Ii M, Yamamoto H, Adachi Y, Maruyama Y, Shinomura Y. Role of matrix metalloproteinase-7 (matrilysin) in human cancer invasion, apoptosis, growth, and angiogenesis. *Experimental Biology and Medicine (Maywood)*. 2006;23(1):20-27.

396. Sanchez-Lopez R, Alexander CM, Behrendtsen O, Breathnach R, Werb Z. Role of zinc-binding- and hemopexin domain-encoded sequences in the substrate specificity of collagenase and stromelysin-2 as revealed by chimeric proteins. *Journal of Biological Chemistry*. 1993;268(10):7238-47.

397. Stamenkovic I. Extracellular matrix remodelling: the role of matrix

metalloproteinases. *The Journal of Pathology*. 2003;200(4):448-464.

398. Itoh Y, Kajita M, Kinoh H, Mori H, Okada A, Seiki M. Membrane type 4 matrix metalloproteinase (MT4-MMP, MMP-17) is a glycosylphosphatidylinositol-anchored proteinase. *Journal of Biological Chemistry*. 1999;274(1):34260-34266.

399. Vihinen P, Kähäri VM. Matrix metalloproteinases in cancer: Prognostic markers and therapeutic targets. *International Journal of Cancer*. 2002;99(2):157-166.

400. Kessenbrock K, Plaks V, Werb Z. Matrix Metalloproteinases: Regulators of the tumor microenvironment. *Cell*. 2010;141(1):52-67.

401. Belkin AM, Akimov SS, Zaritskaya LS, Ratnikov BI, Deryugina EI, Strongin AY. Matrix-dependent proteolysis of surface transglutaminase by membrane-type metalloproteinase regulates cancer cell adhesion and locomotion. *Journal of Biological Chemistry*. 2001;276(21):18415-18422.

402. Belkin AM, Zemskov EA, Hang J, Akimov SS, Sikora S, Strongin AY. Cell-surface-associated tissue transglutaminase is a target of MMP-2 proteolysis. *Biochemistry*. 2004;43(37):11760-11769.

403. Stephens P. Crosslinking and G-protein functions of transglutaminase 2 contribute differentially to fibroblast wound healing responses. *Journal of Cell Science*. 2004;117(15):3389-3403.

404. Satpathy M, Shao M, Emerson R, Donner DB, Matei D. Tissue transglutaminase regulates matrix metalloproteinase-2 in ovarian cancer by modulating cAMP-response element-binding protein activity. *Journal of Biological Chemistry*. 2009;284(23):15390–15399.

405. Goldman MB, Cramer DW. The epidemiology of endometriosis. *Progress in Clinical and Biological Research*. 1990;323(1):15-31.

406. Grzechocińska B, Dąbrowski F, Cyganek A, Panek G, Wielgoś M. The role of metalloproteinases in endometrial remodelling during menstrual cycle. *Ginekologia Polska*. 2017;88(6):337-342.

407. Sternlicht MD, Werb Z. How matrix metalloproteinases regulate cell behavior. *Annual Review of Cell and Developmental Biology*. 2001;17(4):463-516.

408. Livingstone M, Fraser IS. Mechanism of abnormal uterine bleeding. *Human Reproduction Update*. 2002;8(1):60-67.

409. Goffin F, Munaut C, Frankenne F, Perrier d'Hauterive S, Béliard A, Fridman V, Foidart JM. Expression pattern of metalloproteinases and tissue inhibitors of matrix-metalloproteinases in cycling human endometrium. *Biology of Reproduction*. 2003;69(3):976-984.

410. Noguchi Y, Sato T, Hirata M, Hara T, Ohama K, Ito A. Identification and characterization of extracellular matrix metalloproteinase inducer in human endometrium during the menstrual cycle *in vivo* and *in vitro*. *The Journal of Clinical Endocrinology and Metabolism*. 2003;88(12):6063-6072.

411. Osteen KG, Yeaman GR, Bruner-Tran KL. Matrix metalloproteinases and endometriosis. *Seminars in Reproductive Medicine*. 2003;21(23):155-68

412. Kennedy S, Bergqvist A, Chapron C, D'Hooghe T, Dunselman G, Greb R, Hummelshoj L, Prentice A, Saridogan E. Eshre special interest group for endometriosis and endometrium guideline development group and Eshre guideline for the diagnosis and treatment of endometriosis. *Human Reproduction*. 2005;20(10):2698-2704.

413. Braza-Boïls A, Salloum-Asfar S, Marí-Alexandre J, Arroyo AB, González-Conejero R, Barceló-Molina M, Martínez C. Peritoneal fluid modifies the microRNA

expression profile in endometrial and endometriotic cells from women with endometriosis. *Human Reproduction*. 2015,30(10):2292-2302.

414. Ryan IP, Schriock ED, Taylor RN. (1994). Isolation, characterization, and comparison of human endometrial and endometriosis cells *in vitro*. *The Journal of Clinical Endocrinology & Metabolism*. 1994;78(3):642-649.

415. Gargett CE, Schwab KE, Zillwood RM, Nguyen HPT, Wu D. Isolation and culture of epithelial progenitors and mesenchymal stem cells from human endometrium. *Biology of Reproduction*. 2009;80(6):1136-1145.

416. Kruitwagen RF, Poels LG, Willemsen WN, de Ronde IJ, Jap PH, Roll R. Endometrial epithelial cells in peritoneal fluid during the early follicular phase. *Fertil and Steril*. 1991;55(2):297-303.

417. Telci D, Collighan RJ, Basaga H, Griffin M. Increased TG2 expression can result in induction of transforming growth factor β1, causing increased synthesis and deposition of matrix proteins, which can be regulated by nitric oxide. *Journal of Biological Chemistry*. 2009;284(43):29547-29558.

418. Peskin AV, Winterbourn CC. A microtiter plate assay for superoxide dismutase using a water-soluble tetrazolium salt (WST-1). *Clinica Chimica Acta*. 2000;293(2):157-166.

419. Ding DC, Chu TY, Chiou SH, Liu HW. Enhanced differentiation and clonogenicity of human endometrial polyp stem cells. *Differentiation.* 2011;81(3):172-180.

420. Zlatska AV, Rodnichenko AE, Gubar OS, Zubov DO, Novikova SN, Vasyliev RG. Endometrial stromal cells: isolation, expansion, morphological and functional properties. *Experimental Oncology*. 2017;39(3):197-202.

421. Cao M, Chan RW, Yeung WS. Label-retaining stromal cells in mouse endometrium

awaken for expansion and repair after parturition. *Stem Cells and Development*. 2014;24(5):768-780.

422. Gargett CE, Schwab KE, Deane JA. Endometrial stem/progenitor cells: the first 10 years. *Human Reproduction Update*. 2016;22(2):137-163.

423. Sarma D, Iyengar P, Marotta TR, terBrugge KG, Gentili F, Halliday W. Cerebellar endometriosis. *American Journal of Roentgenology*. 2004;182(13):1543-1546.

424. Gui B, Valentini AL, Ninivaggi V, Marino M, Iacobucci M, Bonomo L. Deep pelvic endometriosis: don't forget round ligaments. Review of anatomy, clinical characteristics, and MR imaging features. *Abdominal Imaging*. 2014;39(3):622-632.

425. Meuleman C, Vandenabeele B, Fieuws S, Spiessens C, Timmerman D, D'Hooghe T. High prevalence of endometriosis in infertile women with normal ovulation and normospermic partners. *Fertility and Sterility*. 2009;92(1):68-74.

426. Adamson GD, Pasta DJ. Endometriosis fertility index: the new, validated endometriosis staging system. *Fertility and Sterility*. 2010;94(5):1609-1615.

427. Bulletti C, Coccia ME, Battistoni S, Borini A. Endometriosis and infertility. *Journal of Assisted Reproduction and Genetics*. 2010;27(8):441-447.

428. Jiménez-López J, Muñoz-Hernando L, Marqueta- Marques L, Alvarez-Conejo C, Tejerizo-García Á, Lopez-Gonzalez G, Muñoz-Gonzalez JL. Endometriosis: Alternative methods of medical treatment. *International Journal of Women's Health*. 2015;7(7):595-603.

429. Simoens S, Hummelshoj L, D'Hooghe T. Endometriosis: cost estimates and methodological perspective. *Human Reproduction Update*. 2007;13(5):395-404.

430. Sourial S, Tempest N, Hapangama DK. Theories on the Pathogenesis of

endometriosis. *International Journal of Reproductive Medicine*. 2014;15(7):1–9.

431. Sampson JA. The escape of foreign material from the uterine cavity into the uterine veins. *American Journal of Obstetrics and Diseases of Women and Children*. 1918;78(1):161-175.

432. Sampson JA. The development of the implantation theory for the origin of peritoneal endometriosis. *American Journal of Obstetrics and Gynecology*. 1940;40(5):549-557.

433. Sampson JA. Metastatic or embolic endometriosis due to the menstrual dissemination of endometrial tissue into the venous circulation. *American Journal of Pathology*. 1927;3(1):93-110.

434. Chan RW, Gargett CE. Identification of label-retaining cells in mouse endometrium. *Stem Cells*. 2006;24(11):1529-1538.

435. Gargett CE, Nguyen HP, Ye L. Endometrial regeneration and endometrial stem/progenitor cells. *Reviews in Endocrine and Metabolic Disorders*. 2012;13(4):235-251.

436. Hendijani F. Explant culture: An advantageous method for isolation of mesenchymal stem cells from human tissues. *Cell Proliferation*. 2017;50(2):12334-12347.

437. Fuchs E, Tumbar T, Guasch G. Socializing with the neighbors. *Cell*. 2004;116(6):769-778.

438. Watt FM, Fujiwara H. Cell-extracellular matrix interactions in normal and diseased skin. *Cold Spring Harbor Perspectives in Biology*. 2011;3(4):5124-5137.

439. Pera MF, Tam PPL. Extrinsic regulation of pluripotent stem cells. *Nature*. 2010;465(7299):713-720.

440. Reichert D, Friedrichs J, Ritter S, Käubler T, Werner C, Bornhäuser M, Corbeil D. Phenotypic, morphological and adhesive differences of human hematopoietic progenitor cells cultured on murine versus human mesenchymal stromal cells. *Scientific Reports*. 2015;26(5):15680-15695.

441. Barry FP, Murphy JM. Mesenchymal stem cells: clinical applications and biological characterization. *The International Journal of Biochemistry and Cell Biology*. 2004;36(4):568-584.

442. Rossignoli F, Caselli A, Grisendi G. Isolation, characterization, and transduction of endometrial decidual tissue multipotent mesenchymal stromal/stem cells from menstrual blood. *BioMed Research International*. 2013;31(12):901821-901833.

443. Sahoo AK, Das JK, Nayak S. Isolation, culture, characterization, and osteogenic differentiation of canine endometrial mesenchymal stem cell. *Veterinary World*. 2017;10(12):1533-1541.

444. Ghobadi F, Rahmanifar F, Mehrabani D, Tamadon A, Dianatpour M, Zare S, Razeghian Jahromi I. Endometrial mesenchymal stem stromal cells in mature and immature sheep: An in vitro study. *International Journal of Reproductive BioMedicine*. 2018;16(2):83-92.

445. Dominici M, Le Blanc K, Mueller I, Slaper-Cortenbach I, Marini F, Krause D, Deans R, Keating A, Prockop Dj, Horwitz E. Minimal criteria for defining multipotent mesenchymal stromal cells. *The International Society for Cellular Therapy position statement Cytotherapy*. 2006;8(4):315-327.

446. Schwab KE, Gargett CE. Co-expression of two perivascular cell markers isolates mesenchymal stem-like cells from human endometrium. *Human Reproductive*. 2007;22(11):2903-2911.

447. Koçak P, Canikyan S, Batukan M, Attar R, Şahin F, Telci D. Comparison of enzymatic and nonenzymatic isolation methods for endometrial stem cells. *Turkısh Journal of Biology*. 2016;40(2):1081–1089.

448. Masuda H, Anwar SS, Bühring HJ, Rao R, Gargett CE. A novel marker of human endometrial mesenchymal stem-like cells. *Cell Transplantation*. 2012;21(10):2201-2214.

449. Hu J, Zeng B, Jiang X. The expression of marker for endometrial stem cell and fibrosis was increased in intrauterine adhesious. *International Journal of Clinical and Experimental Pathology*. 2015;8(2):1525-1534.

450. Zuo W, Xie B, Li C. The clinical applications of endometrial mesenchymal stem cells. *Biopreservation and Biobanking*. 2018;16(2):158-164.

451. Barragan F, Irwin JC, Balayan S, Erikson DW, Chen JC, Houshdaran S, Giudice LC. (2016). Human endometrial fibroblasts derived from mesenchymal progenitors inherit progesterone resistance and acquire an inflammatory phenotype in the endometrial niche in endometriosis. *Biology of Reproduction*. 2016;94(5):118-129.

452. Xiao W, Gao Z, Duan Y, Yuan W, Ke Y. Notch signaling plays a crucial role in cancer stem-like cells maintaining stemness and mediating chemotaxis in renal cell carcinoma. *Journal of Experimental and Clinical Cancer Research*. 2017;36(1):41-54.

453. Wang Z, Yan X. CD146, a multi-functional molecule beyond adhesion. *Cancer Letters*. 2013;330(2):150-162.

454. Lehmann JM, Holzmann B, Breitbart EW, Schmiegelow P, Riethmuller G, Johnson JP. Discrimination between benign and malignant cells of melanocytic lineage by two novel antigens, a glycoprotein with a molecular weight of 113,000 and a protein with

a molecular weight of 76, 000. *Cancer Research*. 1987;47(2):841-845.

455. Ouhtit A, Gaur RL, Abd Elmageed ZY, Fernando A, Thouta R, Trappey AK, Abdraboh ME, El Sayyad HI, Rao P, Raj MG. Towards understanding the mode of action of the multifaceted cell adhesion receptor CD146. *Biochimica et Biophysica Acta*. 2009;17(95):130-136.

456. Hu J, Zeng B, Jiang X, Hu L, Meng Y, Zhu Y, Mao M. The expression of marker for endometrial stem cell and fibrosis was increased in intrauterine adhesious. *International Journal of Clinical and Experimental Pathology*. 2015;8(2):1525-1534.

457. Wang Y, Hu C, Dong R, Huang X, Qiu H. Platelet-derived growth factor-D promotes ovarian cancer invasion by regulating matrix metalloproteinases 2 and 9. *Asian Pacific Journal of Cancer Prevention*. 2011;12(2):3367-3370.

458. Matei D, Kelich S, Cao L, Menning N, Emerson RE, Rao J, Sledge GW. PDGF BB induces VEGF secretion in ovarian cancer. *Cancer Biology and Therapy*. 2007;6(12):1951-1959.

459. Madsen CV, Dahl Steffensen K, Waldstrøm M, Jakobsen A. Immunohistochemical expression of platelet-derived growth factor receptors in ovarian cancer patients with long-term follow-up. *Pathology Research International*. 2012;12(9):851432.

460. Yamamoto S, Tsuda H, Takano M. Expression of platelet-derived growth factors and their receptors in ovarian clear-cell carcinoma and its putative precursors. *Modern Pathology*. 2008;21(2):115-124.

461. Matsumoto H, Nasu K, Nishida M, Ito H, Bing S, Miyakawa I. Regulation of proliferation, motility, and contractility of human endometrial stromal cells by platelet-derived growth factor. *The Journal of Clinical Endocrinology and Metabolism*. 2005;90(6):3560-3567.

462. Zemskov EA, Loukinova E, Mikhailenko I, Coleman RA, Strickland DK, Belkin AM. Regulation of platelet-derived growth factor receptor function by integrin-associated cell surface transglutaminase. *Journal of Biological Chemistry*. 2009;284(24):16693-16703.

463. Chen J, Luo Y, Huang H. CD146 is essential for PDGFRβ-induced pericyte recruitment. *Protein Cell*. 2018;9(8):743-747.

464. De Macédo P, Marrano C, Keillor JW. A direct continuous spectrophotometric assay for transglutaminase activity. *Analytical Biochemistry*. 2000;285(1):16–20.

465. Keillor JW, Clouthier CM, Apperley KYP, Akbar A, Mulani A. Acyl transfer mechanisms of tissue transglutaminase. *Bioorganic Chemistry*. 2014;57(12):186-197.

466. Greenberg CS, Birckbichler PJ, Rice RH. Transglutaminases: multifunctional cross-linking enzymes that stabilize tissues. *The FASEB Journal*. 1991;5(15):3071-3077.

467. Achyuthan KE, Greenberg CS. Identification of a guanosine triphosphate-binding site on guinea pig liver transglutaminase. Role of GTP and calcium ions in modulating activity. *Journal of Biological Chemistry*. 1987;262(4):1901-1916.

468. Brosens I, Benagiano G. Endometriosis, a modern syndrome. *Indian Journal of Medical Research*. 2011;133(6):581-593.

469. Griffin M, Casadio R, Bergamini CM. Transglutaminases: Nature's biological glues. Biochemical Journa. 2002;368(2):377-396.

470. Iwahashi M, Muragaki Y, Ooshima A, Yamoto M, Nakano R. Alterations in distribution and composition of the extracellular matrix during decidualization of the human endometrium. *Reproduction*. 1996;108(1):147–155.

471. Khorram O, Lessey BA. Alterations in expression of endometrial endothelial nitric

oxide synthase and αvβ3 integrin in women with endometriosis. *Fertility and Sterility*. 2002;78(4):860-864.

472. Alpay Z, Saed GM, Diamond MP. Female infertility and free radicals: potential role in adhesions and endometriosis. *Journal of the Society for Gynecologic Investigation*. 2006;13(6):390-398.

473. Ota H, Igarashi S, Hatazawa J, Tanaka T. Endothelial nitric oxide synthase in the endometrium during the menstrual cycle in patients with endometriosis and adenomyosis. *Fertility and Sterility*. 1998;69(2):303-308.

474. Yoshiki N. Expression of inducible nitric oxide synthase in human cultured endometrial stromal cells. *Molecular Human Reproduction*. 1999;5(4):353-357.

475. Lai TS, Hausladen A, Slaughter TF, Eu JP, Stamler JS, Greenberg CS. Calcium regulates s-nitrosylation, denitrosylation, and activity of tissue transglutaminase. *Biochemistry*. 2001;40(16):4904-4910.

476. Siegel M, Khosla C. Transglutaminase 2 inhibitors and their therapeutic role in disease states. *Pharmacology and Therapeutics*. 2007:115(2):232-245.

477. Lessey BA, Young SL. Integrins and other cell adhesion molecules in endometrium and endometriosis. *Seminars in Reproductive Medicine*. 1997;15(3):291-299.

478. Lessey BA. The use of integrins as for the assessment of uterine receptivity. *Fertility and Sterility.* 1994;61(8):812-814.

479. Hayashi K, Hayashi M, Jalkanen M, Firestone JH, Trelstad RL, Bernfield M. Immunocytochemistry of cell surface heparan sulfate proteoglycan in mouse tissues. A light and electron microscopic study. *Journal of Histochemistry and Cytochemistry*. 1987;35(10):1079-1088.

480. Potter SW, Morris JE. Changes in histochemical distribution of cell surface heparan sulfate proteoglycan in mouse uterus during the estrous cycle and early pregnancy. *The Anatomical Record*. 1992;234(3):383-390.

481. San Martin S, Soto-Suazo M, Zorn TMT. Perlecan and syndecan-4 in uterine tissues during the early pregnancy in mice. *American Journal of Reproductive Immunology*. 2004;52(8):53-59.

482. Chelariu-Raicu A, Wilke C, Brand M, Starzinski-Powitz A, Kiesel L, Schüring AN, Götte M. Syndecan-4 expression is upregulated in endometriosis and contributes to an invasive phenotype. *Fertility and Sterility*. 2016;106(2):378-385.

483. Kim H, Choi DS, Chang SJ. The expression of syndecan-1 is related to the risk of endometrial hyperplasia progressing to endometrial carcinoma. *Journal of Gynecologic Oncology*. 2010;21(1):50–55.

484. Nikoo S, Ebtekar M, Jeddi-Tehrani M, Shervin A, Bozorgmehr M, Vafaei S, Zarnani AH. Menstrual blood-derived stromal stem cells from women with and without endometriosis reveal different phenotypic and functional characteristics. *Molecular Human Reproduction*. 2014;20(9):905-918.

485. Fesus L, Davies PJ, Piacentini M. Apoptosis: molecular mechanisms in programmed cell death. *European Journal of Cell Biology*. 1991;56(2):170-177.

486. Melino G, Annicchiarico-Petruzzelli M, Piredda L. Tissue transglutaminase and apoptosis: sense and antisense transfection studies with human neuroblastoma cells. *Molecular and Cellular Biology*. 1994;14(10):6584-6596.

487. Oliverio S, Amendola A, Di Sano F, Farrace MG, Fesus L, Nemes Z, Piredda L, Spinedi A, Piacentini M. Tissue transglutaminase-dependent posttranslational modification of the retinoblastoma gene product in promonocytic cells undergoing

apoptosis. *Molecular and Cellular Biology*. 1997;17(3):6040-6048.

488. Hornung D. Chemokine bioactivity of RANTES in endometriotic and normal endometrial stromal cells and peritoneal fluid. *Molecular Human Reproduction*. 2001;7(2):163-168.

489. Hornung D, Chao VA, Vigne JL, Wallwiener D, Taylor RN. Thiazolidinedione Inhibition of Peritoneal Inflammation. *Gynecologic and Obstetric Investigation*. 2003;55(1):20–24.

490. Lebovic DI, Kavoussi SK, Lee J, Banu SK, Arosh JA. PPARγ activation inhibits growth and survival of human endometriotic cells by suppressing estrogen biosynthesis and PGE2 signaling. *Endocrinology*. 2013;154(12):4803-4813.

491. Lee MH, Reynisdottir I, Massague J. Cloning of p57KIP2, a cyclin-dependent kinase inhibitor with unique domain structure and tissue distribution. *Genes and Development*. 1995;9(6):639-649.

492. Ito Y, Matsuura N, Sakon M, Miyoshi E, Noda K, Takeda T, Monden M. Expression and prognostic roles of the G1-S modulators in hepatocellular carcinoma: p27 independently predicts the recurrence. *Hepatology*. 1999;30(1):90-99.

493. Hunter T, Pines J. Cyclins and cancer II: Cyclin D and CDK inhibitors come of age. *Cell*. 1994;79(4):573-582.

494. Ohtsubo M, Theodoras AM, Schumacher J, Roberts JM, Pagano M. Human cyclin E, a nuclear protein essential for the G1-to-S phase transition. *Molecular and Cellular Biology*. 1995;15(5):2612-2624.

495. Chu IM, Hengst L, Slingerland JM. The Cdk inhibitor p27 in human cancer: prognostic potential and relevance to anticancer therapy. *Nature Reviews Cancer*. 2008;8(4):253-267.

496. Lee J, Banu SK, Rodriguez R, Starzinski-Powitz A, Arosh JA. Selective blockade of prostaglandin E2 receptors EP2 and EP4 signaling inhibits proliferation of human endometriotic epithelial cells and stromal cells through distinct cell cycle arrest. *Fertility and Sterility.* 2010;93(8):2498-506.

497. Schor E, da Silva IDC, Sato H, Baracat EC, Girão MJBC, de Freitas V. P27Kip1 is down-regulated in the endometrium of women with endometriosis. *Fertility and Sterility*. 2009;91(3):682-686.

498. Salamonsen LA, Woolley DE. Matrix metalloproteinases in normal menstruation. *Human Reproduction*. 1996;11(2):124-133.

499. Salamonsen LA, Butt AR, Hammond FR, Garcia S, Zhang J. Production of endometrial matrix metalloproteinases, but not their tissue inhibitors, is modulated by progesterone withdrawal in anin vitro model for menstruation. *The Journal of Clinical Endocrinology and Metabolism*. 1997;82(5):1409-1415.

500. Sillem M, Prifti S, Monga B, Arslic T, Runnebaum B. Integrin-mediated adhesion of uterine endometrial cells from endometriosis patients to extracellular matrix proteins is enhanced by tumor necrosis factor alpha (TNFα) and interleukin-1 (IL-1). *European Journal of Obstetrics & Gynecology and Reproductive Biology*. 1999;87(2):123–127.

501. Bruner-Tran KL, Eisenberg E, Yeaman GR, Anderson TA, McBean J, Osteen KG. Steroid and cytokine regulation of matrix metalloproteinase expression in endometriosis and the establishment of experimental endometriosis in nude mice. *The Journal of Clinical Endocrinology & Metabolism*. 2002;87(10):4782-4791.

502. Osteen KG. Progesterone action in the human endometrium induction of a unique tissue environment which limits matrix metalloproteinase MMP expression. *Frontiers in Bioscience*. 2003;8(4):78–86.

503. Szamatowicz J. Matrix metalloproteinase-9 and tissue inhibitor of matrix metalloproteinase-1: a possible role in the pathogenesis of endometriosis. *Human Reproduction*. 2002;17(2):284-288.

504. Bruner-Tran KL, Webster-Claır D, Osteen KG. Experimental endometriosis. *Annals of the New York Academy of Sciences*. 2002,955(1):328-339.

505. Braundmeier AG, Fazleabas AT, Nowak RA. Extracellular matrix metalloproteinase inducer expression in the baboon endometrium: menstrual cycle and endometriosis. *Reproduction*. 2010;140(6):911-920.

506. Bryan NS, Grisham MB. Methods to detect nitric oxide and its metabolites in biological samples. *Free Radical Biology and Medicine*. 2007;43(5):645-657.

507. Kumar A, Hu J, LaVoie HA, Walsh KB, DiPette DJ, Singh US. Conformational changes and translocation of tissue-transglutaminase to the plasma membranes: role in cancer cell migration. *BMC Cancer*. 2014;11(14):256-270.

508. D'Hooghe TM. Endometriosis, retrograde menstruation and peritoneal inflammation in women and in baboons. *Human Reproduction Update*. 2002;8(1):84-88.

509. Bruner-Tran K.L, Mokshagundam S, Herington JL, Ding T, Osteen KG. Rodent models of experimental endometriosis: identifying mechanisms of disease and therapeutic targets. *Current Women s Health Reviews*. 2018;14(2):173–188.

510. Bruner KL, Matrisian LM, Rodgers WH, Gorstein F, Osteen KG. Suppression of matrix metalloproteinases inhibits establishment of ectopic lesions by human endometrium in nude mice. *Journal of Clinical Investigation*. 1997;99(12):2851-2857.

511. Awwad JT, Sayegh RA, Tao X J, Hassan T, Awwad ST, Isaacson K. The SCID mouse: An experimental model for endometriosis. *Human Reproduction*.

1999;14(12):3107-3111.

512. Fortin M, Lépine M, Pagé M, Osteen K, Massie B, Hugo P, Steff AM. An improved mouse model for endometriosis allows noninvasive assessment of lesion implantation and development. *Fertility and Sterility.* 2003;80(2):832-838.

513. Fortin M, Lépine M, Merlen Y, Thibeault I, Rancourt C, Gosselin D, Hugo P, Steff AM. Quantitative assessment of human endometriotic tissue maintenance and regression in a noninvasive mouse model of endometriosis. *Molecular Therapy*. 2004;9(4):540-547.

APPENDIX A: ETHICAL APPROVAL FORM

T.C. YEDİTEPE ÜNİVERSİTESİ

Sayı : 37068608-6100-15-1075
Konu: Etik kurul Başvurusu hk.

26 / 06 / 2015

İlgili Makama (Sayın Dilek Telci)

Yeditepe Üniversitesi Moleküler Hücre Biyolojisi Bölümü Doç.Dr. Dilek Telci'nin sorumlu olduğu "**Doku Transglutaminaz enziminin endometriozis patogenezi üzerine etkisi**" isimli araştırma projesine ait KAEK Başvuru Dosyası (1089 kayıt sayılı KAEK Başvuru Dosyası), Yeditepe Üniversitesi Klinik Araştırmalar Etik Kurulu tarafından 24.06.2015 tarihli toplantıda incelenmiştir.

Kurul tarafından yapılan inceleme sonucu, çalışmanın yapılmasında etik ve bilimsel açıdan uygun olduğuna karar verilmiştir. (Karar No: **63/509**).

Bilginizi ve gereğini saygılarımla arz ederim.

Prof. Dr. Turgay ÇELİK
Yeditepe Üniversitesi
Klinik Araştırmalar Etik Kurulu Başkanı

Yeditepe Üniversitesi 26 Ağustos Yerleşimi, İnönü Mahallesi Kayışdağı Caddesi 34755 Ataşehir / İstanbul
T. 0216 578 00 00 www.yeditepe.edu.tr F. 0216 578 02 99